THE CERATA OF MELIBE LEONINA (GOULD, 1859) (MOLLUSCA; NUDIBRANCHIA). MORPHOGENESIS, NEUROGENESIS, AUTOTOMY AND REPUGNATORIAL GLANDS

by

LOUISE ROBERTA PAGE
B.Sc., University of Alberta, 1975
M.Sc., University of Alberta, 1978

A DISSERTATION SUBMITTED IN PARTIAL FULFILLMENT

OF THE REQUIREMENTS FOR THE DEGREE OF

DOCTOR OF PHILOSOPHY

in the Department

of

Biology

We accept this dissertation as conforming
to the required standard

[redacted]
Dr. G.O. Mackie (supervisor)

[redacted]
Dr. T.W. Pearson

[redacted]
Dr. A.R. Fontaine

[redacted]
Dr. M.E. Corcoran

[redacted]
Dr. M. Paul

[redacted]
Dr. D. Paul

[redacted]
Dr. D.J. Prior

UNIVERSITY OF VICTORIA

Supervisor: Professor George O. Mackie

ABSTRACT

Larval and metamorphic development of Melibe leonina, as determined from histological sections, is similar to that of other planktotrophic nudibranch larvae except that the rudiments of the postmetamorphic cerata appear during the larval stage. Using semi-serial thin sections, I examined ceratal development from the larval mantle fold and neurogenesis of the pleural/ceratal (PC) nerve. The proximal segment of the PC nerve is established initially by outgrowing axons of central motoneurons. Morphological evidence suggests outgrowing axons are guided by a supporting cell and by the basal lamina of the mantle fold epithelium. The distal portion of the PC nerve is pioneered by ingrowing axons from peripheral sensory cells.

Ceratal autotomy, which allows escape from crab predators, requires breakage of the epidermis, longitudinal muscle bands, ceratal nerve and digestive gland. Ultrastructural observations show that two circular nerves, originating from the ceratal nerve, lie within the autotomy plane; one runs beneath the epidermis, the other surrounds the ceratal branch of the digestive gland. Innervated granule-filled cells (GC) lie within the perineurium of these nerves and extend processes to the basal laminae and associated connective tissue of the four structures that cross the autotomy plane. Degranulation of GC and disruption of basal laminae accompany autotomy. I suggest that autotomizing stimuli (pinching the ceras) elicit neurally-mediated release of GC granules, which disrupts basal laminae and connective tissue structures within the autotomy plane. Tissue separation is assisted by strong muscular contractions.

Each ceras of M. leonina contains a peripheral nervous system consisting of several small ganglia that give rise to distal nerves. Efferent neurons within the ganglia are

recruited by strong afferent stimuli and fire semisynchronously to produce a train of large amplitude spike bursts in extracellular recordings from all nerves emanating from the ganglia. The spike bursts precede ceratal autotomy. I argue that these neurons are presynaptic to ceratal muscles that help accomplish ceratal autotomy.

The repugnatorial glands of the cerata are composed of two types of secretory cells invested with muscle cells. Glandular secretion requires direct touch to ciliated sensory cells adjacent to the secretory pore and sea star tube feet reduce the stimulus threshold for secretion.

Examiners:

[redacted]

Dr. G.O. Mackie (supervisor)

[redacted]

Dr. T.W Pearson

[redacted]

Dr. A.R. Fontaine

[redacted]

Dr. M.E. Corcoran

[redacted]

Dr. M. Paul

[redacted]

Dr. D. Paul

[redacted]

Dr. D.J. Prior

TABLE OF CONTENTS

LIST OF TABLES

LIST OF FIGURES

ACKNOWLEDGEMENTS

It is a pleasure to thank the many people who helped in the production of this dissertation.

Ms. C. Pennachetti-Carolsfeld, Mr. J. Carolsfeld, Dr. M. Byrne, and Mr. I. Boyd helped with specimen collections; Mr. J. Deitrich, Dr. B.J. Crawford, Dr. T. Lacalli, Dr. C. Weber, and Dr. C.L. Singla provided helpful suggestions regarding electron microscopy; and J. Carolsfeld, Dr. D. Paul, and Dr. G.O. Mackie taught and assisted me with techniques of neurophysiology. Dr. C. Mills donated the photographs shown in Figs. 60 and 61. Thanks also to Mr. T. Gore for photographic assistance, and Mr. R. Scheurle and his assistants for their diligent maintenance of the seawater system at the University of Victoria.

This dissertation has benefited from input by my examining committee and from comments on earlier drafts by Dr. S.C. Kempf and several anonymous reviewers (first section of Ch. 1), Dr. A.R. Fontaine (Ch. 2), Dr. D. Paul (Ch. 3), and Dr. G.O. Mackie (all Chs.).

Dr. A.O.D. Willows provided laboratory facilities at Friday Harbor Laboratories, University of Washington, where all my neurophysiological work was done, and Dr. R.O. Brinkhurst allowed use of a photomicroscope for photographing histological sections in Ch. 1.

By the example of his own research, Dr. G.O. Mackie motivates others to ask and find ways of answering interesting biological questions. I have greatly benefited from his lectures, discussions, and technical and financial assistance. He has been a friend and teacher who has encouraged my research even when others might have faltered.

Finally, I am grateful to my husband, Richard Page, for much assistance with the computer, for discussions of my research, and for his patience. My mother, Mrs. A.I.

Bickell, donated her time to care for my children during some of my many hours in the photographic darkroom.

Funding for this research was provided by three University of Victoria graduate student fellowships and an NSERC research grant to G.O. Mackie.

GENERAL INTRODUCTION

Extant opisthobranch molluscs exhibit several independent morphoclines of shell reduction and loss (Morton, 1963; Thompson, 1976). The shell is entirely lacking in all members of the order Nudibranchia. Loss of the shell in opistibranchs is correlated with a variety of structural elaborations of the dorsum. The most striking elaboration is the cerata (from the Greek 'ceras', meaning horn), a collective term for all forms of dorsal, non-cephalic appendages in non-dorid nudibranchs. Cerata exhibit a great deal of interspecific variation according to parameters such as size, shape, number, and presence or absence of branches of the digestive gland (see MacFarland, 1966). Additional sources of variation include ability to autotomize, type and number of epidermal glands, and presence of cnidosacs that house nematocysts sequestered from cnidarian prey. This structural diversity suggests that no single suite of functions can be assigned to the cerata of all species.

Evolutionary loss of the shell in nudibranchs is accompanied by loss of the mantle cavity and pallial organs, including the ctenidia (gill). Eighteenth century malacologists debated about whether or not cerata replaced the ctenidia as organs of gas exchange (see Herdman, 1890a). Although this role is now generally accepted for cerata (Morton, 1958; Hyman, 1967), the issue has never been resolved through experimental investigation.

The fact that cerata have replaced the ancestral, protective shell, at least in position, and the observation that nudibranchs are rarely preyed upon (Herdman, 1890b; Thompson, 1960; Russell, 1966) hint that cerata may be defensive structures.

In the mid-1800s, Alder and Hancock (1845-1854; cited by Herdman [1890a]) reported seeing nematocysts within the ceratal apices of aeolids having a transparent epidermis. Herdman (1890a) subsequently confirmed this observation and showed that nematocysts are clustered within cells of a special chamber ('cnidophorus sac') that communicates with

the ceratal branch of the digestive gland and with the external environment via a pore at the tip of the ceras. Grosvenor (1903) and Cuénot (1907) showed that the nematocysts of aeolids are derived from their cnidarian prey. This remarkable ability to retain undischarged nematocysts has been the subject of most subsequent studies on nudibranch cerata (Glaser, 1910; Graham, 1938; Kepner, 1943; Thompson and Bennett, 1969; Cockburn, 1976; Day and Harris, 1978). Beginning with Herdman (1890a), it has been assumed that the sequestered nematocysts are used for defense by their surrogate hosts, yet Day and Harris (1978) point-out that the only direct evidence for this comes from an abstract by Allen (1976) in which he describes nematocysts within swollen mouth tissue of a shiner perch that had mouthed the aeolid, Hermissenda crassicornis. However, Cockburn (1976) failed to find nematocysts within the mouths of sculpins after they had attacked H. crassicornis.

Thompson (1960) and Edmunds (1966) examined evidence for other ways in which cerata may defend against predators, including crypsis through ceratal colour and shape, acidic secretions and defensive chemicals elaborated by ceratal epidermal glands, and ceratal autotomy. Autotomy ('self-cutting') is the ability to rapidly detach an appendage when the appendage receives a threatening stimulus.

Since Johannes' (1963) report that a strong smelling mucus released by Phyllidia varicosa is toxic to some crustaceans and fish, and the subsequent identification of the toxic material by Burreson et al. (1975), who found it to be a novel sesquiterpenoid, organic chemists have succeeded in isolating many unusual metabolites from nudibranchs (see reviews by Schulte and Scheuer, 1982; Gustafson and Anderson, 1985). Many of the substances are derived from prey organisms of the nudibranchs and some have been shown to deter predation by fish (see Gunthorpe and Cameron, 1987). Despite the interest in the chemistry of nudibranch metabolites, nothing is known of the detailed structure of

epidermal glands that might release these substances, nor has their been studies examining the role of nudibranch defensive chemicals within an ecological context, such as that of Young et al. (1986) on the marine pulmonate Onchidella borealis.

Even less is known about ceratal autotomy. Indeed Stasek's (1967) review of autotomy within the Mollusca is mainly a catalogue of superficial descriptions of autotomy in a variety of molluscs. Since then, Hodgson (1984) performed a histological and electron microscopical study of the potential autotomy sites along the siphons of two species of Solen (Bivalvia). He concluded that these sites were zones of weakness due to a reduction of connective tissue, and speculated that the breakage of the longitudinal muscle bands within the siphons is achieved by rapid contractions of circular and radial muscles that "compress, elongate and break the longitudinal muscle fibres." The histological study of Kress (1968) failed to show a zone of reduced connective tissue within the base of the deciduous cerata of three species of Doto (Nudibranchia), but he did identify a 'granular zone' in this region. Although opisthobranchs have been the subject of many neurophysiological studies (see Kandel, 1976; 1979), nothing is known about the neuronal control of autotomy.

Diversity among nudibranch cerata is not limited to structure and function. Developmental studies show that cerata of all species are not homologous, but may be derived from larval mantle fold tissue or larval pedal tissue (Tardy, 1970; Thompson, 1962; Bonar and Hadfield, 1974; Bonar, 1976). None of these studies examined ceratal morphogenesis in detail.

The intent of my dissertation is to contribute information toward a better understanding of the development and functional morphology of nudibranch cerata. I studied the cerata of Melibe leonina (Gould, 1852), a large dendronotid nudibranch that can occur at very high density within eel grass and kelp beds along the west coast of North

America. General anatomical and histological descriptions of this animal have been given by Kjerschow-Agersborg (1921; 1923a; 1923b) and Hurst (1968), aspects of its behaviour have been provided by Kjerschow-Agersborg (1921; 1923a), Hurst (1968), and Ajeska and Nybakken (1976), and the neural control of swimming behaviour has been studied by S. Thompson (Hopkins Marine Laboratory, Stanford University; personal communication, 1982; manuscript in preparation). M. leonina is remarkable among nudibranchs for its method of feeding; a large oral hood that surrounds the mouth is used to engulf zooplankton within the surrounding water. The species does not sequester nematocysts within its cerata, but the cerata will autotomize if pinched and the ceratal epidermis (as well as that of the oral hood and general dorsum) contains distinctive, multicellular glands.

In the first part of Ch. 1, I give a general description of larval and metamorphic development of M. leonina, showing precocious development of the cerata during the larval stage. This section has been modified from a published paper by Bickell (Page) and Kempf (1983). All technical work (larval culture and preparation of histological sections) and interpretation of results included in this version are my own. The second part of Ch. 1 is an ultrastructural investigation of ceratal morphogenesis including the development of the peripheral nerve that innervates these appendages. Peripheral nerve formation during normal development has not been described previously for any mollusc. The results are compared to those of recent studies on neurogenesis in insects.

In Ch. 2, I describe structural specializations for accomplishing ceratal autotomy. The morphological results indicate that, unlike the autotomizing siphonal segments of Solen, the autotomy plane of M. leonina is not a zone of inherent weakness. Instead, its fine structure before and after autotomy suggests an autotomy mechanism akin to that hitherto known only in echinoderms (reviewed by Wilkie, 1984). By virtue of their size and ease of isolation, autotomizing ligaments and tendons of echinoderms may be more

amenable to studies of the physico-chemical mechanism of tissue breakage accompanying autotomy, but the nervous system of nudibranchs is much more conducive to investigation of the neural control of this event. In Ch. 3, I describe one aspect of the neurophysiological control of ceratal autotomy in M. leonina.

Finally, Ch. 4 gives an ultrastructural description of repugnatorial glands from the cerata of M. leonina. My behavioural and morphological observations suggest the effective stimulus and mechanism of discharge for these glands and the effectiveness of their secretory product for repelling various predators.

LITERATURE CITED

Alder, J., and A. Hancock. 1845-1854. Monograph of the British Nudibranchiate Mollusca. pt. 3, Ray Society, London.

Allen, J.K. 1976. Function of nematocysts in eolid nudibranchs. Western Soc. Malac. Ann. Rep. 9: 30 (abstract).

Ajeska, R.A., and J.W. Nybakken. 1976. Contributions to the biology of Melibe leonina (Gould, 1852) (Mollusca: Opisthobranchia). Veliger 19: 19-26.

Bickell, L.R., and S.C. Kempf. 1983. Larval and metamorphic morphogenesis in the nudibranch Melibe leonina (Mollusca: Opisthobranchia). Biol. Bull. 165: 119-138.

Bonar, D.B. 1976. Molluscan metamorphosis: a study in tissue transformation. Am. Zool. 16: 573-591.

Bonar, D.B., and M.G. Hadfield. 1974. Metamorphosis of the marine gastropod Phestilla sibogae Bergh (Nudibranchia: Aeolidacea). I. Light and electron microscopic analysis of larval and metamorphic stages. J. exp. mar. Biol. Ecol. 16: 227-255.

Burreson, B.J., P.J. Scheuer, J. Finer, and J. Clardy. 1975. 9-Isocyanopupukeanane, a marine invertebrate allomone with a new sesquiterpene skeleten. J. Am. chem. Soc. 97: 4763-4764.

Cockburn, T.C. 1976. The Role of the Cerata in the Aeolid Nudibranchs Hermissenda crassicornis (Eschscholtz, 1831) and Aeolidia papillosa (Linnaeus, 1761). Ph.D. dissertation, University of Victoria, 215 pp.

Cuénot, L. 1907. L' origine des nematocystes des Eolidiens. Arch. Zool. éxp. Gen. 6: 22-102.

Day, R.M., and L.G. Harris. 1978. Selection and turnover of coelenterate nematocysts in some aeolid nudibranchs. Veliger 21: 104-109.

Edmunds, M. 1966. Protective mechanisms in the Eolidacea (Mollusca, Nudibranchia). J. Linn. Soc. (Zool.) 46: 27-71.

Glaser, O.C. 1910. The nematocysts of eolids. J. exp. Zool. 9: 117-142.

Graham, A. 1938. The structure and function of the alimentary canal of aeolid molluscs, with a discussion of their nematocysts. Trans. roy. Soc. Edinburgh 59: 267-307.

Grosvenor, G.H. 1903. On the nematocysts of aeolids. Proc. roy. Soc. Lond. 72: 462-486.

Gunthorpe, L., and A.M. Cameron. 1987. Bioactive properties of extracts from Australian dorid nudibranchs. Mar. Biol. 94: 39-43.

Gustafson, K., and R.J. Andersen. 1985. Chemical studies of British Columbia nudibranchs. Tetrahedron 41: 1101-1108.

Herdman, W.A. 1890a. On the structure and function of the cerata or dorsal papillae in some nudibranchiate Mollusca. Quart. J. microsc. Sci. 31: 41-63.

Herdman, W.A. 1890b. Some experiments on feeding fishes with nudibranchs. Nature (Lond.) 42: 201-203.

Hodgson, A.N. 1984. Use of the intrinsic musculature for siphonal autotomy in the Solenacea (Mollusca: Bivalvia). Trans. roy. Soc. S. Afr. 45: 129-137.

Hurst, A. 1968. The feeding mechanism and behavior of the opisthobranch Melibe leonina. Symp. zool. Soc. Lond. 22: 151-166.

Hyman, L.H. 1967. The Invertebrates vol. 4, The Mollusca, vol. 1. McGraw-Hill, New York. 792 pp.

Johannes, R.E. 1963. A poison-secreting nudibranch (Mollusca: Opisthobranchia). Veliger 5: 104-105.

Kandel, E.R. 1976. Cellular Basis of Behavior. W.H. Freeman, San Fransisco, 727 pp.

Kandel, E.R. 1979. Behavioral Biology of Aplysia: A Contribution to the Comparative Study of Opisthobranch Molluscs. W.H. Freeman, San Fransisco. 463 pp.

Kepner, W.A. 1943. The manipulation of the nematocysts of Pennaria tiarella by Aeolis pilata. J. Morph. 73: 297-311.

Kjerschow-Agersborg, H.P. von Wold. 1921. Contribution to the knowledge of the nudibranchiate mollusk, Melibe leonina (Gould) Amer. Nat. 55: 222-253.

Kjerschow-Agersborg, H.P. von Wold. 1923a. A critique on Professor Harold Heath's Chioraera dalli, with special reference to the use of the foot in the nudibranchiate mollusk, Melibe leonina Gould. Nautilus 36: 86-96.

Kjerschow-Agersborg, H.P. von Wold. 1923b. The morphology of the nudibranchiate mollusk Melibe (syn. Chioraera) leonina (Gould). Quart. J. microsc. Sci. 67: 507-592.

Kress, A. 1968. Untersuchungen zur Histologie, Autotomie und Regeneration dreier Doto - Arten Doto coronata, D. pinnatifida, D. fragilis (Gastropoda, Opisthobranchiata). Revue suisse Zool. 75: 225-303.

MacFarland, F.M. 1966. Studies of Opisthobranchiate Mollusks of the Pacific Coast of North America. Calif. Acad. Sci. Memoirs 6: 1-546.

Morton, J.E. 1958. Molluscs: An Introduction to Their Form and Function. Harper and Bros., New York. 232 pp.

Morton, J.E. 1963. The molluscan pattern: evolutionary trends in a modern classification. Proc. Linn. Soc. (Zool.) 174: 53-72.

Russell, E. 1966. An investigation of the palatability of some marine invertebrates to four species of fish. Pac. Sci. 20: 452-460.

Schulte, G.R., and P.J. Scheuer. 1982. Defense allomones of some marine mollusks. Tetrahedron 38: 1857-1863.

Stasek, C.P. 1967. Autotomy in the mollusca. Occ. Pap. Calif. Acad. Sci. 61: 1-44.

Tardy, J. 1970. Contribution a l' étude des métamorphoses chez les nudibranches. Ann. Sci. nat. Zool. 12: 299-370.

Thompson, T.E. 1960. Defensive adaptations in opisthobranchs. J. mar. biol. Ass., U.K. 39: 123-134.

Thompson, T.E. 1962. Studies on the ontogeny of Tritonia hombergi Cuvier (Gastropoda, Opisthobranchia) Phil. Trans. roy. Soc. Lond. 245B: 171-281.

Thompson, T.E. 1976. Biology of Opisthobranch Molluscs, vol. I. Ray Society, Lond. 207 pp.

Thompson, T.E., and I. Bennett. 1969. Physalia nematocysts: utilized by molluscs for defense. Science 166: 1532-1533.

Wilkie, I.C. 1984. Variable tensility in echinoderm collagenous tissues. A review. Mar. Behav. Physiol. 11: 1-34.

Young, C.M., P.G. Greenwood, and C. Powell. 1986. The ecological role of defensive secretions in the intertidal pulmonate Onchidella borealis. Biol. Bull. 171: 391-404.

Chapter 1

LARVAL AND METAMORPHIC DEVELOPMENT OF THE NUDIBRANCH MELIBE LEONINA (GOULD, 1852), WITH EMPHASIS ON THE MORPHOGENESIS OF THE CERATA AND PLEURAL/CERATAL NERVES

INTRODUCTION

Opisthobranch molluscs are an assemblage of diverse and often highly derived adult morphs, yet the young larvae of these gastropods have a conservative structure and a general pattern of developmental events up to metamorphosis is recognizable (Thompson, 1958; 1962; Tardy, 1970; Thiriot-Quiévereux, 1970; 1977; Bonar and Hadfield, 1974; Kempf and Willows, 1977; Kriegstein, 1977a; b; Switzer-Dunlap and Hadfield, 1977; Chia and Koss, 1978; Bickell and Chia, 1979; additional references reviewed by Bonar, 1978a). Deviations from this general pattern can often be interpreted as ontogenic anticipation of unique structural features of the postmetamorphic phase or special features to facilitate the success of settlement and metamorphosis or survival of young juveniles in the adult habitat (Chia and Koss, 1978; 1982; Switzer-Dunlap, 1978; Bickell and Chia, 1979).

Metamorphosis of shell-less opisthobranch larvae is a much more radical event than that which occurs in prosobranch larvae (generalized accounts of metamorphosis given by Fretter [1969] for prosobranchs, and Bonar [1978a] for opisthobranchs). In nudibranchs, metamorphic events include loss of the shell and operculum, with concomitant changes in body shape and symmetry, gut configuration and structure, and nervous system anatomy. Studies of metamorphic morphogenesis may reveal tissue derivations that are useful for phylogenetic inferences (Tardy, 1970; Bonar and Hadfield, 1974). This is particularly important for nudibranchs because the extreme modification, diversity, and convergence that characterizes the adult morphs make phylogenetic hypotheses difficult to assess (Morton, 1963; Ghiselin, 1965).

In the first part of this chapter, I describe the larval and metamorphic development of the nudibranch, Melibe leonina (Gould, 1852), by means of observations of living animals and histological sections through sequential developmental stages. I compare the results to those of other studies and discuss the significance of several unorthodox developmental

features, such as the precocious development of the ceratal rudiments during the larval stage.

In the second part of this chapter I give an ultrastructural description of the premetamorphic morphogenesis of the primary cerata and the peripheral nerve that innervates these appendages. Although much information is available on neuronal mechanisms underlying gastropod behaviour (see Kater et al., 1975; Kandel, 1976; 1979), relatively little is known about neurodevelopment within this group. Existing studies include early light microscopical works on general development of the nervous system (reviewed by Raven, 1958), contemporary studies on the development of central neuronal somata (Shacher et al., 1979a; b; Jacob, 1984; Kempf et al., 1987), and studies on regenerating axons of adult neurons (Price, 1977; Murphy and Kater, 1978; 1980; Bullock et al., 1980; Bullock and Kater, 1981; Wong et al., 1981; Barker et al., 1982; Hadley et al., 1982; Schacher, 1985).

In the juvenile and adult stages of M. leonina, the cerata are petaloid in shape and arranged along two rows down the dorsum of the body (Fig. 1). Each ceras is innervated by a separate ceratal nerve and the ceratal nerves arise as sequential branches of the ipsilateral pleural nerve (see Chs. 2 and 3). Ceratal rudiments and their innervation develop during the larval stage, but anatomical distinction between the pleural and ceratal nerves in late stage larvae and recently metamorphosed animals (post-larvae) is arbitrary because only one pair of cerata is present. Therefore, I use the name pleural/ceratal (PC) nerve for the nerve extending from the pleural ganglion into the cerata of the larva and post-larva.

The right PC nerve is particularly amenable to developmental study because: 1) the distance travelled by the nerve in the larva is relatively short (approximately 100 µm), which facilitates serial electron microscopical reconstructions; 2) it is the only nerve

extending between the CNS and the cerata; and 3) during its initial development, the nerve projects through an environment that is structurally simple.

MATERIALS AND METHODS

Adult M. leonina and their egg masses were collected from eel grass beds located in Shoal Bay, Lopez Island (San Juan Archipelago, Washington, U.S.A.) and in Patricia Bay, Vancouver Island (British Columbia, Canada).

Laboratory hatched larvae were cultured at an initial density of 2 to 3 larvae/ml in bowls containing 100 ml of filtered (Millipore prefilter no. AP2004700) natural seawater with 10,000 cells/ml of the alga Pavlova (Monochrysis) lutheri (Carolina Biological Supply). Larvae were transferred to fresh culture medium at 1 or 2 day intervals. Details of the algal culture method, and the method of transferring larvae to fresh culture medium have been described by Bickell et al. (1979). The antibiotics streptomycin sulfate (50 µg/ml) and penicillin G (60 µg/ml) (Switzer-Dunlap and Hadfield, 1977) were added at 2 to 6 day intervals. Cultures were maintained at a temperature of 12 to 14 degrees Centigrade.

Young juveniles of M. leonina were fed a mixture of unidentified ciliates harvested from various types of decomposing animal tissue (sea urchin eggs, crushed limpets, chunks of sea pen). This diet was supplemented with nauplii of harpacticoid copepods.

Eleven developmental stages were processed for histological examination. Larvae were fixed at hatching, mantle fold retraction, two stages during mantle fold hypertrophy, and full development of the ceratal rudiments and propodium (metamorphic competence). Metamorphic stages were fixed at the time of velum loss, shell loss, and 5, 10, 24, and 48 hours after loss of the larval shell. The primary fixative for all stages consisted of phosphate-buffered (pH 7.6) 2.5% glutaraldehyde made isosmotic to seawater with 0.34M NaCl (Cloney and Florey, 1968). Larval stages were anaesthetized prior to fixation by placing them in 3 ml of seawater and 7 drops of 2% procaine. After 15 min at room temperature, 0.5 ml of a saturated solution of chlorobutanol in seawater was added and the vessel placed on ice for 10 min. Anaesthetized larvae were placed in primary fixative

for 30 min, followed by a 1 hr treatment in a mixture of equal parts primary fixative and 10% ethylenediaminotetraacetic acid (disodium salt) to decalcify the larval shells (Bonar and Hadfield, 1974). Metamorphic stages were anaesthetized for 5 min in 1 part saturated chlorobutanol solution and 9 parts filtered seawater on ice and transferred to primary fixative for 1 hr. After several rinses in 2.5% sodium bicarbonate buffer (pH 7.2), all larval and metamorphic stages were post-fixed for 1 hr in 2% osmium tetroxide in bicarbonate buffer. Fixed animals were dehydrated in ethanol, rinsed in propylene oxide, and embedded in a plastic prepared by substituting Poly/Bed 812 (Polysciences) for Epon 812 in the recipe of Luft (1961).

For general description of development, embedded specimens were serially sectioned at 1 µm thickness and stained with Richardson's stain (Richardson et al., 1960).

For ultrastructural observations of cerata and PC nerve development, ribbons of serial sections were cut with a Diatome diamond knife on a Reichert ultramicrotome and picked up on copper mesh grids (no. 100) having a Formvar or Parlodian support film. Although grid bars obscured some of the sections, this method was adequate for tracing small bundles of axons and groups of sensory cells. Individual axons could not be followed. Sections were stained for 20 min in aqueous uranyl acetate at 60 degrees Centigrade, followed by 10 min in lead citrate at room temperature, and were viewed with a Philips EM 300.

RESULTS

A. Larval and Metamorphic Development

1. Structure at Hatching

The veliger larvae of Melibe leonina hatch from the benthic egg mass approximately 10 days after oviposition and are structurally similar to the young planktotrophic veligers of other opisthobranchs. At hatching, the larval body is small and morphologically simple relative to the size and complexity that is achieved by the end of the obligatory larval stage (compare Figs. 2 and 3).

The veliger has two major body regions: a cephalopedal mass and a visceropallial mass. The cephalopedal mass consists of the two ciliated lobes of the velum that effect swimming and capture of food particles, and a small pointed foot that bears a circular operculum on its posterior face (Figs. 2, 4).

The visceropallial mass includes a functional digestive tract, the so-called larval kidney complex, the larval shell with its underlying perivisceral epithelium, and the mantle fold epithelium (Figs. 2, 4).

The digestive tract is composed of an esophagus, a stomach, a large left and much smaller right digestive gland, and an intestine (Figs. 2, 4, 5). After leaving the stomach, the intestine recurves anteriorly towards the anus located in the floor of the right mantle cavity (Fig. 5). The position of the anus indicates partial torsion of the larval gut. The larval stomach has two major divisions that Thompson (1959) termed the ventral and dorsal stomach. The ventral stomach consists of a ciliated region that receives the openings of the esophagus and digestive glands and an area lined by a gastric shield (Fig. 4). The dorsal stomach is lined on three sides by a band of densely packed, transversely beating cilia (Fig. 6). A sparsely ciliated groove extends down the upper wall of the dorsal

stomach (Fig. 6). The manner in which food particles are transported and digested by the gut of opisthobranch veligers has been described previously (Thompson, 1959; Bickell et al., 1981; Kempf, 1982).

The larval kidney complex is a cluster of distinctive yet heterogeneous cells located adjacent to the anus on the right side of the veliger (Figs. 2, 4). The function of these cells, which degenerate at metamorphosis, is not clear. Two nephrocysts, which are uniquely larval structures whose function is enigmatic but may involve storage or excretion of waste material (Bonar, 1978a), are located on either side of the esophagus (Fig. 6).

At the aperture of the larval shell, the perivisceral epithelium becomes the mantle fold epithelium (Fig. 7). It extends from the rim of the larval shell to the cephalic epidermis and can be subdivided into two components: shell-secreting cells attached to the rim of the larval shell and cells that line the floor of the mantle cavity.

The muscle systems of the veliger of M. leonina extend through both the cephalopedal and visceropallial portions of the larval body. The base of the large larval retractor muscle is attached to the posterior end of the shell via specialized cells of the perivisceral epithelium (Bonar, 1978b) and branches extend anteriorly into the tissues of the foot and velum. A bundle of accessory pedal retractor muscles originates on the pedal epithelium underlying the operculum and extends over the ventral lip of the shell to insert on the perivisceral epithelium immediately ventral to the anus. Contraction of the larval retractor and accessory pedal retractor muscles pulls the larval body and operculum into the shell cavity. In addition, a diffuse system of slender visceral muscles is associated with the digestive tract and with the mantle fold and perivisceral epithelium.

At the time of larval hatching in M. leonina, the only central ganglia that are clearly recognizable in one µm sections are a pair of small cerebral ganglia connected dorsally

over the esophagus by the cerebral commissure (Fig. 6). Sensory structures include a pair of statocysts within the base of the foot (Figs. 2, 4), and tufts of stiff cilia extending from the sides and apex of the foot (Fig. 2).

2. Larval Morphogenesis

The sketches in Figure 8 show three larval stages of Melibe leonina: the hatching stage, the eyespot - mantle retraction stage (16 to 20 days post-hatching), and the stage at which the larvae become capable of settlement and metamorphosis (30 to 48 days post-hatching). The shell increases in length from 149 µm (S.D. 9 µm) at hatching to 250 µm (S.D. 3 µm) (Fig. 8). As described below, morphogenetic events occur throughout the larval phase but tend to be concentrated within the latter half of development.

The mantle fold of M. leonina veligers undergoes a series of major morphogenetic changes during the larval stage. After secreting shell material during the initial portion of larval development, the mantle fold epithelium detaches from the rim of the shell and is pulled posteriorly (Figs. 8b, 9), presumably by slender muscles that extend from the mantle fold and larval kidney complex to various sites on the gut and perivisceral epithelium. Cells within the retracted mantle fold epithelium subsequently proliferate and hypertrophy and eventually form the rudiments of the primary cerata (Figs. 3, 8c, 10). Detailed description of this process is given in section B. Hypertrophied mantle fold cells also extend a short distance over the lateral side of the large left digestive gland and along the right side towards the anus.

The foot of the larva is enlarged considerably by proliferation of the pedal epithelial cells (compare Figs. 4, 9, 10). During the latter half of development, foot growth is accompanied by the differentiation of intrinsic pedal muscles and of large pedal glands that expand within the pedal haemocoel as they become filled with secretory product. These events ultimately result in the development of the propodium, a large swelling on the

proximal, ventral surface of the foot (Figs. 3, 10). The full development of the propodium and the concurrent growth of a dense covering of cilia over the ventral surface of the foot enables crawling, a behaviour that provides a convenient marker identifying metamorphically competent opisthobranch veligers.

The cephalic epithelium that lies immediately behind the velar lobes also proliferates and hypertrophies during the latter part of the larval development of M. leonina (compare Figs. 9 and 10). This band of columnar cephalic epithelium will form the epidermis of the postmetamorphic oral hood.

The basic structure of the gut is preserved throughout the larval phase, although the digestive tract grows considerably and the cells of the stomach and left digestive gland accumulate lipid deposits (Fig. 10). In late stage larvae, a vestigial radular rudiment becomes evident as a slight evagination of the ventral wall of the distal esophagus (Fig. 10), but neither radular teeth nor muscles differentiate in association with this outpocketing as typically occurs during the development of other opisthobranch larvae (see Bonar, 1978a).

The nervous system of M. leonina becomes extensively elaborated during larval development. By the time of mantle retraction, the pedal and pleural ganglia have become recognizable, the cerebral ganglia have enlarged, and a pair of eyespots have differentiated (Fig. 9). Between the stages of mantle retraction and the onset of metamorphosis, the buccal and rhinophoral ganglia differentiate.

Three additional developments that occur during the larval phase of M. leonina are the development of the pulsating larval heart soon after mantle retraction, the appearance of the adult kidney rudiment adjacent to the larval kidney complex and intestine, and the enlargement of the gonadal rudiment (Fig. 10).

3. Metamorphosis

Larvae of M. leonina do not require a specific, external chemical cue for the induction of metamorphosis. After full development of the propodium, larvae of this species settle onto the foot, exhibit a brief period of crawling, and commence metamorphosis.

The events of metamorphosis that are seen during external inspection of this process are shown in Figures 11 through 16. The first superficial indication that metamorphosis is irreversibly underway is the dissociation of the ciliated velar cells (Fig. 12), followed by loss of the operculum and the larval shell (Figs. 13, 14). The time interval between settlement and shell loss is variable but is usually between 12 and 24 hours. During and following shell loss, the cerata and oral hood undergo a period of rapid and pronounced enlargement (Figs. 15, 16).

Serial sections of M. leonina fixed at various stages after settlement reveal that much structural reorganization and tissue morphogenesis occurs during metamorphosis. Some of these changes are illustrated diagrammatically in Fig. 17.

Beginning soon after the dissociation of the velar cells, the trunk of the larval retractor muscle becomes detached from the posterior wall of the shell. Subsequent contractions of this muscle appear to pull the visceral mass out of the shell in a manner similar to that described for other nudibranchs (Bonar and Hadfield, 1974; Bonar, 1976; Bickell et al., 1981). The larval retractor and accessory pedal retractor muscles degenerate following shell loss.

During and immediately following shell loss, the hypertrophied mantle fold epithelium spreads posteriorly and laterally over the stomach and digestive glands and anteriorly toward the hypertrophied epithelium of the presumptive oral hood (Figs. 17a to 17c and Fig. 18). The fate of the perivisceral epithelium is not apparent; it may be sloughed into the environment or overgrown and subsequently phagocytized. Nevertheless, the lateral

and posterior margins of the mantle fold epithelium are continuous with the pedal epithelium by 5 hours after shell loss.

The loss of the shell and operculum at metamorphosis permits a broadening of the connection between the visceral mass and the foot (Figs. 17d to 17g). In M. leonina, this process appears to be facilitated by a large increase in the volume of the haemal space within the foot and surrounding the viscera. Inspection of living animals and histological sections of metamorphosing M. leonina give the impression that a large volume of external fluid has passed through the body wall and into the haemolymph. A similar but much more pronounced expansion of the haemal space accompanies the rapid enlargement of the cerata (compare Figs. 19 and 20) and the oral hood during and following shell loss. As these structures expand, the surface area of their covering epithelia is increased by conversion from a columnar to squamous epithelial type. A marked increase in the vesiculation of the epithelial cells occurs concurrently with their shape change (Figs. 19, 20, 21). Each ceras contains longitudinal and circular muscle fibres and isolated tufts of stiff cilia arise from the ceratal epidermis (Figs. 20, 21).

The anus, larval kidney complex, and adult kidney rudiment of M. leonina are displaced posteriorly following shell loss, presumably by the posterior migration of the mantle fold epithelium that surrounds the anus and by the broadening of the connection between the foot and visceral mass (Figs. 17a, 17b). Subsequently, the anus moves dorsally to its definitive location slightly to the right of the mid-sagittal plane and the larval kidney complex degenerates. The proximal end of the intestine continues to exit from the dorsal side of the posterior end of the stomach (Figs. 17g, 23).

The diagrams shown in Figures 17d to 17g illustrate the positional changes exhibited by the organs of the larval digestive system during metamorphosis of M. leonina. Unlike the process of gut metamorphosis in the dorid nudibranch Doridella steinbergae (Bickell et

al., 1981), the stomach of M. leonina does not undergo additional torsional displacement at metamorphosis, nor does it shift to the mid-dorsal surface of the large left digestive gland. Although the left digestive gland continues to reside beside the stomach, a dramatic enlargement of the right digestive gland gradually displaces the stomach to a central position within the visceral mass (Figs. 17g, 22). Soon after shell loss, both the left and right digestive glands begin to extend into the expanded haemocoel of their respective ceras (Figs. 21, 22).

The conversion of the phytoplanktotrophic larva to the carnivorous juvenile - adult necessitates extensive changes of the tissues composing the larval gut. The cells of the densely ciliated band (style sac) have completely dissociated by the time the post-larva has lost the shell and the gastric shield subsequently peels away from its underlying cells (Fig. 24). Soon thereafter, the cells that produced the larval gastric shield and the cells of the vestibule begin to produce the cuticular material that lines the stomach of the postmetamorphic animal (Kjerschow-Agersborg, 1923b) (Fig. 25).

Differentiation of muscles within the periphery of the oral hood enables it to close (compare Figs. 26 and 27) if a tactile stimulus is applied to the ventral surface of the hood. M. leonina is able to capture and ingest ciliates using the oral hood and oral lips at approximately 2.5 days after shell loss.

During metamorphosis, the cerebral and pleural ganglion on each side fuse to form a pair of cerebropleural ganglia and the neuropil region of all central ganglia enlarges. Several neuronal somata within the pleural portion of the cerebropleural ganglia become noticeably larger (10 µm diameter) than adjacent ganglionic cell bodies (3 to 5 µm diameter) (Fig. 28). The rhinophoral ganglia become associated with two distinctive patches of oral hood epithelium, which are the presumptive rhinophores (Fig. 29). As the oral hood expands, each rhinophoral ganglion is carried apart from the ipsilateral cerebral ganglion but the two remain connected by a rhinophoral nerve (Fig. 29).

The initial hood tentacles appear as 8 small papillae distributed around the periphery of the oral hood (Fig. 16). In living animals, particularly after the onset of feeding, prominent nerve tracts can be seen extending from the cerebral ganglia to each hood tentacle (Fig. 26). The cerebral nerves terminate at small clusters of cells (peripheral hood ganglia) at the base of the developing hood tentacles (Fig. 30). The epithelium of each hood tentacle gives rise to several tufts of stiff cilia and additional ciliary tufts occur on the ventral surface of the hood.

B. Morphogenesis of the Ceratal Rudiments and Pleural/Ceratal Nerves

Although the metamorphically competent larva of M. leonina has two ceratal rudiments and two PC nerves, I describe the development of these structures on the right side only, unless stated otherwise.

1. Ceratal Rudiments

The development of the ceratal rudiments during the larval stage can be divided into four stages: 1) mantle fold retraction from the aperture of the larval shell, 2) onset of mitoses by cells of the presumptive ceratal rudiments, 3) onset of cellular differentiation within the presumptive ceratal rudiments (mitoses continue during this stage), and 4) complete, premetamorphic development of the ceratal rudiments.

As previously stated, the mantle fold epithelium has two functionally distinct areas: a ridge of shell-secreting cells attached to the aperture of the larval shell, and cells lining the floor of the mantle cavity. The latter portion, which extends to the cephalic epidermis, will be called the floor epithelium.

Immediately after mantle fold retraction, the thickened ridge of former shell-secreting cells persists at the periphery of the mantle fold. In addition, a ridge of cuboidal cells is present within the otherwise squamous floor epithelium and is located a short distance proximal to the former shell-secreting cells (Fig. 31). Slender processes of mantle retractor muscles insert periodically on the basal lamina of the floor epithelium thickening and haemocoelic cells are clustered immediately beneath the thickening (Fig. 31).

Following mantle fold retraction, the former shell-secreting cells show signs of cytoplasmic deterioration (Fig. 32), whereas the cells composing the thickening of the floor epithelium and the associated population of subepithelial, haemocoelic cells begin to multiply (Figs. 33 and 34). The floor epithelium thickening on the right side of the larva is the presumptive, right ceratal rudiment. By the midpoint of the mitotic phase, the shell-secreting cells are no longer present (Fig. 34). None of the epithelial cells of the presumptive ceratal rudiment show signs of cellular differentiation at this stage.

Continued mitotic activity within the presumptive ceratal rudiment eventually forms a prominent mound of many epithelial and subepithelial cells at the periphery of the floor epithelium (Fig. 35). Stage 3 begins with the onset of primary sensory cell differentiation; these are the first epithelial cells to differentiate within the rudiment. Fig. 36 shows a pair of primary sensory cells at an advanced stage of maturation in a stage 3 ceratal rudiment. These cells occur in clusters of usually 3 to 6 and their cytoplasm is more electron-lucent than other epithelial and subepithelial cells. Each has a subepithelial cell body, an apical, ciliated dendrite that traverses the thickness of the epithelium together with other dendrites of the cluster, and a basal axon (Figs. 35 and 36; basal axons not shown). Detailed description of the ceratal sensory cells in postmetamorphic animals is given in Ch. 4.

Sections through stages 3 and 4 of ceratal rudiment development show various phases of sensory cell differentiation and suggest the following sequence of events. The first morphological signs of impending sensory cell differentiation are an increased electron-lucency of a cluster of cells within the epithelium and the attachment of one or more centrioles to their apical plasmalemma (Fig. 37 and inset). Subsequently, the nucleus and perinuclear cytoplasm of each cell migrates beneath the basal lamina (Fig. 38). Finally, the cytoplasm remaining within the thickness of the epithelium matures into a dendrite, with longitudinally arrayed microtubules, apical cilia, and mitochondria clustered beneath the ciliary basal bodies, and the subepithelial soma extends an axon. The axons of each cluster of sensory cells remain bound together as they travel toward the anterior margin of the ceratal rudiment.

At the stage of metamorphic competence, the left and right ceratal rudiments form two, prominent conical masses overtop the visceral mass (Fig. 10). As shown in Fig. 39, the epidermis consists of pseudostratified columnar epithelium and a solid mass of subepidermal cells fills the interior. In addition to sensory cells, at least four other cell types have differentiated by this stage: subepidermal muscles (Fig. 40), one or two very large, subepidermal glandular cells with a duct that opens at or near the apex of the ceratal rudiment (Fig. 39), and two types of intraepidermal secretory cells. Many of the subepidermal cells are presumptive muscle cells, as evidenced by isolated clumps of myofilaments within their cytoplasm.

One of the intraepidermal secretory cell types (type A) has a large central vacuole filled with a diffuse flocculence and sometimes concentric lamellae (Figs. 39 and 41). Bundles of microtubules lie adjacent to the limiting membrane of the central vacuole and the cells are innervated (Fig. 41). These characteristics are very similar to the type A secretory cell of the repugnatorial glands of M. leonina, as described in Ch. 4.

The second type of intraepidermal secretory cell type (type B) has a very large Golgi that elaborates many secretory vesicles filled with electron-dense material (Figs. 41 and 42).

2. Pleural/Ceratal (PC) Nerve

The pleural ganglia begin to differentiate sometime between larval hatching and mantle fold retraction. At mantle fold retraction stage, two nerves extend from the right pleural ganglion. As shown diagrammatically in Fig. 43, the larger nerve extends towards the larval kidney complex and terminal intestine, whereas the much smaller nerve, composed of 4 to 6 axons, travels beneath the floor epithelium towards the periphery of the mantle fold. The small nerve is the presumptive PC nerve. The larval kidney nerve and the PC nerve usually leave the pleural ganglion separately, although in one sectioned larva, the PC nerve originated as a branch from the larval kidney nerve shortly after the latter emerged from the right pleural ganglion.

In the 'neck' region of the larva, where the cephalic epidermis meets the floor epithelium of the mantle fold, the small PC nerve is associated with a non-neural supporting cell (Figs. 43 and 44). The supporting cell occurs at the only point where the developing PC nerve must change direction along its trajectory between the pleural ganglion and the presumptive ceratal rudiment (Fig. 43).

Towards the periphery of the PC nerve's trajectory at mantle retraction stage, it is closely associated with the basal lamina of the floor epithelium (Fig. 45). In the two larvae sectioned at this stage, the axon bundle appears to dissipate into slender cytoplasmic processes prior to reaching the thickened epithelium of the presumptive ceratal rudiments. The processes are also associated with the basal lamina of the overlying floor epithelium (Fig. 46). Although small, electron-dense vesicles were occasionally present within axons composing the PC nerve (Fig. 45), no synaptic terminals were identified at any point along

its length at mantle retraction stage. Therefore, the apparent structural dissipation of the distal extremity of the PC nerve may represent growth cone filopodia of the constituent axons.

During the mitotic phase of ceratal rudiment morphogenesis, the number of axons composing the developing PC nerve remains small but three significant changes occur relative to mantle retraction stage: 1) additional, supporting cells become associated with the nerve (Figs. 47A,B, 49, and 51); 2) actual contact between the peripheral segment of the nerve and the overlying basal lamina of the floor epithelium is lost (Fig. 50); and 3) the nerve meets and follows a band of muscle that extends along the anterolateral margin of the proliferating ceratal rudiment (Figs. 51 and 52) and neuromuscular synapses are present (Fig. 52).

The PC nerve remains small during the period of initial sensory cell differentiation within the ceratal rudiments (Fig. 53 and inset). The axons composing the nerve do not appear to travel into the rudiment but remain associated with the muscle around its anterolateral margin (Figs. 53 and 54). Axon fascicles arising from newly differentiated sensory cells within the ceratal rudiment (Figs. 55, 56, and 57) extend to the area where the PC nerve innervates the basal muscle fibres (Fig. 54). The method of section preparation did not permit the sensory cell axons to be followed beyond their merger with the PC nerve. However, the number of axons within the PC nerve appeared approximately the same in stages sectioned before and after onset of ceratal sensory cell differentiation (compare Figs. 47A,B and 48 with Fig. 53 and inset), suggesting that primary sensory axons do not project back to the pleural ganglion at this stage of development.

During the final phase of cellular differentiation leading to the complete, premetamorphic development of the ceratal rudiments, the number of axons within the PC

nerve increases tremendously (Fig. 58). I made no attempt to determine the source or targets of individual axons within this large nerve.

Figure 59 shows the right PC nerve in a post-larva of M. leonina at approximately 48 hours after shell loss. After leaving the fused cerebropleural ganglion, the nerve bifurcates; the smaller branch extends to the body wall immediately anterior to the ceras and the larger branch extends into the ceras. This figure is referred to again in the Discussion.

DISCUSSION

A. Larval and Metamorphic Development

Although the developmental events that occur during the larval stage of M. leonina are similar in kind and sequence to those of other opisthobranchs, three unusual features occur: the absence of radular teeth, the appearance of presumptive oral hood tissue, and the precocious development of the primary cerata.

The almost complete omission of the radula - odontophore complex from the sequence of developmental events in M. leonina eliminates an unnecessary energy expenditure as this structure has no larval function and is not required for food capture or ingestion in the adult. However, the small size of newly metamorphosed nudibranchs may preclude feeding on the same type of prey or in the same manner as the adults of their species. At least one species of nudibranch utilizes its radula to graze on an organic surface film until sufficiently large enough to exploit the preferred prey of the adult stage (Perron and Turner, 1977). Juveniles of M. leonina cannot employ this type of interim feeding due to the lack of a radula. Instead, metamorphosis in M. leonina involves rapid differentiation of the oral hood, thereby permitting young juveniles to capture small prey in a manner similar to that employed by the adult. Selective pressures acting to promote the rapid formation of the oral hood during metamorphosis may have resulted in the preliminary development of this structure during the final part of the larval stage.

Hypertrophy of the larval cephalic epidermis has not been noted in premetamorphic veligers of dorid nudibranchs, which tend to lack a large oral veil over the mouth, but is shown in drawings by Thompson (1962) of premetamorphic veligers of Tritonia hombergi (Dendronotacea) and by Tardy (1970) of Aeolidiella alderi (Aeolidacea). The juveniles and adults of both these species have a prominent oral veil that is derived from this hypertrophied cephalic tissue. These observations confirm that the oral hood of M. leonina and the oral veil of other nudibranchs are homologous structures.

The appearance of ceratal rudiments in the larval stage of nudibranchs has not been reported previously, although many aeolids and dendronotids have been reared in the laboratory. It has been suggested that the cerata of nudibranchs provide an increased surface area for gas exchange with the environment (see Morton, 1958). This hypothesis is strengthened by the fact that the metabolically active digestive gland often extends into the cerata. Ajeska and Nybakken (1976) found that oxygen consumption/gm body weight was an inverse function of animal size in M. leonina. They suggested that the higher metabolic rate of young juveniles reflects the fact that they must actively seek-out their benthic prey, whereas larger animals simply extend their hood into the surrounding waters to intercept passing zooplankton. Of the 6 species of newly metamorphosed opisthobranchs that I have observed, young juveniles of M. leonina are by far the most active; the others tend to be sluggish grazers on the prey organism that induced their metamorphosis. Together, these observations suggest that the development of ceratal rudiments during the larval stage of M. leonina and their rapid expansion and invasion by the left and right digestive glands during metamorphosis may be neccessary to sustain a high oxygen demand resulting from an active juvenile life style.

I will comment on additional aspects of ceratal rudiment morphogenesis in section B of this discussion.

My study of larval development and metamorphosis of M. leonina provides the second histological description of gut metamorphosis in a planktotrophic nudibranch veliger. As in the dorid nudibranch, Doridella steinbergae (Bickell et al., 1981), the morphologically complex stomach of M. leonina veligers is transformed to the post-metamorphic stomach by dissociation of the cells composing the ciliated band (style sac) and loss of the gastric shield. In Doridella steinbergae, Bickell et al. (1981) speculated that the gastric shield was lost by dissociation of the underlying cells. Observations made in the present study

indicate that the gastric shield is simply sloughed from the gut wall; the underlying cells are retained and subsequently secrete a portion of the cuticle that lines the stomach of the postmetamorhic stage.

The stomach of M. leonina does not undergo additional torsional displacement during metamorphosis, as observed in D. steinbergae (Bickell et al., 1981), nor does it exhibit complete detorsion, as described for the aeolid nudibranch Phestilla sibogae (Bonar and Hadfield, 1974). In M. leonina, the dorso-lateral position of the anus and the fact that the intestine emerges from the dorsal aspect of the stomach are postmetamorphic vestiges of the torted larval digestive tract.

Larval settlement and metamorphosis has been observed in three species of dendronotid nudibranchs. Tritonia hombergi is typical of many opisthobranchs (see Hadfield, 1978) in that metamorphosis will occur only in the presence of its postmetamorphic prey, Alcyonium digitatum (Thompson, 1962). Larval metamorphosis of Tritonia diomedea is promoted by the preferred pennatulacean prey of the adults, but will also occur without this external inducer. Kempf and Willows (1977) suggested that the absence of absolute dependence on an external metamorphic trigger in T. diomedea may relate to the fact that adults will also feed on several other pennatulaceans. In M. leonina, the presence of a substratum appears to be the only requirement for the onset of larval settlement and metamorphosis. The prey of young juveniles (which were benthic ciliates and crustacean nauplii in this study and benthic crustaceans and bivalve spat in the field study of Ajeska and Nybakken, 1976) probably occur ubiquitously on marine substrates, and the zooplanktonic prey of larger juveniles and adults is continuously transported through coastal waters. Therefore, the need for specific metamorphic induction to ensure a benthic food source (Thompson, 1964; Todd, 1981) seems unnecessary in this species.

Despite the apparent absence of environmental induction of metamorphosis, populations of M. leonina are consistently found in eel grass and kelp beds located in protected waters (Kjerschow-Agersborg, 1923a; Hurst, 1968; Ajeska and Nybakken, 1976). Pelagic individuals of this species, which include the larvae and postmetamorphic animals that have become dislodged from a surface (Hurst, 1968), may become passively concentrated in areas of reduced water flow. The buoyant fronds of eel grass and certain large kelp species that are typical of these locations might be expected to promote the survival of M. leonina because the plants provide a submerged, tidally adjusting substratum (M. leonina cannot withstand atmospheric exposure) that is suspended within the upper levels of the water column where the flow of plankton-carrying currents is greatest.

B. Morphogenesis of the Ceratal Rudiments and the Pleural/Ceratal Nerve

1. Ceratal Rudiments

With one exception (Bonar and Hadfield, 1974; Bonar, 1976), previous histological studies of nudibranch development have shown that the larval mantle fold gives rise to the dorsal epidermis of the postmetamorphic stage (Thompson, 1958; 1962; Tardy, 1970; Bickell, 1978; Bickell and Chia, 1979). These studies have not indicated whether the shell-secreting cells of the mantle fold participate in this process. In M. leonina, I have shown degeneration of the shell-secreting cells following mantle retraction.

An unusual feature of the mantle fold hypertrophy process in M. leonina is the conspicuous proliferation of haemocoelic cells beneath the epithelium of the presumptive ceratal rudiments. Previous histological accounts of mantle fold hypertrophy leading to the

formation of the dorsal epidermis in nudibranch larvae describe proliferation and enlargement of mantle fold epithelial cells only. These studies were done on dorid nudibranchs, which lack cerata (Thompson, 1958; Bickell and Chia, 1979), or on species in which cerata begin to develop after metamorphosis (Thompson, 1962; Tardy, 1970). In M. leonina, some of the subepithelial cells are cell bodies of primary sensory cells, others are differentiated muscle fibres, and most of the remainder are presumptive muscle cells. Premetamorphic development of ceratal muscles enables movement of the primary cerata of M. leonina immediately after shell loss. One function of ceratal movements (lateral 'flicks' in response to light touch) in young juveniles is to deflect ciliates and benthic nauplii, which have crawled onto the cerata, to the substrate alongside the foot where they can be captured by a lateral swing of the oral hood (Page; unpublished observations).

Although I cannot speculate on the function of the very large, subepidermal gland cells that differentiate within the primary cerata, the two intraepidermal secretory cells are interesting because of their similarity to the two secretory cell types within the repugnatorial glands of adult M. leonina (see Ch. 4). This is particularly apparent for the type A cells in both the ceratal rudiment and the mature repugnatorial gland. Although the type B cell of the ceratal rudiment lacks the ordered, parallel lamellae of rough endoplasmic reticulum and the large central storage vacuole of the type B cell within the repugnatorial gland, both have a similar elaborate Golgi and a highly electron-dense secretory product. The types A and B secretory cells in both the ceratal rudiments and the mature repugnatorial gland are innervated.

The possibility that the intraepidermal secretory cells in the ceratal rudiments are preliminary components of the repugnatorial glands has two implications: 1) the benthic stage of M. leonina has a chemical defense system even from the time of shell loss, and 2) defensive chemical in M. leonina is obtained by de novo synthesis, not from prey-derived

metabolites as occurs in most other nudibranchs (see reviews by Schulte and Scheuer [1982] and Faulkner and Ghiselin [1983]; for exceptions see Cimino et al. [1983; 1985] and Gustafson and Andersen [1985]).

2. Pleural/Ceratal (PC) Nerve

My observations on the development of the right PC nerve show that the proximal portion is formed initially by a small group of axons extending from the right pleural ganglion, rather than by ingrowing axons of peripheral sensory cells. Sections through the presumptive PC nerve at mantle retraction stage show structural connection with the pleural ganglion but not with the epithelial cells of the presumptive ceratal rudiment, and sensory cells within the presumptive ceratal rudiments do not begin to differentiate until 1 to 2 weeks (under laboratory culture conditions) after the proximal portion of the PC nerve tract has formed. Appearance of additional axons within the PC nerve does not become marked until after the onset of sensory cell differentiation within the presumptive ceratal rudiment.

It is instructive to compare my preliminary observations on peripheral nerve development in M. leonina to those obtained from studies on insect neurogenesis. Recently, insect model systems have yielded detailed and impressive information about neuronal development because differentiating neurons can be individually identified at many stages of their development, and the preparations are amenable to various cell marking techniques and to experimental manipulations.

In 1976, C.M. Bate showed that certain peripheral nerves of the antenna and thoracic limb buds of a grasshopper (Locusta migratoria) embryo are established initially by the ingrowing axons of one (limb bud) or two (antennae) pairs of sensory neurons that differentiate from the ectodermal epithelium near the distal tip of these embryonic appendages. The axons of these so-called pioneer neurons, a term originally coined by

Ross Harrison (1910) during his observations of regenerating axons in frogs, are subsequently followed to the central ganglia by axons of later differentiating sensory neurons within the epidermis of the appendage. Bate's (1976) observations on peripheral nerve formation by pioneering axons of peripheral sensory cells have been confirmed and extended in antennae (Ho and Goodman, 1982; Berlot and Goodman, 1984), limb buds (Keshishian, 1980; Bentley and Keshishian, 1982; Ho and Goodman, 1982; Bentley and Caudy, 1983; Caudy and Bentley, 1986a; b), and cerci (Shankland and Bentley, 1983) of the grasshopper embryo, the cerci of cricket embryos (Edwards and Chen, 1979; Edwards, 1982), and the imaginal wing disc of Drosophila (Murray et al., 1984). Similarly, in the freshwater crustacean Daphnia magna, the optic nerve connecting the retina of the eye with the optic lamina of the optic ganglion is pioneered by a pair of early differentiating axons from retinal photoreceptors, which are followed by axons of later differentiating photoreceptors (detailed description given in review by Flaster et al., 1982).

Other studies on the grasshopper embryo have shown that initial fibre tracts within the CNS are also established by axons of pioneering neurons (see reviews by Goodman et al., 1984; Bastiani et al., 1985). Furthermore, some peripheral fibre tracts in grasshoppers are pioneered by outgrowing axons of centrally located motoneurons, rather than ingrowing axons of peripheral sensory neurons (Ho and Goodman, 1982). This appears to be the case for the pioneering axons that form the proximal segment of the PC nerve in M. leonina, because their peripheral target is the muscle band along the anterolateral border of the developing ceratal rudiment.

Pioneering axons in both the CNS and periphery of insects often follow a circuitous, yet stereotyped route before reaching their target. This suggests that axonal growth cones are guided by extrinsic cues within the local environment through which they navigate, rather than by a chemical attractant diffusing from their targets. Indeed, pioneering growth

cones follow their normal pathways in surgically isolated antennae and limb buds of grasshoppers (Berlot and Goodman, 1984) and imaginal wing discs of Drosophila (Blair and Palka, 1985; Blair et al., 1985). Extensive testing of this hypothesis has led to the notion that axonal growth cones follow a labelled pathway that consists of a chronological sequence of recognition events between growth cone filopodia and surface molecules located on cellular or extracellular components in the embryonic environment. For example, research reviewed by Bastiani et al. (1985) indicates that the formation of the first three axon fascicles in the ventral nerve cord of grasshopper embryos involves seven key choices by seven pioneer axons. The choices provide examples of recognition events between pioneering axonal growth cones and basement membrane, a glial cell, and other axons.

In the grasshopper leg, Bentley and Keshishian (1982) initially proposed that three 'guidepost cells', distributed at intervals within the limb bud, provide the only cues directing the axonal growth cones of pioneering sensory axons. The guidepost cells are immature neurons and their recognition by pioneering sensory axons appears to be another example of a labelled pathways phenomenon. However, subsequent studies on grasshopper antennae and legs suggested that directed extension of pioneering axons within the distal portion of the appendage may be guided also by directional information encoded on the epithelium or basal lamina of the developing appendage, probably as a gradient of substrate adhesiveness (Bentley and Caudy, 1983a; Berlot and Goodman, 1984). Detailed studies by Caudy and Bentley (1986a; b) confirmed this notion but the authors found evidence that the guidpost cells manifest an attraction for growth cone filopodia that dominates over that of the epithelial basal lamina. Although the two distal guidepost cells may not be necessary for correct routing of pioneering sensory neurons, the most proximal guidepost cell is manditory (Bentley and Caudy, 1983b).

Research on peripheral nerve development within the imaginal wing discs of the moth, Manduca sexta also suggests that an adhesive gradient expressed on the basal lamina of the wing disc epithelium may assist in guiding the growth cones of peripheral sensory cells (Nardi, 1983). However, neither proximo-distal epithelial gradients nor guidepost cells are necessary to orient the pioneering growth cones of sensory axons in Drosophila imaginal wing discs (Blair and Palka, 1985; Blair et al., 1985). The guidance mechanism that establishes these neural pathways remains unknown.

Researchers studying insect model systems have been able to test their hypotheses about axonal guidance by experimental manipulation, usually in the form of selective cell ablation. Nevertheless, purely descriptive studies of other preparations have suggested mechanisms of peripheral nerve formation similar in principle to those elucidated in insects. Recently, Eisen et al. (1986) and Myers et al. (1986) have been able to individually identify several motoneurons in the spinal cord of embryonic zebrafish (Brachydanio rerio) for which the entire process of axonogenesis can be watched directly in living embryos. Their descriptive observations "strongly suggest that the primary motor growth cones are seeking and using cues in the environment as they grow to their targets". The authors suspect that these cues reside on certain connective tissue structures, the horizontal septum and the myosepta, within the environment navigated by the pioneering growth cones.

In my descriptive study of PC nerve development in M. leonina, I noted a close association between the initial bundle of outgrowing axons (at mantle retraction stage) and a supporting cell in the 'neck' region of the larva, where the nerve must change direction to proceed to the presumptive ceratal rudiment. A second association was noted between the peripheral extremity of the axon bundle and the basal lamina of the overlying mantle floor epithelium. I propose that the supporting cell in the neck region may act as a

guidepost cell for the pioneering axons of the PC nerve, and the basal lamina of the floor epithelium may provide subsequent directional cues.

The peripheral target for the outgrowing pioneer axons of the PC nerve is the muscle band extending around the anterolateral margin of the presumptive ceratal rudiment. This muscle was not recognized in sections through larvae at mantle retraction stage. Possibly, the outgrowing pioneer axons recognize progenitor cells of this muscle, with the subsequent interaction resulting in differentiation of the muscle cells and synapse formation by the axons. In the grasshopper embryo, muscle progenitor cells provide guidance cues for the outgrowing axons of their innervating motoneurons (Ball et al., 1985), and the crucial influence of exploratory nerve fibres on muscle differentiation has be documented in vertebrates (see Filogamo, 1981).

In the metamorphically competent larva of M. leonina, the ceratal tissues and the PC nerve are crowded together due to the preceding period of rapid tissue growth within the cramped confines of the larval shell. However, when the haemocoel of the post-larva expands after metamorphic shell loss, it is clear that the PC nerve bifurcates into two branches as it approaches the ceras (Fig. 59). The smaller of the two branches extends to the body wall immediately anterior to the ceras. I propose that this branch, along with the proximal segment of the PC nerve, is the fibre tract pioneereed by the outgrowing motoneurons from the pleural ganglion at mantle retraction stage.

The motoneuron axons that pioneer the proximal segment of the PC nerve, and presumably the small branch to the dorsal body wall anterior to the ceras, do not appear to extend past their muscle target, at least until sometime into the cellular differentiation phase of ceratal rudiment morphogenesis. Instead, these early motoneurons are met at the base of the enlarging ceratal rudiment by ingrowing axon fascicles from peripheral sensory cell clusters. These initial sensory axon fascicles may erect a framework for the

later establishment of nerve fibre tracts within the ceras; providing a guidance substrate for ingrowing axons of later differentiating sensory cells and possibly for outgrowing motor axons arriving along the PC nerve. My observations suggest that the larger branch of the PC nerve, which extends into the ceras (Fig. 59), is pioneered by ingrowing axons of peripheral, ceratal sensory cells that unite with the previously established fibre tract pioneered by outgrowing motoneurons from the pleural ganglion. This hypothesis requires further investigation.

In summary, my morphological evidence suggests that only the pleural component of the PC nerve is pioneered by outgrowing central motoneurons within the pleural ganglion, whereas the ceratal component is pioneered by ingrowing axons of ceratal sensory cells. It might be expected that the latter process is repeated each time a ceras is regenerated after ceratal autotomy.

LITERATURE CITED

Ajeska, R.A., and J.W. Nybakken. 1976. Contributions to the biology of Melibe leonina (Gould, 1852) (Mollusca: Opisthobranchia). Veliger 19: 19-26.

Ball, E.E., R.K. Ho, and C.S. Goodman. 1985. Development of neuromuscular specificity in the grasshopper embryo: guidance of motoneuron growth cones by muscle pioneers. J. Neurosci. 5: 1808-1819.

Barker, D.L., R.G. Wong, and S.B. Kater. 1982. Separate factors produced by the CNS of the snail Heliosoma stimulate neurite outgrowth and choline metabolism in cultured neurons. J. Neurosci. Res. 8: 419-432.

Bastiani, M.J., C.Q. Doe, S.L. Helfand, and C.S. Goodman. 1985. Neuronal specificity and growth cone guidance in grasshopper and Drosophila embryos. Trends Neurosci. 8: 257-266.

Bate, C.M. 1976. Pioneer neurones in an insect embryo. Nature (Lond.) 260: 54-55.

Bentley, D., and M. Caudy. 1983a. Navigational substrates for peripheral pioneer growth cones: limb-axis polarity cues, limb-segment boundaries, and guidepost neurons. Cold Spring Harbor Symp. quant. Biol. 48: 573-585.

Bentley, D., and M. Caudy. 1983b. Pioneer axons lose directed growth after selective killing of guidepost cells. Nature (Lond.) 304: 62-65.

Bentley, D., and H. Keshishian. 1982. Pathfinding by peripheral pioneer neurons in grasshoppers. Science 218: 1082-1087.

Berlot, J., and C.S. Goodman. 1984. Guidance of peripheral pioneer neurons in the grasshopper: adhesive heirarchy of epithelial and neuronal surfaces. Science 223: 493-495.

Bickell, L.R. 1978. Larval Development, Metamorphosis, and Juvenile Feeding of Doridella steinbergae (Lance) (Opisthobranchia: Nudibranchia). M.Sc. thesis, University of Alberta. 226 pp.

Bickell, L.R., and F.-S. Chia. 1979. Organogenesis and histogenesis in the planktotrophic veliger of Doridella steinbergae (Opisthobranchia: Nudibranchia). Mar. Biol. 52; 291-313.

Bickell, L.R., F.-S. Chia, and B.J. Crawford. 1981. Morphogenesis of the digestive system during metamorphosis of the nudibranch Doridella steinbergae (Gastropoda): conversion from phytoplanktivore to carnivore. Mar. Biol. 62: 1-16.

Blair, S., and J. Palka. 1985. Axon guidance in cultured wing discs and disc fragments of the Drosophila wing. Dev. Biol. 108: 411-419.

Blair, S., M.A. Murray, and J. Palka. 1985. Axon guidance in cultured epithelial fragments of the Drosophila wing. Nature (Lond.) 315: 406-408.

Bonar, D.B. 1976. Molluscan metamorphosis: a study in tissue transformation. Am. Zool. 16: 573-591.

Bonar, D.B. 1978a. Morphogenesis at metamorphosis in opisthobranch molluscs. Pp. 177-196 in Settlement and Metamorphosis of Marine Invertebrate Larvae, F.-S. Chia and M.E. Rice, eds. Elsevier/North-Holland, New York.

Bonar, D.B. 1978b. Fine structure of muscle insertions on the larval shell and operculum of the nudibranch Phestilla sibogae (Mollusca: Gastropoda) before and during metamorphosis. Tiss. Cell 10: 143-152.

Bonar, D.B., and M.G. Hadfield. 1974. Metamorphosis of the marine gastropod Phestilla sibogae Bergh (Nudibranchia: Aeolidacea). I. Light and electron microscopic analysis of larval and metamorphic stages. J. exp. mar. Biol. Ecol. 16: 227-255.

Bulloch, A.G.M., S.B. Kater, and A.D. Murphy. 1980. Connectivity changes in an isolated molluscan ganglion during in vivo culture. J. Neurobiol. 11: 531-546.

Bulloch, A.G.M., and S.B. Kater. 1981. Selection of a novel connection by adult molluscan neurons. Science 212: 79-80.

Caudy, M., and D. Bentley. 1986a. Pioneer growth cone morphologies reveal proximal increases in substrate affinity within leg segments of grasshopper embryos. J. Neurosci. 6: 364-379.

Caudy, M., and D. Bentley. 1986b. Pioneer growth cone steering along a series of neuronal and non-neuronal cues of different affinities. J. Neurosci. 6: 1781-1795.

Chia, F.-S., and R. Koss. 1978. Development and metamorphosis of the planktotrophic larvae of Rostanga pulchra (Mollusca: Nudibranchia). Mar. Biol. 46: 109-119.

Chia, F.-S., and R. Koss. 1982. Fine structure of the larval rhinophores of the nudibranch, Rostanga pulchra, with emphasis on the sensory receptor cells. Cell Tiss. Res. 225: 235-248.

Cimino, G., S. de Rosa, S. de Stefano, G. Sodano, and G. Villani. 1983. Dorid nudibranch elaborates its own chemical defense. Science 219: 1237-1238.

Cimino, G., S. de Rosa, S. de Stdfano, R. Morrona, and G. Sodano. 1985. The chemical defense of nudibranch molluscs. Tetrahedron 41: 1093-1100.

Cloney, R.A., and E. Florey. 1968. Ultrastructure of cephalopod chromatophore organs. Z. Zellforsch. mikrosk. Anat. 89: 250-280.

Edwards, J.S. 1982. Pioneer fibers. The case for guidance in the embryonic nervous system of the cricket. Pp. 255-266 in Current Topics in Neurobiology. Neuronal Development, N.C. Spitzer, ed. Plenum Press, New York.

Edwards, J.S., and S.-W. Chen. 1979. Embryonic development of an insect sensory system, the abdominal cerci of Acheta domesticus. Wilhelm Roux's Arch. 186: 151-178.

Eisen, J.S., P.Z. Myers, and M. Westerfield. 1986. Pathway selection by growth cones of identified motoneurons in live zebrafish embryos. Nature (Lond.) 320: 269-271.

Faulkner, D.J., and M.T. Ghiselin. 1983. Chemical defense and evolutionary ecology of dorid nudibranchs and some other opisthobranch gastropods. Mar. Ecol. Prog. Ser. 13: 295-301.

Filogamo, G. 1981. The first stage in myoblast development: skeletal muscles, myocardium, and iris. Pp. 171-187 in Studies in Developmental Biology, Essays in Honor of Viktor Hamburger, W.M. Cowan, ed. Oxford University Press, New York and Oxford.

Flaster, M.S., E.R. Macagno, and R.S. Schehr. 1982. Mechanisms for the formation of synaptic connections in the isogenic nervous system of Daphnia magna. Pp. 267-296 in Current Topics in Neurobiology. Neuronal Development, N.C. Spitzer, ed. Plenum Press, New York.

Fretter, V. 1969. Aspects of metamorphosis in prosobranch gastropods. Proc. Malacol. Soc. Lond. 38: 375-386.

Ghiselin, M.T. 1965. Reproductive function and the phylogeny of opisthobranch gastropods. Malacologia 3: 327-378.

Goodman, C.S., M.J. Bastiani, C.Q. Doe, S. duLac, S.L. Helfand, J.Y. Kuwada, and J.B. Thomas. 1984. Cell recognition during neuronal development. Science 225: 1271-1279.

Gustafson, K., and R.J. Anderson, 1985. Chemical studies of British Columbian nudibranchs. Tetrahedron 41: 1101-1108.

Hadfield, M.G. 1978. Metamorphosis in marine molluscan larvae: an analysis of stimulus and response. Pp. 165-175 in Settlement and Metamorphosis of Marine Invertebrate Larvae, F.S. Chia and M.E. Rice, eds. Elsevier/North Holland, New York.

Hadley, R.D., R.G. Wong, S.B. Kater, D.L. Barker, and A.G.M. Bulloch. 1982. Formation of novel central and peripheral connections between molluscan central neurons in organ cultured ganglia. J. Neurobiol. 13: 217-230.

Harrison, R. 1910. The outgrowth of the nerve fiber as a mode of protoplasmic movement. J. exp. Zool. 9: 787-846.

Ho, R.K., and C.S. Goodman. 1982. Peripheral pathways are pioneered by an array of central and peripheral neurones in grasshopper embryos. Nature (Lond.) 297: 404-406.

Hurst, A. 1968. The feeding mechanism and behavior of the opisthobranch Melibe leonina. Symp. zool. Soc. Lond. 22: 151-166.

Jacob, M.H. 1984. Neurogenesis in Aplysia californica resembles nervous system formation in vertebrates. J. Neurosci. 4: 1225-1239.

Kandel, E.R. 1976. Cellular Basis of Behavior. Freeman, San Fransisco, 727 pp.

Kandel, E.R. 1979. Behavioral Biology of Aplysia: a contribution to the comparative study of opisthobranch molluscs. W.H. Freeman, San Fransisco, 463 pp.

Kater, S.B., C.B. Heyer, and C.R.S. Kaneko. 1975. Identifiable neurons and invertebrate behavior. Pp. 1-51 in Neurophysiology (Physiology, Series 1, vol.3, MTP Internat. Rev. Sci.) Butterworths, London.

Kempf, S.C. 1982. Acquisition, Storage and Utilization of Nutrients by the Embryos and Larvae of Opisthobranch Molluscs. Ph.D. dissertation, University of Hawaii, 287 pp.

Kempf, S.C., B. Masinovsky, and A.O.D. Willows. 1987. A simple neuronal system characterized by a monoclonal antibody to SCP neuropeptides in embryos and larvae of Tritonia diomedea (Gastropoda, Nudibranchia). J. Neurobiol. 18: 217-236.

Kempf, S.C., and A.O.D. Willows. 1977. Laboratory culture of the nudibranch Tritonia diomedea Bergh (Tritonidae: Opisthobranchia) and some aspects of its behavioral development. J. exp. mar. Biol. Ecol. 30: 261-276.

Keshishian, H. 1980. The origin and morphogenesis of pioneer neurons in the grasshopper metathoracic leg. Dev. Biol. 80: 388-397.

Kjerschow-Agersborg, H.P. von Wold. 1923a. A critique on Professor Harold Heath's Chioraera dalli, with special reference to the use of the foot in the nudibranchiate mollusk, Melibe leonina Gould. Nautilus 36: 86-96.

Kjerschow-Agersborg, H.P. von Wold. 1923b. The morphology of the nudibranchiate mollusk Melibe (syn. Chioraera) leonina (Gould). Quart. J. microsc. Sci. 67: 507-592.

Kriegstein, A.R. 1977a. Development of the nervous system of Aplysia californica. Proc. nat. Acad. Sci. 74: 375-378.

Kriegstein, A.R. 1977b. Stages in the post-hatching development of Aplysia californica. J. exp. Zool. 199: 275-288.

Luft, J.H. 1961. Improvements in epoxy resin embedding methods. J. biophys. biochem. Cytol. 9: 409-414.

Morton, J.E. 1958. Molluscs: An Introduction to Their Form and Function. Harper and Bros., New York. 232 pp.

Morton, J.E. 1963. The molluscan pattern: evolutionary trends in a modern classification. Proc. Linn. Soc., Lond. 174: 53-72.

Murphy, A.D., and Kater, S.B. 1978. Specific reinnervation of a target organ by a pair of identified molluscan neurons. Brain Res. 156: 322-328.

Murphy, A.D., and S.B. Kater. 1980. Sprouting and functional regeneration of an identified neuron in Heliosoma. Brain Res. 186: 251-272.

Murray, M.A., M. Schubinger, and J. Palka. 1984. Neuron differentiation and axon growth in the developing wing of Drosophila melanogaster. Dev. Biol. 104: 259-273.

Myers, P.Z., J.S. Eisen, and M. Westerfield. 1986. Development and axonal outgrowth of identified motoneurons in the zebrafish. J. Neurosci. 6: 2278-2289.

Nardi, J.B. 1983. Neuronal pathfinding in developing wings of the moth Manduca sexta. Dev. Biol. 95: 163-174.

Perron, F.E., and R.D. Turner. 1977. Development, metamorphosis, and natural history of the nudibranch Doridella obscura Verrill (Corambidae: Opisthobranchia). J. exp. mar. Biol. Ecol. 27: 171-185.

Price, C.H. 1977. Regeneration in the central nervous system of a pulmonate mollusc, Melampus. Cell Tiss. Res. 180: 529-536.

Raven, C.P. 1958. Morphogenesis: The Analysis of Molluscan Development. Pergamon Press, New York. 311 pp.

Richardson, K.C., L. Jarrett, and E.H. Finke. 1960. Embedding in epoxy resins for ultrathin sectioning in electron microscopy. Stain Technol. 35: 313-323.

Schacher, W., E.R. Kandel, and R. Woolley. 1979a. Development of neurons in the abdominal ganglion of Aplysia californica. I. Axosomatic synaptic contacts. Dev. Biol. 71: 163-175.

Schacher, W., E.R. Kandel, and R. Woolley. 1979b. Development of neurons in the abdominal ganlgion of Aplysia californica. II. Nonneural support cells. Dev. Biol. 71: 176-190.

Schacher, S. 1985. Differential synapse formation and neurite outgrowth at two branches of the metacerebral cell of Aplysia in dissociated cell culture. J. Neurosci. 5: 2028-2034.

Schulte, G.R., and P.J. Scheuer. 1982. Defensive allomones of some marine mollusks. Tetrahedron 38: 1857-1863.

Shankland, M., and D. Bentley. 1983; Sensory receptor differentiation and axonal pathfinding in the cercus of the grasshopper embryo. Dev. Biol. 97: 468-482.

Switzer-Dunlap, M. 1978. Larval biology and metamorphosis of aplysiid gastropods. Pp. 197-206 in Settlement and Metamorphosis of Marine Invertebrate larvae, F.S. Chia and M.E. Rice, eds. Elsevier/North-Holland, New York.

Switzer-Dunlap, M., and M.G. Hadfield. 1977. Observations on development, larval growth and metamorphosis of four species of Aplysiidae (Gastropoda, Opisthobranchia) in laboratory culture. J. exp. mar. Biol. Ecol. 29: 245-261.

Tardy, J. 1970. Contribution a l'étude des métamorphoses chez les nudibranches. Ann. Sci. nat. Zool. 12: 299-370.

Thiriot-Quiévreux, C. 1970. Transformations histologiques lors de la métamorphose chez Cymbulia peroni de Blainville (Mollusca: Opisthobranchia). Z. Morphol. Tiere 67: 106-117.

Thiriot-Quiévreux, C. 1977. Véligère planctotrophe du doridien Aegires punctilucens (D'Orbigny) (Mollusca: Nudibranchia: Notodorididae): description et métamorphose. J. exp. mar. Biol. Ecol. 26: 177-196.

Thompson, T.E., 1958. The natural history, embryology, larval biology, and post-larval development of Adalaria proxima (Alder and Hancock) (Gastropoda, Opisthobranchia). Phil. Trans. roy. Soc. Lond. B242: 1-57.

Thompson, T.E., 1959. Feeding in nudibranch larvae. J. mar. biol. Assoc. U.K. 38: 239-248.

Thompson, T.E., 1962. Studies on the ontogeny of Tritonia hombergi Cuvier (Gastropoda, Opisthobranchia). Phil. Trans. roy. Soc. Lond. B245: 171-281.

Thompson, T.E., 1964. Grazing and the life cycles of British nudibranchs. Pp. 275-297 in Grazing in Terrestrial and Marine Environments. D.J. Crisp, ed. Blackwell Scientific Publ., Oxford.

Todd, C.D. 1981. The ecology of nudibranch molluscs. Oceanogr. mar. Biol. Ann. Rev. 19: 141-234.

Wong, R.G., R.D. Hadley, S.B. Kater, and G.C. Hauser. 1981. Neurite outgrowth in molluscan organ and cell cultures: the role of conditioning factor(s). J. Neurosci. 1: 1008-1021.

Figure 1: Juvenile of Melibe leonina at 2.5 months after metamorphosis showing the foot (F), double row of petaloid cerata (C) containing dendritic branches of the digestive gland, and oral hood (OH) surrounding the mouth. The oral hood bears peripheral hood tentacles (HT) and a pair of rhinophores (R) mounted on a rhinophoral process (RP). The arrowhead indicates the position of the anus.

Figure 2: Photomicrograph of a live larva of M. leonina immediately after hatching showing the velum (VE), foot (F), and statocyst (S) of the cephalopedal mass and the stomach (ST), right and left digestive gland (RD and LD, respectively), intestine (I), larval kidney complex (LK), mantle fold (MF), and shell (SH) of the visceropallial mass. The arrowheads indicates a tuft of long, stiff cilia at the apex of the foot.

Figure 3: Photomicrograph of a live larva of M. leonina nearing the stage of metamorphic competence showing the right eye (EY), propodium (P), enlarged stomach (ST), left digestive gland (LD), and the shell (SH), statocyst (S), and velum (VE). The arrowheads indicate the rudiments of the primary cerata.

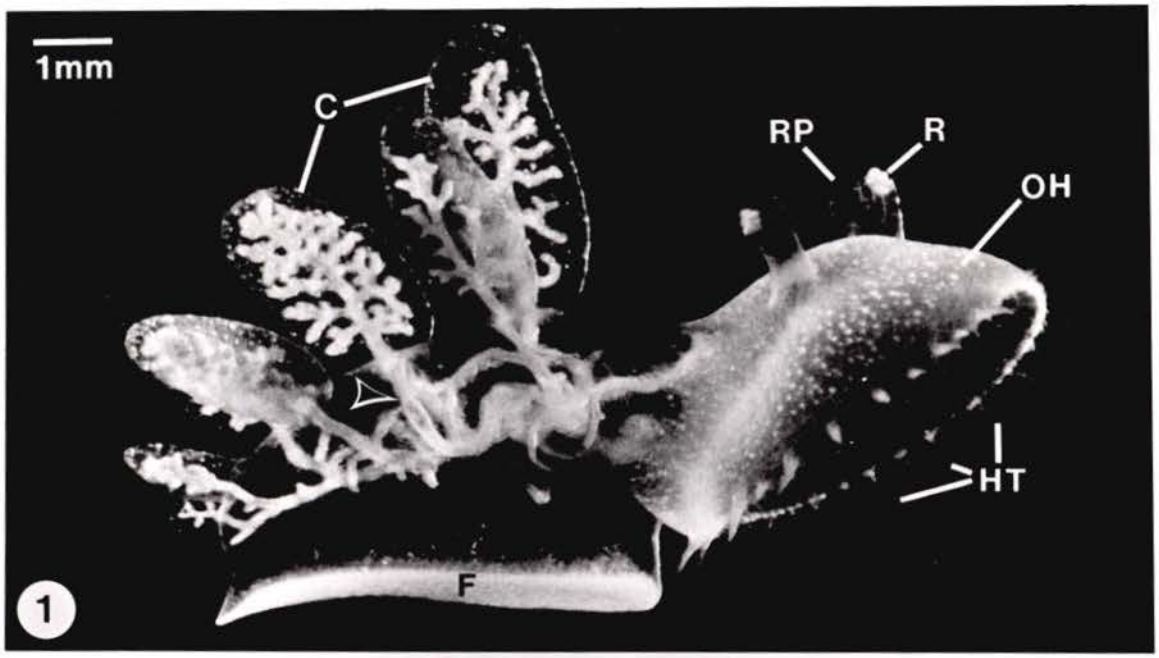
1mm
C
RP
R
OH
HT
F
1

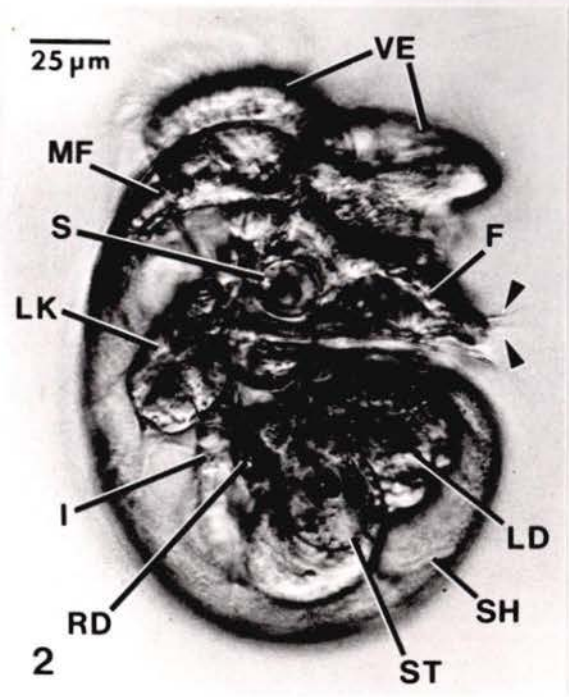
25 µm
VE
MF
S
F
LK
I
LD
RD
SH
ST
2

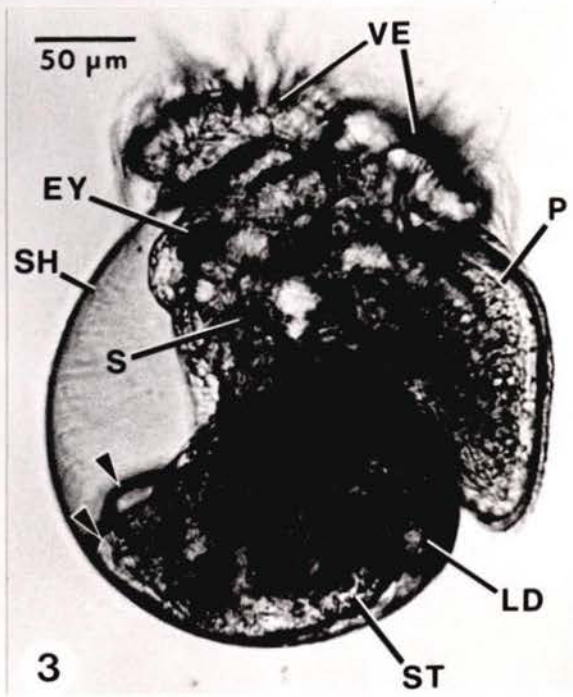
50 µm
VE
EY
P
SH
S
LD
ST
3

Figure 4: Oblique sagittal section of a newly hatched larva of M. leonina that passes through the foot (F), operculum (O), statocyst (S), and velum (VE) of the cephalopedal mass and the stomach (ST), left digestive gland (LD), intestine (I), larval kidney complex (LK), perivisceral epithelium (PV), and mantle fold (MF) of the visceropallial mass. The section shows the vestibule (V) and gastric shield (arrowheads) of the larval stomach.

Figure 5: Frontal section through a newly hatched larva showing the small right and large left digestive gland (RD and LD, respectively) flanking the stomach (ST). Also note the torted intestine (I) that terminates at the anus (A) in the mantle cavity on the right side. MF, mantle fold.

Figure 6: Frontal section through a newly hatched larva showing the sparsely ciliated groove (CIG) and band of dense cilia (arrowheads) within the dorsal part of the larval stomach. Other abbreviations: CG, cerebral ganglion; E, esophagus; I, intestine; N, nephrocyst; and VE, velar lobes.

Figure 7: Detail of the mantle fold on the right side of a newly hatched larva. The mantle fold (MF) is a continuation of the perivisceral epithelium (PV). MC, mantle cavity; VE, velum.

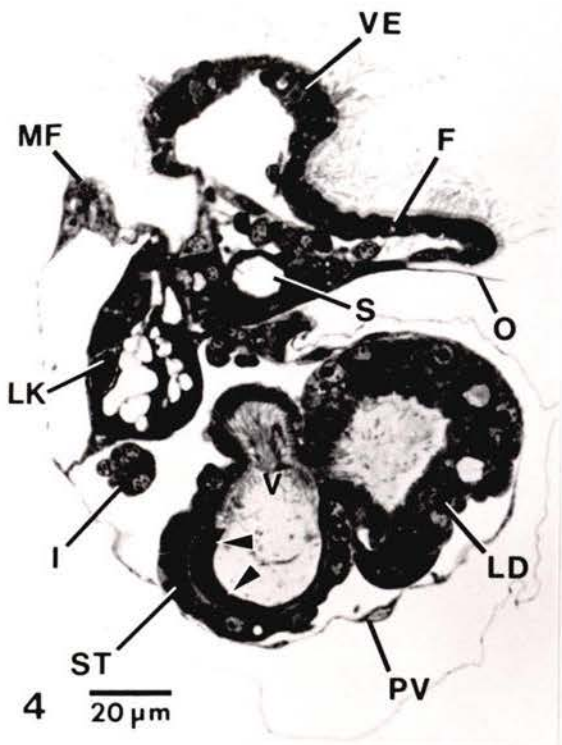
VE
MF
F
S
O
LK
V
I
LD
ST
PV
20 µm

4

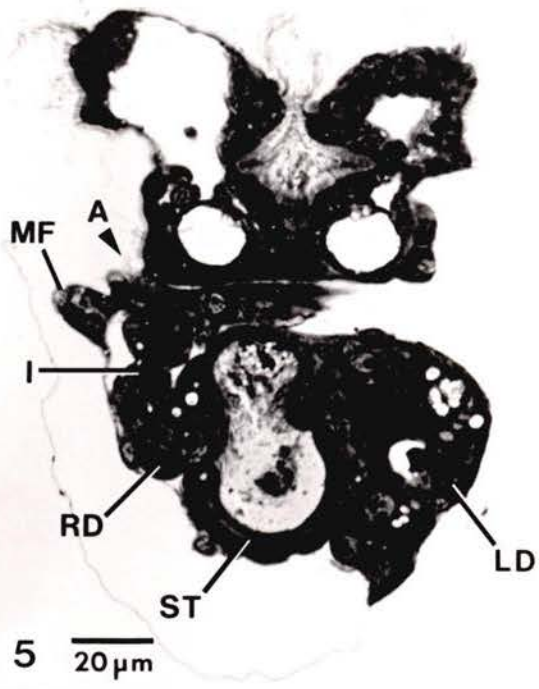
A
MF
I
RD
LD
ST
20 µm

5

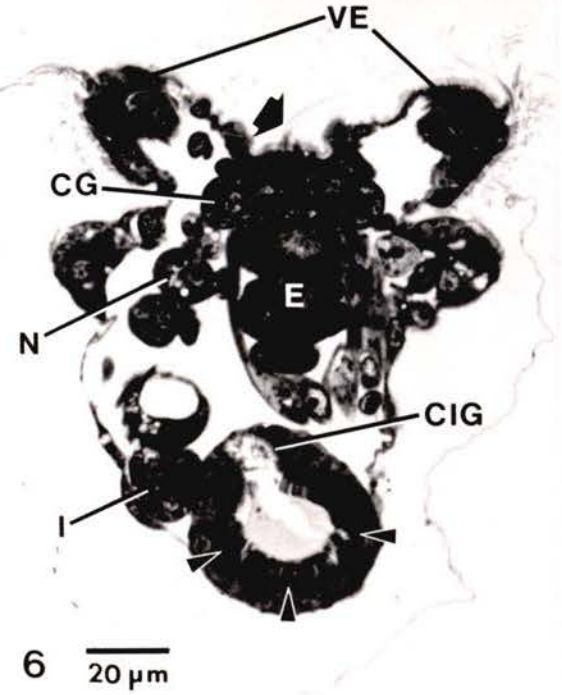
VE
CG
E
N
CIG
I
20 µm

6

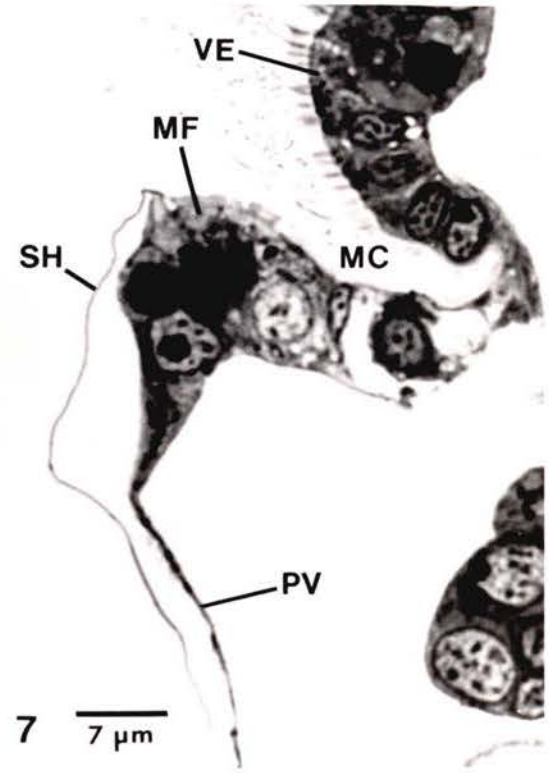
VE
MF
SH
MC
PV
7 µm

7

Figure 8: Growth rate of the shell during the larval development of M. leonina. The points indicate the mean length of a minimum of five larvae and the vertical bars show the standard deviation. Diagrams of the newly hatched stage (a), the mantle retraction stage (b), and the late larval stage (c) correspond in approximate size and age to the sites indicated by arrows on the graph. Abbreviations: C, ceras; CE, hypertrophied cephalic epithelium; EY, eye; F, foot; I, intestine; LD, left digestive gland; MF, mantle fold; P, propodium; S, statocyst; SH, shell; ST, stomach; VE, velum.

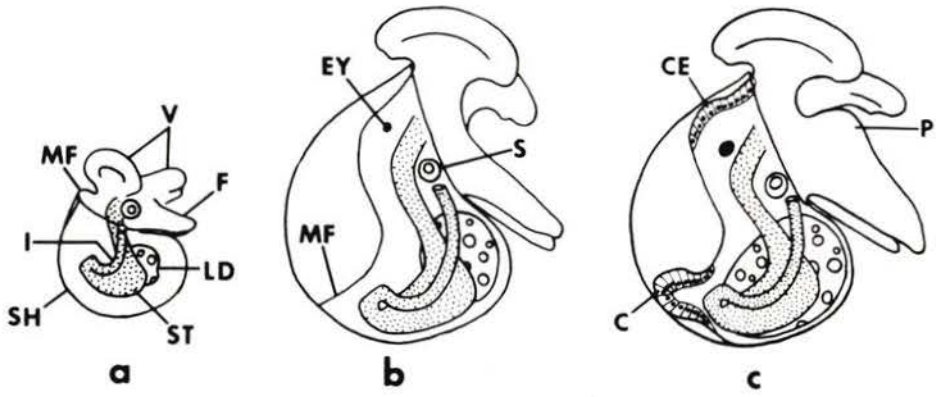
V
MF
F
I
LD
SH
ST
a
EY
S
MF
b
CE
P
C
c

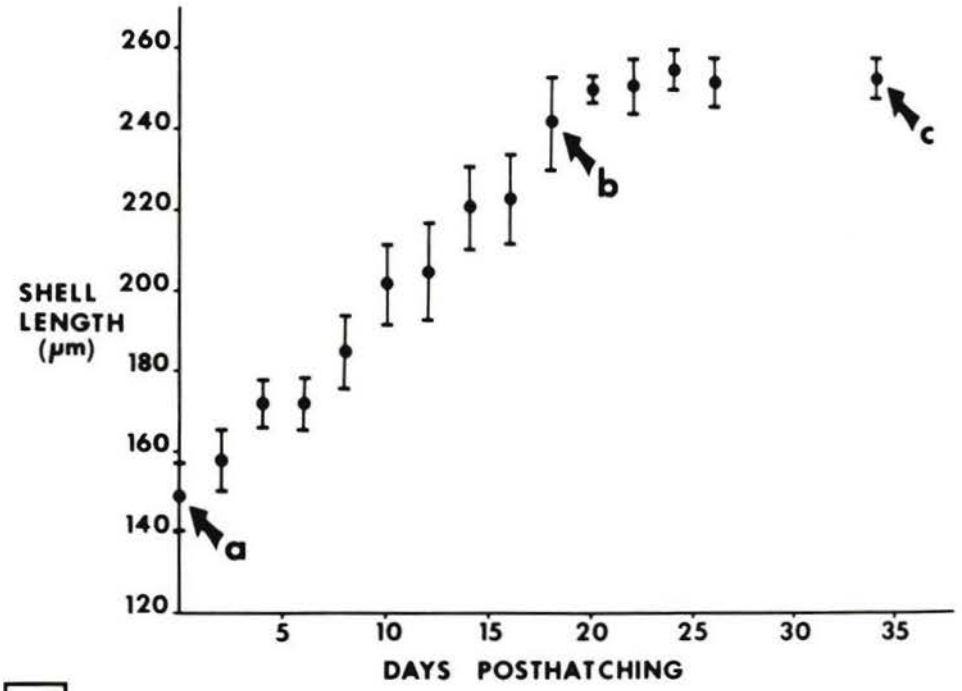
260
240
220
200
180
160
140
120
SHELL LENGTH (μm)
a
b
c
5
10
15
20
25
30
35
DAYS POSTHATCHING

8

Figure 9: Sagittal section through a larva of M. leonina in which the mantle fold (MF) has retracted from the aperture of the shell. Note the eye (EY), statocyst (S), cerebral ganglion (CG), pedal ganglion (PG), and pleural ganglion (PLG) of the larval nervous system and the thin cephalic epithelium (CE), the foot (F), and the gonadal rudiment (G). Other abbreviations: ST, stomach; RD, right digestive gland; and I, intestine.

Figure 10: Sagittal section through a metamorphically competent larva of M. leonina showing the hypertrophied cephalic epithelium (CE), the right ceratal rudiment (C), the propodial swelling (P) on the ventral surface of the foot, the enlarged gonadal rudiment (G), and many large lipid deposits (arrowheads) within the walls of the stomach (ST) and left digestive gland (LD). A vestigial radular rudiment (asterisk) has evaginated from the ventral wall of the esophagus (E) at the level of the cerebral commissure (CC).

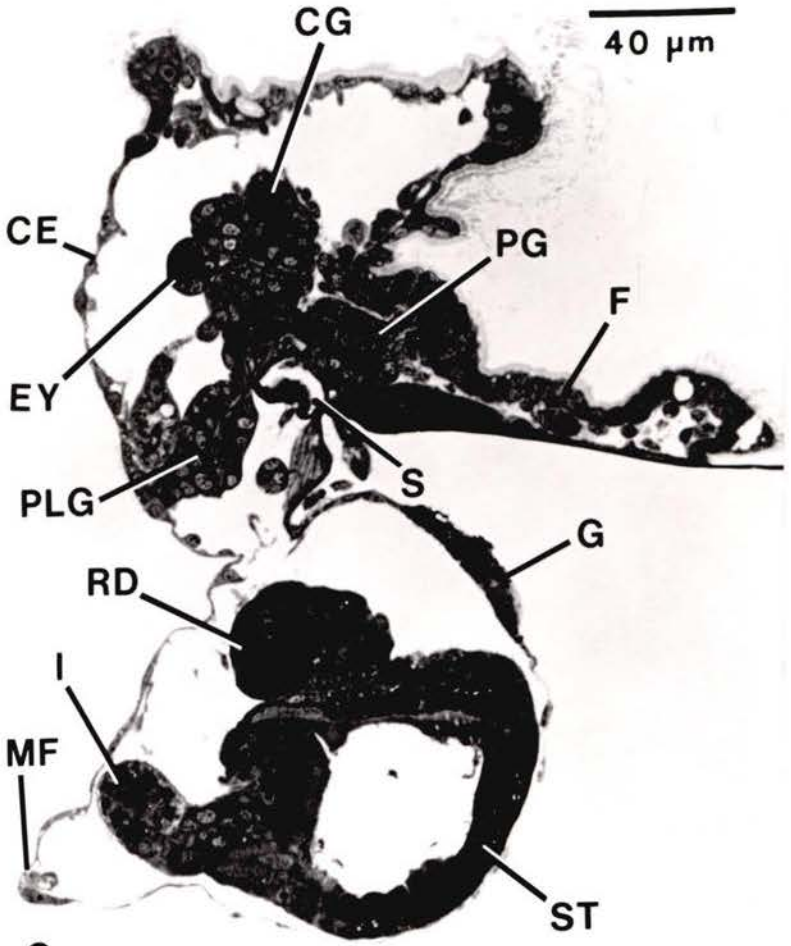

9

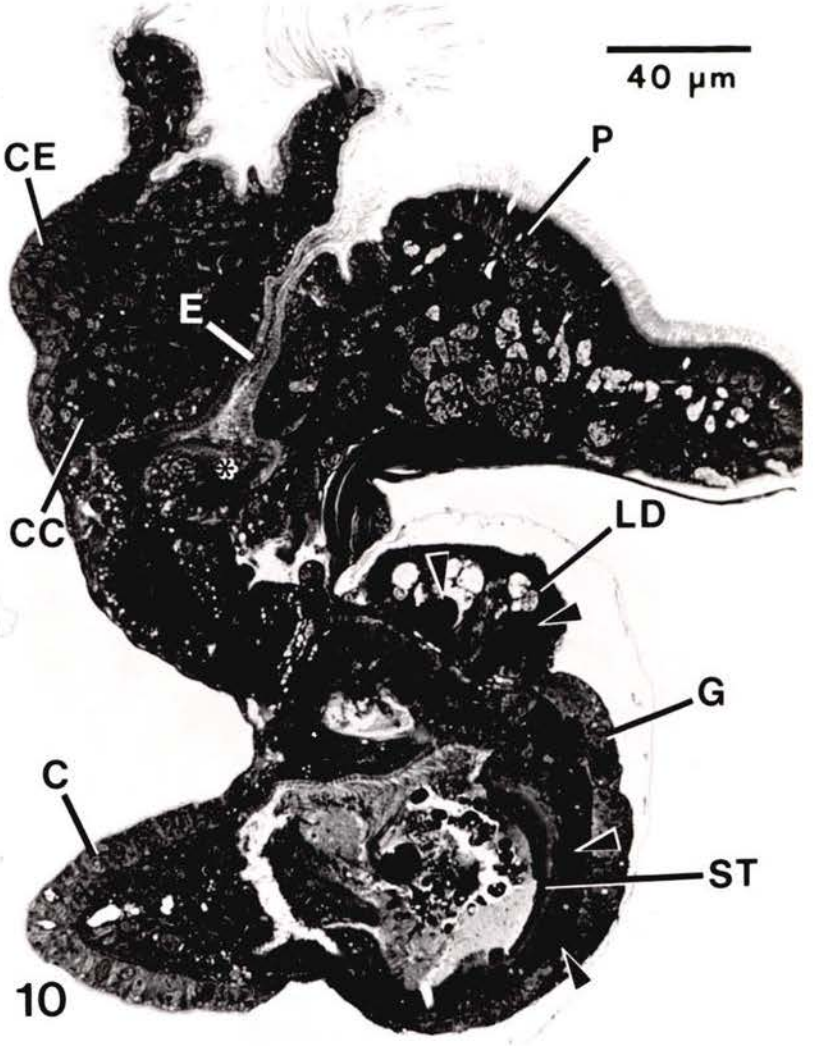

10

Figures 11 to 16: Photomicrographs of a live larva of M. leonina during successive stages of metamorphosis.

Figure 11: Dorsal view of a larva of M. leonina that has settled onto the foot in preparation for metamorphosis. The stomach (ST), left digestive gland (LD) and eyes (EY) are visible through the transparent larval shell (SH). The velar lobes (VE) are retracted but still intact.

Figure 12: Onset of metamorphosis. The slurry of cells indicated by the arrow are dissociated velar cells. Inset: lateral view of a post-larva after loss of the ciliated velar cells.

Figure 13: Post-larva withdrawing the visceral mass from the shell (SH).

Figure 14: Post-larva immediately after shell loss. Note the left ceras (C).

Figure 15: Post-larva at 10 hours after shell loss showing the initial expansion of the cephalic epithelium to form the oral hood (OH). Inset: lateral view of a post-larva showing a ceras (C) and the oral hood (OH).

Figure 16: Post-larva at approximately 36 hours after shell loss showing the cerata (C), the dramatic enlargement of the oral hood (OH), and the buds of the initial hood tentacles (HT). R, rhinophore.

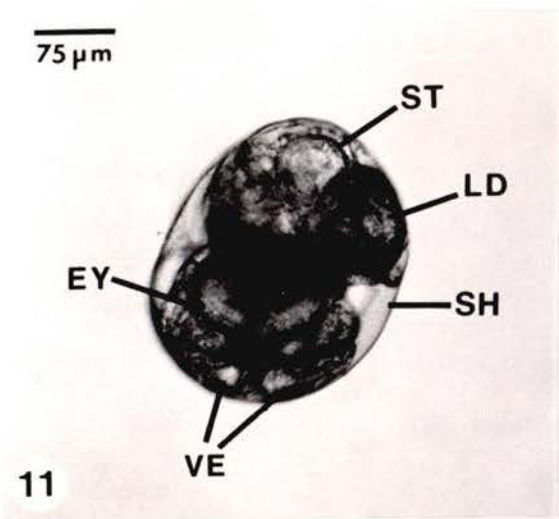

11

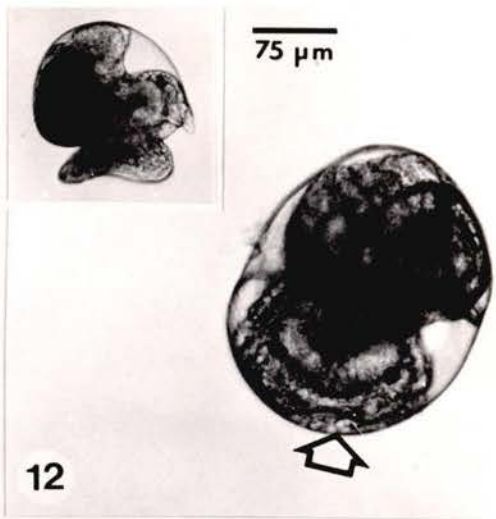

12

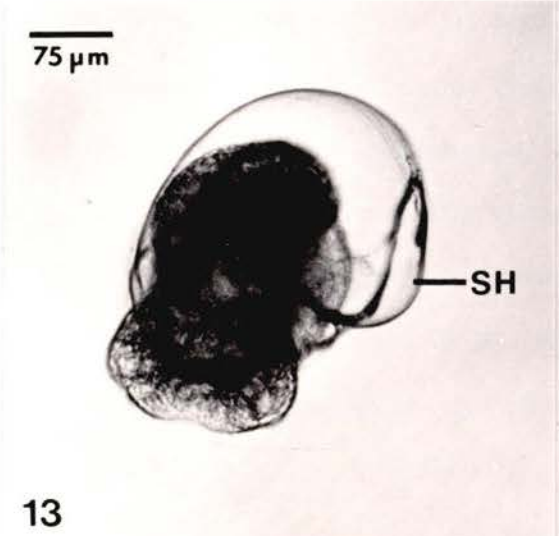

13

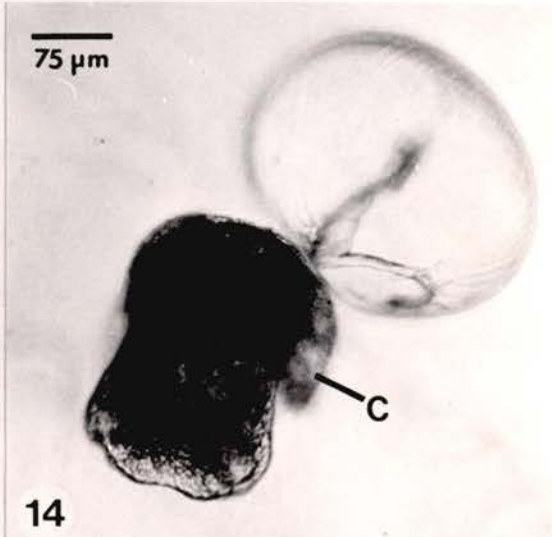

14

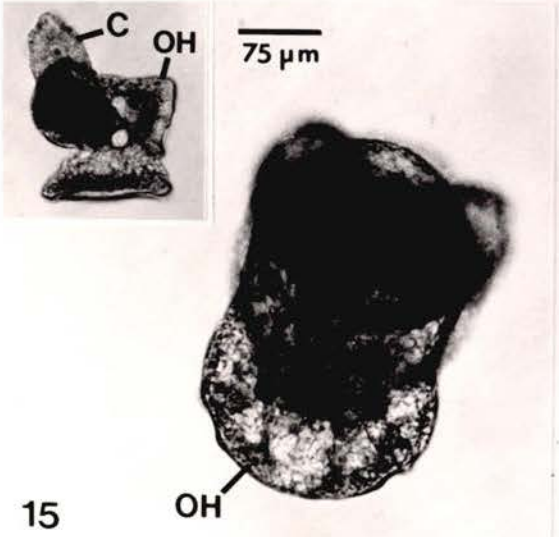

15

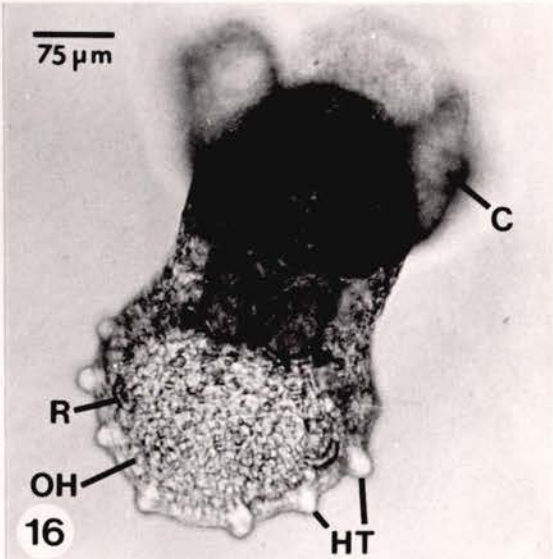

16

Figure 17: Sketches of successive stages during the metamorphosis of M. leonina drawn from reconstructions of serial, one µm sections. Figures 17a to 17c show post-larva at the time of velum loss, and at 5 and 24 hours after shell loss, respectively. These three diagrams illustrate the migratory movements of the hypertrophied mantle fold and cephalic epithelium (the borders of these epithelia are demarcated by broken lines), the invagination of the gonadal rudiment, and the postero-dorsal displacement of the anus. The arrows indicate specific movements of the mantle fold epithelium. Figures 17d to 17g show post-larvae at velum loss, and at 5, 24, and 48 hours after shell loss, respectively. These four diagrams illustrate the size and positional changes undergone by the component organs of the digestive system during metamorphosis. Abbreviations: A, anus; AK, adult kidney rudiment; C, ceras; CE, hypertrophied cephalic epithelium; CG, cerebral ganglion; E, esophagus; EY, eye; F, foot; G, gonadal rudiment; HT, hood tentacle; I, intestine; LD, left digestive gland; LK, larval kidney complex; O, operculum; OH, oral hood; PG, pedal ganglion; R, rhinophore; RD;, right digestive gland; RG, rhinophoral ganglion; S, statocyst; SH, shell; ST, stomach.

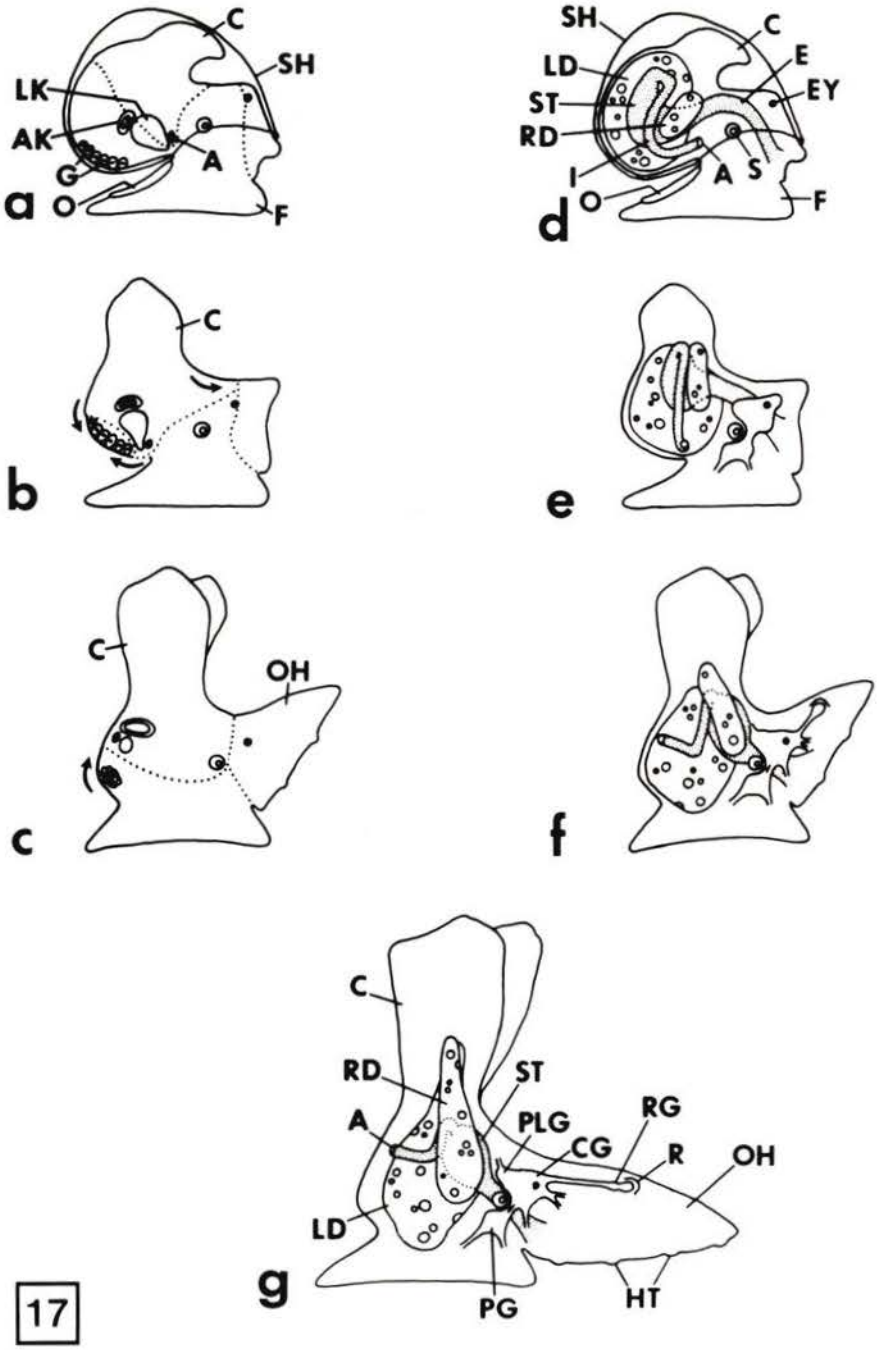
C
SH
LK
AK
G
A
a
O
F
SH
C
E
LD
EY
ST
RD
I
A
S
O
d
F
C
b
e
C
OH
c
f
C
RD
ST
A
PLG
RG
CG
R
OH
LD
g
PG
HT

17

Figure 18: Cross section through the posterior portion of the foot (F) and visceral mass at 5 hours after shell loss. The hypertrophied mantle fold epithelium (arrowheads) has spread over the viceral mass so as to completely cover the large left digestive gland (LD), the adult kidney (AK), and the invaginated rudiment of the gonad (G). A, anus.

Figure 19: Longitudinal section through a primary ceras of a late stage larva of M. leonina. Occasional secretory cells (arrow) are embedded in the pseudostratified columnar epithelium of the ceratal epidermis (CE).

Figure 20: Longitudinal section through the apical portion of a primary ceras at 5 hours after shell loss. The ceratal epidermis (CE) is composed of highly vacuolated, squamous cells and occasional tufts of stiff cilia (arrow). A muscle fiber (MU) traverses the expanded haemocoel (H) of the ceras.

Figure 21: Photomicrograph using Nomarski differential interference contrast optics (NDIC) of a primary ceras of M. leonina during metamorphosis showing the extension of the left digestive gland (LD) into the ceratal haemocoel and patches of stiff cilia (arrows) arising from the ceratal epidermis (CE).

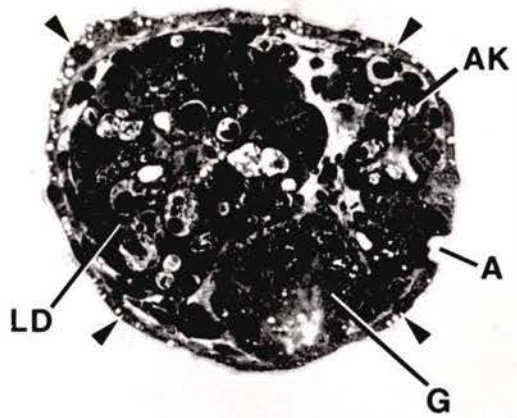

18

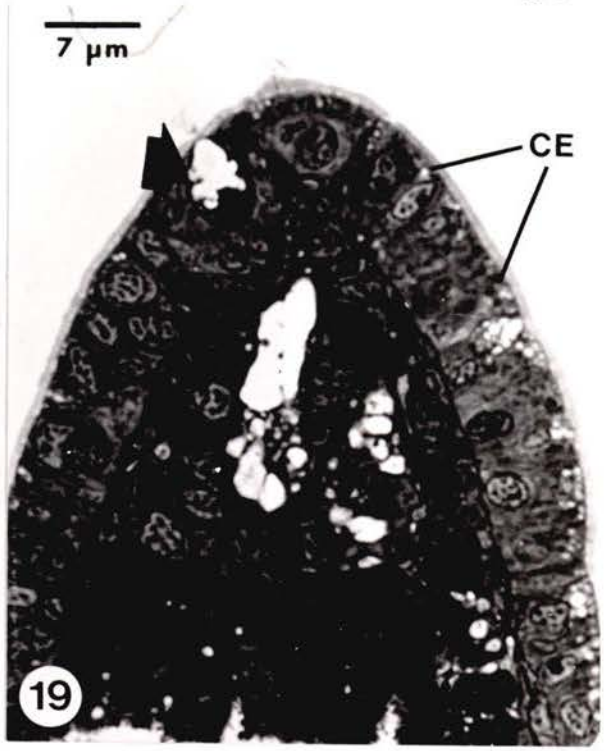

19

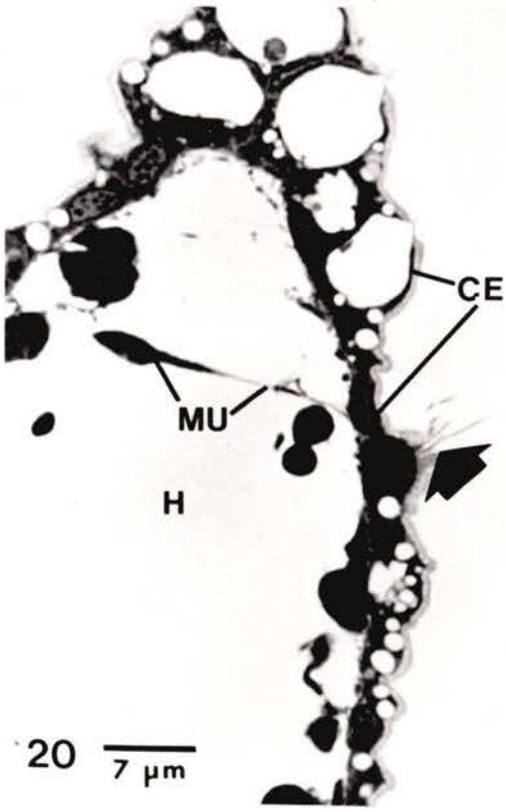

20 7 µm

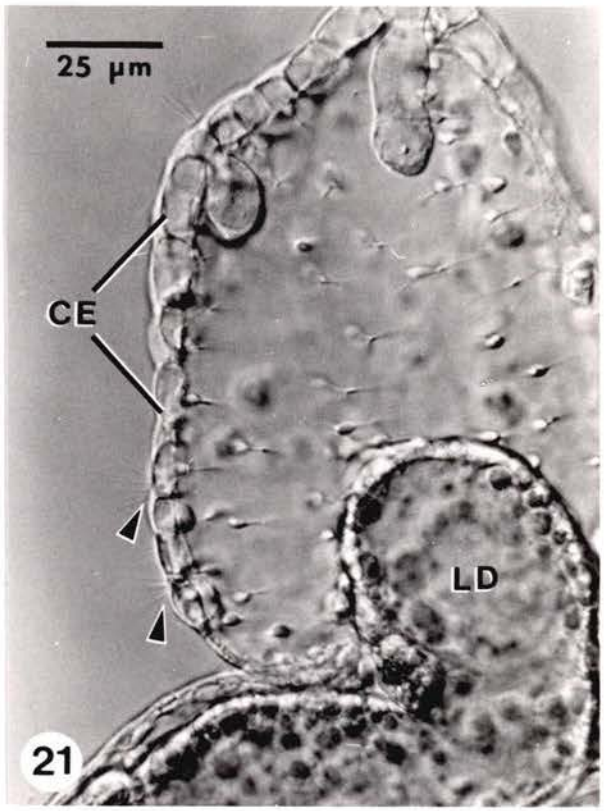

21

Figure 22: Cross section of M. leonina at 5 hours after shell loss that passes through the left and right digestive glands (LD and RD, respectively) where they enter the stomach (ST). Both glands are beginning to project into their respective ceras (C).

Figure 23: Cross section of M. leonina at 5 hours after shell loss showing the emergence of the intestine (I) from the dorsal side of the posterior end of the stomach (ST). The left digestive gland (LD) and degenerating larval kidney complex (LK) are also shown.

Figure 24: High magnification of the stomach area of Fig. 22. The larval gastric shield (large arrows), which can be recognized by the presence of small hyaline rods (small arrowheads) embedded in the shield matrix, is sloughing into the lumen of the stomach (ST).

Figure 25. High magnification of the wall of the stomach (ST) at 24 hours after shell loss. The arrowheads indicate the cuticle that lines the inner side of the gastric epithelium in postmetamorphic animals.

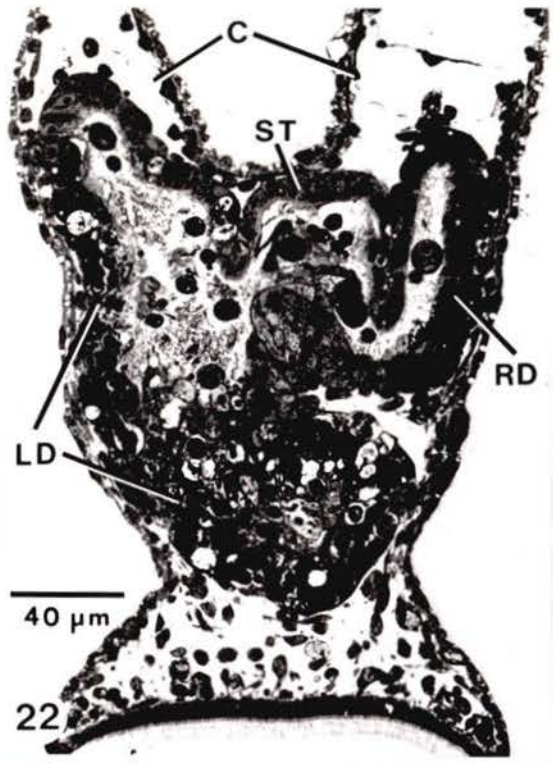

22

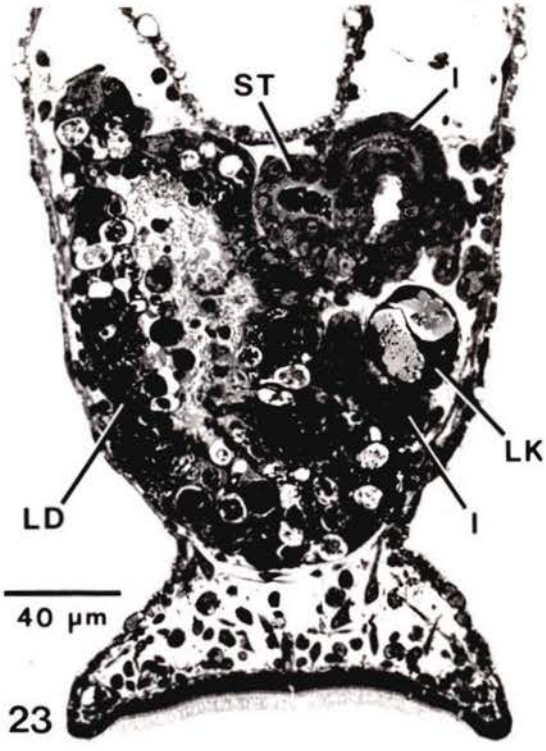

23

24

25

Figure 26: Ventral view of M. leonina at 5 days after shell loss showing the extended oral hood (OH). Nerve tracts (arrowheads) extend from the cerebral ganglia (CG) to the buds of the peripheral hood tentacles (HT). C, ceras.

Figure 27: Same animal as that in Fig. 26 showing closure of the oral hood by contraction of peripheral hood muscles.

Figure 28: Slightly oblique cross section through the esophageal region of M. leonina at 24 hours after shell loss showing the buccal ganglia (BG), pleural part (PLG) of the fused cerebropleural ganglia, pedal ganglia (PG), a pleuropedal connective (PPC), and a statocyst (S). The arrow indicates an enlarged neuronal soma within the right pleural ganglion.

Figure 29: Slightly oblique cross section through the base of the oral hood (OH) and the anterior end of the foot (F) at 24 hours after shell loss showing the developing rhinophore (R), its underlying rhinophoral ganglion (RG), and a rhinophoral nerve (arrowhead). CG, cerebral ganglion; EY, eyespot.

Figure 30: Photomicrograph (NDIC) of a peripheral portion of the oral hood showing a cerebral nerve (CN) extending to a peripheral hood ganglion (HG). A tuft of stiff cilia (arrow) extends from the tentacle bud.

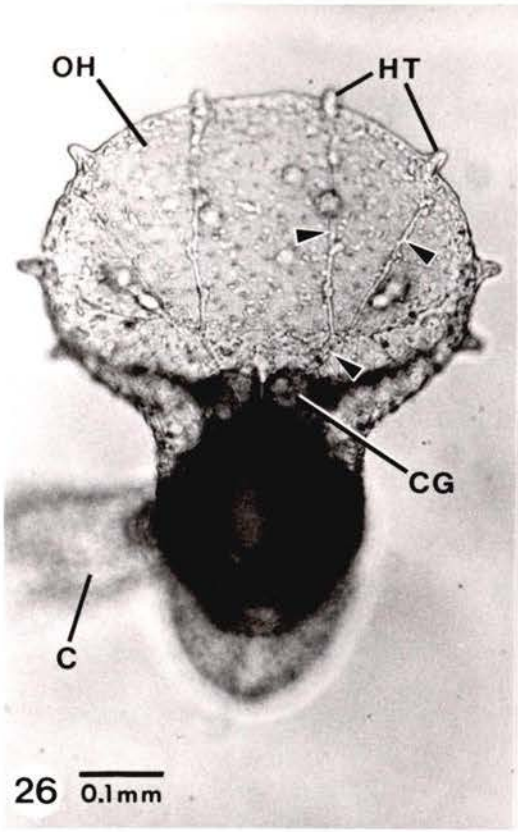
OH
HT
CG
C
26 0.1mm


27 0.1mm

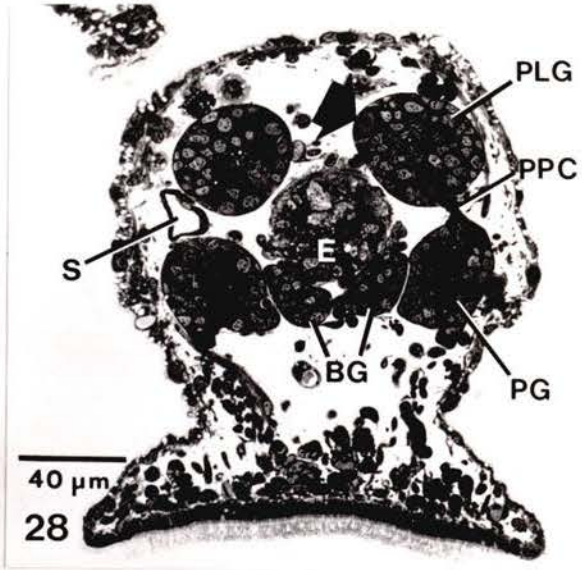
PLG
PPC
S
E
BG
PG
40 µm
28

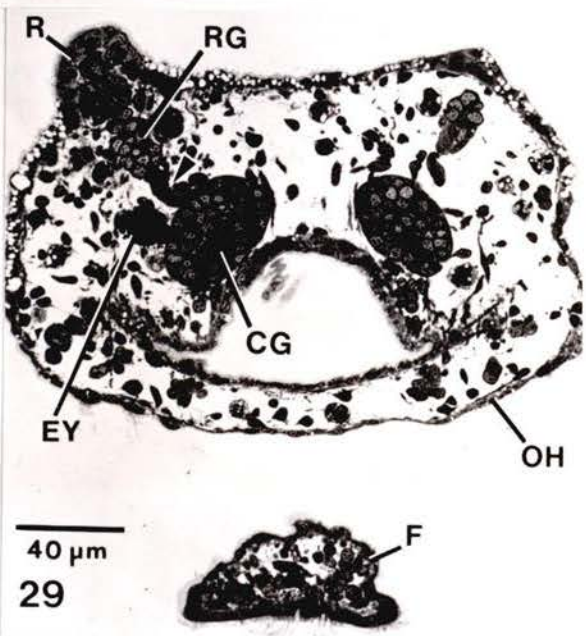
R
RG
CG
EY
OH
40 µm
29
F


30
HG
CN
7 µm

Figure 31: Low magnification, transmission electronmicrograph (TEM) showing the perivisceral epithelium (PV) and mantle fold of larval M. leonina at mantle retraction stage (long. section from the right side of the mid-sagittal plane). The mantle fold consists of a ridge of former shell-secreting cells (SS) and a floor epithelium (FE) composed of squamous cells except for a peripheral band of thickened epithelial cells (E) with associated subepithelial cells (SE). Other abbreviations: I, intestine; MC, mantle cavity; MR, short segment of mantle retractor muscle fibres. Scale bar = 5 µm.

Figure 32: TEM of deteriorating, former shell-secreting cells shortly after mantle fold retraction. Abbreviations are: CD, extracellular, cytoplasmic debris; L, autolysosomes; N, necrotic cytoplasm; SH, decalcified larval shell. Scale bar = 1 µm.

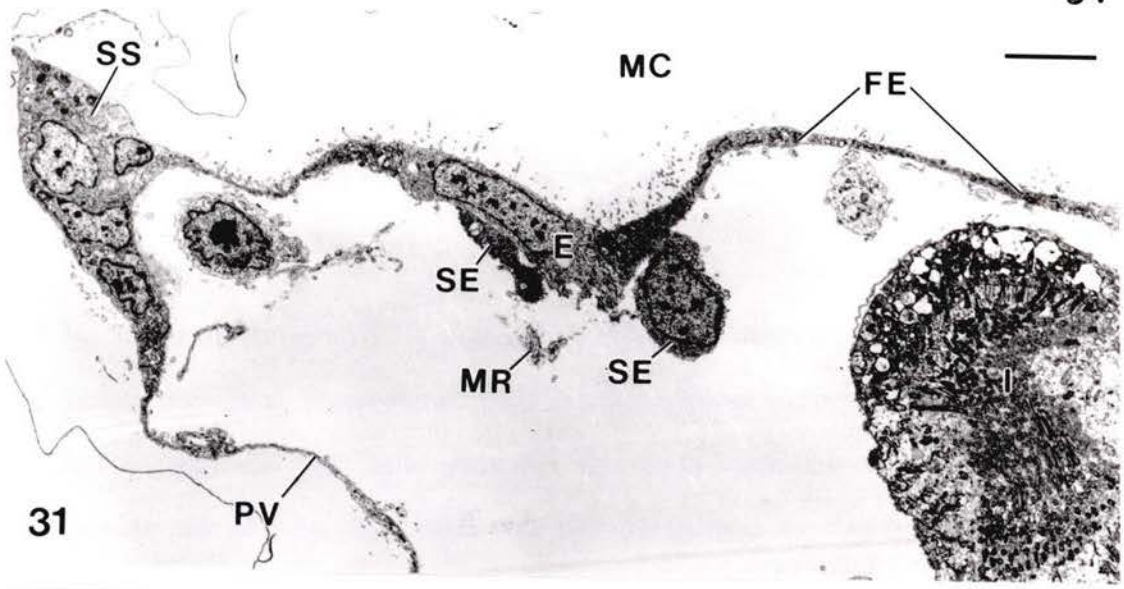

31

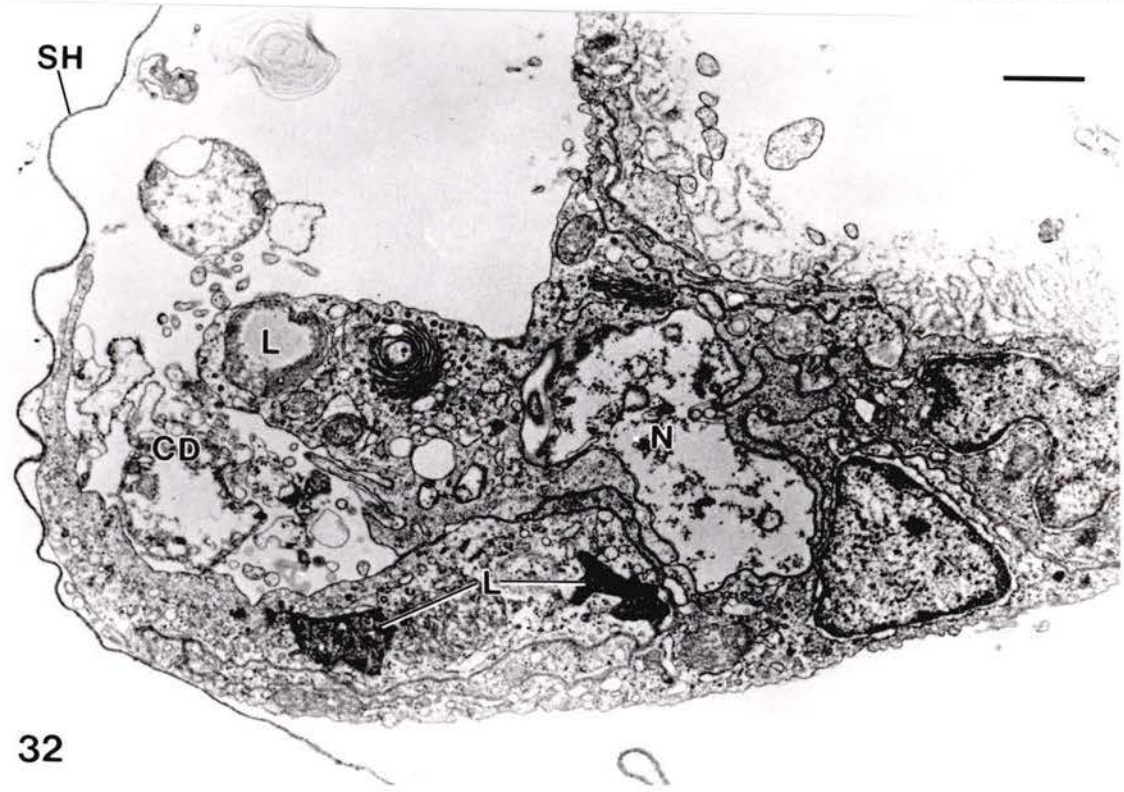

32

Figure 33: TEM through the zone of thickened mantle floor epithelial cells (E) and associated subepithelial cells (SE) that constitute the presumptive ceratal rudiment during early mitotic phase. The arrow indicates a mitotic subepithelial cell. Scale bar = 2 μm.

Figure 34: Low magnification, TEM through the right, presumptive ceratal rudiment (CR) during mid-mitotic phase showing the marked increase in numbers of epithelial (E) and subepithelial (SE) cells compared to mantle retraction stage. Arrowheads indicate mitotic cells. Squamous cells continue to form the remainder of the floor epithelium (FE) but the shell-secreting cells have disappeared by this stage. I, intestine. Scale bar = 5 μm.

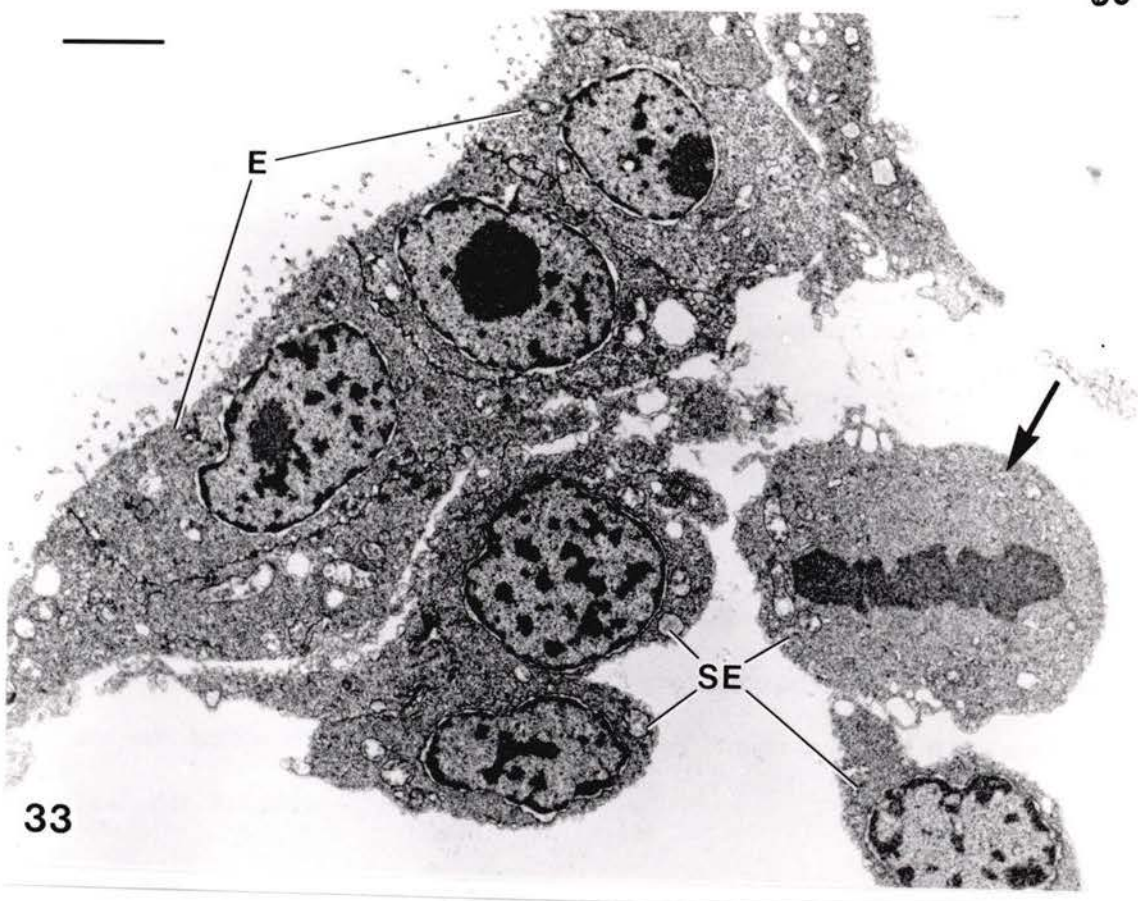

33

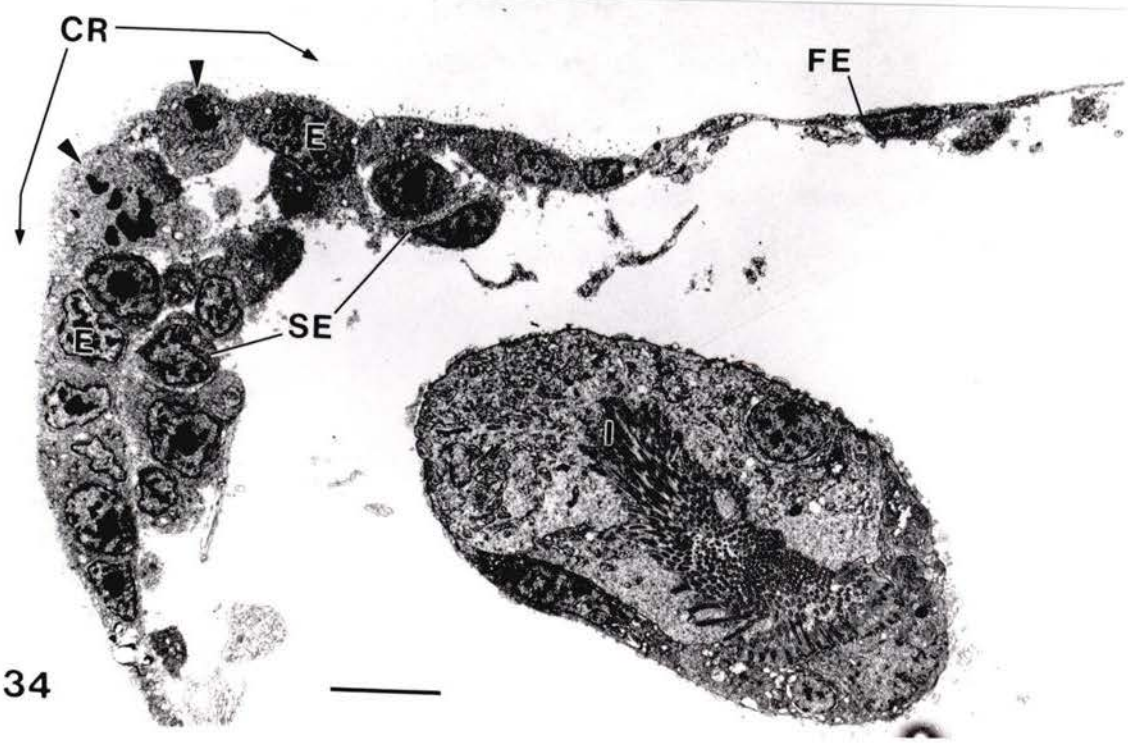

34

Figure 35: Low magnification, TEM through the ceratal rudiment during an early period of cellular differentiation phase. Note the large population of epidermal epithelial cells (E) and subepidermal cells (SE) and the cell body of a primary sensory cell (SC). Intraepidermal dendrites are indicated by an arrowhead. Scale bar = 5 µm.

Figure 36: TEM of ceratal, primary sensory cells at an advanced stage of maturation showing the subepithelial cell bodies (CB) and intraepidermal dendrites (D). Boundary between the epidermal and subepidermal cell layers is indicated by arrowheads. Scale bar = 2 µm.

Figure 37: TEM of two sensory cells (SC) at an early stage of maturation. A centriole is associated with the apical plasmalemma (arrow; enlarged in inset), but the nuclei are still within the epidermal layer (E). Basal lamina indicated by arrowheads. Scale bar = 1 µm.

Figure 38: TEM of two maturing sensory cells. The nucleus (N1) and perinuclear cytoplasm of one has migrated beneath the basal lamina (BL) of the ceratal epidermal epithelium (E); the remaining cytoplasm (arrowheads) stays within the epidermal layer. The nucleus (N2) of the neighboring sensory cell has not yet migrated through the basal lamina. Scale bar = 1 µm.

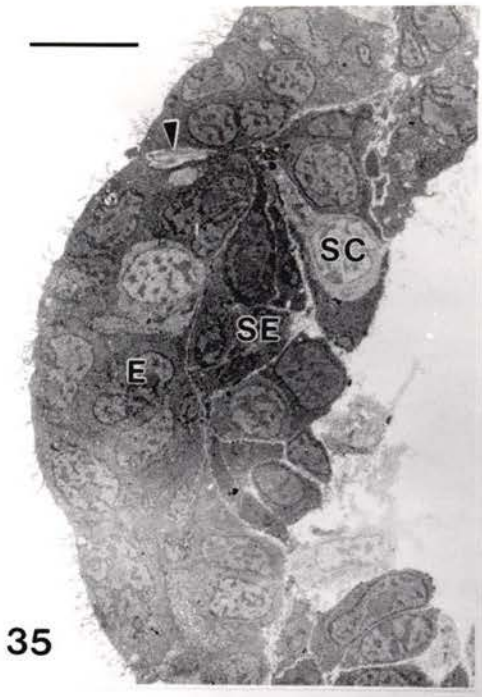

35

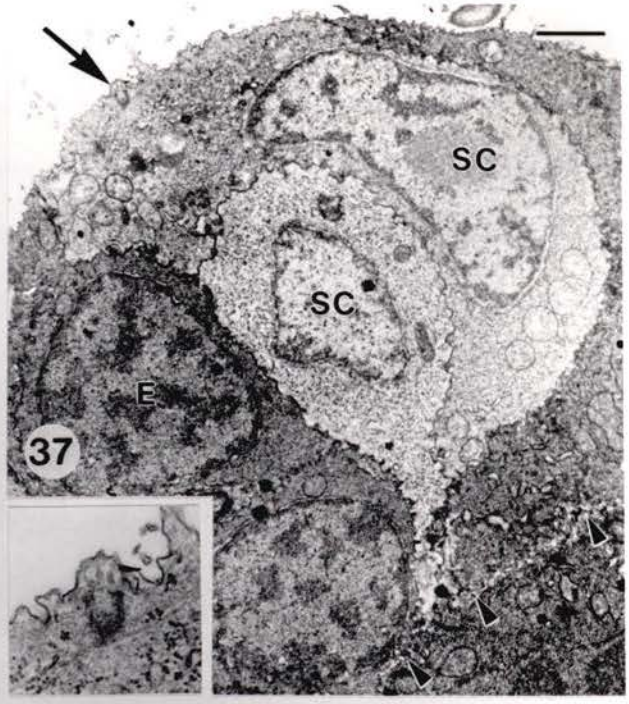

37

36

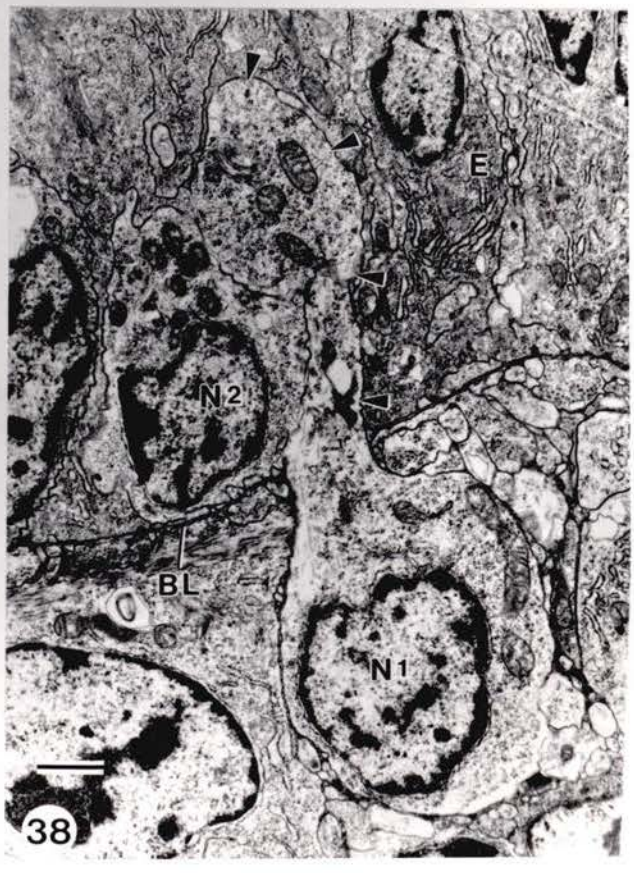

38

Figure 39: TEM of a longitudinal section through the cone-shaped ceratal rudiment of a metamorphically competent larva. The pseudostratified epithelium (E) of the ceratal epidermis includes a bundle of ciliated sensory dendrites (D), a type A secretory cell (AS), and a type B (BS) secretory cell. The solid mass of subepidermal cells (SE) includes two large subepidermal gland cells (SG). Scale bar = 5 µm.

Figure 40: TEM showing circular and longitudinal muscle fibres (CM and LM, respectively) beneath the epidermal basal lamina (arrowheads) of the ceratal rudiment in a metamorphically competent larva. Scale bar = 0.5 µm.

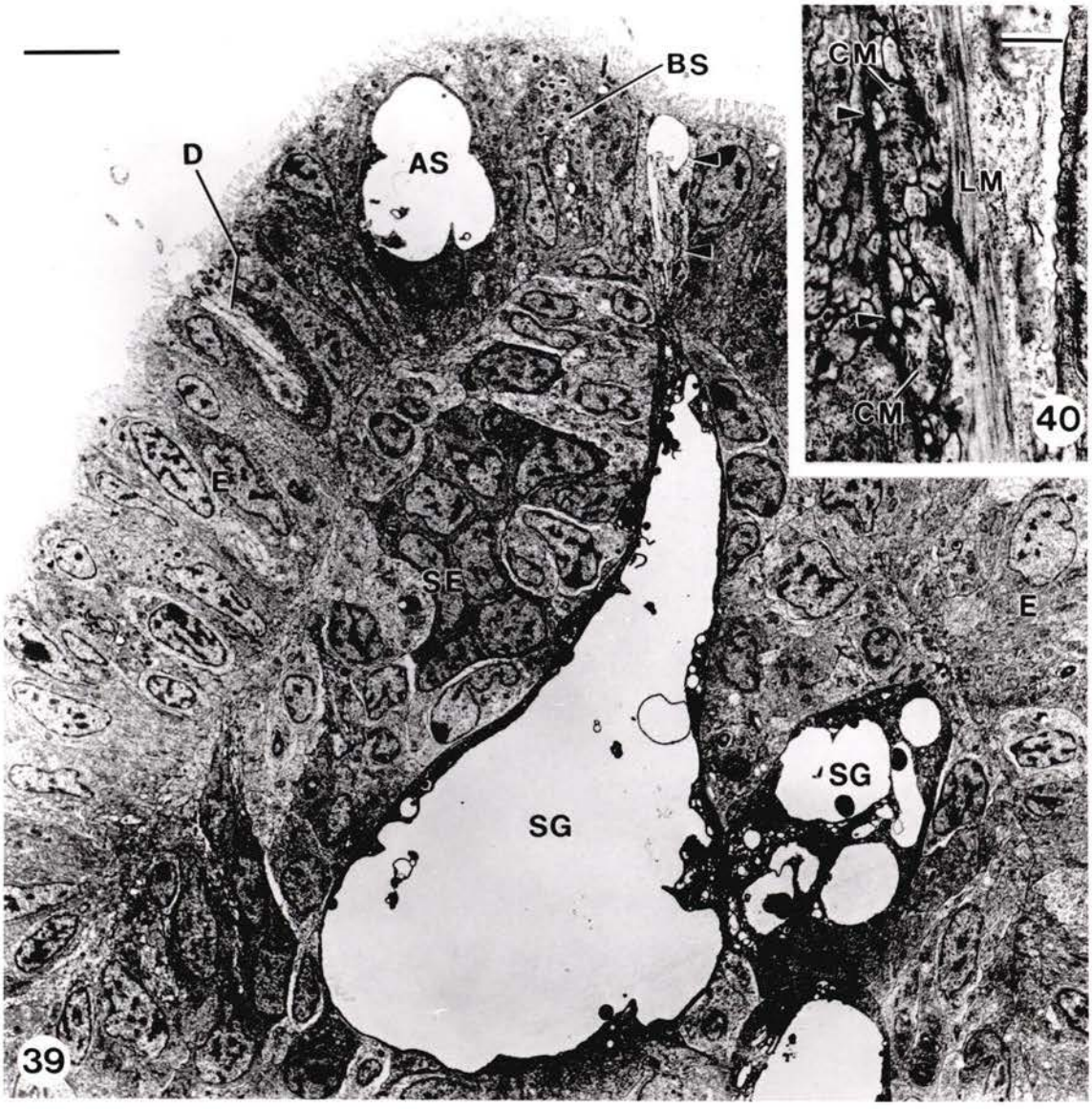
BS
AS
D
E
SE
SG
SG
E
39
CM
LM
CM
40

Figure 41: TEM of the basal half of a type A secretory cell (AS) within the ceratal rudiment epidermis at the stage of metamorphic competence. Note the large, intracellular storage vacuole (CV), the bundles of microtubules (arrowheads) adjacent to the limiting membrane of the storage vacuole, and the neuroglandular synapse (arrow). A type B secretory cell (BS) is also shown. Scale bar = 1 μm.

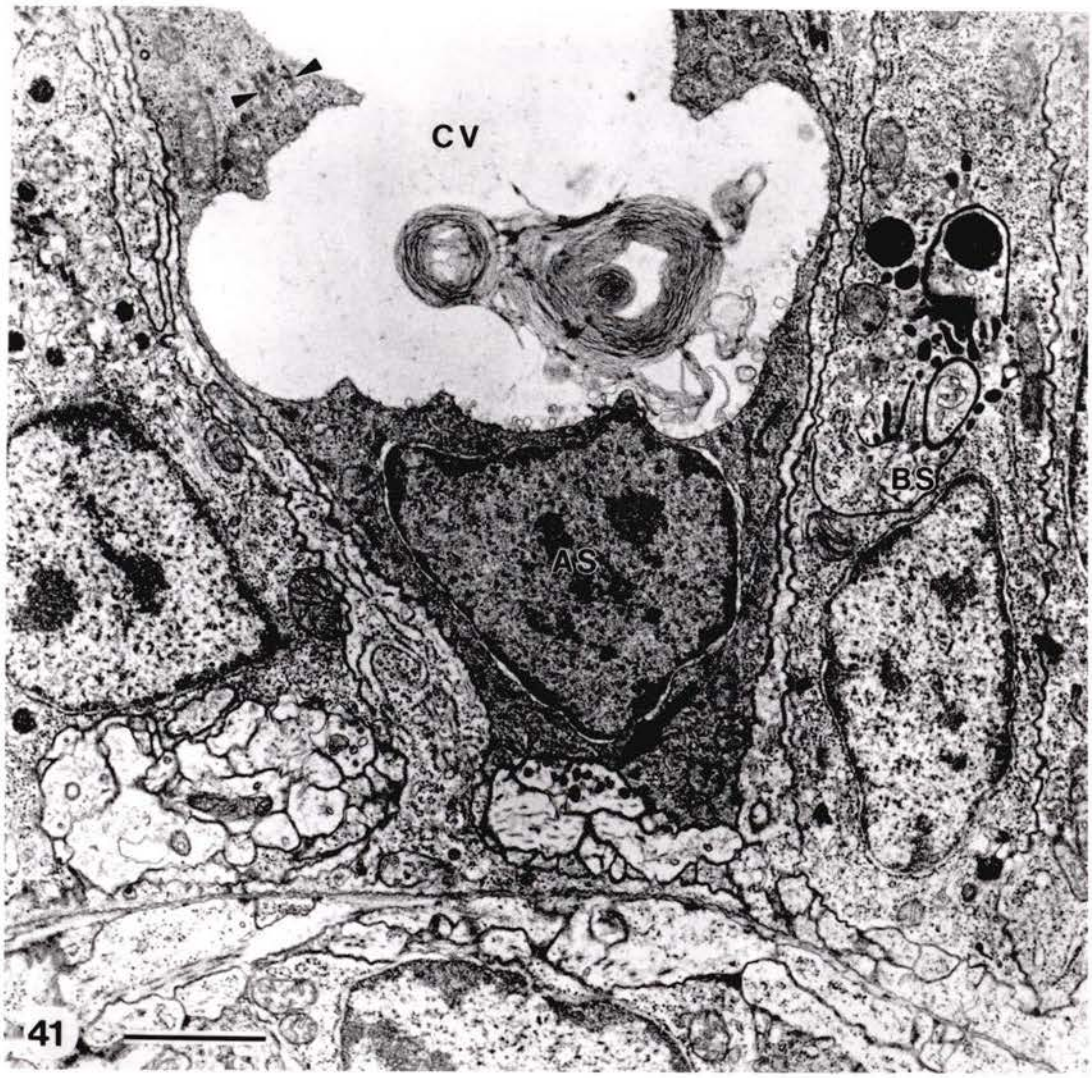
CV
BS
AS
41

Figure 42: TEM through two type B secretory cells (BS) within the ceratal rudiment epidermis at the stage of metamorphic competence. Note the elaborate Golgi (G), the secretory vesicles containing very electron-dense product (arrowheads), and the neuroglandular synapse (arrow). BL, basal lamina. Scale bar = 1 μm.

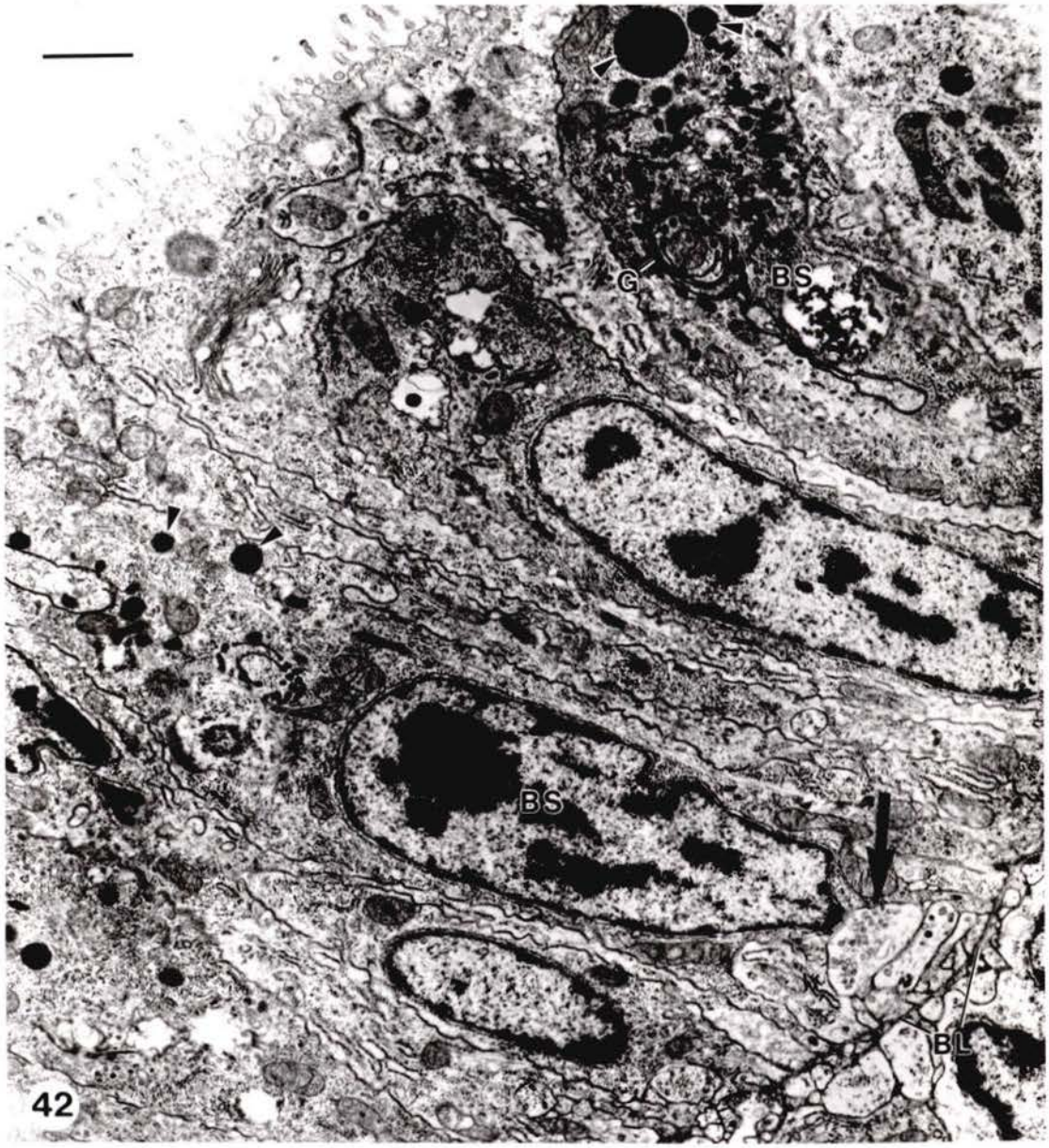
G
BS
BS
BL
42

Figure 43: Sketch of larval M. leonina (right side) at mantle retraction stage showing components of the nervous system associated with the right pleural ganglion and mantle fold (reconstructed from semi-serial sections; nerve diameters exaggerated; nervous tissue stippled). Two peripheral nerves extend from the pleural ganglion (PLG): the larger nerve (LKN) runs toward the larval kidney complex (LK) and the smaller, pleural/ceratal nerve (PC) runs beneath the floor epithelium (FE) of the mantle fold but does not yet meet the peripheral thickening (E) of this epithelium. The PC nerve is associated with a supporting cell (arrow labelled x) at the junction of the floor epithelium with the cephalic epidermis (CE). Micrographs through the PC nerve at positions labelled x, y, and z on this diagram are shown in Figs. 44, 45, and 46, respectively. Other abbreviations: CG, cerebral ganglion; CE, cephalic epidermis; F, foot; I, intestine; PG, pedal ganglion; PV, perivisceral epithelium; S, statocyst; SH, shell; SS, former shell-secreting cells; ST, stomach; VE, velum.

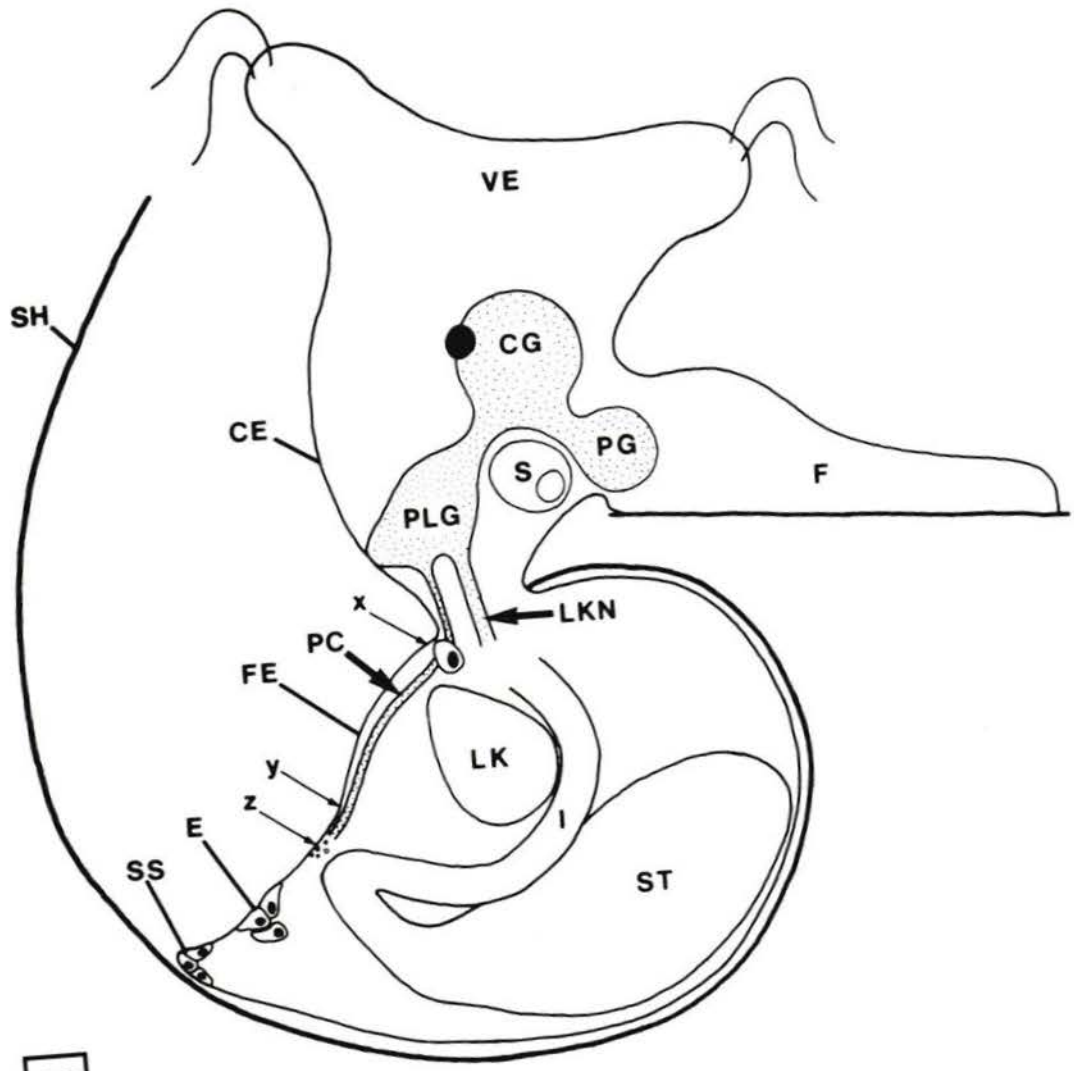

43

Figures 44 to 46: Profiles of the PC nerve at three locations along its trajectory at mantle retraction stage (see Fig. 43). The micrographs were obtained from sagittal sections of the larva in which the PC nerve runs tangentially through the sections. The progenitor cells of the presumptive ceratal rudiments (CR) are beyond the left side of each micrograph.

Figure 44: TEM of the supporting cell (SU) associated with axons of the PC nerve at the junction of the cephalic epidermis (CE) and the floor epithelium (FE) of the mantle fold. Scale bar = 1 µm.

Figure 45: TEM of the PC nerve at a distal point along its trajectory. Note the close association between the axonal bundle and the basal lamina of the overlying floor epithelium (FE). Arrowheads indicate cytoplasmic processes located distal to the PC nerve profile. Scale bar = 1 µm.

Figure 46: Terminal portion of the PC nerve. Although two of the profiles have dimensions and cytoplasmic features of axons (A), most of the profiles are through slender cytoplasmic processes (arrowheads) spread over the basal lamina of the overlying floor epithelium (FE). The small arrows indicate muscle fibres around the wall of the intestine (I). Scale bar = 1 µm.

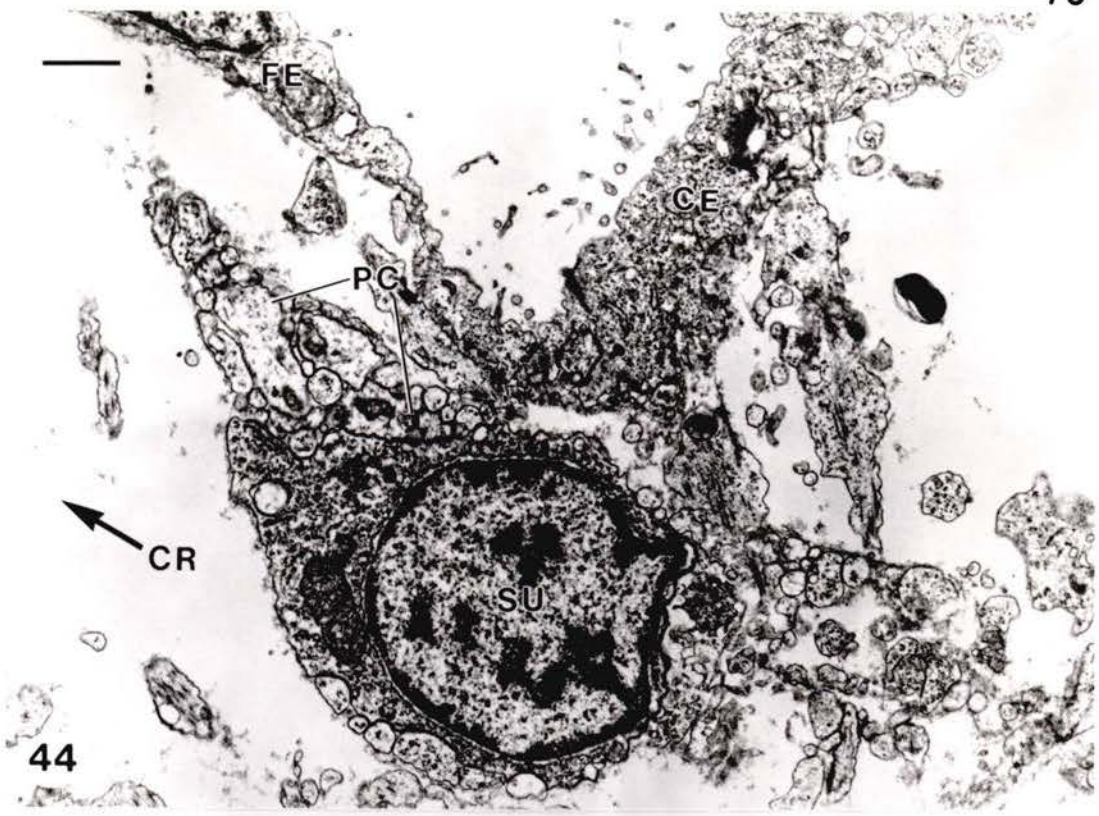
FE
CE
PC
CR
SU
44

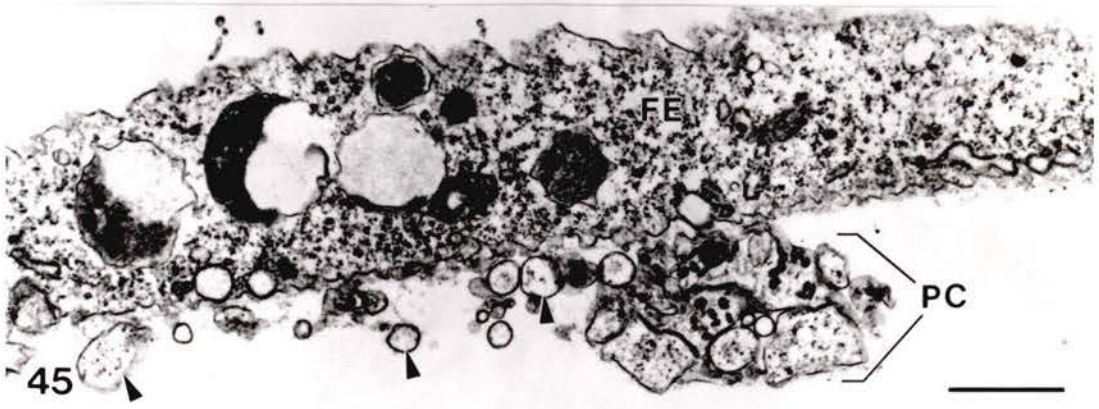
FE
PC
45

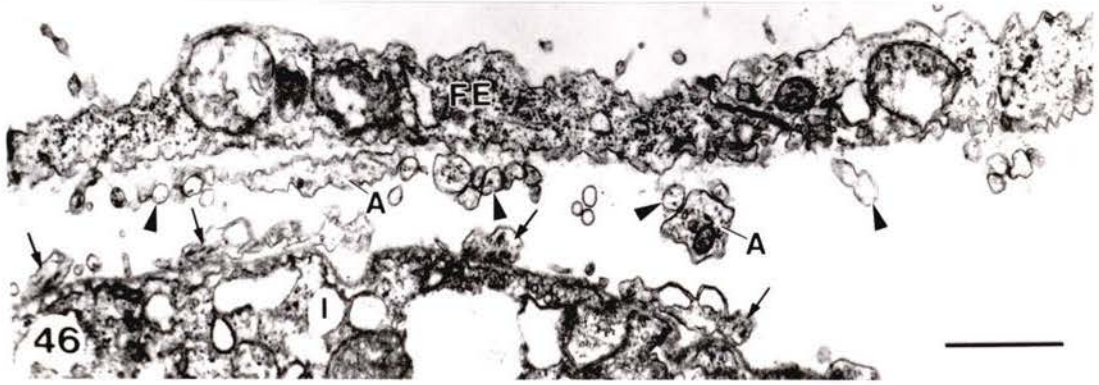
FE
A
A
I
46

Figure 47A,B: TEM collage of two frontal sections taken from the same specimen at the onset of the mitotic phase, but separated by a depth of 10 to 15 µm. Section A passes through the right pleural ganglion (PLG) and cephalic epidermis (CE) of the larva; section B passes through the floor epithelium (FE) of the mantle fold and the presumptive ceratal rudiment (CR). Collectively, the two sections pass through the PC nerve at 5 points, indicated by numbered arrows. Arrow 1 indicates the ganglionic root of the PC nerve; arrow 2 shows the PC nerve and associated supporting cell at the junction of cephalic epidermis and floor epithelium (enlarged in Fig. 48); arrow 3 shows a second supporting cell associated with the PC nerve (see Fig. 49); arrow 4 shows a subterminal section through the nerve (see Fig. 50); and arrow 5 shows the PC nerve associated with a muscle band at the anterior margin of the presumptive ceratal rudiment (see Figs. 51 and 52). Other abbreviations: CG, cerebral ganglion; E, esophagus. Scale bar = 10 µm.

Figure 48: TEM; enlargement of the PC nerve profile indicated by arrow 2 in Fig. 47A,B showing the PC nerve and supporting cell (SU) in the 'neck' region of the larva. Scale bar = 0.5 µm.

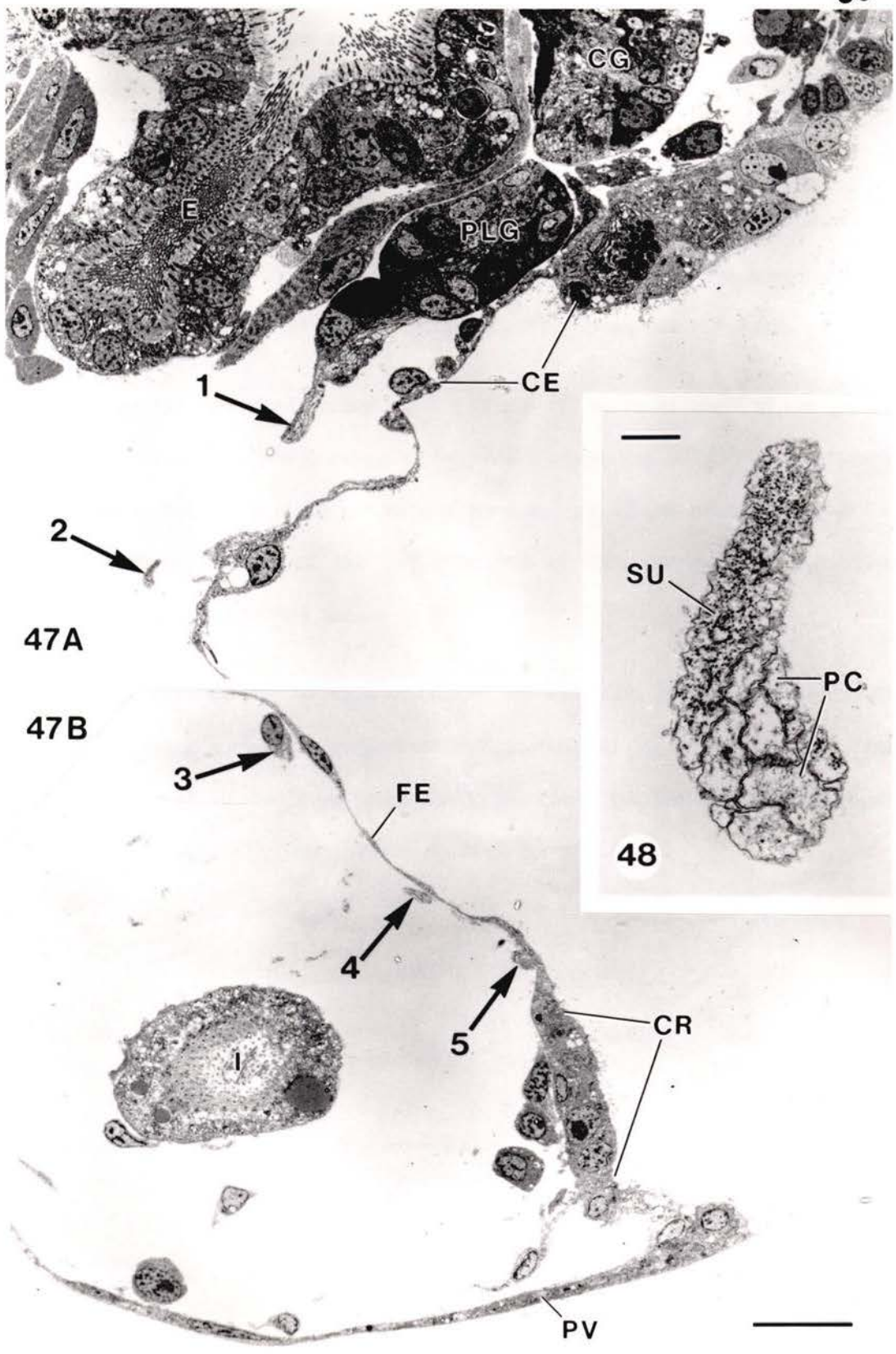
CG
E
PLG
CE
1
2
47A
47B
3
FE
4
5
I
CR
PV
SU
PC
48

Figure 49: TEM of the PC nerve and associated supporting cell in the area indicated by arrow 3 in Fig. 47A,B. The supporting cell is distal to that in the 'neck' region. Scale bar = 0.5 µm.

Figure 50: TEM showing a subterminal region of the PC nerve at onset of the mitotic phase. The axons are not intimately associated with the basal lamina (arrowheads) of the overlying floor epithelium (FE). Scale bar = 0.5 µm.

Figure 51: TEM through the terminal portion of the PC nerve at onset of the mitotic phase. The axon bundle is extending between a supporting cell (SU) and a muscle fibre (MU) that runs along the anterolateral margin of the presumptive ceratal rudiment (located beyond the upper margin of this micrograph). FE, floor epithelium. Scale bar = 1 µm.

Figure 52: TEM through the terminal portion of the PC nerve at onset of the mitotic phase showing a neuromuscular synapse (demarcated by arrowheads) onto the muscle fibre (MU) that runs along the anterolateral margin of the presumptive ceratal rudiment. FE, floor epithelium. Scale bar = 0.5 µm.

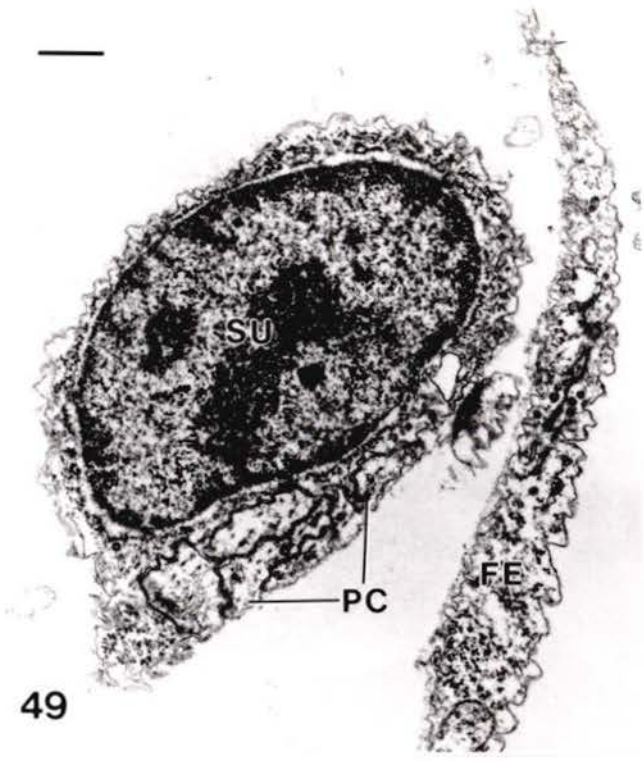

49

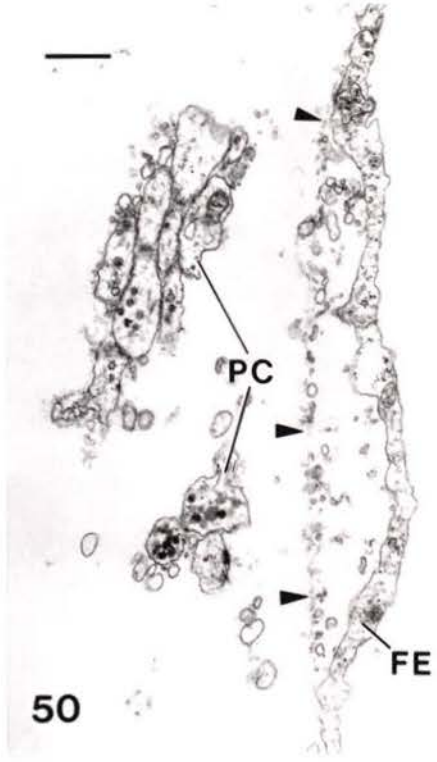

50

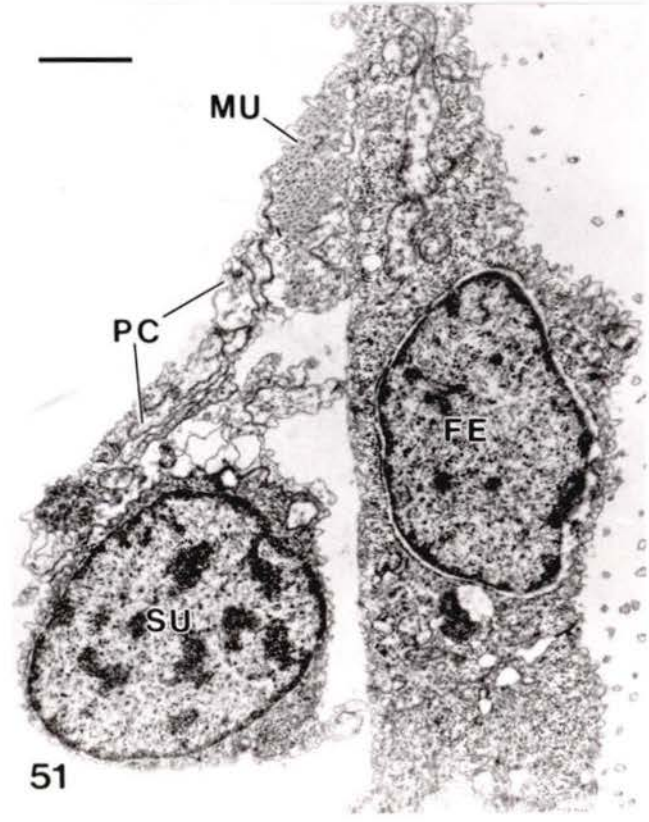

51

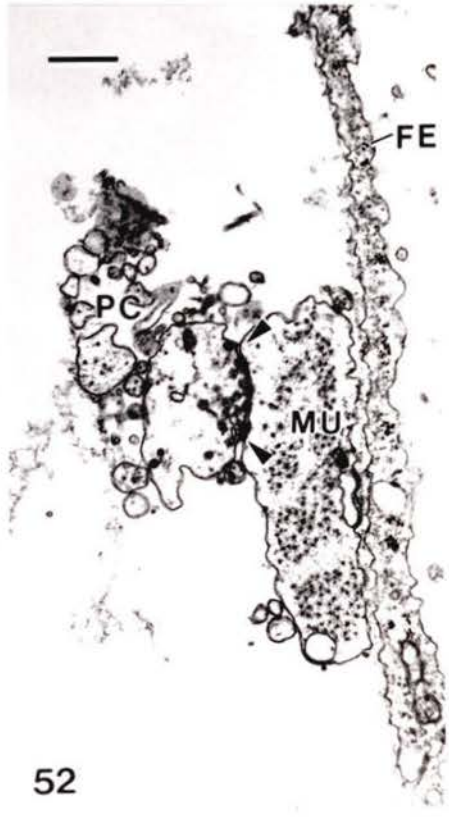

52

Figure 53: Low magnification TEM of a frontal section through larval M. leonina during early cellular differentiation phase showing two profiles through the right PC nerve (arrows) as it extends to the base of the presumptive ceratal rudiment (CR). The inset is an enlargement of one of these profiles (scale bar of inset = 1 µm). Although most of the presumptive ceratal rudiment is outside the plane of section, the boxed region is located at its anterolateral margin, where the PC nerve merges with an axon fascicle from a cluster of peripheral sensory cells. Enlargement of the boxed area is shown in Fig. 54. Other abbreviations: E, esophagus; LD, left digestive gland; LRM;, larval retractor muscle; S, left statocyst. Scale bar = 10 µm.


S
E
LRM
PC
PC
LD
CR
53

Figure 54: TEM; enlargement of boxed area in Fig. 53. Anterolateral margin of right ceratal rudiment showing merger of the PC nerve and an axon fascicle (AF) derived from a cluster of peripheral sensory cells. The PC nerve is associated with a muscle band (MU) at the base of the presumptive ceratal rudiment and the arrow indicates a neuromuscular synapse. E, epidermis. Scale bar = 1 µm.

Figures 55 to 57: Sections through three regions of the cluster of 5 peripheral, ceratal sensory cells that produced the axon fascicle shown in Fig. 54.

Figure 55: TEM; intraepidermal dendrites (arrowheads). One of the neighboring cells has an electron-lucent cytoplasm but an intraepithelial nucleus (not shown); it may be a sixth sensory cell in the process of differentiating. E, ceratal epidermis. Scale bar = 0.5 µm.

Figure 56: TEM; subepidermal sensory cell bodies (arrowheads). BL, basal lamina of epidermis; SE, subepidermal cells. Scale bar = 2 µm.

Figure 57: TEM; axons (arrowheads), bundled together as a fascicle, shortly after emerging from the sensory cell bodies. SE;, subepidermal cells. Scale bar = 0.5 µm.

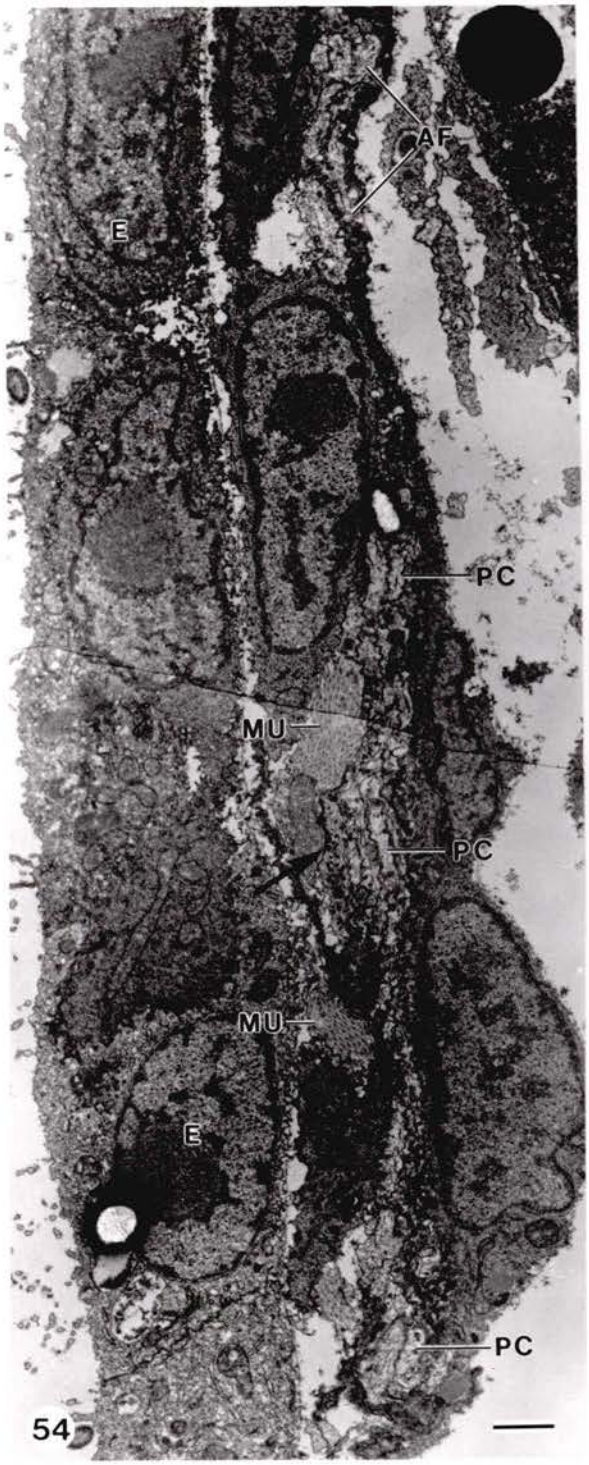
AF
E
PC
MU
PC
MU
E
PC
54

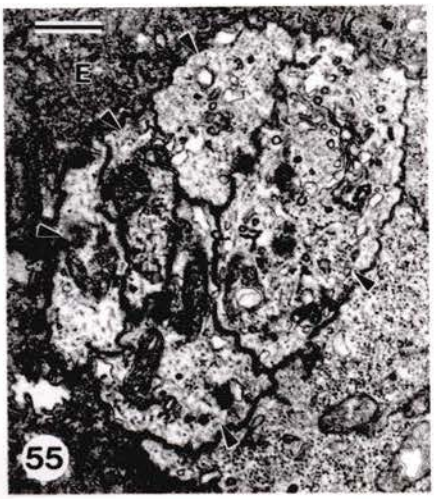
E
55

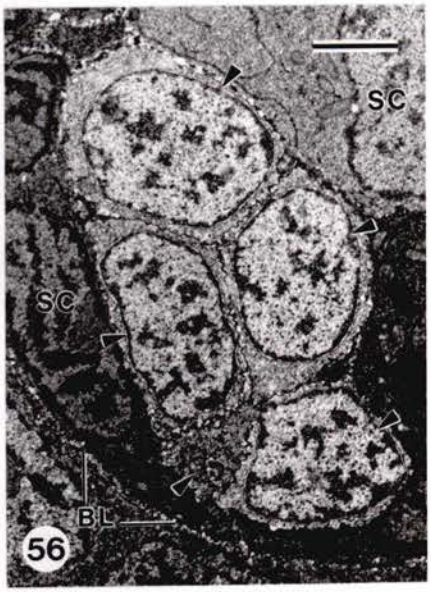
SC
SC
BL
56

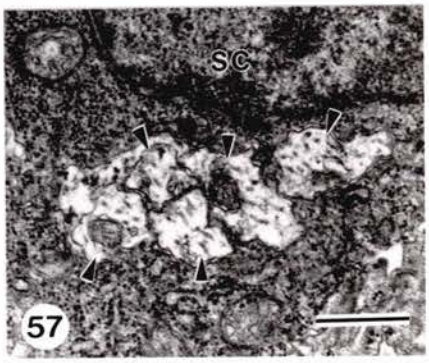
SC
57

Figure 58: TEM of a slightly oblique cross section through the PC nerve and associated supporting cell (SU) in a metamorphically competent larva. The nerve contains over 100 axons. MU, subepidermal muscle fibres. Scale bar = 1 µm.

Figure 59: Photomicrograph (NDIC) of a post-larva of M. leonina at approximately 48 hours after shell loss showing the right cerebropleural ganglion (CPG; produced by metamorphic fusion of the larval cerebral and pleural ganglia) and the PC nerve. The open arrow indicates a bifurcation of the PC nerve; one of the branches is out of the plane of focus but the small, solid arrow is parallel to its route. I propose that the proximal segment of the PC nerve (large, solid arrow) and the branch to the dorsal body wall (small, broken arrow) immediately anterior to the ceras (C) are pioneered by outgrowing motor axons from the larval pleural ganglion, whereas the second branch (small, solid arrow) that runs into the ceras is pioneered by ingrowing axons of peripheral sensory cells. Other abbreviations: F, foot; OH, oral hood. Scale bar = 50 µm.

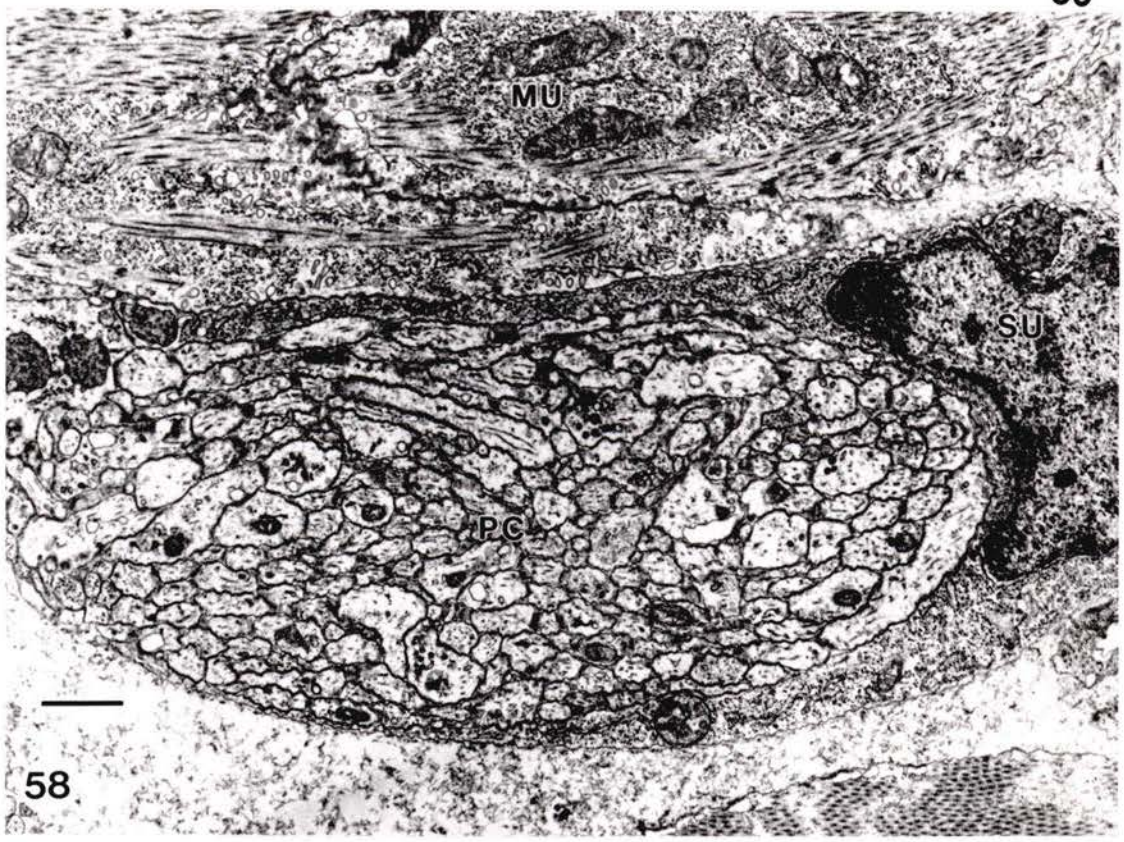

58

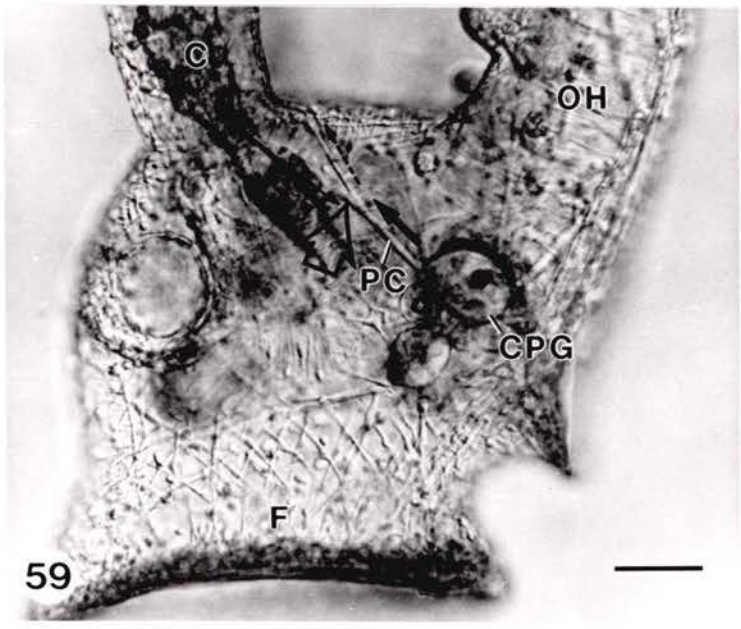

59

Chapter 2

FUNCTIONAL MORPHOLOGY OF THE CERATAL AUTOTOMY ZONE IN THE NUDIBRANCH MELIBE LEONINA (GOULD, 1852)

INTRODUCTION

Frédéricq (1883) invented the term 'autotomie' to describe the ability of some animals to rapidly discard a part of their body following a threatening external stimulus applied directly to the detachable appendage. He interpreted the behaviour as a means of escaping predators. For some lizards, there is good evidence that tail autotomy may provide a decoy to distract an attacker or may allow escape after a predator has trapped the tail (Congdon, et al., 1974; Dial and Fitzpatrick, 1983). Instances of tissue loss related to reproduction or to the normal ontogenetic development of animals were not included in the original definition of autotomy. This distinction, although controversial, has been upheld by Riggenbach (1903), Stasek (1967), and Emson and Wilkie (1980).

Research before and after Frédéricq's (1883) study has shown that autotomy is widespread among animals. The most thorough mechanistic studies have been confined to certain members of the Echinodermata (see reviews by Emson and Wilkie, 1980; Wilkie, 1984), the Arthropoda (see reviews by McVean, 1975; 1982), the Amphibia (Wake and Dresner, 1967), and the Reptilia (Sheppard and Bellairs, 1972). Stasek (1967) reviewed the many instances of autotomy described for molluscs. However, with the exception of a study by Hodgson (1984) on siphonal autotomy in the Solenacea (Bivalvia), little is known about the mechanism or physiological control of autotomy in the Mollusca.

Wake and Dresner (1967) and McVean (1975) point out that the process of autotomy must incorporate two components: a mechanism for detachment and a mechanism for wound closure and healing. Stasek (1967), Wilkie (1978a) and, in a subsequent paper, McVean (1982) suggest that provision for regeneration at the wound site should also be included as a component of autotomy. It might be expected that unique anatomical and physiological characteristics are associated with the autotomy zone(s) of each species to facilitate detachment, wound closure, and regeneration.

The speed and apparent ease with which autotomy occurs after appropriate stimulation may superficially suggest a zone of structural weakness at the detachment site. Nevertheless, for any one species this must remain speculative until the region of the autotomy plane is carefully examined morphologically. In salamanders that show a constriction at the base of their tails, Wake and Dresner (1967) have provided histological evidence of structural weakness at the sites of skin breakage and vertebral and myotome separation. However, in echinoderms such as the brittlestar Ophiocomina nigra studied by Wilkie (1978a; b; 1979) and Wilkie and Emson (1987), the potential autotomy planes along the length of the arms are not structurally fragile. Instead, weakness develops only after a neurally mediated reduction in the tensile strength of collagenous structures, including the intervertebral ligament and adjacent muscle tendons, within the autotomy plane.

Regardless of whether the autotomy plane is inherently or only potentially weak, muscular activity usually plays some role in the detachment process (Riggenbach, 1903). Leg autotomy in crabs such as Carcinus maenas is accomplished when a special arrangement of muscles and their tendons are directed by a distinct orchestration of nervous activity to cause rupture of cuticular specializations at the base of the leg (McVean, 1973; McVean, 1974; McVean and Findlay, 1976). In the absence of the autotomizing nervous signals, all but one of these muscles are also responsible for the normal walking movements of the leg. Alternatively, in salamanders with basal constrictions of their tails, Wake and Dresner (1967) have argued that local muscular activity may assist tail detachment, but actual breakage can only occur if the salamander is allowed to twist its trunk while the tail is held by an outside agency.

Many nudibranch and ascoglossan molluscs are notable for the apparent ease with which their cerata detach from the dorsal body wall following aversive stimuli (Thompson, 1960; Edmunds, 1966; Stasek, 1967; Kress, 1968; Ros, 1976). So-called 'deciduous'

cerata are possessed by Melibe leonina (Gould, 1852), a large dendronotid nudibranch that inhabits eel grass and kelp beds along the west coast of North America (see Ajeska and Nybakken, 1976). The cerata of M. leonina are petaloid in shape and are arranged in order of decreasing size in two rows along the dorsal surface of this nudibranch (Fig. 60). In living animals, the otherwise translucent epidermis is marked by an opaque line around the narrowed basal region of each ceras (Fig. 61). This line marks the autotomy plane, which is where the ceras separates from the dorsal body wall during autotomy.

Previous histological studies have failed to suggest specific hypotheses for the mechanism of ceratal autotomy in nudibranchs. Several authors have identified a muscular sphincter at the base of the deciduous cerata of various nudibranchs (Graham, 1938; Baba and Hamatani, 1965; Kress, 1968) and Kress (1968) identified a 'granular zone' at the base of the cerata of three species of Doto. These authors did not elaborate on the actual mechanism of autotomy.

I examined the ultrastructure of the ceratal autotomy zone of M. leonina in the hope that detailed morphological information will suggest a mechanism for ceratal autotomy in this nudibranch. I found that ceratal autotomy is accompanied by disruption of connective tissue structures within the autotomy plane and by degranulation of cells associated with these connective tissue structures. Contraction of sphincter and longitudinal muscles on either side of the autotomy plane appears to help rupture tissues.

MATERIALS AND METHODS

Adult specimens of Melibe leonina measuring approximately 5 cm in relaxed foot length were collected from the eel grass bed in Patricia Bay, Vancouver Island by SCUBA divers. Juveniles having a relaxed foot length of approximately 0.5 cm were reared in the laboratory (see Ch. 1) from egg masses also collected from Patricia Bay.

Prior to fixation, animals were lightly anaesthetized in an artificial seawater solution containing an excess of magnesium ions (recipe according to Audesirk and Audesirk, 1980). This procedure was necessary to prevent excessive constriction of the ceratal autotomy plane when the specimens were placed in fixative.

Following anaesthesia, a portion from the base of a ceras was cut from each adult and pinned to a small block of Sylgard (Dow-Corning) before being immersed in primary fixative for 5 hours. Juveniles were fixed whole for 5 hours. The primary fixative consisted of a 2.5% solution of glutaraldehyde in phosphate buffer (pH 7.6), with 0.34M NaCl added to make the fixative isosmotic with seawater (Cloney and Florey, 1968). After several rinses in 2.5% sodium bicarbonate (pH 7.2), the tissue was placed in a 1:1 mixture of 4% osmium tetroxide and sodium bicarbonate buffer. Ethanol dehydration and infiltration with Epon 812 followed standard procedure. Thin sections were stained for 20 min at 60 degrees C in aqueous uranyl acetate, followed by 10 min at room temperature in lead citrate and were photographed with a Philips EM300.

Preliminary examination of one µm thick sections and of thin sections showed that the structural organization of the autotomy zone was much easier to reconstruct in juveniles than adults because the amount of tissue (e.g. size of muscle bundles) is much less. Therefore, a series of sections through the intact autotomy zone of a juvenile ceras was prepared by cutting one to three 1 µm sections alternating with five to seven grids of thin sections (ceras oriented longitudinally) until the autotomy zone was sectioned completely.

The basic structure of the autotomy zone revealed by this specimen was confirmed by examining thin sections through selected regions of a ceratal autotomy zone in a second juvenile and through the autotomy zone of an adult ceras.

Autotomized cerata for ultrastructural observations were obtained by two methods. Firstly, autotomy was induced by a pinch with forceps to cerata of adults prior to their fixation, in which case no anaesthesia preceded fixation. Secondly, cerata were occasionally autotomized when lightly anaesthetized juveniles were placed in fixative. Subsequent preparation of autotomized cerata for electron microscopy followed the procedure outlined above.

RESULTS

A. Behaviour During Ceratal Autotomy

When a ceras of M. leonina is grasped firmly by forceps, the base of the held appendage becomes greatly constricted and eventually separates from the dorsal body wall at the level of this constriction. The muscles of the ceras are capable of contraction for many hours after autotomy, but the autotomized ceras shows little spontaneous movement. In addition to ceratal autotomy, pinching a ceras causes the whole animal to contract and eventually induces the swimming behaviour described by Hurst (1968). Swimming may begin before or after actual separation of the ceras.

In laboratory aquaria, crab attacks on M. leonina often cause one or more cerata to autotomize. However, a ceras autotomizes only when grasped by the chela of the crab; neighbouring cerata do not autotomize. Indeed, if an animal is secured to a Sylgard-lined dish by pins through non-ceratal parts of the body, none of the cerata show basal constriction even when pins are placed close to the insertion of a ceras. If a ceras of this animal is grasped by forceps, it becomes contracted around its base and eventually autotomizes, but the basal regions of adjacent cerata remain relaxed. These observations suggest that each ceras must receive direct trauma to initiate events leading to its autotomy.

After a ceras detaches, the resultant wound in both the ceras and the dorsal body wall is closed by continued constriction of the tissues on both sides of the autotomy plane (Fig. 62). Presumably, the circumferential contraction around the respective wounds is effected by sphincter muscles that lie on either side of the autotomy plane. Furthermore, as the epidermis separates at the autotomy plane, the ceratal tissue surrounding the wound is pulled away from the site of detachment in a manner suggesting contraction of longitudinal muscles within the ceras.

Autotomized cerata are subsequently regenerated. In juveniles measuring 0.5 cm in relaxed foot length, regenerative buds appear at the site of ceratal detachment within 2 to 3 days after autotomy (n=4).

Populations of M. leonina were sampled to determine the extent of ceratal losses in the field. Two samples of 41 and 81 animals, respectively, were collected from different locations around southern Vancouver Island at different times of year. Sixty-five (53.3%) of the 122 animals were in the process of regenerating lost cerata and 35 of these had more than one regenerative bud.

B. Structure of the Ceratal Autotomy Zone

1. Intact Ceras

Dissections of M. leonina show that 4 major structures extend across the autotomy plane at the base of each ceras (Fig. 63): the epidermis, a branch of the digestive gland, the ceratal nerve (originating from the pleural nerve), and longitudinal muscle bands that originate within the dorsum of the body (proximal to the autotomy zone) and insert near the apex of the ceras. Although the digestive gland and the ceratal nerve eventually undergo extensive branching within each ceras, they both enter as a single undivided trunk. In addition to these 4 structures, the complex system of fluid-filled haemal sacs, which provides M. leonina with its hydraulic skeleton, extends from the body into each of the cerata.

As previously described, a pair of sphincter muscles flank the intact autotomy plane. I will use the term 'autotomy zone' to describe the region that includes the autotomy plane and its adjacent sphincter muscles (Fig. 63).

Ultrastructural details of these components of the ceras and identification of additional components are given below.

a. Epidermis

Most of the epidermis covering the cerata and the adjacent dorsal body wall of juvenile M. leonina is composed of highly vacuolated squamous epithelial cells (Fig. 64). However, around the base of each ceras, the cells of the epidermis become cuboidal. The resultant epidermal thickening is most consistent and pronounced on the body side of the autotomy plane (Fig. 65), where many of the epithelial cells contain large nuclei with 1 or 2 prominent nucleoli. Mitotic cells are not unusual in this region of the epidermis. A less pronounced thickening of the epidermis may occur on the ceratal side of the autotomy plane (Fig. 65), but this is not consistently present. However, in regions that show an epidermal thickening on both the body and ceratal side of the autotomy plane, the two are joined by 1 or 2 epidermal cells that are lower in height than those of the adjacent thickenings (Fig. 65).

b. Autotomy Plane Nerve and Granule-Filled Cells

Serial sections through the autotomy zone show that a prominent bundle of axons completely encircles the base of the ceras just beneath the ceratal epidermis. This nerve, which I call the autotomy plane nerve (APN), lies between the two sphincter muscles at the base of the ceras and is therefore positioned at the exact level of the autotomy plane (Fig. 65). Serial sections also show that the APN arises from the ceratal nerve after the latter has entered the ceras but before it gives rise to major branches within the ceras.

Somata and cytoplasmic processes of distinctive, granule-filled cells (GC) are intimately associated with the APN along its entire course around the base of the ceras (Figs. 66 and 67). The GC are contained within the perineurium of the APN and the cytoplasmic

extensions of the GC intermingle with the axons of the APN (Fig. 67). Each GC contains a large nucleus with prominent nucleolus (Fig. 66) and the perinuclear cytoplasm contains mitochondria, polyribosomes, smooth and rough endoplasmic reticulum, and several Golgi bodies (Fig. 68). The Golgi give rise to primary vesicles containing an electron-dense material (Fig. 68) that appear to be precursors of the larger (max. 280 nm diameter) membrane-bounded dense granules that are characteristic of this cell (Figs. 67, 68, 69, and 70). Most of the latter occur within cytoplasmic processes of the granule-filled cells, where smooth endoplasmic reticulum is also abundant (Fig. 69).

The axons composing the APN show occasional interneuronal synapses but most of the synaptic profiles I observed were onto the somata and cytoplasmic processes of GC (Fig. 70). A mixture of clear and dense vesicles are present on the presynaptic side of the axon - GC synaptic contacts.

Along the entire length of the APN, cytoplasmic extensions from the GC contact the basal lamina of the overlying epidermis in the restricted region of the autotomy plane (Figs. 65, 66, and 69). Furthermore, processes of the GC are closely associated with the longitudinal muscle bands where the latter intersect the autotomy plane. Further description of this association is given in section d.

The APN with its associated granule-filled cells is probably responsible for the opaque line that circumscribes the base of each ceras in living M. leonina.

c. Sphincter Muscles

Of the two bands of circular muscle (sphincters) that flank the autotomy plane, the band on the body (proximal) side of the autotomy plane is larger (Fig. 65). The size difference is due to the relative number of constituent muscle fibres. The general fine structural features of the sphincter muscles are typical of gastropod non-striated muscle (Fig. 71) (see Plesch, 1977).

The sphincter muscle on the body side of the autotomy plane lies immediately beneath the prominent thickening of the epidermis. A meshwork of connective tissue fibrils invests the individual muscle cells of this sphincter and binds the whole to its overlying ridge of epidermal cells (Figs. 71 and 72). Although the connective tissue fibrils are likely some form of collagen, they measure only 15 to 20 nm in diameter and are not banded.

Hemidesmosome-like structures occur frequently along the sarcolemma of the sphincter muscles (Fig. 71). Nunzi and Franzini-Armstrong (1981), studying the smooth muscle portion of a scallop adductor muscle, termed these hemifasciae adherentes to distinguish the fact that actin-containing filaments (the thin myofilaments), rather than intermediate filaments (tonofilaments), insert on the sarcoplasmic side of the membrane specialization. Twarog et al. (1973) and Nunzi and Franzini-Armstrong (1981) suggest that hemifasciae adherentes mediate attachment of intracellular thin myofilaments onto extracellular filament networks. Direct junctional complexes between neighbouring muscle cells were rarely observed. Epidermal cells are anchored to their underlying basal lamina by hemidesmosomes (Fig. 72).

Small bundles of axons lie alongside the sphincter muscles and these form occasional neuromuscular synapses (Fig. 73).

d. Longitudinal Muscles

Like the sphincter muscles, the longitudinal muscles of the ceras lack obvious cross or oblique striations. The muscle cells composing each longitudinal muscle band are held in staggered register by connective tissue and many hemifasciae adherentes are located along their sarcolemmae (Fig. 76). Each longitudinal band passes close to the inner side of the two sphincter muscles as it extends from the ceras into the body proper (Figs. 74 and 76). Concentrations of connective tissue fibrils are located where the longitudinal and sphincter muscles are juxtaposed (Fig. 76).

The longitudinal muscle bands actually penetrate through the APN-GC complex where the former cross the autotomy plane (Fig. 74). At the point of penetration, the individual fibres of the muscle band are interspersed with cytoplasmic processes of the GC (Fig. 75).

In some sections, it appears that the longitudinal muscle bands show a structural discontinuity where they traverse the autotomy plane. As shown in Fig. 75, a narrow, irregular plate of connective tissue extends across the band so that longitudinal muscles from the ceras insert on one side of the plate and longitudinal muscles from the body insert on the opposite side. The extensions of GC interdigitate with the muscle fibres on the ceratal side of the connective tissue plate.

Profiles of neuromuscular synapses onto longitudinal muscle cells were found (Fig. 77).

Figure 78 is a summary diagram showing the basic arrangement and interrelationships of the APN, the two sphincter muscles, and the longitudinal muscle bands within the ceratal autotomy zone of M. leonina.

e. Gliointerstitial Cells

Gliointerstitial cells, with their network of granule-filled cytoplasmic processes, are associated with the muscle cells of the sphincters (Figs. 71 and 79) and the longitudinal bands (Fig. 74), and with the small groups of axons that occur adjacent to the muscle tissue. A detailed review of the structure and distribution of these cells within molluscs has been given by Nicaise (1973). Apart from their association with peripheral nerves and muscles, the most distinguishing characteristic of gliointerstitial cells is their content of membrane-bounded granules having average dimensions of 250 to 350 nm in width and 350 to 450 nm in length. Nicaise (1973) stated that gliointerstial cells may have a trophic function or may be involved in the ionic regulation of neurons and muscle. Cholinesterases and calcium ions have been cytochemically identified within the storage granules.

In my tissue sections of M. leonina, the membrane-bounded granules within the gliointerstitial cells and those of the GC associated with the APN are both electron-dense, yet the two are easily distinguishable. The granules of the gliointerstitial cells are larger (max. 400 nm diameter) than those of the GC (max. 280 nm diameter) and gliointerstitial granules consistently show irregular swelling of the limiting membrane away from the granular product (compare Figs. 80 and 81).

f. Digestive Gland

Throughout the cerata of M. leonina, the digestive gland is invested with occasional fibres of circular muscles. However, where the trunk of the digestive gland enters the base of each ceras, it is encircled by two prominent sphincter muscles that lie on either side of the autotomy plane. Figures 82 and 83 show the digestive gland sphincter situated on the body side of the autotomy plane. The distance between the sphincters of the digestive gland is greater than that between the two subepidermal sphincters.

In the mid-region of the lateral side of the ceras, the APN extends at least two branches toward the digestive gland (Fig. 85). Each branch merges with a single nerve ring that completely encircles the digestive gland between the two digestive gland sphincters (Figs. 82 and 84). Somata of the GC are located at intervals along the centrally directed branches of the APN and along the entire course of the nerve ring encircling the digestive gland (Figs. 84 and 86). Granule-filled processes of the GC are apposed to the basal lamina of the digestive gland cells (Figs. 84 and 86) and to occasional profiles of muscle fibre (non-sphincter) associated with the gland.

g. Ceratal Nerve

In each ceras, the trunk of the ceratal nerve crosses the autotomy plane in the mid-region of the lateral side of the ceras. At the point of intersection, the ceratal nerve

becomes associated with one of the branches of the APN extending toward the digestive gland. The APN branch, with accompanying GC, actually penetrates the perineurium of the ceratal nerve (Fig. 87) and granule-filled cytoplasmic processes of the GC are closely applied to this perineurium (Fig. 88).

Figure 89 is a diagram summarizing the distribution of the various nerves and connectives found within the base of a ceras and the adjacent body wall of M. leonina.

2. Autotomized Ceras

After ceratal autotomy, the various tissues within the base of the ceras are compressed together (Fig. 90) due to contraction of muscles in the area. Nevertheless, the following observations were made from longitudinal thin sections through the base of the autotomized ceras.

The subepidermal sphincter muscle on the ceratal side of the autotomy plane remains bound by connective tissue to the overlying basal lamina of the ceratal epidermis and to the underlying longitudinal muscle bands (Figs. 90 and 91). Dissections of autotomized cerata confirm that these two attachments are maintained throughout the process of autotomy. However, the longitudinal muscle bands terminate immediately proximal to their association with the sphincter muscle (Fig. 90).

The subepidermal sphincter muscle and the broken ends of the longitudinal muscle bands border on a bundle of axons that lies immediately beneath the area of ceratal epidermis that has detached from the dorsal body wall of the nudibranch (Fig. 90). The position of this axonal bundle, relative to the subepidermal sphincter muscle and the epidermis identify it as the APN. However, whereas the APN of the intact ceras includes GC with cytoplasmic processes containing many membrane-bounded dense granules, very few granules are present in the APN of an autotomized ceras (Fig. 92). For example, in Fig. 85 of a non-autotomized ceras there is a combined total of 95 granule profiles within

the section through the APN and the adjacent nerve ring around the digestive gland (the granules within the nerve branch extending between the APN and digestive gland nerve ring are not included in this tally), whereas only 11 granules are present in a corresponding region of the autotomized ceras shown in Fig. 90.

The basal lamina underlying the ceratal epidermis is easily recognizable up to and including the level of the subepidermal sphincter muscle (Fig. 91). Beyond the sphincter, a rim of epidermis only one to two cells thick is retained by the detached ceras. These epidermal cells, which overlie the APN, are noteworthy because they lack a basal lamina (Fig. 92).

The detached stump of the digestive gland often protrudes slightly from the epidermal wound following ceratal autotomy (Fig. 90). A sphincter muscle corresponding to that on the ceratal side of the autotomy plane constricts the trunk of the digestive gland above the level of detachment (Fig. 90).

Due to the extreme constriction of tissues at the base of autotomized cerata, I was unable to positively identify the subdivision of the APN that encircles the digestive gland in the region of the autotomy plane. However, clusters of dense granules, like those associated with the GC of this nerve ring in intact cerata, were rarely found alongside the detached stump of the digestive gland.

DISCUSSION

My descriptions of ceratal autotomy by live Melibe leonina and, particularly, of the ultrastructure of the autotomy zone before and after separation suggest that GC granules and muscle contraction participate in the autotomy mechanism. Interpretation of the role of these two elements is given below.

A. Granule-Filled Cells (GC)

I propose that the central mechanism facilitating ceratal autotomy involves the GC associated with the autotomy plane nerve (APN) and its offshoot, the nerve ring that encircles the digestive gland. Granule-filled cytoplasmic processes from the GC impinge on the basal laminae and associated connective tissue of every major structure that extends from the ceras into the body proper: the epidermis, longitudinal muscle bands, ceratal nerve, and digestive gland. Furthermore, existing evidence indicates that contacts by granule-filled processes of GC are restricted to the region where these four structures separate during ceratal autotomy. Thin sections through randomly chosen locations along the ceras, outside the autotomy zone, and along the periphery of the oral hood showed gliointerstitial cells but no cells similar to the GC of the ceratal autotomy zone.

The GC are extensively innervated by axons within the APN and therefore must be effectors responsive to neural stimuli. Neural involvement in autotomy is suggested by the fact that each ceras is autotomized only after it receives a strong mechanical stimulus, even at some distance from the autotomy plane, and the response may occur within seconds of the stimulus. Additional evidence for neural involvement is given in Ch. 3.

The foregoing observations, combined with morphological data showing relatively few GC granules in autotomized cerata and absence of basal laminae where structures have separated, suggest that neural signals elicit exocytosis of GC granules that disrupt

adjacent basal laminae and possibly associated connective tissue fibrils. Deprived of these strengtheng elements, it might be expected that epithelial, muscular, and nervous tissue would be highly susceptible to disjunction. Indeed, close inspection of the process of epidermal separation along the ceratal autotomy plane of M. leonina recalls Stasek's (1967) translation of Quoy and Gaimard's (1832) description of pedal autotomy in the prosobranch Harpa ventricosa: "...the separation resembl[es] an ungluing rather than a tearing of tissues".

Rapid, irreversible loss of tensile strength by collagenous structures is the central mechanism of autotomy in echinoderms. Three of the best studied cases are: arm autotomy in the ophiuroid, Ophiocomina nigra (Wilkie, 1978a; b; 1979; Wilkie and Emson, 1987), arm autotomy in the crinoid, Florometra serratissima (Holland and Grimmer, 1981), and evisceration in the dendrochirotid holothurian, Eupentacta quinquesemita (Byrne, 1985a; b; 1986). Evisceration requires tissue breakage at three widely separated sites within the animal.

Breakage at the autotomy planes of these three echinoderms usually involves mechanical failure of interstitial connective tissue (ligaments and dermal tissue), which contains banded fibrils resembling vertebrate type I collagen (see Wilkie, 1984). However, Wilkie and Emson (1987) have recently shown that autotomizing muscle tendons within the arms of O. nigra are derived from the basal lamina of muscle cells and consist of non-banded fibrils resembling collagen type IV embedded within a markedly carbohydrate-rich matrix. In addition, Byrne (1985a) noted disruption of muscle basal laminae in the autotomizing introvert of E. quinquesemita and dissociation of peritoneum from the basal lamina at two other autotomizing sites during evisceration of this holothurian.

Echinoderm autotomy is an extreme and irreversible expression of a more widespread ability by many echinoderm collagenous structures to rapidly, yet reversibly, switch

between extensible and inextensible ('catch') states (see reviews by Emson and Wilkie, 1980; Wilkie, 1984; Motokawa, 1984). Although the mechanism for this phenomenon is still speculative, a number of studies, particularly the excellent work of Hidaka and Takahashi (1983) on the catch apparatus of echinoid spines, suggest that collagen fibrils themselves are not broken down during the extensible state. Instead, collagen fibrils can slip past one another during the extensible state, but become locked in place during the catch state. Similarly, degradation of collagen fibrils does not appear to occur during autotomy in echinoderms (Wilkie, 1978a; Holland and Grimmer, 1981; Byrne, 1985a).

It is currently thought that the collagen fibrils of these variable tensility connective tissues are interlinked by non-covalent interactions with and between ground substance proteoglycans and glycoproteins. Variable tensility may result from alteration of these weak (particularly electrostatic) interactions by active control of local pH or cation concentration (see Wilkie, 1984; Motokawa, 1984). This hypothesis is consistent with in vitro results, obtained from a number of echinoderm collagenous structures, showing sensitivity of their mechanical properties to pH, ionic strength, divalent cation concentration (particularly calcium ion), and calcium ion chelators (Wilkie, 1978b; 1983; Smith et al., 1981; Eylers, 1982; Hidaka, 1983; Byrne, 1985b).

The variable tensility connective tissues of echinoderms are infiltrated by cytoplasmic processes of acidophilc cells that, in electron micrographs, contain large, spherical or oval dense-cored vesicles (LDVs) (see review by Wilkie, 1984). Using histochemical techniques, Wilkie (1979) found evidence of glycoprotein and calcium within the granules of the arm autotomy zones in the ophiuroid, O. nigra. He speculated that the glycoprotein may trigger autotomy changes in collagenous structures by chelating calcium ions within the extracellular matrix or by a more subtle cation exchange mechanism. Wilkie and Emson (1987) showed a bleaching of the granular product within the LDVs of autotomizing

muscle tendons in O. nigra. However, Holland and Grimmer (1981) found ultrastructural evidence of granule exocytosis in autotomizing arms of the crinoid, F. serratissima. Their scanning electron micrographs of calcareous ossicles adjacent to the level of arm breakage show erosion of the ossicles, suggesting exposure to an acid medium or calcium chelator during the autotomy process. Byrne (1985a) failed to find evidence of LDV degranulation in autotomizing tissues of the holothurian E. quinquesemita. She (Byrne, 1986), along with Smith and Greenberg (1973) propose that a chemical factor, which can be isolated from coelomic fluid of eviscerating holothurians, directly or indirectly triggers the mechanical failure of collagenous structures during evisceration.

Except for holothurian evisceration, their is good evidence that reversible tensility changes and irreversible autotomy phenomena in echinoderms are under direct nervous control. For example, ophiuroid arm autotomy occurs within seconds after an adequate stimulus. Anaesthetics block the response in vivo and also block the rapid drop in tensile strength of the intervertebral ligament induced in vitro by elevated potassium ion concentration (Wilkie, 1978b). Hyponeural nerves are associated with the granule-filled cells ('juxtaligamental cells') within the arm autotomy zones of O. nigra (Wilkie, 1979). The catch apparatus of sea urchin spines, which is capable of reversible changes in tensile strength, becomes extensible following application of adrenalin and stiffens following application of acetylcholine (Hidaka and Takahashi, 1983).

The ceratal autotomy plane of M. leonina, examined before and after autotomy, reveals several striking structural similarities to autotomy planes within echinoderms. Firstly, the autotomy plane of M. leonina is not inherently fragile. This is also true of the autotomy planes of echinoderms, as first emphasized by Wilkie (1978a) while studying ophiuroid arm autotomy. Secondly, prior to ceratal autotomy, granule-filled cytoplasmic processes of GC impinge on basal laminae and associated connective tissue fibrils of all ceratal

structures where they cross the autotomy plane, and degranulation occurs coincident with ceratal separation. The granules and cytoplasmic features of the GC are structurally similar to the LDVs and their synthesizing cells associated with autotomizing and variable tensility connective tissues in echinoderms (Wilkie, 1979; 1984). Thirdly, the GCs of M. leonina and the granular cells associated with echinoderm autotomy zones are innervated. Finally, autotomy in M. leonina and in echinoderms is accompanied by disruption of connective tissue structures within the autotomy plane.

Prior to my study on ceratal autotomy in M. leonina, there had been no evidence from any phylum other than Echinodermata for rapid, neurally mediated control of the mechanical integrity of collagenous structures. In mammals, the softening of collagenous structures associated with the ovarian follicle during ovulation and within the uterine cervix and symphysis pubis during pregnancy and partuition, and the degradation of uterine collagen following partuition appear to be effected by enzymatic activity. These processes are under hormonal control and require hours or weeks rather than seconds to develop (see Rondell, 1970; Jeffery and Koob, 1980; Steinetz et al., 1980).

Additional research is required to determine if the connective tissue structures within the ceratal autotomy plane of M. leonina are collagenous, and to determine if enzymatic activity or control of chemical microenvironment is responsible for the breakdown of these structures. Future work should focus on examining the biochemical nature of GC granules by means of histochemical, cytochemical, and other methods.

It would be interesting to examine the fine structure of autotomy planes within other molluscs to search for the presence of granule-filled cells as described here for M. leonina. It is intriguing that Kress (1968), using light microscopy, identified a granular zone around the base of the deciduous cerata of three species of Doto (Nudibranchia), although the GC granules of M. leonina are not resolvable in one µm sections. In the only

other ultrastructural study of the autotomy plane of a mollusc, Hodgson (1984) concluded that siphonal autotomy in two species of Solen (Bivalvia) is simply the result of muscular action and an inherent weakness of the autotomy planes in the form of reduced connective tissue. He does not describe granule-filled cells within the potential autotomy sites.

B. Muscles

Although the GC may provide the major mechanism for ceratal autotomy in M. leonina, the muscles of the ceras must play a contributory role. In living M. leonina, the most obvious structural change that immediately precedes ceratal autotomy is the marked contraction of the sphincter muscles and, less obviously, contraction of the longitudinal muscle bands.

The longitudinal muscle bands are composed of a staggered array of individual muscle cells in parallel alignment. Direct membrane junctional complexes between neighbouring muscle cells of the longitudinal bands are rare. Instead, muscle cells are indirectly linked to their neighbours via connective tissue fibrils, which are anchored to the sarcolemma by frequent hemifasciae adherentes. Twarog et al. (1973) and Nunzi and Franzini-Armstrong (1981) suggest that hemifasciae adherentes in molluscan non-striated muscle may allow some of the very large tension generated by these muscles to be safely transferred to connective tissue components. Normally, the connective tissue binding each longitudinal muscle band is sufficiently strong to withstand the tensile stress experienced during contraction of the component muscle cells, resulting in a shortening of the entire muscle band. However, if this connective tissue suddenly lost tensile strength where the longitudinal muscle bands cross the autotomy plane (presumably by the action of exocytosed granules from the GC), muscle cells on either side of the weakened connective tissue would separate when the muscle band contracted.

On either side of the autotomy plane, the longitudinal muscle bands are attached to the epidermis via the two sphincter muscles. Consequently, once the longitudinal muscle bands have broken, tensile stress must be transmitted to the epidermis at the level of the autotomy plane. Cytoplasmic extensions from the GC are associated with the epidermis at the level where this stress would be experienced.

At least three functions can be envisaged for contraction of the subepidermal sphincter muscles during autotomy. Firstly, sphincter contraction must prevent haemal fluid from leaving the ceras during contraction of the longitudinal muscle bands. This would provide the ceras with a rigid hydraulic skeleton, allowing the contracting longitudinal muscle bands on the ceratal side of the autotomy plane to generate the large tensile stresses that help to separate tissues. Secondly, sphincter contraction may assist in breaking the longitudinal muscle bands by exerting an additional stress, directed at right angles to that generated by contraction of the muscle band itself, on the autotomy planes of these muscles. Finally, as previously suggested by Graham (1938) for the ceratal sphincter muscles of several aeolids, a major function of the subepidermal and digestive sphincters must be for wound closure to prevent haemolymph loss following ceratal autotomy. McVean (1982) proposed that autotomy may have evolved initially as a means to limit the effect on the whole animal of random injuries sustained by an appendage. By converting all types of severe damage to one predictable injury, "all regenerating and wound healing resources can then be invested in this region" (McVean, 1982).

My morphological and behavioural evidence suggests that GC and ceratal muscles are synaptically driven to provide the direct mechanism for ceratal autotomy. Nevertheless, I cannot eliminate the possibility that a neurosecretory substance, released into the haemocoel from a site outside the autotomy zone, might play a facilitory role. This possibility is discussed further in Ch. 3.

C. Function of Ceratal Autotomy

Stasek (1967) characterized autotomy in the Mollusca by a list of 11 conditions, which might apply equally well to other animals. His final two conditions state that autotomy must be functionally advantageous (presumably for escape), and additional behaviours may exist together with autotomy to facilitate escape from predators. The high incidence of regenerating cerata in field populations of M. leonina argue that ceratal autotomy is a frequent and important act during the life of this nudibranch. The three most probable potential predators of M. leonina in its natural environment are seastars, fish, and crabs. As described in Ch. 4, predatory seastars do not trigger ceratal autotomy by M. leonina; most of these predators are repelled by secretions from the repugnatorial glands of this nudibranch. At least some fish are also repelled by the product of the repugnatorial glands, although the nudibranch will autotomize cerata if roughly mouthed. Predatory crabs, however, attack and eat M. leonina without hesitation. During over 50 hours of underwater observations on a dense population of M. leonina in Monterey Harbor (California, U.S.A.), Ajeska and Nybakken (1976) saw only five instances of predation on M. leonina and all five were by the kelp crab Pugettia producta. On several occasions, I observed M. leonina escape from the grasping chelae of an attacking crab by autotomizing one or more cerata held by the crab. The escape was facilitated by subsequent swimming behaviour by the nudibranch, which carried the slug beyond the grasp of the crab. Water currents in the natural environment would surely assist the latter part of this escape strategy. Edmunds (1966) has also speculated that ceratal autotomy may protect nudibranchs from crab predators.

Ceratal loss in M. leonina is a classic example of autotomy according to Frédéricq's (1883) original definition of the term. Evidence presented in this chapter suggests a mechanism for ceratal detachment and wound closure. The following chapter provides some insight into the neurological control of the event.

LITERATURE CITED

Ajeska, R.A., and J. Nybakken. 1976. Contributions to the biology of Melibe leonina (Gould, 1852) (Mollusca: Opisthobranchia). Veliger 19: 19-26.

Audesirk, G., and T. Audesirk. 1980. Complex mechano-receptors in Tritonia diomedea 1. Responses to mechanical and chemical stimuli. J. comp. Physiol. 141: 101-109.

Baba, K., and I. Hamatani. 1965. The anatomy of Sakuraeolis enosimensis (Baba, 1930) N.G. (=Hervia ceylonica (?) Eliot, 1913) (Nudibranchia - Eolidoidea). Publ. Seto mar. biol. Lab. 13: 103-113.

Byrne, M. 1985a. Ultrastructural changes in the autotomy tissues of Eupentacta quinquesemita (Selenka) (Echinodermata: Holothuroidea) during evisceration. Pp. 413-420 in Proceedings of the Fifth International Echinoderm Conference, Galway, B.F. Keegan and B.D.S. O'Connor, eds. A.A. Balkema, Rotterdam.

Byrne, M. 1985b. The mechanical properties of the autotomy tissues of the holothurian Eupentacta quinquesemita and the effects of certain physico-chemical agents. J. exp. Biol. 117: 69-86.

Byrne, M. 1986. Induction of evisceration in the holothurian Eupentacta quinquesemita and evidence for the existence of an endogenous evisceration factor. J. exp. Biol. 120: 25-39.

Cloney, R.A., and E. Florey. 1968. Ultrastructure of cephalopod chromatophore organs. Z. Zellforsh. mikrosk. Anat. 89: 73-79.

Congdon, J.D., L.J. Vitt, and W.W. King. 1974. Geckos: adaptive significance and energetics of tail autotomy. Science, N.Y. 184: 1370-1380.

Dial, B.E., and L.C. Fitzpatrick. 1983. Lizard tail autotomy: function and energetics of postautotomy tail movement in Scincella lateralis. Science, N.Y. 219: 391-393.

Edmunds, M. 1966. Protective mechanisms in the Eolidacea (Mollusca Nudibranchia). J. Linn. Soc. (Zool.) 46: 27-71.

Emson, R.H., and I.C. Wilkie. 1980. Fission and autotomy in echinoderms. Oceanogr. mar. Biol. Ann. Rev. 18: 155-250.

Eylers, J.P. 1982. Ion-dependent viscosity of holothurian body wall and its implications for the functional morphology of echinoderms. J. exp. Biol. 99: 1-8.

Frédéricq, L. 1883. Sur l'autotomie ou mutilation par voie réflexe comme moyen de défense chez les animaux. Arch. Zool. exp. gén, Sér.2, 1: 413-426.

Graham, A. 1938. The structure and function of the alimentary canal of aeolid molluscs, with a discussion on their nematocysts. Trans. roy. Soc. Edinburgh 59: 267-307.

Hidaka, M. 1983. Effects of certain physico-chemical agents on the mechanical properties of the catch apparatus of the sea-urchin spine. J. exp. Biol. 103: 15-29.

Hidaka, M., and K. Takahashi. 1983. Fine structure and mechanical properties of the catch apparatus of the sea-urchin spine, a collagenous connective tissue with muscle-like holding capacity. J. exp. Biol. 103: 1-14.

Hodgson, A.N. 1984. Use of the intrinsic musculature for siphonal autotomy in the Solenacea (Mollusca: Bivalvia). Trans. roy. Soc. S. Afr. 45: 129-138.

Holland, N.D., and J.C. Grimmer. 1981. Fine structure of syzygial articulations before and after arm autotomy in Florometra serratissima (Echinodermata: Crinoidea). Zoomorph. 98: 169-183.

Hurst, A. 1968. The feeding mechanism and behavior pattern of the opisthobranch Melibe leonina. Symp. zool. Soc. Lond. 22: 151-166.

Jeffery, J.J., and T.H. Koob. 1980. Endocrine control of collagen degradation in the uterus. Pp. 135-145 in Dilation of the Uterine Cervix, F. Naftolin and P.G. Stubblefield, eds. Raven Press, New York.

Kress, A. 1968. Untersuchungen zur Histologie, Autotomie und Regeneration dreier Doto - Arten Doto coronata, D. pinnatifida, D. fragilis (Gastropoda, Opisthobranchiata). Revue suisse Zool. 75: 225-303.

McVean, A. 1973. Autotomy in Carcinus maenas (Decapoda: Crustacea). J. Zool., Lond. 169: 349-364.

McVean, A. 1974. The nervous control of autotomy in Carcinus maenas. J. exp. Biol. 60: 423-436.

McVean, A. 1975. Autotomy. Comp. Biochem. Physiol. 51A: 497-505.

McVean, A. 1982. Autotomy. Pp. 107-132 in Biology of Crustacea, vol. 4, D.C. Sandeman and H.L. Atwood, eds. Academic Press, New York.

McVean, A., and I. Findlay. 1976. Autotomy in Carcinus maenas: the role of the basi-ischiopodite posterior levator muscles. J. comp. Physiol. 110: 367-381.

Motokawa, T. 1984. Connective tissue catch in echinoderms. Biol. Rev. 59: 255-270.

Nicaise, G. 1973. The gliointerstitial system of molluscs. Int. Rev. Cytol. 34: 251-332.

Nunzi, M.G., and C. Franzini-Armstrong. 1981. The structure of smooth and striated portions of the adductor muscle of the valves in a scallop. J. ultrastruct. Res. 76: 134-148.

Plesch, 1977. An ultrastructural study of the musculature of the pond snail Lymnaea stagnalis (L.). Cell Tiss. Res. 180: 317-340.

Quoy, J.R.C., and J.P. Gaimard. 1832. Voyage de decouvertes de l'Astrolabe. Paris. Zoologie 2: 1-686.

Riggenbach, E. 1903. Die Selbstverstummelung der Tiere. Ergebrisse der Anatomie und Entwicklungsgeschichte 12: 782-903.

Rondell, P. 1970. Follicular processes in ovulation. Fedn. Proc. Fedn. Am. Socs. exp. Biol. 29: 1875-1879.

Ros, J. 1976. Sistemas de defensa en los opisthobranquios. Oecologia Aquatica 2: 41-71.

Sheppard, L., and A. d'A. Bellairs. 1972. The mechanism of autotomy in Lacerta. Brit. J. Herpetol. 4: 276-286.

Smith, G.N., and M.J. Greenberg. 1973. Chemical control of the evisceration process in Thyone briareus. Biol. Bull. 144: 421-436.

Smith, D.S., S.A. Wainwright, J. Baker, and M.L. Cayer. 1981. Structural features associated with movement and 'catch' of sea-urchin spines. Tissue and Cell 13: 299-320.

Stasek, C.R. 1967. Autotomy in the Mollusca. Occ. Pap. Calif. Acad. Sci. No. 61: 1-44.

Steinetz, B.G., E.M. O'Byrne, and R.L. Kroc. 1980. The role of relaxin in cervical softening during pregnancy in mammals. Pp. 156-177 in Dilation of the Uterine Cervix, F. Naftolin and P.G. Stubblefield, eds. Raven Press, New York

Thompson, T.E. 1960. Defensive adaptations in opisthobranchs. J. mar. biol. Ass. U.K. 39: 123-134.

Twarog, B.M., M.H. Dewey, and T. Hikado. 1973. The structure of Mytilus smooth muscle and the electrical constants of the resting muscle. J. gen. Physiol. 61: 207-221.

Wake, D.B., and I.G. Dresner, 1967. Functional morphology and evolution of tail autotomy in salamanders. J. Morph. 122: 265-306.

Wilkie, I.C. 1978a. Functional morphology of the autotomy plane of the brittlestar Ophiocomina nigra (Abildgaard) (Ophiuroidea, Echinodermata). Zoomorphology 91: 289-305.

Wilkie, I.C. 1978b. Nervously mediated change in the mechanical properties of a brittlestar ligament. Mar. Behav. Physiol. 5: 289-306.

Wilkie, I.C. 1979. The juxtaligamental cells of Ophiocomina nigra (Abildgaard) (Echinodermata: Ophiuroidea) and their possible role in mechano-effector function of collagenous tissue. Cell Tiss. Res. 197: 515-530.

Wilkie, I.C. 1983. Nervously mediated change in the mechanical properties of the cirral ligaments of a crinoid. Mar. Behav. Physiol. 9: 229-248.

Wilkie, I.C. 1984. Variable tensility in echinoderm collagenous tissues: a review. Mar. Behav. Physiol. 11: 1-34.

Wilkie, I.C., and R.H. Emson. 1987. The tendons of Ophiocomina nigra and their role in autotomy (Echinodermata, Ophiuroida). Zoomorphology 107: 33-44.

Figure 60: Ventral view of a live specimen of M. leonina showing the foot (F), the large oral hood (OH) surrounding the slit-like mouth (M), and the two rows of petaloid cerata (C) extending from the dorsal surface of the nudibranch. Scale bar = 1 cm.

Figure 61: Single ceras (C) of M. leonina in lateral view showing the opaque line (arrowhead) that marks the ceratal autotomy plane. The branched structure within the ceras is an extension of the digestive gland (DG). Scale bar = 4 mm.

Figure 62: Light micrograph showing the wound (W) in the dorsal body wall of M. leonina after autotomy of a ceras. Note the contracted sphincter muscle (arrowheads) that surrounds the wound. Scale bar = 0.5 mm.

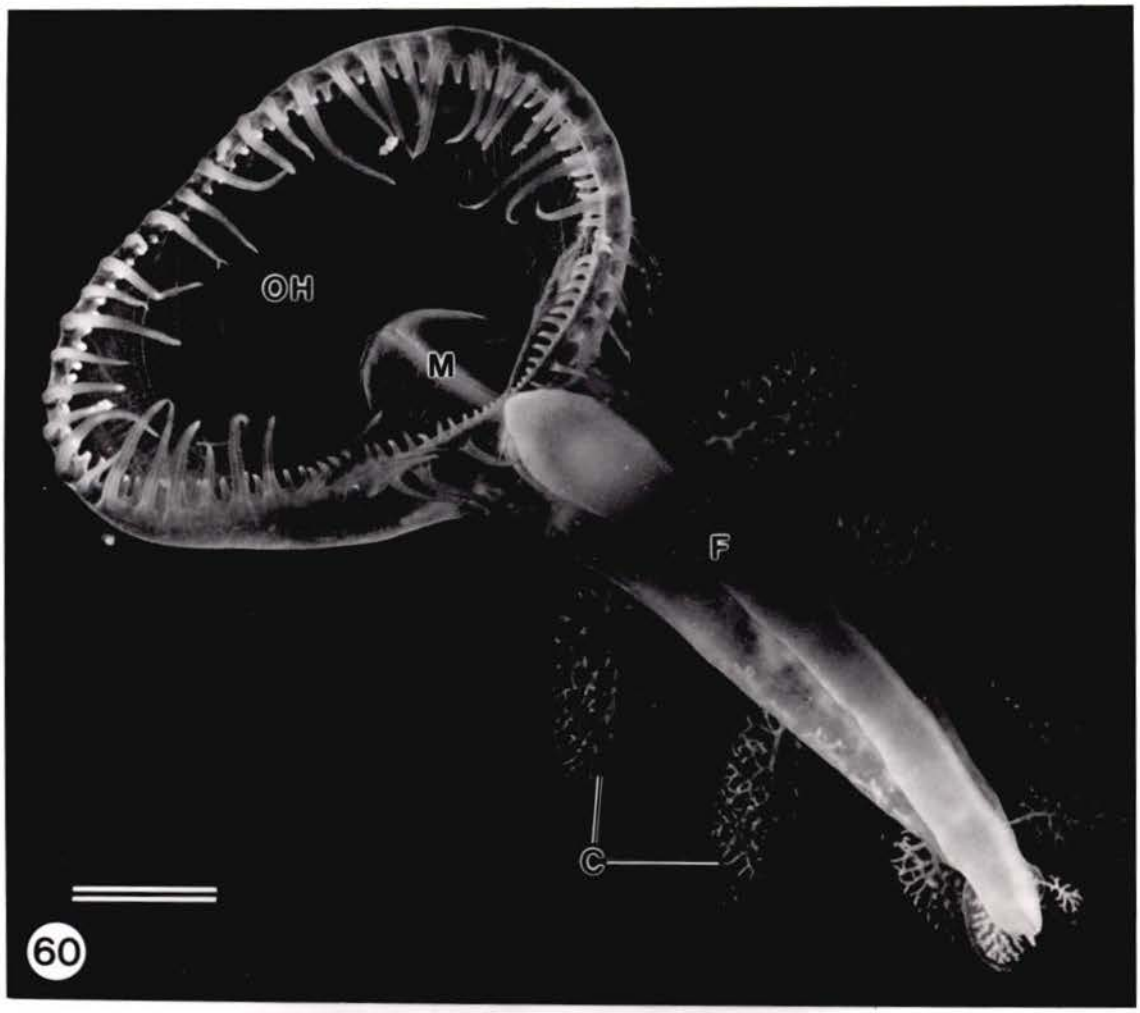

60

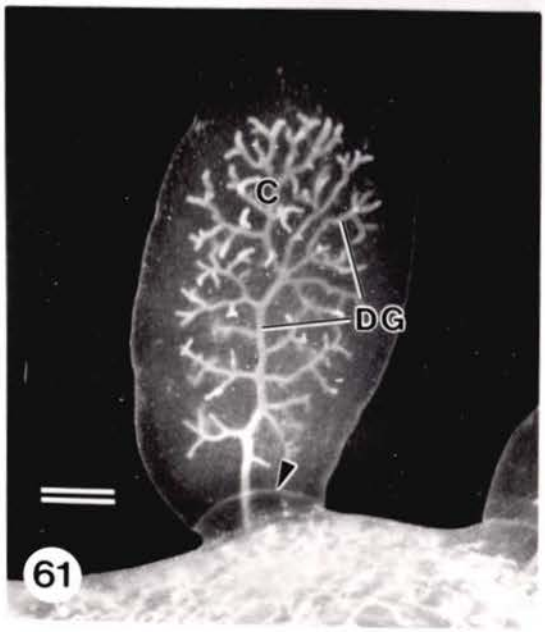

61

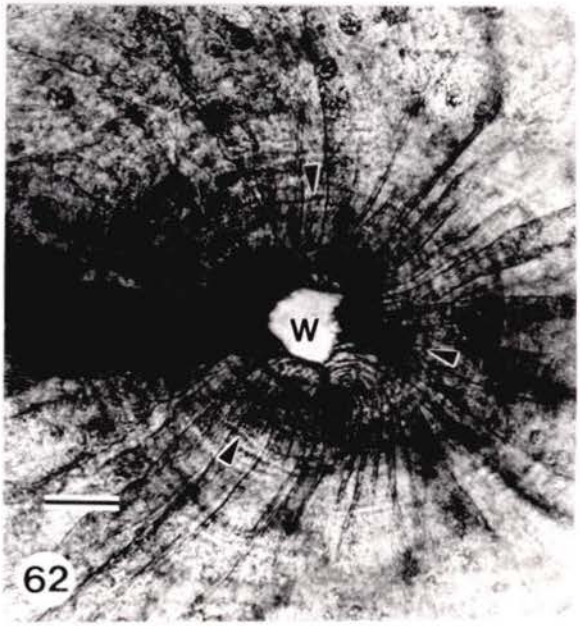

62

Figure 63: Sketch of a ceras of M. leonina showing structures that can be seen during dissection. Abbreviations are: AP, autotomy plane; AZ, autotomy zone; CN, ceratal nerve; DG, digestive gland; E, epidermis; LM, longitudinal muscle bands (only two shown); PN, pleural nerve; SM, sphincter muscle. Drawing not to scale.

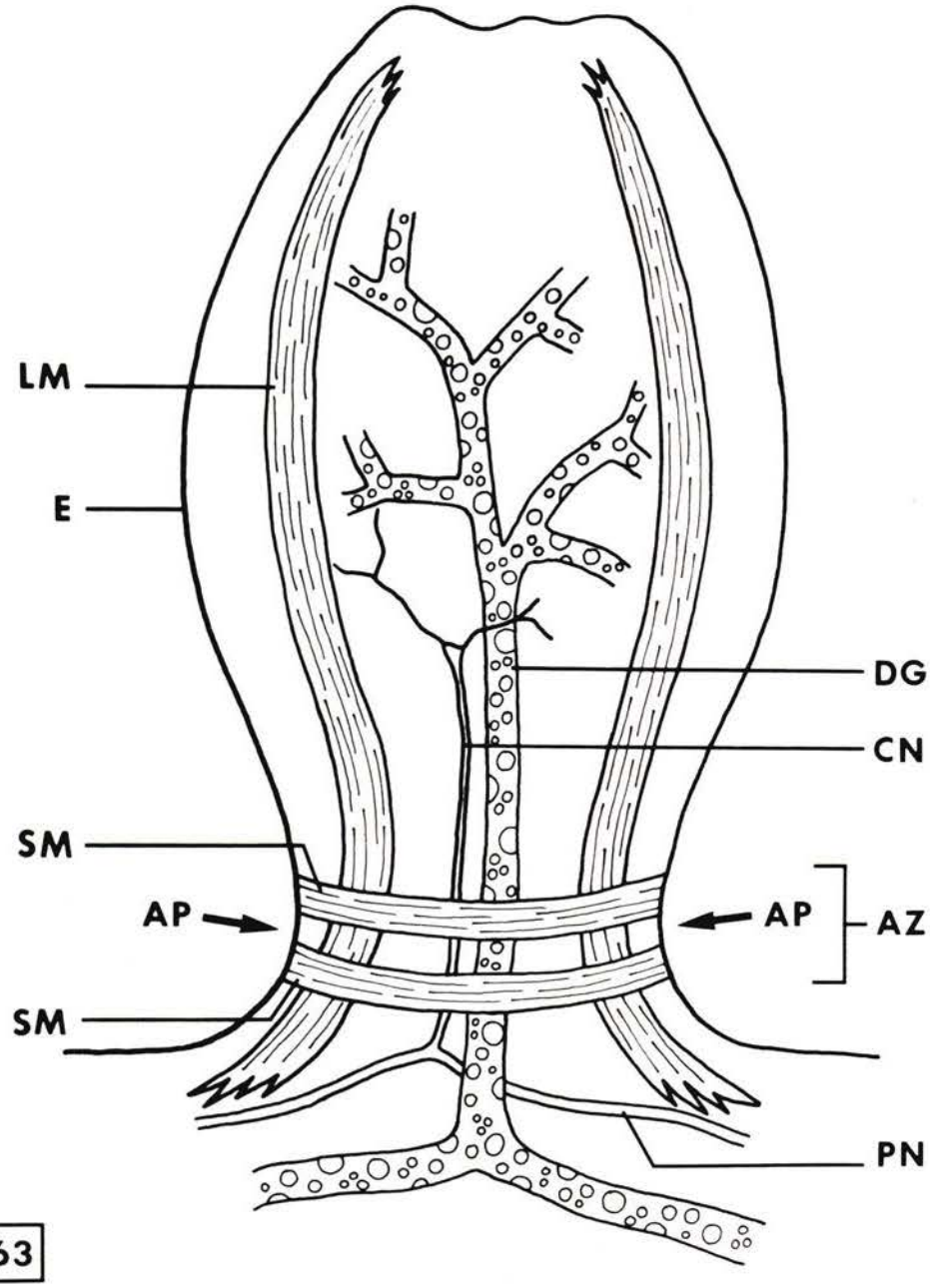

63

Figure 64: Transmission electronmicrograph (TEM) at low magnification showing the vacuolated, squamous epithelial cells forming much of the general ceratal epidermis (E) of M. leonina. Note subepidermal muscle fibres (MU). Scale bar = 5 µm.

Figure 65: TEM at low magnification showing a longitudinal section through the ceratal autotomy zone of M. leonina. The autotomy plane nerve (APN) lies at the level of the autotomy plane (large arrow labelled AP) and is flanked on either side by subepidermal sphincter muscles (SM). The epidermis (E) overlying the subepidermal sphincters is thickened, particularly on the body side of the APN. The latter epidermal cells have large nuclei (N) with prominent nucleoli. Scale bar = 5 µm.

Figure 66: TEM showing detail of the autotomy plane nerve from a tissue section neighboring that in Fig. 65. Note the axons (A) and a cell body of a granule-filled cell (GC). The arrowheads indicate where cytoplasmic processes of granule-filled cells come into close contact with the overlying epidermis (E). Scale bar = 3 µm.

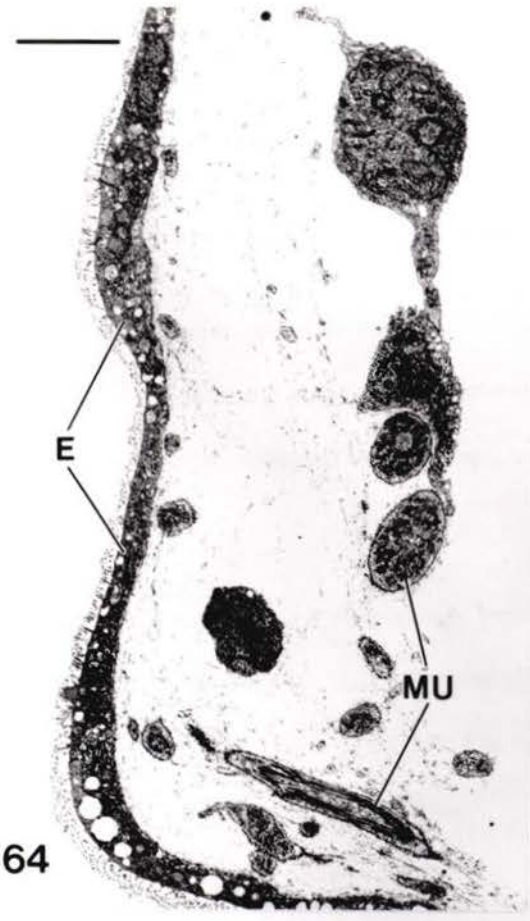

64

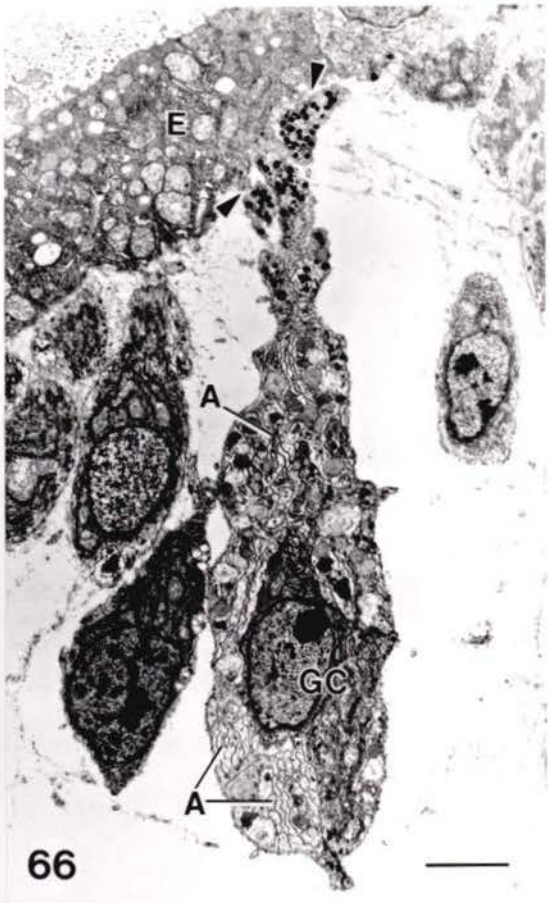

66

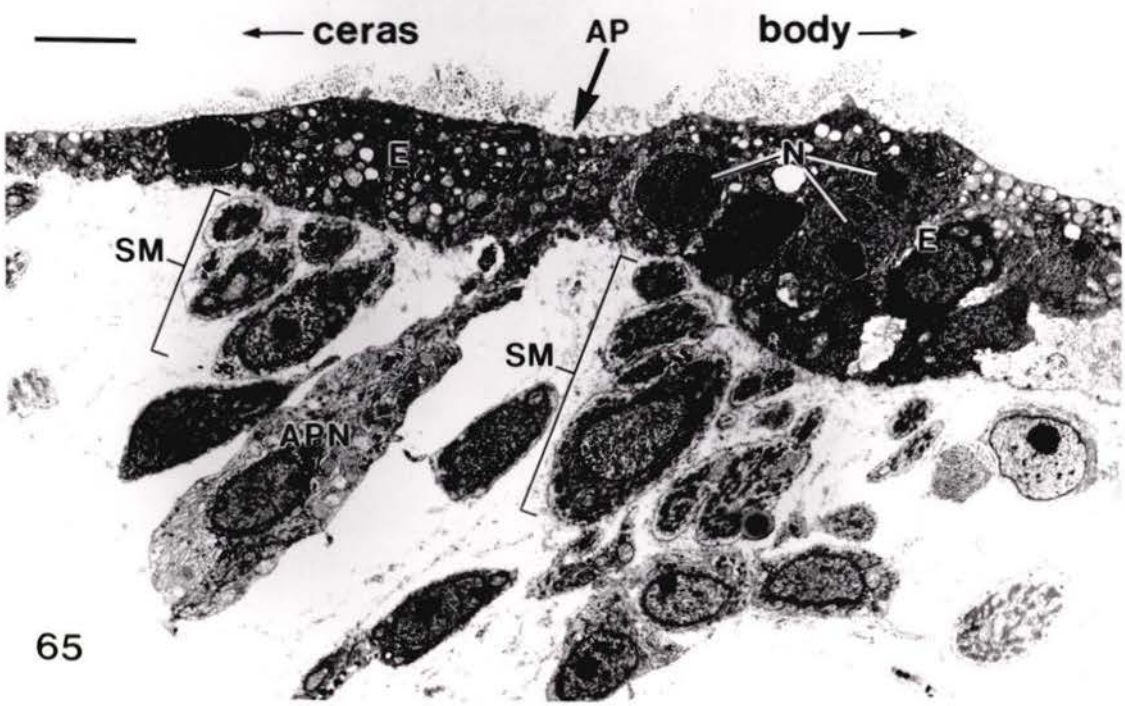

65

Figure 67: TEM of a granule-filled cell (GC) showing the nucleus (N) and a cytoplasmic process (demarcated by arrowheads) located alongside axons (A) of the autotomy plane nerve. The asterisk indicates where an axon forms a synapse onto the cytoplasmic process of the GC. Scale bar = 1 µm.

Figure 68: TEM showing the nucleus (N) and perinuclear cytoplasm of a granule-filled cell. The primary vesicles (arrowheads) produced by the Golgi (G) give rise to the characteristic, electron-dense granules (GR) within these cells. Scale bar = 0.5 µm.

Figure 69: TEM showing cytoplasmic processes from granule-filled cells (GC) closely applied to the basal lamina (asterisks) of the epidermis (E) at the level of the autotomy plane (enlarged from Fig.66). Arrowheads indicate smooth endoplasmic reticulum. Scale bar = 0.5 µm.

Figure 70: TEM showing detail of a synapse (demarcated by arrowheads) between an axon (A) within the APN and a cytoplasmic process of a granule-filled cell (GC). Scale bar = 0.5 µm.

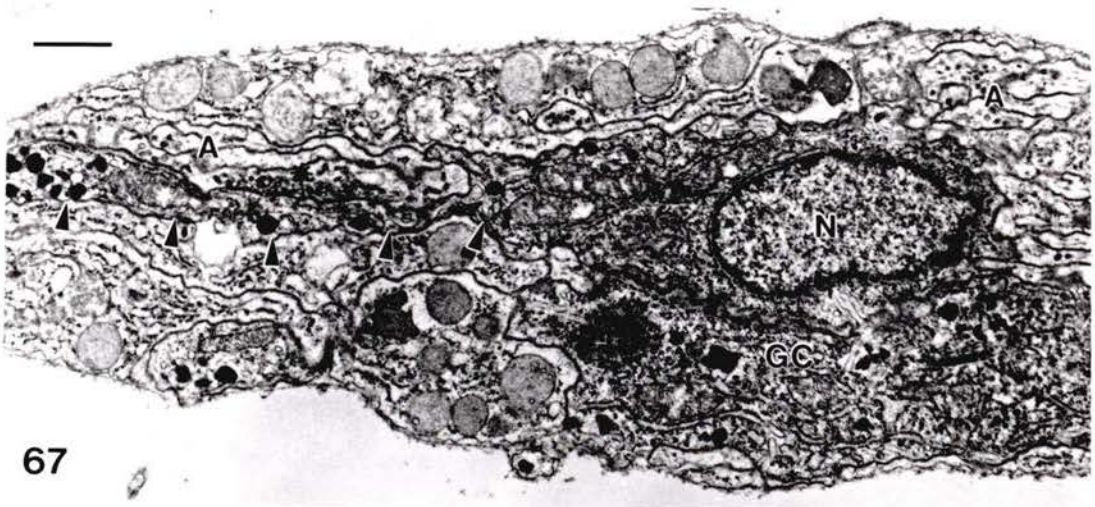

67

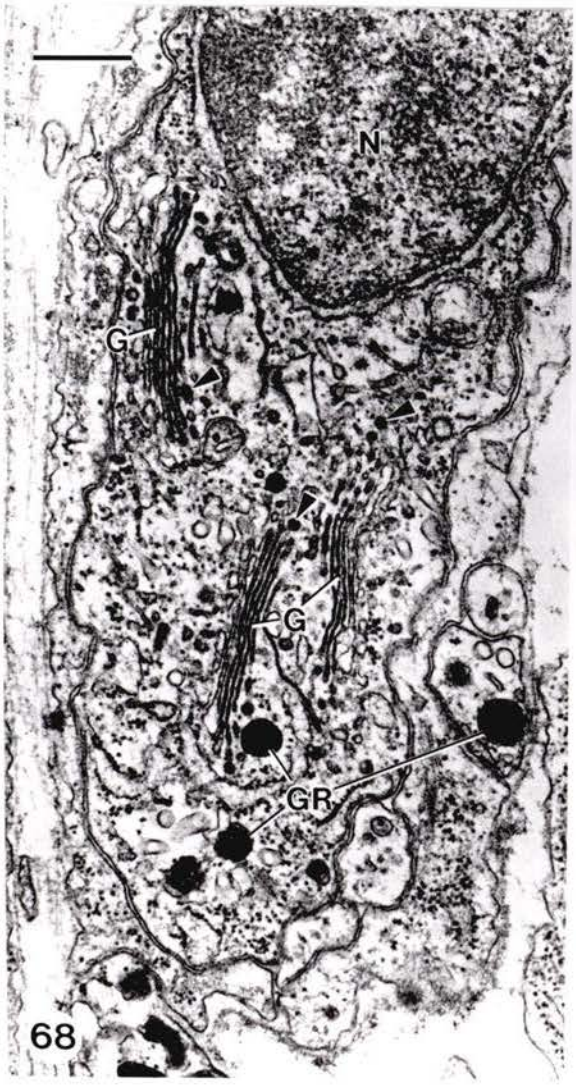

68

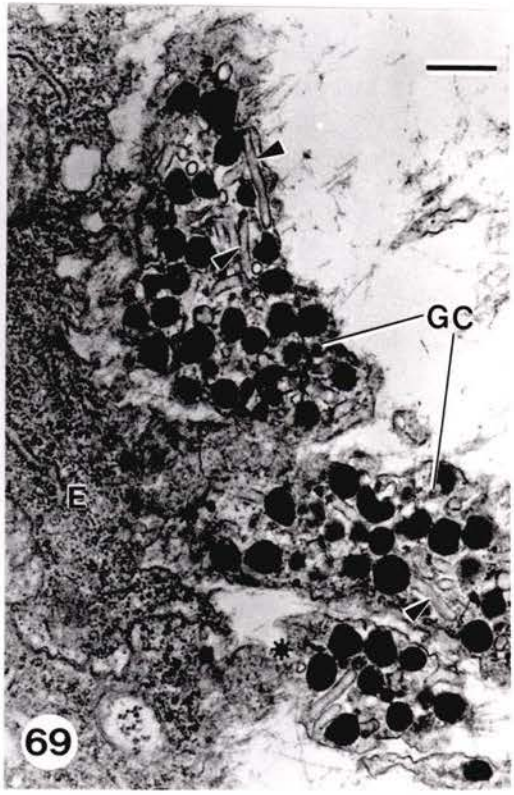

69

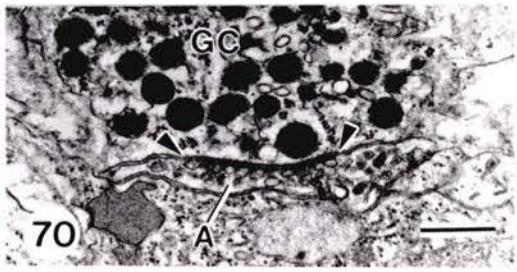

70

Figure 71: TEM of a slightly oblique cross-section through the subepidermal sphincter muscle on the body side of the autotomy plane. The section passes through the nuclei (N) of two muscle cells and through a cytoplasmic process of a gliointerstitial cell (GI). Hemifasciae adherentes (hemidesmosome-like structures) are indicated by arrowheads. Scale bar = 1 µm. Inset: Detail of a hemifascia adherens; S, sarcoplasm. Scale bar = 0.3 µm.

Figure 72: TEM showing the concentration of connective tissue fibrils (CF) between the muscle cells of a subepidermal sphincter (SM) and the overlying epidermis (E). Hemidesmosomes (arrowheads), with associated tonofilaments (T), attach the basal membrane of the epidermal cells to the basal lamina. Scale bar = 0.5 µm.

Figure 73: TEM of a neuromuscular synapse (arrowhead) onto a fibre of subepidermal sphincter muscle (SM). Scale bar = 0.5 µm.

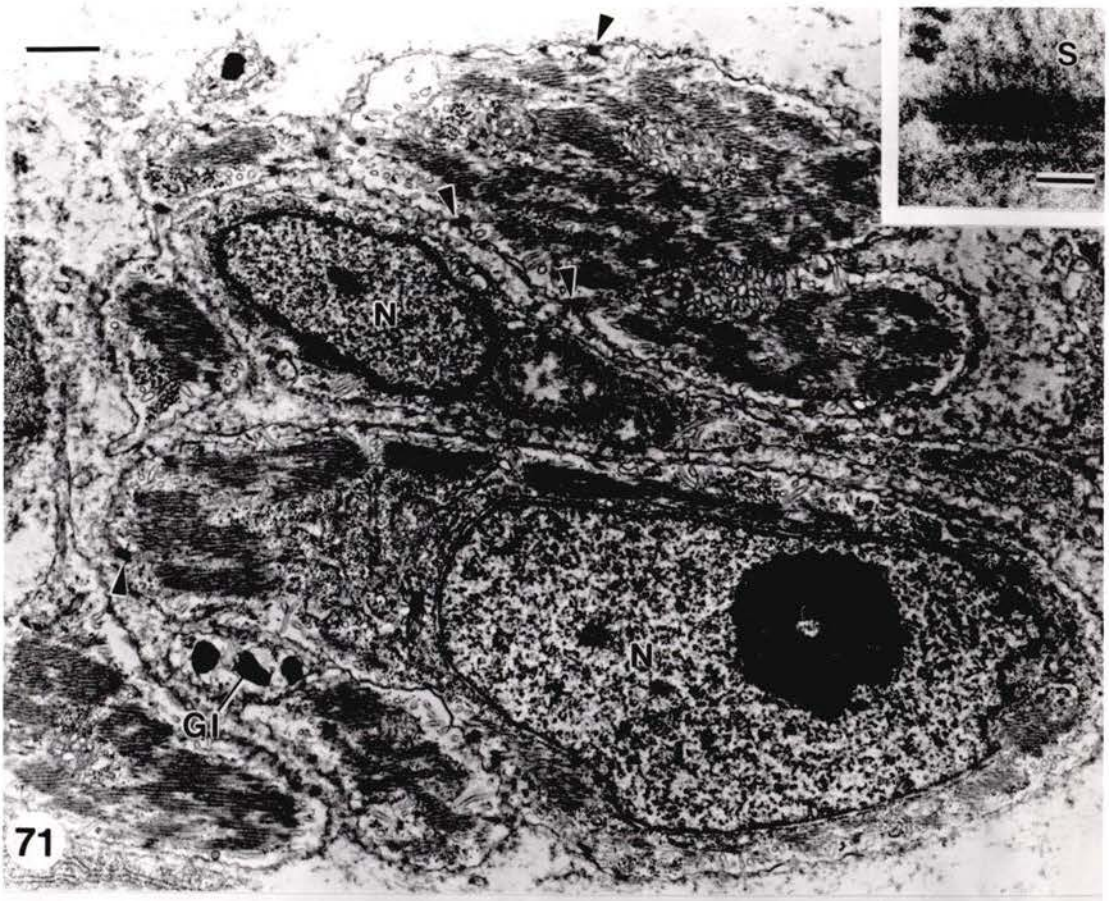
S
N
N
GI
71

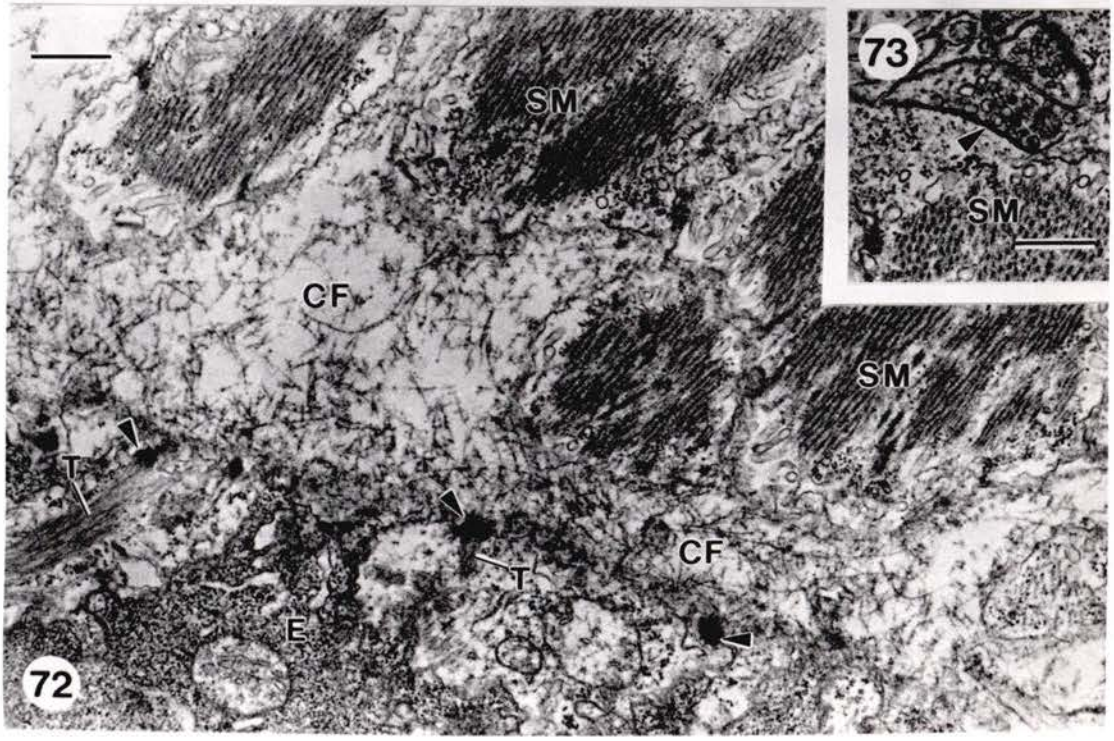
73
SM
SM
CF
SM
T
T
CF
E
72

Figure 74: TEM of a longitudinal section through the ceratal autotomy zone where a longitudinal muscle band (LM) penetrates the autotomy plane nerve (APN) with associated granule-filled cells (GC). The subepidermal sphincter muscles (SM) are situated close to the epidermis (E) on one side and the longitudinal muscle bands (LM) on the other side. Cytoplasmic processes of gliointerstitial cells (GI) are associated with the longitudinal muscle bands. Scale bar = 5 µm.

Figure 75: TEM showing an enlargement of the area in Fig. 74 where the longitudinal muscle band (LM) penetrates the autotomy plane nerve. Note the irregular plate of connective tissue (asterisks) extending across the muscle band and between (arrowheads) the muscle fibres themselves. Processes of granule-filled cells (GC) interdigitate with the muscle fibres on the ceratal side of the connective tissue plate. Scale bar = 1 µm.

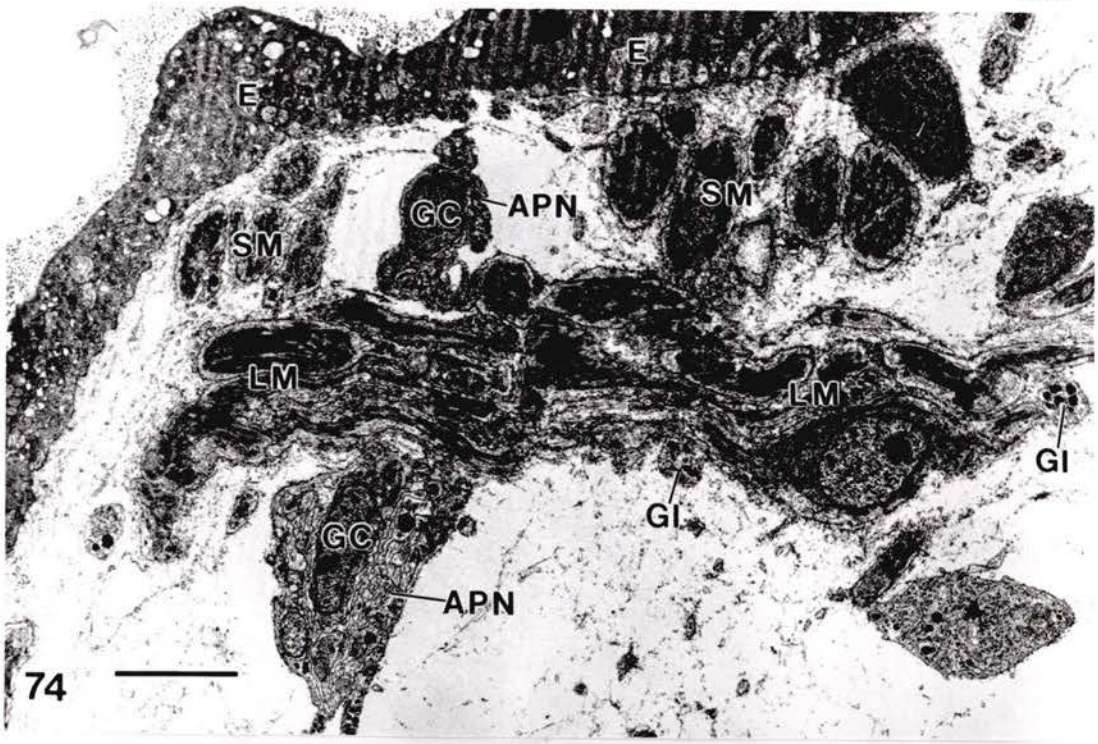
E
E
GC
APN
SM
SM
LM
LM
GI
GI
GC
APN
74

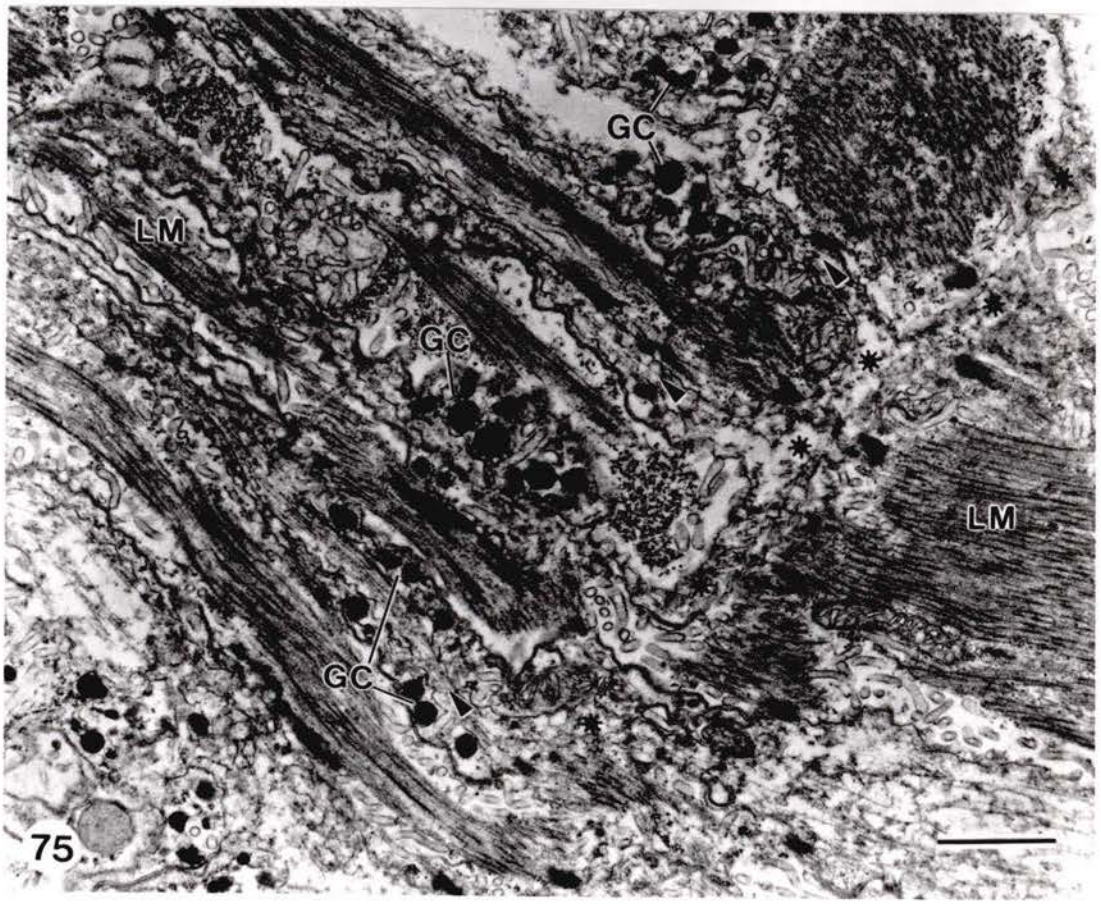
GC
LM
GC
LM
GC
75

Figure 76: TEM showing concentration of connective tissue fibrils (asterisks) between longitudinal muscles (LM) and a circular fibre of the subepidermal sphincter muscle (SM). Arrowheads indicate hemifasciae adherentes along the sarcolemmae of the two muscle types. Scale bar = 0.5 µm.

Figure 77: TEM of a neuromuscular synapse (demarcated by arrowheads) onto a longitudinal muscle fibre (LM). Scale bar = 0.3 µm.

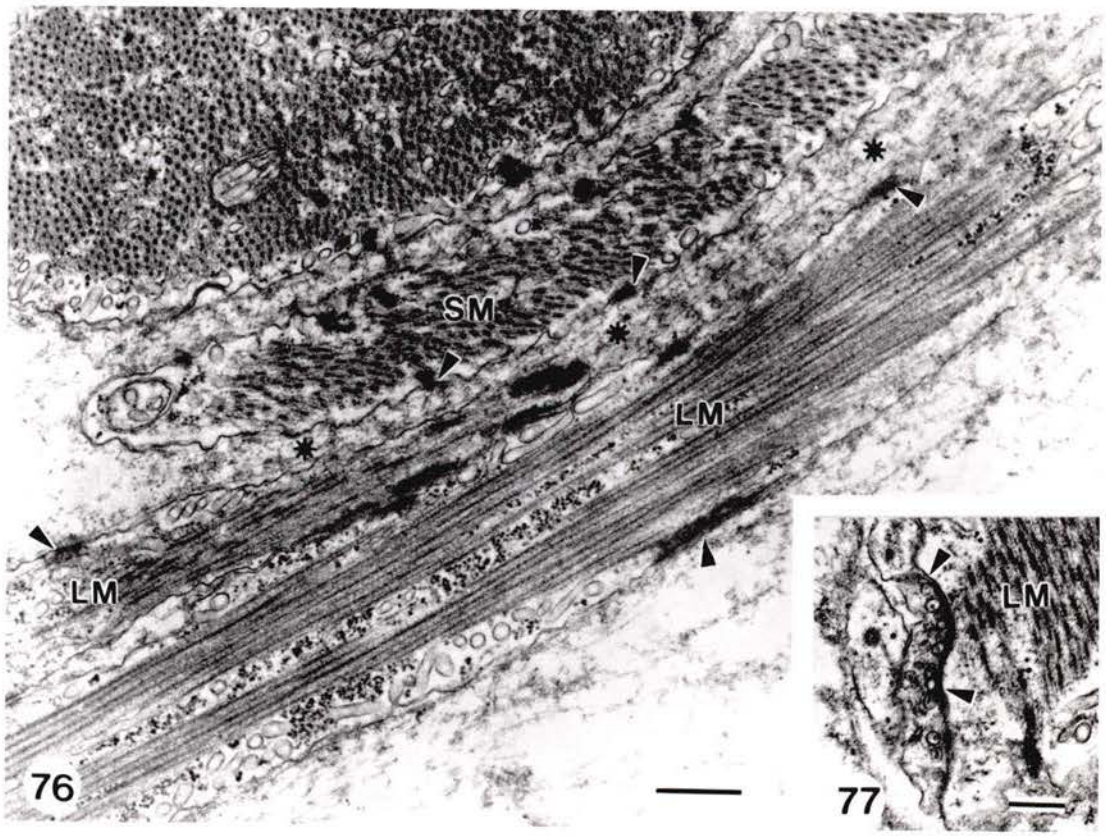
SM
LM
LM
76
LM
77

Figure 78: Summary diagram of the relationships between the major structures associated with the body wall in the ceratal autotomy zone of M. leonina. The digestive gland and ceratal nerve are not shown. The small x's indicate where two structures are joined by connective tissue fibrils. The autotomy plane nerve (APN), which arises as a branch of the ceratal nerve, runs immediately beneath the epidermis (E) at the level of the autotomy plane (AP) and is flanked on either side by a subepidermal sphincter muscle (SM). The sphincter muscles are attached to the overlying epidermis. Within the autotomy zone (AZ), the longitudinal muscle bands (LM) are attached to the two sphincter muscles and are enveloped by the autotomy plane nerve. Drawing not to scale.

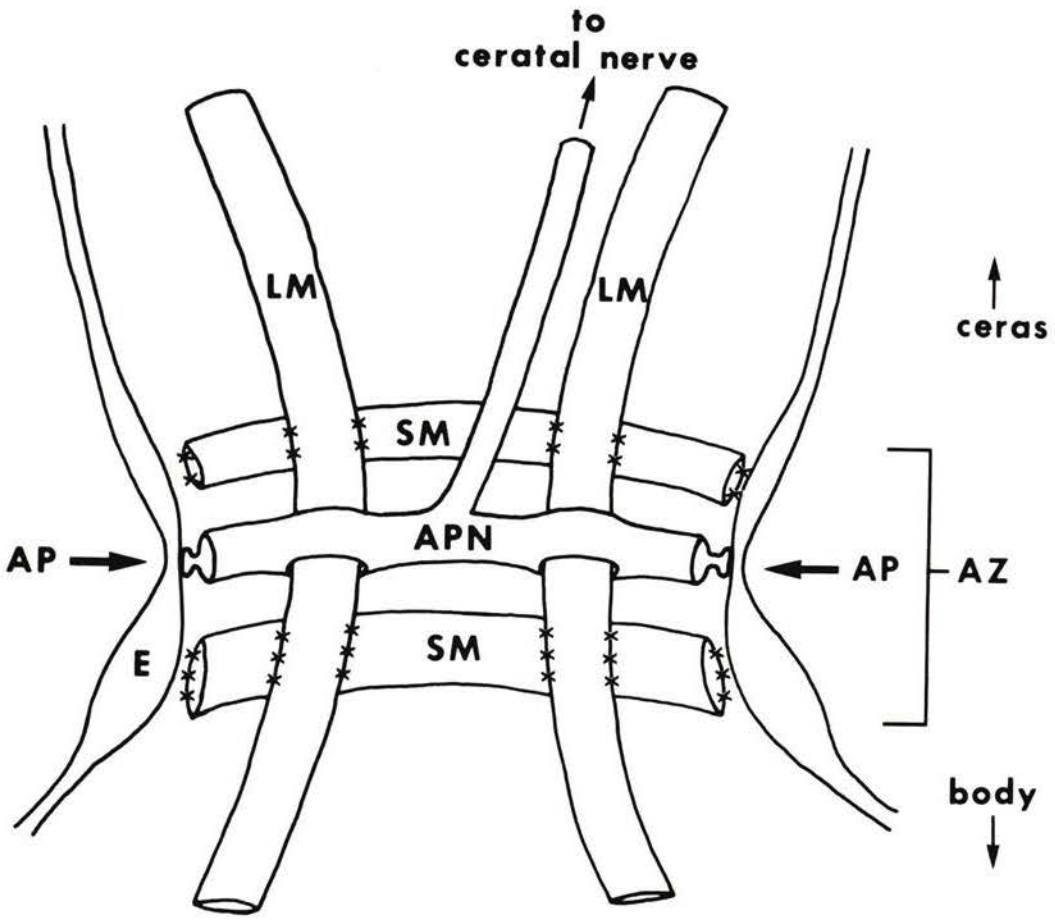

78

Figure 79: TEM of a gliointerstitial cell (GI), with characteristic granules (arrowheads), associated with several muscle cells (MU). Scale bar = 1 μm.

Figure 80: TEM of granules within a cytoplasmic process of a GC associated with the autotomy plane nerve. Scale bar = 0.3 μm.

Figure 81: TEM of granules within a cytoplasmic process of a gliointerstitial cell. Scale bar = 0.3 μm

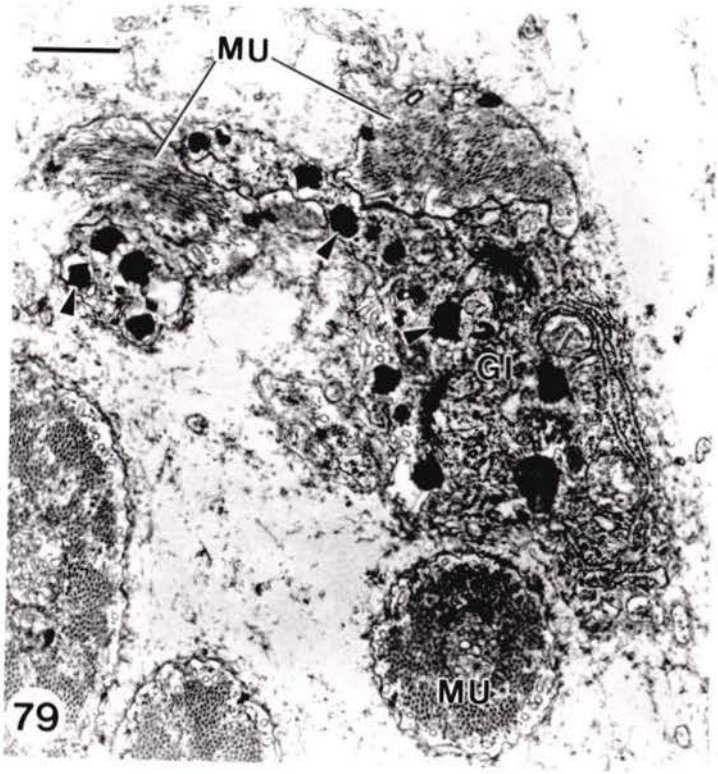
MU
GI
MU
79

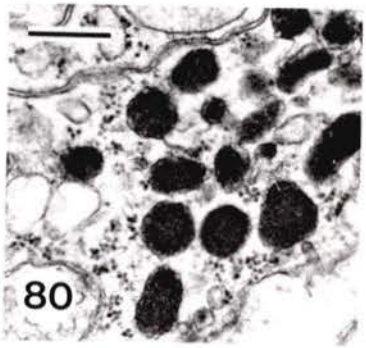
80

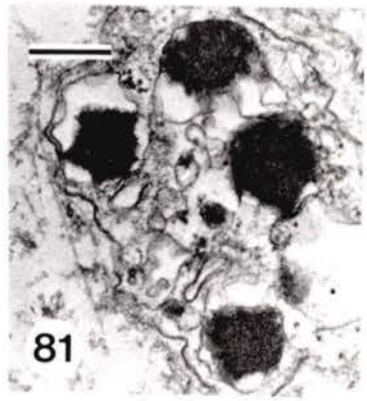
81

Figure 82: TEM at low magnification of a longitudinal section through the digestive gland (DG) where it extends across the autotomy zone. The large sphincter muscle (DS) is located on the body side of the autotomy plane. A second large sphincter on the ceratal side of the autotomy plane is beyond the upper edge of this micrograph. The arrows indicate two profiles of the nerve ring that encircles the digestive gland at the level of the autotomy plane (see Fig. 84 for enlargement of one of these profiles). Scale bar = 10 µm.

Figure 83: TEM of a cross-section through a portion of one of the major sphincters (DS) surrounding the digestive gland (DG) (enlarged from Fig. 82). Scale bar = 2 µm.

Figure 84: TEM of a cross-section through the nerve ring (NR) that surrounds the digestive gland (DG) (enlarged from Fig. 82). Note the cell body (GC) and cytoplasmic processes (arrowheads) of granule-filled cells. Scale bar = 2 µm.

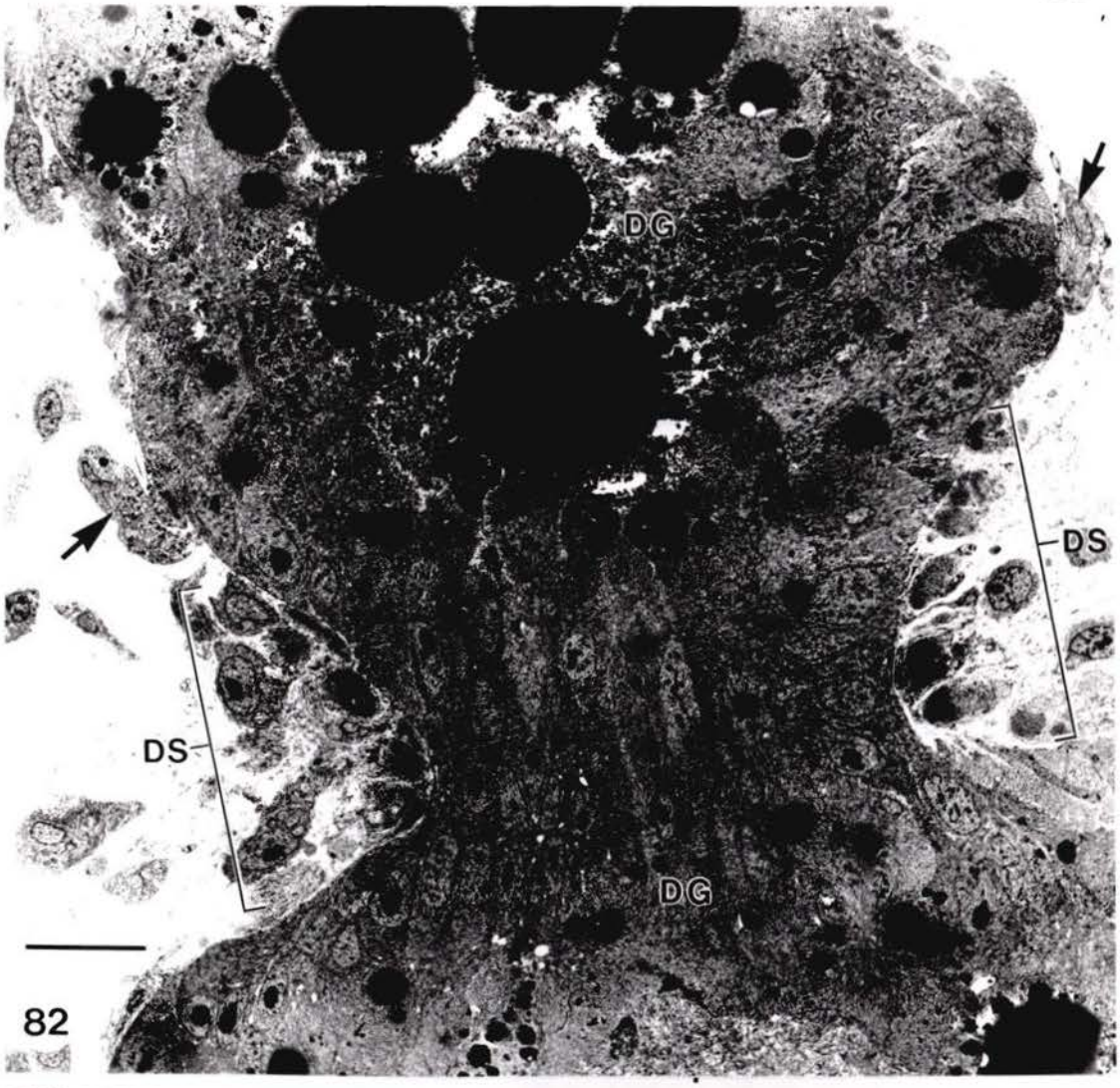

82

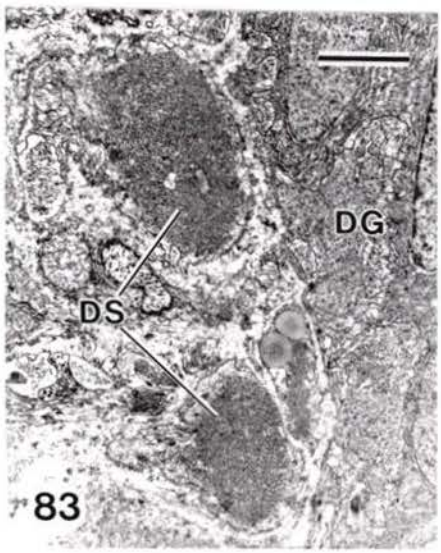

83

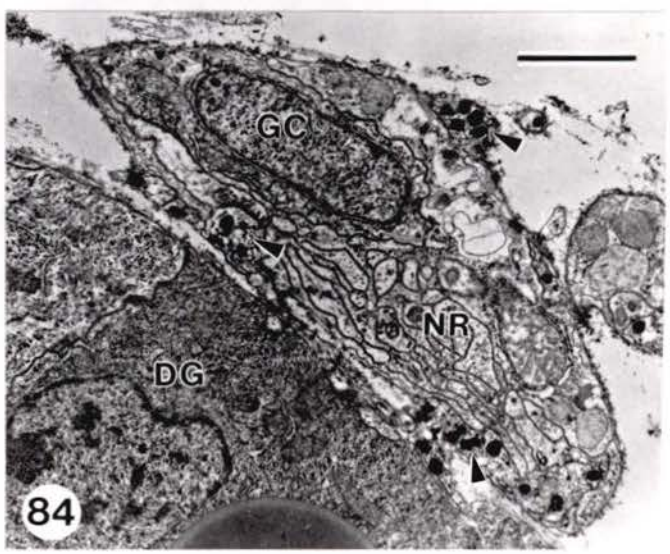

84

Figure 85: TEM at low magnification showing a branch (arrows) of the autotomy plane nerve (APN) that extends to the wall of the digestive gland (DG). Other abbreviations are: CN, ceratal nerve as it approaches the autotomy plane; DS, digestive gland sphincter (body side of the autotomy plane); E, epidermis; and, SM subepidermal sphincer muscles. Scale bar = 10 µm.

Figure 86: TEM showing where a branch (arrow) of the autotomy plane nerve unites with the nerve ring (NR) that encircles the digestive gland (DG) at the level of the autotomy plane (enlarged from Fig. 85). Profiles of axons (A) and cell bodies of granule-filled cells (GC) are present within the nerve ring. Arrowheads indicate granule-filled cytoplasmic processes adjacent to the wall of the digestive gland. Scale bar = 2 µm.

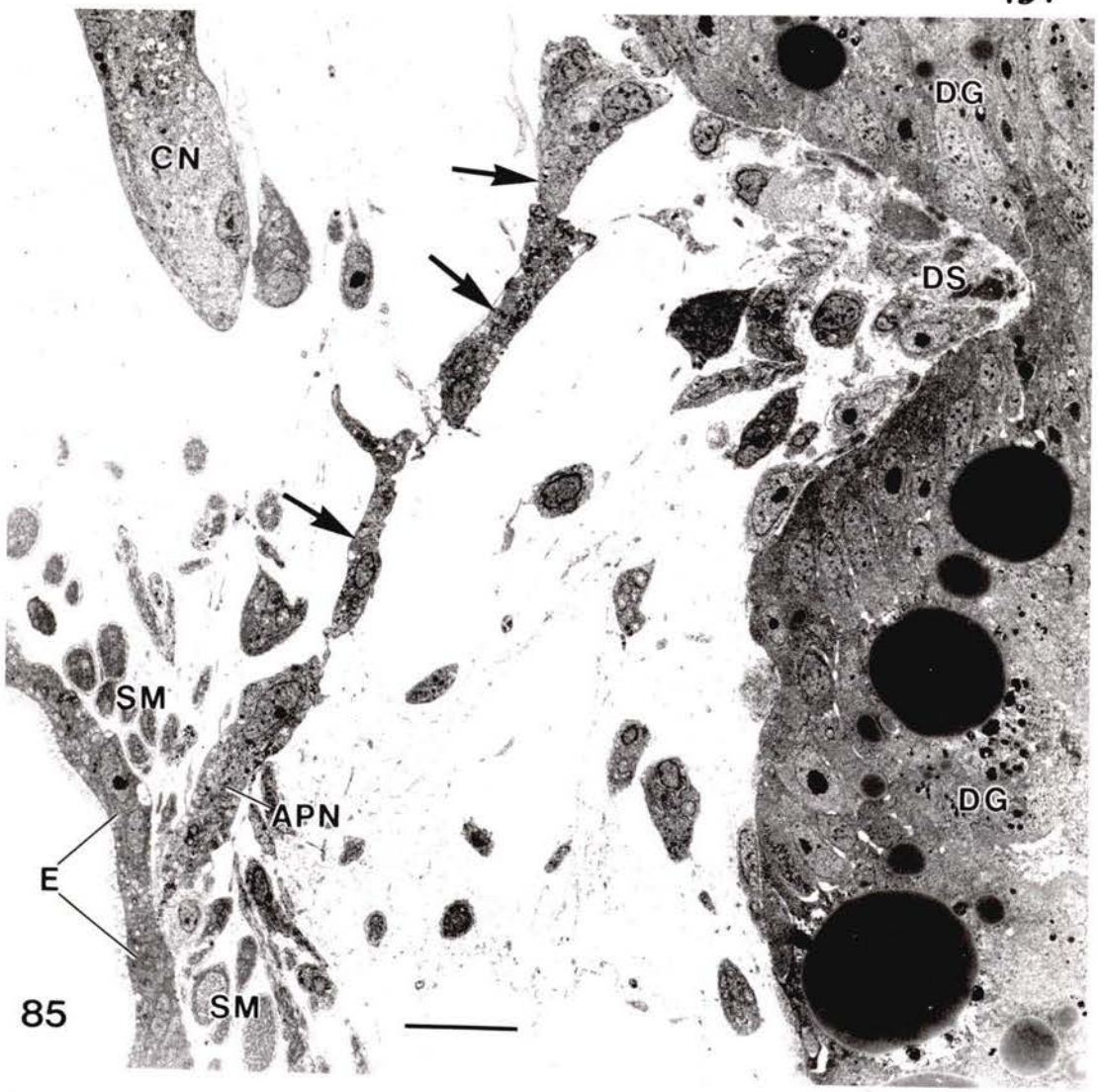

85

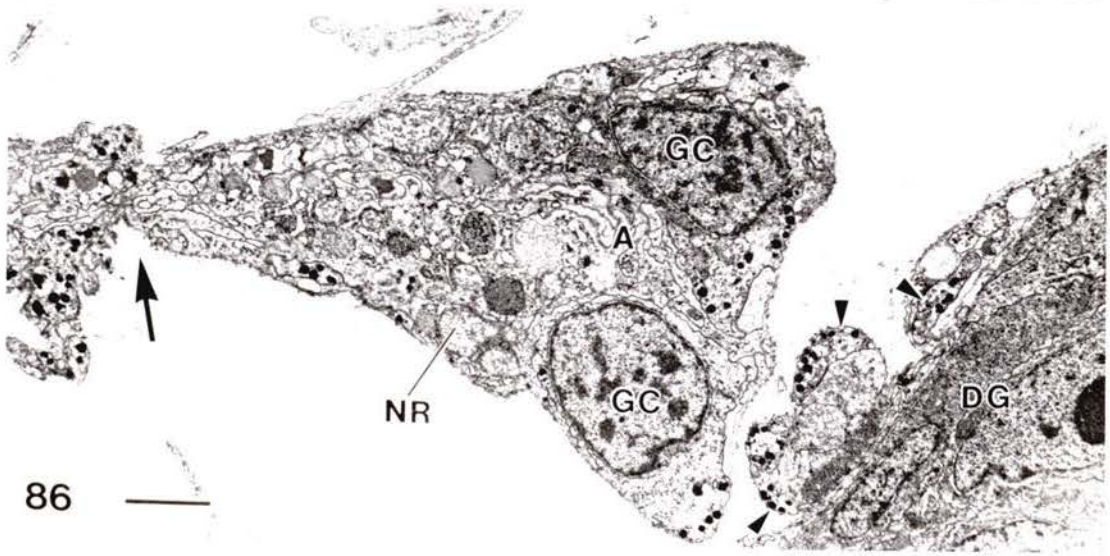

86

Figure 87: TEM of a longitudinal section through the ceratal autotomy zone where the ceratal nerve (CN) penetrates an extension of the autotomy plane nerve (APN). The ceratal nerve runs obliquely through the section. A granule-filled cell (GC) lies within the perineurium of the ceratal nerve. Scale bar = 3 µm.

Figure 88: A peripheral portion of the ceratal nerve (CN) within the autotomy plane showing cytoplasmic processes of granule-filled cells (large arrows) lying adjacent to the perineurium (small arrows) of the ceratal nerve. Scale bar = 1 µm.

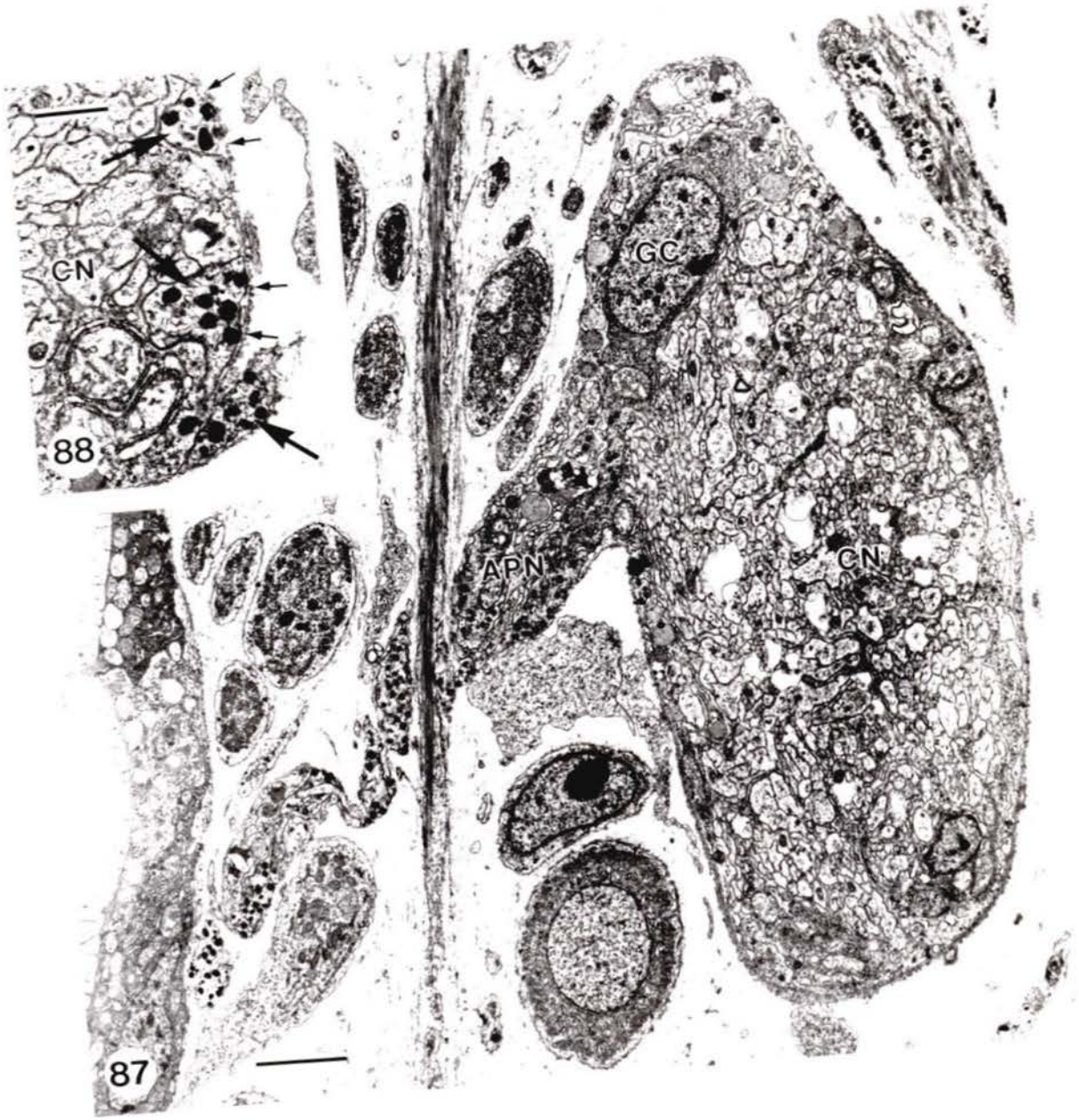
CN
88
GC
APN
CN
87

Figure 89: Summary diagram of the major nerves located within the base of the ceras and adjacent dorsum of the body in M. leonina. The stippled nerves are those that include granule-filled cells. The ceratal nerve (CN), after arising from the pleural nerve (PN), enters the ceras and gives rise to a connective (CO) that links the ceratal nerve with the circular autotomy plane nerve (APN). The APN lies immediately beneath the ceratal epidermis at the level of the autotomy plane (large arrows labelled AP). Two or more branches (small arrows) of the autotomy plane nerve extend to a nerve ring (NR) that encircles the digestive gland (DG). Two major sphincter muscles (DS) surround the digestive gland on either side of the nerve ring. The occasional circular muscles associated with the digestive gland are not shown. Drawing not to scale.

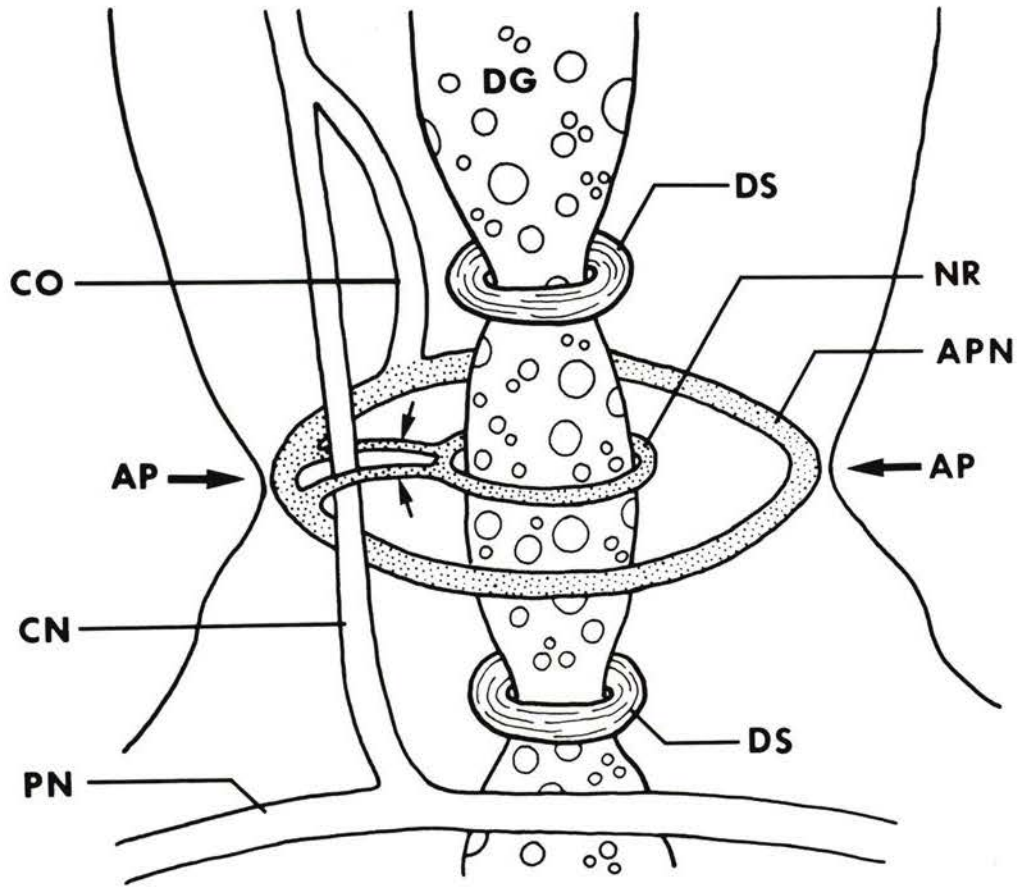

89

Figure 90: TEM of a low magnification, longitudinal section through an autotomized ceras adjacent to the level of detachment. The detached stump of the digestive gland (DG) protrudes slightly beyond where the epidermis (E) has broken (large arrow). The autotomy plane nerve (APN) lies beneath the terminal epidermal cells (see Fig. 92) and the longitudinal muscle band (LM) has broken just beyond its association with the subepidermal sphincter muscle (SM), where the LM meets the APN. The digestive gland (DG), prior to its point of breakage, is constricted by a large sphincter muscle (DS) and by occasional circular mucles (OC) that invest this organ. Scale bar = 10 µm.


LM
DG
E
LM
DS
SM
E
APN
OC
DG
DS
90
OC

Figure 91: TEM of the subepidermal sphincter muscle (SM) within an autotomized ceras (enlarged from Fig. 90). Connective tissue fibrils (CT) are concentrated between the epidermis (E) and the muscle cells of the sphincter and between the sphincter muscle cells and an adjacent cell of the longitudinal muscle band (LM). Note the prominent basal lamina (arrowheads) underlying the epidermis. Scale bar = 1 µm.

91

Figure 92: TEM of a terminal epidermal cell (E) and underlying axons of the APN within an autotomized ceras (enlarged from Fig. 90; overlaps Fig. 91). Basal lamina and connective tissue fibrils are not present beneath the epidermal cell overlying the APN; the termination of the epidermal basal lamina, just beyond the subepidermal sphincter muscle (SM) is marked by an arrow. An apparent GC is devoid of granules, but a small cluster of granules (arrowhead) remains within a cytoplasmic process overlying the protruding stump of the digestive gland (DG). Scale bar = 1 µm.


SM
E
GC
APN
DG
92

Chapter 3

NEUROPHYSIOLOGICAL CHARACTERISTICS OF THE CERATAL PERIPHERAL NERVOUS SYSTEM OF MELIBE LEONINA (GOULD, 1852) AND ITS ROLE IN CERATAL AUTOTOMY

INTRODUCTION

Molluscs exhibit a remarkable range in the degree of nervous system centralization. However, even in molluscs with pronounced clustering of neurons into centralized ganglia (the central nervous system; CNS), a large population of peripheral neurons remains (see Bullock and Horridge, 1965). A complete understanding of the neuronal basis of molluscan behaviour and behavioural plasticity must include the contribution of both central and peripheral neurons and possible interactions between them (see Lukowiak and Peretz, 1977; Kandel, 1979).

Three categories of peripheral neurons in bivalves and gastropods have been described, based primarily on location: 1) peripheral, primary sensory cells, often having somata within or beneath the epidermis (see Ch. 4 for references); 2) neurons that occur singly or in small clusters (peripheral ganglia) strung out along peripheral nerves or nerve plexuses (Prior, 1972a; Peretz and Estes, 1974; Carew et al., 1974; Prior and Lipton, 1977; Bailey et al., 1979; Abraham, 1983a, b; earlier literature reviewed by Bullock and Horridge, 1965); and 3) individual neurons located within or alongside muscle bundles (Bowden and Lowry, 1955; Bowden, 1958; Peretz and Estes, 1974; Plesch, 1977). Peripheral neurons are similar to neurons within the CNS with respect to many features of their fine structure (Prior and Lipton, 1977; Bailey et al., 1979), neurophysiological characteristics (Prior, 1972a, b; Peretz and Moller, 1974; Bailey et al., 1979), and neurotransmitter content (Peretz and Estes, 1974). However, unlike central neurons, the exact number and location of peripheral neurons is not strictly predictable between individuals of a species (Peretz and Estes, 1974; Prior and Lipton, 1977; Bailey et al., 1979; see Bullock and Horridge for earlier literature).

The research of Alkon and his co-workers (reviewed by Alkon, 1980) on the photoreceptors and statocyst hair cells of the opisthobranch, Hermissenda (=Phidiana)

crassicornis has provided the only intracellular analysis of molluscan primary receptor cells located outside the CNS. Likewise, there have been few unit recordings from neurons located along distal nerves compared to many from central neurons. To date, intracellular recordings from non-sensory peripheral neurons have come from only three preparations: the siphon of the opisthobranch, Aplysia californica (Bailey et al., 1979; Clark and Kandel, 1984), the siphons of the bivalve, Spisula solidissima (Prior, 1972a, b), and the gill of Aplysia (Peretz and Moller, 1974). These three preparations have yielded important insights into the ways that peripheral neurons can contribute to certain gastropod and bivalve behaviours.

Lukowiak and Jacklet (1972; 1975) reported that the siphon of Aplysia responds to tactile stimulation even in the absence of central innervation and the response can be habituated and dishabituated. This suggests the presence of a peripheral reflex pathway within the siphon. Peripheral neuronal somata are located along the siphonal nerve within the siphon (Lukowiak and Jacklet, 1972; Bailey et al., 1979) and intracellular recordings indicate that all but one, a suspected neurosecretory cell, are motor neurons to siphonal musculature (Bailey et al., 1979). The siphonal musculature is also innervated by central motor neurons with somata in the parietovisceral (abdominal) ganglion (Kupfermann et al., 1974; Perlman, 1979). The motor field of each central siphon motor neuron is much larger than that of individual peripheral motor neurons. Unit recordings showed that both peripheral and central motor neurons receive monosynaptic input from a single population of sensory neurons with somata located in the parietovisceral ganglion (Bailey et al., 1979). Furthermore, repeated spiking of a central sensory cell causes decrement of post-synaptic potentials in both peripheral and central motor neurons and the kinetics of these responses is similar to that of behavioural habituation. The important implication of these results is that the peripheral reflex pathway, which persists in the absence of the

parietovisceral ganglion, is based on axonal reflexes between peripheral axon collaterals of central sensory cells and motor neurons with peripheral cell bodies and axons.

Perlman (1979) reported that defensive siphon withdrawal in Aplysia following weak, medium, or strong tactile stimuli to the siphon is mediated by conjoint participation of peripheral and central motor neurons, with the former contributing 45% of the total response. Lukowiak and Jacklet (1972; 1975) estimated a greater contribution by peripheral neurons during siphon withdrawal. These quantitative response differences may be due to differences in experimental methodology (see Perlman, 1979).

Siphon withdrawal in Aplysia is an example of a single behaviour mediated by combined peripheral and central control of one effector, the siphonal musculature. The siphons of the bivalve, Spisula solidissima provide an example of two separate behaviours, each mediated by different effector muscles, in which peripheral neurons control one behaviour and central neurons control the other.

The peripheral neurons within the siphons of Spisula are grouped into small ganglia located at distal branch points of siphonal nerves that arise from the visceral ganglion (Prior, 1972a, b; Prior and Lipton, 1977). As shown by Prior (1972a), the peripheral neurons are efferents that cause local contractions of the intrinsic siphonal musculature following weak tactile stimuli to the siphons. Stronger tactile stimuli cause siphon withdrawal, which results from the recruited activity of central motor neurons within the visceral ganglion that innervate the siphon retractor muscles. Although he was unable to obtain intracellular recordings from sensory cells presynaptic to either category of motor neurons, Prior (1972b) demonstrated that the ability of peripheral and central motor neurons to discriminate stimulus intensity is due to differences in their membrane electrical properties.

The third preparation in which peripheral reflex pathways have been studied involves the gill of Aplysia. Gill contractions can be induced by direct touch to the gill itself or by touches to the adjacent siphon. The former is a local reflex called the pinnule response; the latter is a remote reflex called the gill-withdrawal reflex (see Kandel, 1979). As discussed below, some disagreement exists regarding the extent of central and peripheral control of gill behaviours in Aplysia. Resolution of the controversy must await additional cellular studies on the peripheral neurons within the gill.

Peretz (1970) reported that the pinnule response can be elicited in gill preparations surgically isolated from the CNS and the response can be habituated and dishabituated. Peretz and others (Peretz, 1970; Peretz and Estes, 1974; Carew et al., 1974) described peripheral neurons within the gill. Some of these form a gill (branchial) ganglion along the course of the branchial nerve from the parietovisceral (abdominal) ganglion. Intracellular recordings from the peripheral gill ganglion, made in conjunction with extracellular nerve recordings and measurements of gill withdrawal responses, suggested to Peretz and Moller (1974) that the peripheral ganglion contains interneurons that regulate the amplitude of the pinnule response. The regulation, which is demonstrable during habituation of the response, may be exerted by varying degrees of presynaptic facilitation to peripheral sensory-to-motor synapses. Unit recordings from the sensory and motor neurons, which Peretz and co-workers believe are also peripherally located, have not been performed (Peretz, 1970; Peretz and Estes, 1974; Peretz and Moller, 1974).

Kupfermann et al. (1971; 1974) and Carew et al. (1974) confirmed Peretz's (1970) observations on the pinnule response. They emphasized that the reflex response is confined to the pinnules stimulated and argued that, even with CNS innervation intact, the peripheral nervous system is both necessary and sufficient for the pinnule response following weak to moderate stimuli. However, Lukowiak and Peretz (1977) argue that

some interaction between central and peripheral neurons can be demonstrated, specifically during habituation and dishabituation.

The gill-withdrawal reflex of Aplysia is a widespread contraction of the gill evoked by tactile stimulation to the siphon (a remote reflex) and the reflex can be habituated, dishabituated, and sensitized (Pinsker et al., 1970; Kandel et al., 1976). The reflex is mediated by sensory and motor neurons both having somata within the parietovisceral ganglion (Kupfermann et al., 1970; 1971; 1974; Castellucci et al., 1970; Carew et al., 1974; Byrne et al., 1978). The sensory neurons are primary receptors (Byrne et al., 1974) and the motor neurons connect monosynaptically with gill muscles (Kupfermann et al., 1971; Carew et al., 1974). All these studies argue that the gill-withdrawal reflex is effected completely or almost completely by central neurons within the parietovisceral ganglion, yet Peretz and co-workers (Peretz et al., 1976; Lukowiak and Peretz, 1977) found that the reflex remains strong after removal of the parietovisceral ganglion. They suggested the gill-withdrawal reflex involves an interaction between the peripheral and central nervous systems. The discrepancy between these results has been partially explained by differences in experimental design, enabling Carew et al. (1979) to develop a rigid experimental protocol in which central neurons evoke 90 to 95% of the gill-withdrawal reflex. Nevertheless, evidence for some involvement of the peripheral nervous system during gill-withdrawal reflex must be accepted, particularly at strong stimulus intensities (Kupfermann et al., 1971; Carew et al., 1979) and during adaptive changes in the reflex (Peretz and Howieson, 1973; Peretz et al., 1976; Lukowiak and Jacklet, 1977).

Under the heading of central ganglia, Bullock and Horridge (1965) include the category of accessory ganglia. According to them, "Most of the accessory ganglia are on nerves to sense organs . . . for example, optic, rhinophore, tentacle, and osphradial." The distinction between accessory and peripheral ganglia is not obvious and may not be appropriate.

Indeed, Bicker et al. (1982) describe the tentacular and rhinophoral ganglia of the opisthobranch Pleurobranchaea californicus as peripheral ganglia. However, the location and number of ganglia associated with major sensory organs is predictable in each member of a gastropod genus (see MacFarland, 1966; Bullock and Horridge, 1965) and at least one of this category, the optic ganglion of the nudibranch Hermissenda crassicornis, contains a fixed number of cells in each individual (Stensaas et al., 1969). These are features typical of molluscan central ganglia rather than peripheral ganglia. Studies by Alkon and his co-workers (see review by Alkon, 1980) on the optic ganglion of Hermissenda, by Chase (1981) on the tentacular ganglion of the pulmonate Achatina fulica, and by Bicker et al. (1982) on the tentacular and rhinophoral ganglia of Pleurobranchaea have shown that these accessory ganglia contain interneurons postsynaptic to receptors within the associated sense organ. None of the cells penetrated were suspected motor neurons.

As described in previous chapters, Melibe leonina is a large dendronotid nudibranch with two rows of large, petaloid cerata along the dorsal body wall. Each ceras is innervated by a single ceratal nerve, which arises from the ipsilateral pleural nerve (Fig. 93), and contains a variable number of peripheral ganglia.

The cerata assume typical postures during feeding and mating (Ajeska and Nybakken, 1976), and swimming (Hurst, 1968). They can be elevated or depressed, either spontaneously or in response to a touch stimulus to the ceras or other body surface. Noxious or strong intensity tactile stimuli to the cerata can release fixed action patterns; high threshold, stereotyped behavioural sequences often involving multiple body parts (see Kandel, 1976; pp. 346-349). For example, touch to a ceras by tube feet of Pycnopodia helianthoides, a predatory seastar that induces dramatic escape responses in many marine gastropods (Feder, 1963), often activates galloping behaviour by M. leonina. Galloping is a method of rapid pedal locomotion (see Kjerschow-Agersborg [1923] for description). Firm

pinching of a ceras induces ceratal autotomy and usually releases swimming behaviour (see Hurst [1968] for description of swimming). Contact by seastars does not induce ceratal autotomy.

I investigated the properties and functions of the peripheral nervous system contained within cerata of M. leonina by means of behavioural observations and extracellular and intracellular neurophysiological analysis. I wished to determine the function of cells within the ceratal peripheral gangla and I was particularly interested in the possible role of the ganglia in the process of ceratal autotomy. In the preceding chapter on the morphology of the ceratal autotomy zone, I suggested that both muscles and granule-filled cells (GC) within each ceras are the effectors of ceratal detachment during autotomy.

MATERIALS AND METHODS

M. leonina was collected from Patricia Bay, Vancouver Island, Canada by SCUBA divers. Animals were held in the flow-through seawater system at Friday Harbor Laboratories, University of Washington, U.S.A. Holding temperatures varied between 9 and 12 degrees Centigrade.

Basal ganglia were prepared for one µm histological sections by first removing them from cerata and then fixing, dehydrating, and embedding in Epon 812 according to the method given in Ch. 2.

Three types of preparations were used for neurophysiological recordings: isolated cerata, isolated basal ganglia with attached nerve trunks, and whole animals.

Isolated cerata were prepared by first severing the ceras by a cut through its narrow base and then pinning it to a petri dish lined with Sylgard (Dow-Corning). The ceras was opened by a cut extending from its base to halfway down the midline of its lateral face. Nerves and ganglia within the ceras were exposed by carefully removing attached connective tissue. During neurophysiological recordings, the petri dish containing the isolated ceras was immersed in a chamber that received continuous irrigation with seawater. Extracellular electrodes held by micromanipulators were attached to various nerves within the ceras as described in the Results.

Intracellular recordings were made from isolated basal ganglia. Each ganglion was removed from the ceras along with lengthy portions of the ceratal nerve and several distal nerves. This was secured to a Sylgard-lined petri dish using spines of the cactus Opuntia. Isolated ganglia were not perfused with seawater during intracellular recordings but the seawater surrounding the preparation was periodically replaced.

Whole animals with intact cerata were prepared for extracellular recordings from a distal nerve within a ceras as described in the Results. Like isolated cerata, each whole animal preparation was continuously irrigated with seawater.

Extracellular suction electrodes were made by drawing out polyethylene tubing. Intracellular electrodes were made from glass microcapillary tubes having a glass filament within the lumen. The latter were filled with 3M KCl and had resistances of 50 to 100 megohms. Neural activity recorded by intracellular and extracellular electrodes was amplified and displayed according to conventional techniques.

Tactile stimuli were applied to the ceratal epidermis with a glass probe mounted on a micromanipulator. Individual seastar tube feet were applied to the ceras by slipping the cylindrical tube foot over the shaft of a micromanipulator-held polyethylene electrode and securing it by applying suction. Cerata were pinched with hand-held forceps. Electrical stimuli to various nerves within the ceras were applied via polyethylene suction electrodes using a stimulator and stimulus isolation unit.

RESULTS

A. Structure of the Cerata

The structure of the cerata of M. leonina is described elsewhere in this dissertation (see Chs. 2 and 4). The following is a brief overview of the major effectors within these appendages and a summary diagram is given in Fig. 94.

Each ceras contains three categories of muscle. The subepidermal muscle plexus consists of a delicate network of circular and longitudinal muscle fibres that mediate local contractions of the ceratal epidermis. Beneath the subepidermal muscles are prominent bands of longitudinal muscles that originate within the dorsum of the body and insert near the apex of each ceras. Contractions of the longitudinal muscle bands on opposing sides of a ceras cause depression or elevation of the appendage. These muscles act against internal turgor pressure maintained by an interconnected system of fluid-filled haemal sacs within each ceras and the adjacent dorsum of the body. Finally, a pair of muscular sphincters is located within the base of each ceras; the sphincters lie on either side of the ceratal autotomy plane (see Ch. 2).

Repugnatorial glands, each consisting of several subepidermal secretory cells enclosed within a muscle capsule, are distributed abundantly throughout the ceratal epidermis (see Ch. 4). Each ceras also contains a highly branched extension of the digestive gland.

B. Organization of the Ceratal Nervous System

Sensory cells with an apical ciliated dendrite, a subepidermal cell body, and a basal axon are clustered beside the pores of the many repugnatorial glands (see Ch. 4). These were the only receptors identified by scanning and electron microscopy, although others may exist.

The exact arrangement of nerves and ganglionic swellings within the cerata of M. leonina is variable both between animals and between cerata from the same animal. Nevertheless, my observations on over 100 dissected cerata have allowed me to recognize a generalized pattern for the gross ceratal neuroanatomy (Fig. 95).

The cerata receive central innervation from the pleural ganglia exclusively. The left and right pleural nerves, after emerging from their respective pleural ganglion (part of the CNS), extend posteriorly beneath the dorso-lateral body wall of the nudibranch and sprout sequential branches into each ipsilateral ceras. These branches are the ceratal nerves (Fig. 93). Additional, usually smaller branches of the pleural nerve extend to non-ceratal body wall and musculature within dorsal and dorso-lateral regions of the nudibranch.

After entering the ceras, the ceratal nerve invariably arrives at a ganglionic swelling that I have termed the ceratal basal ganglion (Fig. 95). The size of this basal ganglion varies between preparations but it is usually the largest cluster of neuronal cell bodies within the ceras. One basal ganglion that I cut into serial one µm sections contained approximately 100 somata measuring 25 µm or less in diameter. Most neuronal somata are arranged as a cellular cap over the neuropil region of the ganglion (Fig. 96).

With few exceptions, one or more of the nerves emerging from the basal ganglion is a connective to one or more secondary ganglia, often located towards the opposite (medial) side of the ceras. As shown in Fig. 95, both the basal ganglion and the secondary ganglia give rise to a variable number of distal nerves.

Microscopic observations of live cerata showed that peripheral branches of the distal nerves extend towards the longitudinal muscle bands, repugnatorial glands, and to the region of the autotomy zone. However, when the present neurophysiological study was undertaken, I had not discovered the two nerve rings (the autotomy plane nerve and its subdivision surrounding the ceratal branch of the digestive gland) located at the level of the autotomy plane (Fig. 95) (see Ch. 2).

C. Neurophysiological Characteristics of Cerata

1. Isolated Cerata: Extracellular Recordings

Excised cerata of M. leonina remain viable for at least 24 hours in seawater at 10 to 12 degrees Centigrade, as evidenced by the fact that muscles continue to contract following a pinch to the epidermis and repugnatorial glands secrete when touched by a probe (see Ch. 4). Therefore, isolated cerata were used for initial neurophysiological investigation of the ceratal peripheral nervous system.

By placing a recording suction electrode on the peripheral, cut end of a distal nerve (see diagram accompanying Fig. 97), I recorded responses during three qualitatively different stimuli to the ceratal epidermis. The stimuli were: touch with a glass probe having a diameter approximating that of a single seastar tube foot, touch with a single tube foot of the seastar Pycnopodia helianthoides, and a firm pinch applied by forceps to the ceratal epidermis. The duration of each stimulus was approximately 1 sec. Neural responses obtained during this type of experiment were assumed to be discharges by primary or secondary sensory neurons. Nevertheless, at least some of the output may represent antidromic impulses of motor axons activated by peripheral sensory-to-motor axonal synapses located distal to the recording electrode. The results of a representative preparation are shown in Fig. 97. The pinch induced the largest neural output in the distal nerve (based on amplitude and frequency of impulses) and the tube foot from Pycnopodia produced a greater response than did glass probe touch. In no instance did a distal nerve exhibit a patterned sequence of impulses following these stimuli.

Results of a second type of experiment showed extensive overlap in the sensory fields innervated by each distal nerve. Responses of two distal nerves were recorded simultaneously during 1 sec touches with a glass probe to four widely separated locations

on the lateral surface of the ceras (see diagram accompanying Fig. 98). Both nerves responded to three of the touches, although the magnitude of the response was obviously different in one of these, and neither nerve responded to the fourth touch (Fig. 98). Distal nerve responses did not markedly outlast the duration of the touch stimulus and did not show an 'off' response following removal of the touch stimulus.

A subsequent experiment examined the type of neuronal activity carried by the ceratal nerve after possible processing of sensory signals by the basal ganglion. The design of this experiment exploited the extensive overlap of sensory fields of distal nerves to directly compare pre- and post-ganglionic neuronal signals during epidermal stimulation. As shown in Fig. 99, one recording electrode (R1) was placed on the peripheral, cut end of a distal nerve as in previous preparations. En passant recording from R1 was undesirable due to possible centrifugal conduction along the distal nerve of signals emerging from the basal ganglion. A second recording electrode (R2) was placed on the ceratal nerve as it emerged from the basal ganglion. Stimuli were applied to the ceratal epidermis in a region likely to give rise to afferent signals within both the cut distal nerve (R1) and the intact distal nerves, thereby enabling these signals to be recorded by R1 but also conducted to the basal ganglion via intact nerves. Figure 99 shows activity recorded from the two nerves in response to 4 different stimuli: a glass probe having a diameter similar to a starfish tube foot (Fig. 99a), a tube foot of the sea star Pisaster ochraceus (Fig. 99b), two different touches by a tube foot of the sea star Pycnopodia (Figs. 99c and 99d), and a firm pinch by forceps to the ceratal epidermis (Fig. 99e).

The response of the distal nerve during each of the 4 stimuli was a non-patterned train of impulses, although the two Pycnopodia tube foot touches and the pinch (latter not shown in Fig. 99e) produced impulses of higher amplitude than touches by the glass probe or Pisaster tube foot (see Fig. 97). The response of the ceratal nerve was also non-patterned

during touches by the glass probe and Pisaster tube foot, and one of the trials with a Pycnopodia tube foot. However, the second application of a Pycnopodia tube foot and the pinch stimulus produced a dramatic response from the ceratal nerve consisting of very high amplitude spikes (often greater than 200 μV) clustered together to form a series of bursts (Figs. 99d and 99e). The spike bursts were superimposed on a background of non-patterned, low amplitude impulses. Once the bursting sequence was initiated within the ceratal nerve, it greatly outlasted the neural activity recorded from the distal nerve. Of 9 preparations in which the bursting was activated by a 1 sec touch by a Pycnopodia tube foot, the output had a mean duration of 9 secs (range 4 to 15 secs). The mean duration of the patterned output after the ceras was pinched, cut, or impaled was 21.5 secs (range 5 to 43 secs; n = 16).

The patterning of the ceratal nerve response (output from the basal ganglion) compared to the non-patterned distal nerve activity (input to the basal ganglion), and the long duration of the ceratal nerve discharge compared to that of the distal nerve argues that neurons responding with the long-lasting train of high amplitude spikes are post-synaptic to afferent input to the basal ganglion.

The stimulus-response characteristics of the patterned discharge were investigated further by applying single electrical stimuli of various intensities, via a suction electrode, to the proximal end of a distal nerve while recording from the ceratal nerve (see diagram accompanying Fig. 100). In the representative preparation shown in Fig. 100, stimuli of 6 V, 1.5 msec and 8 V, 1.5 msec failed to elicit the high amplitude spike bursts, whereas a stimulus of 10 V, 1.5 msec resulted in a train of spike bursts which lasted 12 sec before terminating abruptly. This type of result was duplicated in all preparations (n= 19) and confirms previous indications that the effective stimulus for generating the spike bursts must surpass a precise, critical threshold. Once initiated, the patterned discharge is self-

perpetuating for a period greatly outlasting the stimulus duration (mean duration of patterned discharge activated by electrical stimulus = 7.8 sec; range 3 to 15 secs; n = 19). I also found that the frequency of spike bursts varied (mean frequency = 6.8 bursts/sec; range 4 to 13 bursts/sec; n = 19) and each preparation required a resting period of 1 to 2 secs before a subsequent stimulus of equal voltage and duration could elicit a renewed discharge of spike bursts.

When a preparation like that shown in Fig. 100 was bathed in an artificial seawater solution containing excess Mg^{2+} and reduced Ca^{2+} (recipe from Audesirk and Audesirk [1980]) to eliminate synaptic activity, the patterned output in response to electrical stimulation was not obliterated, although the threshold stimulus for activation was markedly elevated and the spike amplitude and train duration was reduced.

The patterned discharge was also recorded from distal nerves emerging from the basal ganglion, as shown in Fig. 101. The 12 preparations of this experiment showed that all nerves emerging from the basal ganglion, and even those emerging from secondary ganglia, responded to a suprathreshold electrical stimulus applied to either a distal nerve or the ceratal nerve with a long-lasting patterned discharge. This was also true when a Pycnopodia tube foot or a pinch to the ceras provided the suprathreshold stimulus. Furthermore, the bursts were synchronous in any pair of nerves (Figs. 101b and 101c) and in no instance was there a difference in the stimulus threshold for eliciting the bursting discharge in two nerves (compare Figs. 101a and 101b).

I wished to determine if the patterned output of spikes could be generated within distal nerves arising from secondary ganglia after the connective between basal and secondary ganglia had been cut. As shown in Fig. 102, the secondary ganglia, as well as the basal ganglion, can generate the patterned output.

The preparation in Fig. 102 also shows a change in the form of the spike bursts recorded from the ceratal nerve (R1) but not the distal nerve (R2) extending from the secondary ganglion, after the connective was cut. The change consists of a reduction in the number of spiking units within each burst. The simplest explanation for this result is that some of the spiking axons within the ceratal nerve are activated by afferent synapses located proximal to the cut connective (within the basal ganglion), whereas others receive afferent synapses distal to the cut connective (within the secondary ganglion).

2. Isolated Basal Ganglion: Intracellular Recordings

The results described above show that the neurons responsible for the patterned output recorded extracellularly are post-synaptic to afferent fibres and the synaptic exchange occurs within the basal and secondary ganglia. To determine if somata of these neurons are located within the basal ganglion, I made intracellular recordings from basal ganglion cells. A stimulating electrode was applied to one nerve trunk (the S nerve) of an isolated basal ganglion preparation and a recording electrode applied to a second nerve trunk (the R nerve). A total of 18 basal ganglion cells from 6 preparations were penetrated. None showed spontaneous activity and 3 cells failed to respond to all electrical stimuli applied to the S nerve and to intracellular injection of current. These 3 may have been glial cells (D. Prior, 1984; personal communication). Of the remaining 15 cells, 4 categories were recognized.

The two cells in category no. 1 failed to respond to either subthreshold stimuli (insufficient to generate the patterned discharge from the R nerve) or suprathreshold stimuli (sufficient to generate the patterned discharge from the R nerve) but did exhibit action potentials when injected with depolarizing current. The intracellular spikes were not represented in the recording from the R nerve.

The 6 cells in category no. 2 were quiescent following subthreshold stimuli to the S nerve but began spiking soon after a stimulus that generated a patterned discharge within the R nerve. However, the intracellular action potentials did not coincide with the spike bursts recorded from the R nerve and they stopped prior to the end of the burst train in the R nerve (Fig. 103a).

Only a single cell of category no. 3 was penetrated. During the first suprathreshold stimulus to the S nerve, this cell remained silent until the end of the patterned bursting recorded from the R nerve, at which time it exhibited a group of spikes. Subsequent, suprathreshold stimuli applied to the S nerve failed to induce spiking in this cell but a distinct wave of depolarization accompanied the end of the patterned outbursts recorded from the R nerve.

With respect to the focus of this study, the 6 cells in category no. 4 were most interesting. Like the cells in category no. 2, the fourth group failed to respond to subthreshold stimuli applied to the S nerve but began spiking immediately following stimuli that produced the patterned discharge in the R nerve. However, the train of action potentials in the category no. 4 cells began and ended simultaneously with the output of large amplitude spike bursts recorded from the R nerve (Fig. 103b) and each action potential occurred synchronously with each extracellular spike burst (Fig. 103c). Occasionally, during the initial period of spiking, 2 action potentials occurred during a single extracellular burst (Fig. 103b). Prepotentials and epsp's preceded the spikes in category no. 4 neurons (Fig. 103c).

3. Whole Animal Preparation

A number of observations, taken together, suggest that the long-lasting, large amplitude spike bursts carried by all nerves radiating from the basal and secondary ganglia following a suprathreshold stimulus to the ceras may play a role during ceratal

autotomy (see Discussion). To investigate this possibility, I attempted to record extracellularly from a distal nerve of the ceras during the act of ceratal autotomy.

Whole, unanaesthetized specimens of M. leonina were pinned to a Sylgard-lined dish and the central ganglia completely removed by an incision through the epidermis behind the oral hood. One of the cerata was pinned sparingly to the Sylgard and two distal ceratal nerves were exposed by an incision made distal to the autotomy zone. One of these distal nerves was cut quickly and cleanly and its proximal end attached to a recording suction electrode (the R nerve; see diagram accompanying Fig. 104). Because of the trauma resulting from these manipulations to the ceras, many autotomized before electrophysiological recordings could begin. However, I was able to complete the procedure and obtain extracellular recordings from a distal nerve in 12 of approximately 40 attempts. Nevertheless, the injury caused by the surgical procedure resulted in obvious constriction of the sphincter muscles within the autotomy zone before recordings could begin. This constriction suggests that physiological mechanisms that bring about autotomy, though not yet accomplishing the actual separation, were probably begun prior to the onset of electrophysiological recordings.

At the outset of this experiment, I cut the second ceratal distal nerve previously exposed by dissection (the S nerve) while recording from the R nerve. If the cut failed to induce autotomy, the S nerve was attached to a suction stimulating electrode and given electrical stimuli of progressively greater voltage until autotomy occurred. I expected to obtain the patterned discharge from the R nerve immediately before ceratal autotomy. With some qualifications, this was the result obtained. Figures 104a, 104b, and 105 show recordings from three representative preparations. In all of these, autotomy was preceded by a sequence of large amplitude spike bursts within the R nerve that were initiated by a stimulus to the S nerve (cutting the nerve as in Fig. 104a or electrically stimulating the

nerve as in Figs. 104b and 105). Notice that the train of spike bursts continued after autotomy occurred.

In 7 of the 12 preparations, the train of spike bursts was obscured at the time of autotomy and shortly after by a barrage of additional neuronal discharges. An example is shown in Fig. 104b. The barrage likely represents injury discharges of neurons having axons in both the R nerve and in the ceratal nerve, because the latter is pulled apart as the ceras autotomizes (see Ch. 2). Previous results showed that an electrical stimulus to the ceratal nerve could generate the patterned discharge. Therefore, rupture and consequent injury discharges of the ceratal nerve would explain why the patterned discharge is renewed, often with increased frequency of bursts and for long duration, immediately after autotomy takes place.

Figure 105 shows the record from a whole animal preparation in which a short quiescent period occurred between the end of a patterned discharge within the R nerve and the occurrence of autotomy. Injury spiking and a renewal of the patterned discharge were initiated at the time of autotomy. This was found in two of the twelve preparations and a possible interpretation is given in the discussion.

Stimuli to the S nerve that activated the patterned discharge within the R nerve did not always result in autotomy in the whole animal preparations. Nevertheless, patterned discharges were accompanied by abrupt contractions of the sphincter muscles and longitudinal muscle bands whether or not autotomy ensued. Muscle contraction was not monitored quantitatively.

DISCUSSION

Two questions were posed in the introduction to this chapter. Firstly, what is the identity of neurons residing within the ceratal peripheral ganglia? Secondly, is the ceratal peripheral nervous system involved in controlling ceratal autotomy? The results of this study provide at least partial answers to both questions.

A. Identity of Neurons Within Basal Ganglion

The long-lasting, patterned output from the basal ganglion in response to short, unpatterned input indicates that synaptic exchange occurs within this peripheral ganglion. Studies on the Aplysia siphon have shown that synaptic transfer between sensory and motor neurons can occur at peripheral sites and can continue to operate in siphons surgically isolated from the CNS, despite the fact that somata of the sensory cells are located within the CNS (Bailey et al., 1979). Therefore, in M. leonina, somata of sensory neurons or the neurons responsible for the extracellularly recorded bursting pattern, or both, could reside within the CNS. However, intracellular recordings from the category no. 4 neurons suggest that somata of neurons that produce the bursting pattern recorded from ceratal nerves are located in the basal ganglion. These cells show a single (occasionally 2) action potential coincident with each spike burst recorded extracellularly from nerves emanating from the basal ganglion. Furthermore, these cells are silent during subthreshold electrical stimuli delivered to a distal nerve, show synaptic prepotentials and epsp's during spiking, and stop spiking simultaneously with the end of the train of spike bursts carried by an emergent nerve. Because no cells were found that showed intracellular bursts of spikes in synchrony with the extracellular spike bursts in emergent nerves, I suggest that the action potentials of neurons in category no. 4 are somehow synchronized to produce the bursting pattern of neural activity recorded by the extracellular electrodes.

Intracellular recordings in this study were made only from somata within the basal ganglion. Nevertheless, dual extracellular recordings made from distal nerves emanating from the basal and secondary ganglia before and after cutting the connective between these two ganglia provide evidence that a network of category no. 4 neurons resides in secondary as well as basal ganglia and the bursting of each network is synchronized between ganglia. Therefore, the basal and secondary ganglia are probably subdivisions of the same population of neurons that are clustered differently in different cerata. This is similar to the distribution of neuronal somata within the siphonal peripheral ganglia of Spisula (Prior and Lipton, 1977). The terms basal and secondary ganglia are artificial distinctions and I will subsequently refer to all ganglia within the ceras as ceratal ganglia.

Although dual recordings from pairs of category no. 4 neurons were not attempted, the simplist explanation for the proposed synchrony of their action potentials is electrical coupling between these neurons. This explanation is consistent with two other observations. First, high Mg^{2+}, low Ca^{2+} failed to completely block the train of spike bursts elicited by an electrical stimulus to a distal nerve. Blockage would be expected if the response synchrony of category no. 4 neurons were mediated by interconnecting chemical synapses. This result also shows that category no. 4 neurons send axons into nerves extending from the ceratal ganglia. Second, the train of extracellular spike bursts requires a high stimulus intensity for activation. This could be a consequence of electrical coupling between category no. 4 neurons. Populations of electrically coupled neurons have low input resistances due to shunting of current throughout the group, and therefore, these cells require large synaptic currents for depolarization. Carew and Kandel (1977) suggested that electrical coupling among motoneurons innervating the ink gland of Aplysia is part of the reason for the high threshold for activation of these motoneurons.

The three most probable targets, either directly or indirectly, for the category no. 4 neurons are the repugnatorial glands, the granule-filled cells (GC) associated with the autotomy plane nerve, and the ceratal muscles. As described in Ch. 4, both the secretory cells and the muscles of the repugnatorial glands receive chemical synapses and a bundle of axons is associated with each gland. However, discharge of repugnatorial glands was never observed coincident with the patterned discharge. Furthermore, touches by a glass probe or a Pycnopodia tube foot discharged only those glands actually touched (see Ch. 4). The highly localized stimulus-response character of repugnatorial gland discharge and the finding that the patterned discharge, once initiated, is carried by all nerves emerging from the ceratal ganglia is inconsistent with the notion that repugnatorial glands are the target of the pattern generating, category no. 4 neurons. Nevertheless, the possibility remains that the pattern generating neurons act on repugnatorial glands to alter their threshold for discharge. Many of the axons within the nerve bundle associated with each repugnatorial gland are probably primary or secondary sensory axons from adjacent ciliated receptor cells.

The fact that the patterned output is carried by all nerves emerging from the ceratal ganglia also argues against the possibility that granule-filled cells are the target for this signal. As described in Ch. 2, axons that innervate the granule-filled cells appear to arise from the ceratal nerve only. Granule-filled cells will be discussed further in section B below.

The longitudinal muscle bands of the ceras are each composed of a staggered array of muscle fibres that collectively extend from the apex of the ceras into its base and continue into the body proper. Unquantified observations showing contraction of the longitudinal muscle bands and the basal sphincter muscles coincident with the occurrence of the patterned discharge, and the fact that the patterned discharge is carried by nerves

extending from the ceratal ganglia to regions throughout the ceras, suggest that the pattern generating neurons are motor neurons to the longitudinal and sphincter muscles. Proof that pattern generating neurons are presynaptic to muscle fibres requires simultaneous intracellular recordings from both neurons and muscle fibres. I did not attempt this.

The obvious question arising from these results is: What might be the functional importance of generating a train of spike bursts rather than a train of randomly occurring or constant frequency impulses? Studies on the physiology of molluscan neuromuscular junctions have revealed that many molluscan muscles show graded contractions that are proportional to the size of excitatory junctional potentials (Carew et al., 1974; Mayeri et al., 1974; Blankenship et al., 1977; Cohen et al., 1978; Peters and Altrup, 1984). Frequently, these junctional potentials respond to the temporal pattern of arriving neuronal impulses by exhibiting summation, facilitation, and/or post-tetanic potentiation. Cohen et al. (1978) studying the accessory radular closer muscle of Aplysia and Peters and Altrup (1984) studying the pharyngeal muscles of Helix pomatia showed that repetitive burst activity in some motor neurons affected amplitude of muscle excitatory junctional potentials (and thus muscle tension) by causing facilitation within each burst and post-tetanic potentiation between each burst.

However, the patterned train of impulses carried by nerves emanating from the ceratal ganglia of M. leonina does not appear to be generated by a single neuron, but by the semi-synchronous spiking of a group of category no. 4 neurons. Therefore, if the burst pattern is to have temporal effects on the junctional potentials of target muscles, like those described by Cohen et al. (1978) and Peters and Altrup (1984), each muscle must be innervated by at least several of the category no. 4 neurons. Many studies have shown polyneuronal innervation of molluscan muscle cells (Mellon, 1968; Kater et al., 1971;

Carew et al., 1974; Mayeri et al., 1974; Peretz and Estes, 1974; Prior, 1975; Jacklet and Rine, 1977; Cohen et al., 1978; Peters and Altrup, 1984), although Blankenship et al. (1977) and Rock et al. (1977) point-out that apparent polyneuronal innervation of molluscan muscles may be only functional rather than anatomical due to extensive electrical coupling between muscle cells.

The patterned discharge carried by distal nerves within the cerata of M. leonina may effect strong contractions of the longitudinal muscle bundles and sphincter muscles by virtue of polyneuronal innervation of muscle fibres (even if only functional) and plastic properties of the neuromuscular junction that are influenced by the temporal pattern of arriving impulses. This hypothesis awaits testing.

An additional or alternative function for the co-occurrence of action potentials by category no. 4 neurons may be to effect simultaneous contractions of all muscle cells within the longitudinal muscle bands and sphincter muscles (see Mellon, 1968; Prior, 1975; Bailey et al., 1979). During a discussion of the stimulus - response characteristics of several neuromuscular systems in the bivalve, Spisula solidissima, Prior (1975) noted that motoneurons to the fast adductors show highly coincident activity that is correlated with a synchronous contraction of the muscle mass. However, the efferents to the siphon retractor muscle show less coincident activity and this muscle is capable of graded contractions. Therefore, the synchrony of action potentials among category no. 4 neurons, combined with their high threshold for activation, may contribute to the all-or-none nature of the autotomy behaviour.

B. Ceratal Nervous System and Autotomy

As described in Ch. 2, ceratal autotomy in M. leonina is initiated by a strong pinch directly to a ceras and only the pinched ceras is detached. Mechanical insults to other parts of the body, even the dorsal epidermis close to the base of a ceras, fail to cause

autotomy or even contraction of the ceratal sphincter muscles. These observations suggest that receptors for stimuli initiating autotomy are confined to the ceras itself and a separate neural effector system for autotomy exists for each ceras. The finding that autotomy can occur even when the CNS is removed indicates that autotomy is a local response regardless of the location of neuronal somata involved in the response.

Ceratal autotomy is accompanied by marked contractions of the longitudinal muscle bands and the basal sphincter muscles of the ceras. In the previous chapter on the morphology of the autotomy zone, I described how contractions of these two categories of muscle operate together to help detach the ceras. In brief, contraction of the basal sphincter muscles prevents escape of haemal fluid from the ceras so that coincident contractions of the longitudinal muscle bands can generate a high intraceratal turgor pressure. This turgor pressure provides a rigid skeleton for the ceras, allowing continued contractions of the longitudinal muscle bands on either side of the sphincter muscles to exert strong tensile stress at the level of the autotomy plane. For this model to work, all the muscle cells involved must contract synchronously and strongly. In the present chapter, I have argued that the longitudinal muscle bands and the sphincter muscles are the target of the network of pattern generating neurons located within the ceratal ganglia. The hypothesis that pattern generating neurons are part of the neuronal effector system for ceratal autotomy is supported by whole animal preparations showing that autotomy is preceded by stimuli that initiate patterned output in the ceratal distal nerves.

This hypothesis has a potential problem. In laboratory aquaria, touches by tube feet of Pycnopodia to cerata of M. leonina never caused ceratal autotomy, yet in isolated cerata, 35% of the Pycnopodia touches initiated the patterned discharge from nerves emanating from the basal ganglion. Furthermore, in whole animal preparations, electrical stimuli of sufficient strength to generate the patterned discharge were not always sufficient to initiate ceratal autotomy. Two observations may resolve this apparent paradox.

Firstly, the frequency of spike bursts within the patterned discharge and the duration of the discharge were often variable; these factors may affect the strength of response by follower cells. The mean frequency of spike bursts following Pycnopodia touch (5.1 bursts/sec, n = 9) was significantly less than the frequency of spike bursts that followed autotomizing stimuli in whole animal preparations (7.9 bursts/sec, n = 12; $p < 0.05$; Student's t-test for unequal sample sizes). Furthermore, the mean frequency of spike bursts following stimuli that did not result in autotomy in the whole animal preparations (5.3 bursts/sec, n = 11) was also significantly less than the frequency that preceded ceratal autotomy ($p < 0.05$). Data given by Orkand and Orkand (1975) and Blankenship et al. (1977), who studied the neuromuscular physiology of buccal and penis retractor muscles, respectively, of Aplysia, show a marked increase in muscle tension when the impulse frequency of innervating neurons is increased from 5 to 8 Hz. The effect is largely due to facilitation at the neuromuscular junction.

Duration of the patterned output in whole animal preparations was also significantly greater ($p < 0.05$) following autotomizing stimuli (mean = 9.8 sec; time interval between stimulus to onset of autotomy; n = 12) than that following non-autotomizing stimuli (mean = 4.4 sec; n = 11). A more dramatic difference was obtained in isolated cerata, in which the mean duration of the train of spike bursts following touch by a Pycnopodia tube foot was 9 sec (n = 9) compared to a mean duration of 21.5 sec (n = 16) following a strong pinch to the ceras. The similarity between the train duration following Pycnopodia tube foot touches in the isolated ceras and that preceding ceratal autotomy in whole animal preparations may reflect the fact that dissection prior to recording from the latter may have already activated some events leading to autotomy.

The second and possibly more important explanation for the inability of all patterned discharges to cause ceratal autotomy is provided by morphological evidence that muscle

contraction may be of secondary importance for ceratal detachment, subordinate to the disruption of connective tissue structures within the autotomy zone by granule-filled cells (see Ch. 2). Although the granule-filled cells receive many chemical synapses, I have not identified the location or activity characteristics of neuronal somata that innervate these effector cells. However, because the axons innervating the granule-filled cells are contained within a connective that runs proximally from the ceratal nerve to the ring-shaped autotomy plane nerve (Ch. 2; Fig. 89), it is reasonable to propose that the neuronal effectors for the granule-filled cells have their somata within the basal ganglia. The short quiescent period between the cessation of the patterned discharge and the actual occurrence of autotomy in 2 of the 12 whole animal preparations (Fig. 105), may represent a time period necessary for exocytosed granules to complete the disruption of basal laminae and connective tissue structures within the autotomy zone. Because autotomy is a drastic all-or-none behaviour to be employed only in extremely threatening situations, it is likely that motoneurons for granule-filled cells or the granule-filled cells themselves have a very high threshold for activation.

The foregoing observations suggest that synchronous contractions of the longitudinal muscle bands, as directed by category no. 4 neurons, may be part of a general body retraction response to noxious (Pycnopodia touch) or aversive mechanical stimuli. However, only when the muscle contractions are sufficiently strong, and particularly, only when they are coupled to GC degranulation, does autotomy occur. A strong pinch to the ceras is capable of surpassing the critical stimulus threshold for the latter events, but touch by Pycnopodia tube feet is not.

In this and the preceding chapter, I have argued that the longitudinal muscle bands are involved in the mechanism of ceratal autotomy and in this capacity they are directed by neurons within the ceratal ganglia. However, other ceratal responses (elevation and

depression) are exhibited when tactile stimuli are given to non-ceratal body parts and cerata also have characteristic postures during various whole animal behaviours such as feeding and mating (Ajeska and Nybakken, 1976) and swimming (Hurst, 1968). Previous studies on molluscs have shown that both remote reflexes and fixed action patterns are controlled mainly or exclusively by the CNS (see reviews by Kandel, 1976; 1979). Therefore, it would seem that the longitudinal muscle bands within the cerata of M. leonina are under dual or interactive control by both peripheral and central pathways.

Brachyuran crabs are the only animals for which information is available on the neural control of autotomy. As shown by McVean and Findlay (1976), leg autotomy in Carcinus meanas, is accomplished entirely by strong contractions of a specific arrangement of muscles that act on cuticular specializations at the base of the leg. Three of the four muscles involved also function during normal walking movements of the leg. The autotomizing action of the muscles is brought about by signals from phasic motor neurons that are active only during autotomy and are coordinated to commence and terminate firing in a specific temporal pattern (McVean, 1974; McVean and Findlay, 1976).

In general principles, the mechanism of leg autotomy in C. meanas shows some similarities to the mechanism of ceratal autotomy in M. leonina. Of the two muscle groups involved in ceratal autotomy in M. leonina, the longitudinal muscle bands are also functional during other ceratal behaviours, yet strong contractions of the sphincter muscles seem to occur only in preparation for autotomy (however, partial contraction of the sphincter muscles is reversible if ceratal stimulation is insufficient to trigger the entire programme of events necessary for ceratal detachment). Preliminary results reported in this study suggest that, like C. meanas, the coordinated activity of a particular group of neurons directs these two groups of muscles to help bring about autotomy. In C. meanas, muscles act on a specialized region of the cuticle cause its rupture. In M. leonina, the

longitudinal muscle bands act on special regions of basal lamina and connective tissue that become disrupted during autotomy, presumably by exocytosed granules of innervated granule-filled cells (see Ch. 2).

My behavioural, morphological, and neurophysiological evidence suggests that neural circuits within the ceras evoke degranulation of GC and strong contractions of ceratal muscles, which are directly responsible for ceratal autotomy in M. leonina. Nevertheless, I cannot discount the possibility that autotomizing stimuli also cause release of a hormone or neurosecretory substance from cells located outside the autotomy zone. Such a substance within the haemolymph could act directly or indirectly on the effectors of autotomy, possibly to potentiate the event. Factors isolated from the coelomic fluid of eviscerating holothurians and from various tissues of non-eviscerating specimens can initiate evisceration when injected into intact holothurians (Smith and Greenberg, 1973; Byrne, 1986). Evisceration in holothurians involves mechanical failure of connective tissues at several widely separated sites within the animal. Motokowa (1982) isolated a methanol soluble substance and a methanol insoluble substance from holothurian coelomic fluid that increased and decreased, respectively, the stiffness of the collagenous catch apparatus of echinoid spines (see Ch. 2 for additional discussion of variable tensility connective tissues in echinoderms). Dr. Roger Longley (Friday Harbor Laboratories, University of Washinton; personal communication, 1984) found that the first in a series of ceratal autotomies by Phidiana (Hermissenda) crassicornis requires a high intensity stimulus (strong pinch and pull of the ceras), whereas subsequent cerata autotomize following stimuli of much lower intensity. The effect lasts for at least 10 min after the initial autotomy response. The potentiation of subsequent ceratal autotomies in P. crassicornis may be mediated by the product of a neurosecretory cell, which is triggered to secrete into the haemolymph by the initial autotomizing stimulus. Alternatively, the phenomenon may

result from a neurally-mediated sensitization of sensory neurons within the ceras, similar to the sensitization mechanism involving the defensive gill withdrawal reflex in the opisthobranch Aplysia californica (reviewed by Carmardo et al., 1983).

In conclusion, the peripheral nervous system within the cerata of M. leonina is similar to that described for several other molluscan preparations in that at least some of the peripheral neuronal somata are effectors, probably motor neurons. However, in other preparations studied to date, the peripheral effector cells mediate only partial responses or small local responses to weak stimuli, whereas stronger stimuli recruit neurons within the central nervous system that bring about more dramatic defensive responses. The ceras of M. leonina is the first molluscan preparation to show that peripheral effector neurons play an important role, and in fact may be fully responsible, for a dramatic defensive behaviour involving a large structure: ceratal autotomy.

LITERATURE CITED

Abraham, A. 1983a. Light and electron-microscopic investigations into the gastro-intestinal nervous system of the vineyard snail (Helix pomatia). Zeitschrift mikrosk. anat. Forsch. 97: 688-704.

Abraham, A. 1983b. Ultrastructural studies on the gastrointestinal nervous system of Helix pomatia. Acta biol. Szeged. 29: 129-136.

Ajeska, R.A., and J. Nybakken. 1976. Contributions to the biology of Melibe leonina (Gould, 1852). Veliger 19: 19-26.

Alkon, D.L. 1980. Cellular analysis of a gastropod (Hermissenda crassicornis) model of associative learning. Biol. Bull. 159: 505-560.

Audesirk, G., and T. Audesirk. 1980. Complex mechanoreceptors in Tritonia diomedea 1. Responses to mechanical and chemical stimuli. J. comp. Physiol. 141: 101-109.

Bailey, C.H., V.F. Castellucci, J. Koester, and E.R. Kandel. 1979. Cellular studies of peripheral neurons in siphon skin of Aplysia californica. J. Neurophysiol. 42: 530-557.

Bicker, G., W.J. Davis, and E.M. Matera. 1982. Chemoreception and mechanoreception in the gastropod mollusc Pleurobranchaea californica. II. Neuroanatomical and intracellular analysis of afferent pathways. J. comp. Physiol. 149A: 235-250.

Blankenship, J.E., M.K. Rock, and J. Hill. 1977. Physiological properties of the penis retractor muscle of Aplysia. J. Neurobiology. 8: 549-568.

Bowden, J. 1958. The structure and innervation of lamellibranch muscle. Int. Rev. Cytol. 7: 295-335.

Bowden, J., and J. Lowry. 1955. The lamellibranch muscle: innervation. Nature (Lond.) 176: 346-347.

Bullock, T.H., and G.A. Horridge. 1965. Structure and Function in the Nervous Systems of Invertebrates. vol. II, W.H. Freeman, New York. 1719 pp.

Byrne, J., V. Castellucci, and E.R. Kandel. 1974. Receptive fields and response properties of mechanoreceptor neurons innervating siphon skin and mantle shelf in Aplysia. J. Neurophysiol. 37: 1041-1064.

Byrne, J., V. Castellucci, and E.R. Kandel. 1978. Contribution of individual mechanoreceptor sensory neurons to defensive gill-withdrawal reflex in Aplysia. J. Neurophysiol. 41: 418-431.

Byrne, M. 1986. Induction of evisceration in the holothurian Eupentacta quinquesemita and evidence for the existence of an endogenous evisceration factor. J. exp. Biol.: 120:25-39.

Carew, T.J., V.F. Castellucci, J.H. Byrne, and E.R. Kandel. 1979. Quantitative analysis of relative contribution of central and peripheral neurons to gill-withdrawal reflex in Aplysia californica. J. Neurophysiol. 42: 497-509.

Carew, T.J., and E.R. Kandel. 1977. Inking in Aplysia californica. I. Neural circuit of an all-or-none behavioural response. J. Neurophysiol. 40: 692-707.

Carew, T.J., H. Pinsker, K. Rubinson, and E.R. Kandel. 1974. Physiological and biochemical properties of neuromuscular transmission between identified motoneurons and gill muscle in Aplysia. J. Neurophysiol. 37: 1020-1040.

Carmardo, J.S., MlJ. Shuster, S.A. Siegelbaum, and E.R. Kandel. 1983. Modulation of a specific potassium channel in sensory neurons of Aplysia by serotonin and cAMP-dependent protein phosphorylation. Cold Spring Harbor Symp. quant. Biol. 48: 213-219.

Castellucci, V., H. Pinsker, I. Kupfermann, and E. Kandel. 1970. Neuronal mechanisms of habituation and dishabituation of the gill-withdrawal reflex in Aplysia. Science 167: 1745-1748.

Chase, R. 1981. Electrical responses of snail tentacle ganglion to stimulation of the epithelium with wind and odors. Comp. Biochem. Physiol. 70A: 149-155.

Clark, G.A., and E.R. Kandel. 1984. Branch specific heterosynaptic facilitation in Aplysia siphon sensory cells. Proc. natl. Acad. Sci. N.Y. 81: 2577-2581.

Cohen, J.L., K.R. Weiss, and I. Kupfermann. 1978. Motor control of buccal muscles in Aplysia. J. Neurophysiol. 41: 157-180.

Feder, H.M. 1963. Gastropod defensive responses and their effectiveness in reducing predation by starfishes. Ecology 44: 505-512.

Hurst, A. 1968. The feeding mechanism and behaviour of the opisthobranch Melibe leonina. Symp. zool. Soc. Lond. 22: 151-166.

Jacklet, J.W., and Rine. 1977. Facilitation at neuromuscular junctions. Contribution to habituation and dishabituation of the Aplysia gill withdrawal reflex. Proc. natl. Acad. Sci. U.S.A. 74: 1267-1271.

Kandel, E.R. 1976. Cellular Basis of Behavior. An Introduction to Behavioral Neurobiology. W.H. Freeman, San Fransisco. 727 pp.

Kandel, E.R. 1979. Behavioral Biology of Aplysia: A Contribution to the Comparative Study of Opisthobranch Molluscs. W.H. Freeman, San Francisco. 463 pp.

Kandel, E.R., M. Brunelli, J. Byrne, and V. Castellucci. 1976. A common presynaptic locus for the synaptic changes underlying short-term habituation and sensitization of the gill-withdrawal reflex in Aplysia. Cold Spring Harbor Laboratory Symp. quant. Biol. 40: 465-482.

Kater, S.B., C. Heyer, and J.P. Hegmann. 1971. Neuromuscular transmission in the gastropod mollusc Heliosoma trivolis identification of motoneurons. Z. vergl. Physiol. 74: 127-139.

Kjerschow-Agersborg, H.P. Von W. 1923. A critique on professor Harold Heath's Chioraera dalli, with special reference to the use of the foot in the nudibranchiate mollusk, Melibe leonina Gould. Nautilus 36: 86-96.

Kupfermann, I., T.J. Carew, and E.R. Kandel. 1974. Local, reflex, and central commands controlling gill and siphon movements in Aplysia. J. Neurophysiol. 37: 996-1019.

Kupfermann, I., V. Castellucci, H. Pinsker, and E. Kandel. 1970. Neuronal correlates of habituation and dishabituation of the gill-withdrawal reflex in Aplysia. Science 167: 1743-1745.

Kupfermann, I., H. Pinsker, V. Castellucci, and E.R. Kandel. 1971. Central and peripheral control of gill movements in Aplysia. Science 174: 1252-1255.

Lukowiak, K., and J.W. Jacklet. 1972. Habituation and dishabituation: interactions between peripheral and central nervous systems in Aplysia. Science 178: 1306-1308.

Lukowiak, K., and J.W. Jacklet. 1975. Habituation and dishabituation mediated by the peripheral and central neural circuits of the siphon of Aplysia. J. Neurobiol. 6: 183-200.

Lukowiak, K., and B. Peretz. 1977. The interaction between the central and peripheral nervous systems in the mediation of gill withdrawal reflex behavior in Aplysia. J. comp. Physiol. 117: 219-244.

MacFarland, F.M. 1966. Studies of Opisthobranchiate Mollusks of the Pacific Coast of North America. Calif. Acad. Sci., San Francisco. 546 pp.

Mayeri, E., J. Koester, I. Kupfermann, G. Liebeswar, and E.R. Kandel. 1974. Neural control of circulation in Aplysia. I. Motoneurons. J. Neurophysiol. 37: 458-475.

McVean, A. 1974. The nervous control of autotomy in Carcinus maenas. J. exp. Biol. 60: 423-436.

McVean, A., and I. Findlay. 1976. Autotomy in Carcinus maenas: the role of the basi-ischiopodite posterior levator muscles. J. comp. Physiol. 110: 367-381.

Mellon, DeF. Jr. 1968. Junctional physiology and motor nerve distribution in the fast adductor muscle of the scallop. Science 160: 1018-1020.

Motokawa, T. 1982. Rapid change in mechanical properties of echinoderm connective tissues caused by coelomic fluid. Comp. Biochem. Physiol. 73C: 223-229.

Orkand, P.M., and R.K. Orkand. 1975. Neuromuscular junctions in the buccal mass of Aplysia: fine structure and electrophysiology of excitatory transmission. J. Neurobiol. 6: 531-548.

Peretz, B. 1970. Habituation and dishabituation in the absence of a central nervous system. Science 169: 379-381.

Peretz, B., and J. Estes. 1974. Histology and histochemistry of the peripheral neural plexus in the Aplysia gill. J. Neurobiol. 5: 3-19.

Peretz, B., and D.B. Howieson. 1973. Central influence on peripherally mediated habituation of an Aplysia gill withdrawal response. J. comp. Physiol. 84: 1-18.

Peretz, B., J.W. Jacklet, and K. Lukowiak. 1976. Habituation of reflexes in Aplysia: contribution of the peripheral and central nervous systems. Science 191: 396-399.

Peretz, B., and R. Moller. 1974. Control of habituation of the withdrawal reflex by the gill ganglion in Aplysia. J. Neurobiol. 5: 191-212.

Perlman, A.J. 1979. Central and peripheral control of siphon-withdrawal reflex in Aplysia californica. J. Neurophysiol. 42: 510-529.

Peters, M., and U. Altrup. 1984. Motor organization in pharynx of Helix pomatina. J. Neurophysiol. 52: 389-409.

Pinsker, H., I. Kupfermann, V. Castellucci, and E. Kandel. 1970. Habituation and dishabituation of the gill-withdrawal reflex in Aplysia. Science 167: 1740-1742.

Plesch, B. 1977. An ultrastructural study of the innervation of the musculature of the pond snail Lymnaea stagnalis (L.). Cell Tiss. Res. 183: 353-369.

Prior, D.J. 1972a. Electrophysiological analysis of peripheral neurones and their possible role in the local reflexes of a mollusc. J. exp. Biol. 57: 133-145.

Prior, D.J. 1972b. A neural correlate of behavioural stimulus intensity discrimination in a mollusc. J. exp. Biol. 57: 147-160.

Prior, D.J. 1975. A study of the electrophysiological properties of the incurrent siphonal valve muscle of the surf clam, Spisula solidissima. Comp. Biochem. Physiol. 52A: 607-610.

Prior, D.J., and B.H. Lipton. 1977. An ultrastructural study of peripheral neurons and associated non-neural structures in the bivalve mollusc, Spisula solidissima. Tiss. and Cell 9: 223-240.

Rock, M.K., J.E. Blankenship, and F.J. Lebeda. 1977. Penis-retractor muscle of Aplysia: excitatory motor neurons. J. Neurobiol. 8: 569-579.

Smith, G.N., and M.J. Greenberg. 1973. Chemical control of the evisceration process in Thyone briareus. Biol. Bull. 144: 421-436.

Stensaas, L.J., S.S. Stensaas, and O. Trujillo-Cenoz. 1969. Some morphological aspects of the visual system of Hermissenda crassicornis (Mollusca: Nudibranchia). J. ultrastruct. Res. 27: 510.

Figure 93: Sketch of Melibe leonina in dorsal view showing the oral hood (OH), cerata (C), and innervation of the cerata. The pleural nerves (PN) arise from the cerebropleural ganglia of the central nervous system (CNS) and extend branches called ceratal nerves (CN) to the basal ganglion (BG) within each ceras. Not drawn to scale.

Figure 94: Sketch of a ceras of M. leonina showing longitudinal muscle bands (LM), sphincter muscles (SM), a portion of the subepidermal muscle plexus (SP), and repugnatorial glands (RG). Not drawn to scale.

Figure 95: Sketch of a ceras of M. leonina showing general organization of the ceratal nervous system. Abbreviations are: APN, autotomy plane nerve; BG, basal ganglion; CN, ceratal nerve; DN, distal nerves; PN, pleural nerve; SC, sensory cells; and SG, secondary ganglion. The autotomy plane nerve (APN), which encircles the base of the ceras just beneath the epidermis of the autotomy plane, is drawn with broken lines because its existence was not known during this neurophysiological study. The nerve ring encircling the ceratal branch of the digestive gland is not shown. Not drawn to scale.

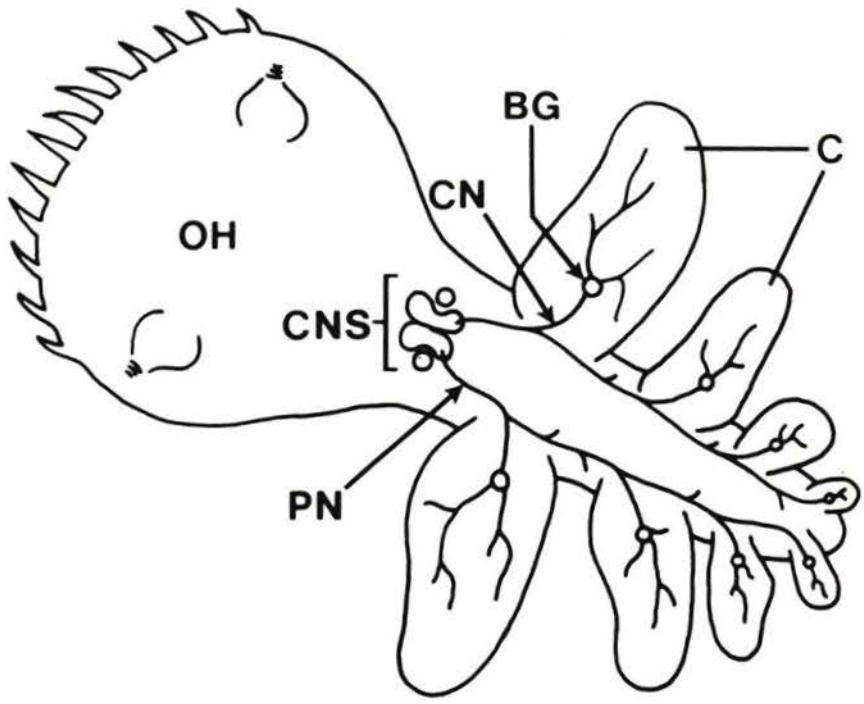

93

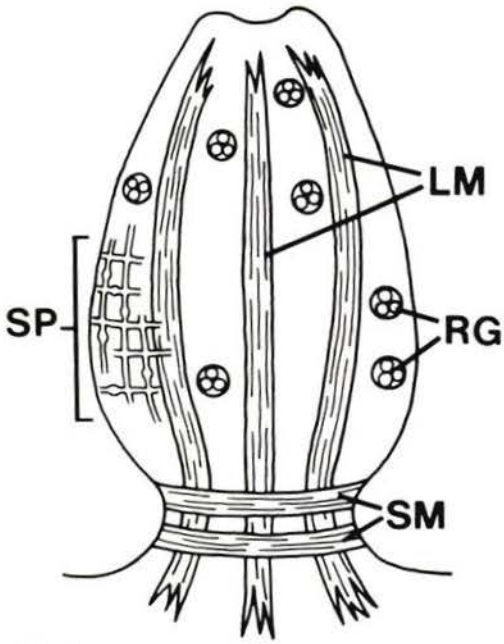

94

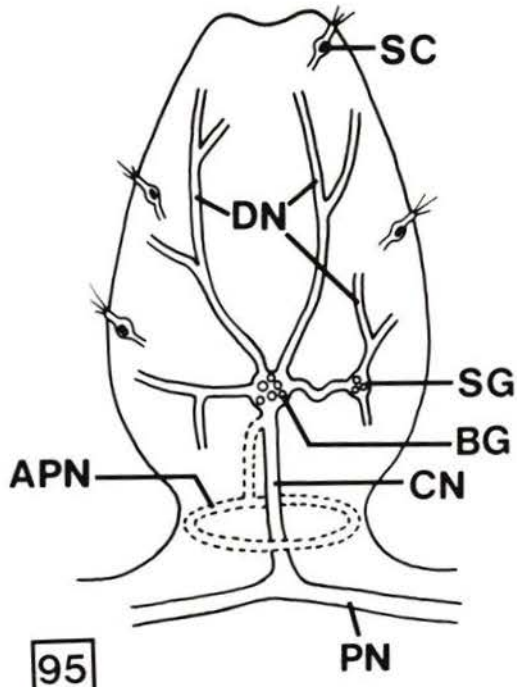

95

Figure 96: Histological section through the basal ganglion (BG), ceratal nerve (CN), and a distal nerve (DN) from a ceras of Melibe leonina. Neuronal somata (arrowheads) are concentrated on one side of the neuropil region (N) of the ganglion. Scale bar = 25 µm.

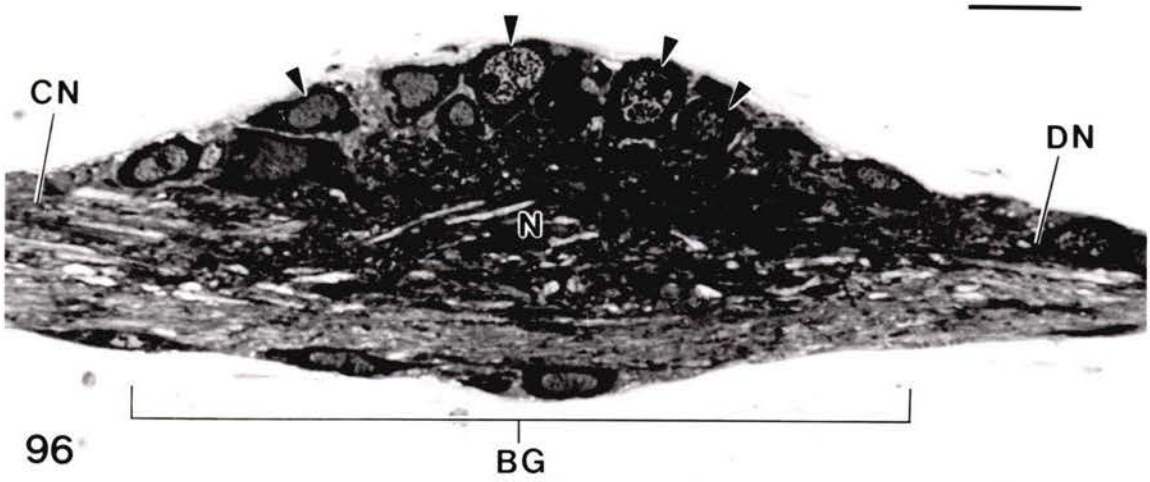

96

Figure 97: Response of a distal nerve, recorded extracellularly (R) as shown on the accompanying diagram, during 3 types of stimuli applied to the ceras:

a.touch by a glass probe; time scale = 500 msec

b. touch by Pycnopodia tube foot

c. pinch by forceps

97

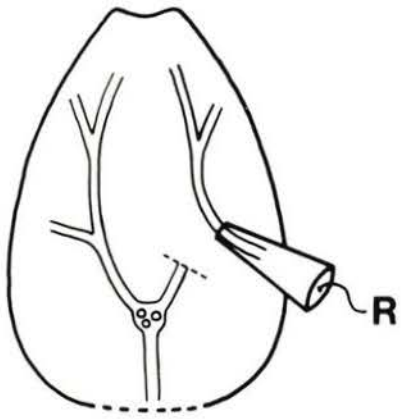

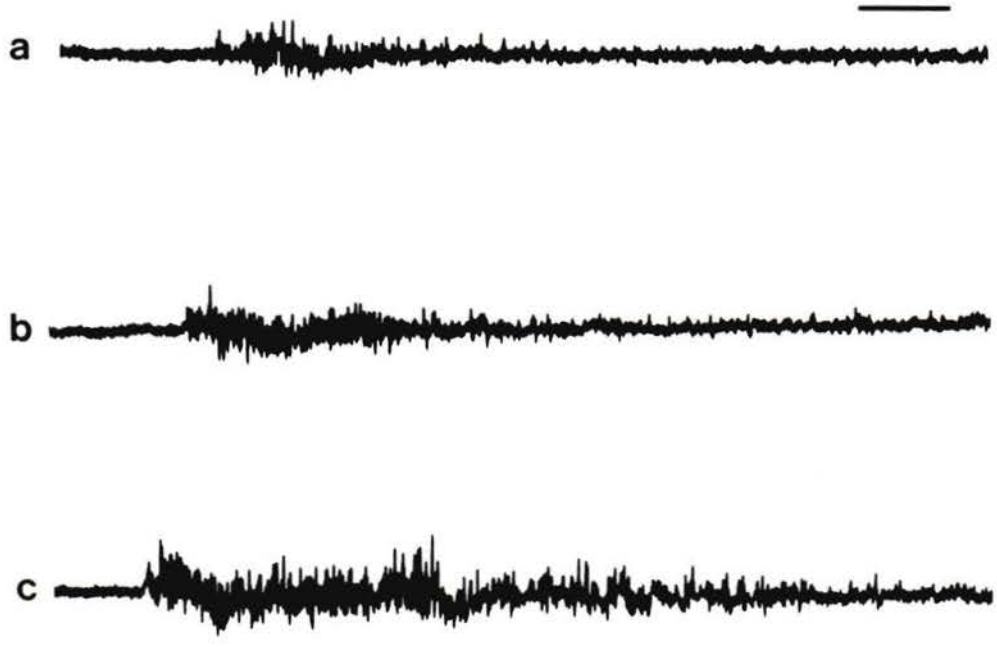

Figure 98: Demonstration of extensive overlap in sensory fields innervated by two distal nerves. The sketch shows positions of extracellular recording electrodes (R1 and R2) on two distal nerves during touches with a glass probe to 4 different sites on the ceratal epidermis. Duration of each touch was approximately 1 sec. Abbreviations are: BG, basal ganlgion; CN, ceratal nerve; and DN, distal nerve. The chart traces, labelled a to d, show responses of the two distal nerves during touches to the corresponding sites marked on the diagram. Time scale = 1 sec

98

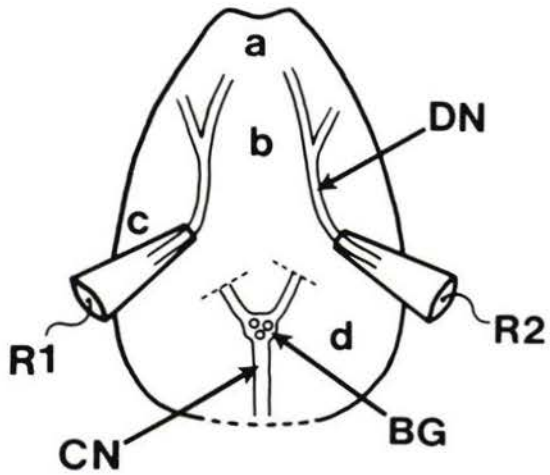

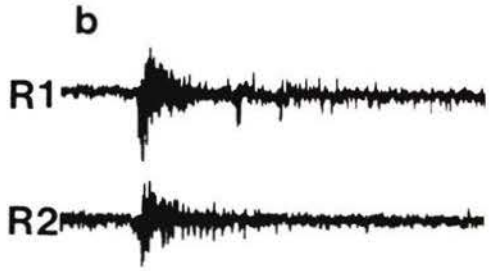

Figure 99: Simultaneous responses of a distal nerve and the ceratal nerve, recorded extracellularly by R1 and R2, as shown on the accompanying diagram, during 4 types of stimuli applied to the ceras:

a. touch by a glass probe; time scale = 200 msec

b. touch by a Pisaster tube foot

c. first touch by a Pycnopodia tube foot

d. second touch by a Pycnopodia tube foot

e. pinch by forceps; distal nerve response not shown; time scale = 100 msec

99

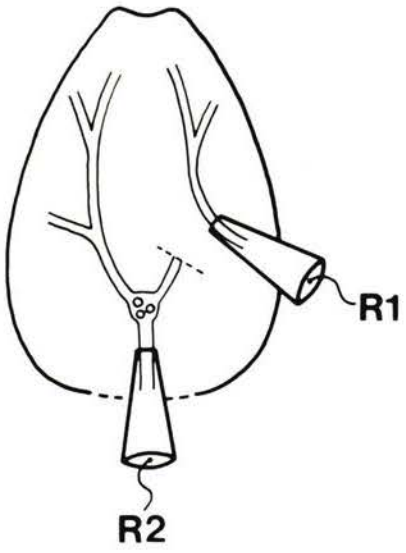

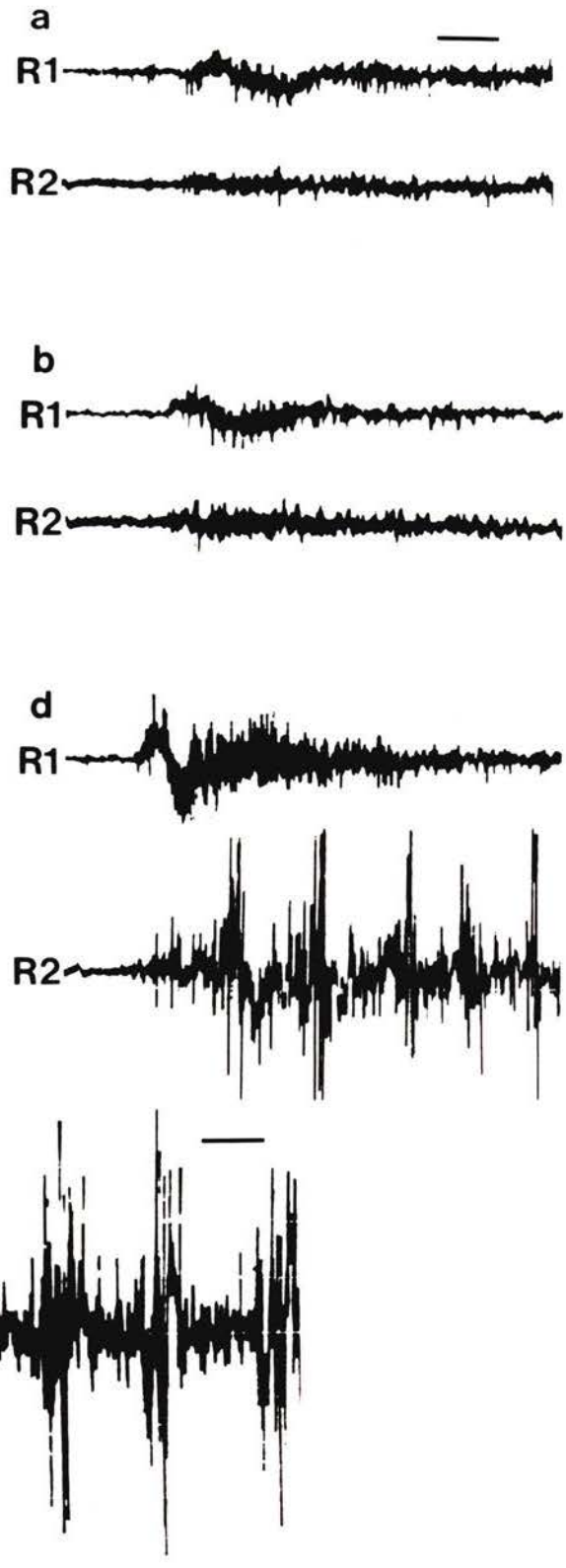

Figure 100: Responses of the ceratal nerve, recorded extracellularly by R as shown on the accompanying diagram, following electrical stimulation via S to the proximal end of a cut distal nerve. The magnitude of the stimuli were:

a. 6 V, 1.5 msec; time scale = 500 msec

b. 8 V, 1.5 msec

c. 10 V, 1.5 msec; the asterisk marks a gap in the chart record of 8 sec.

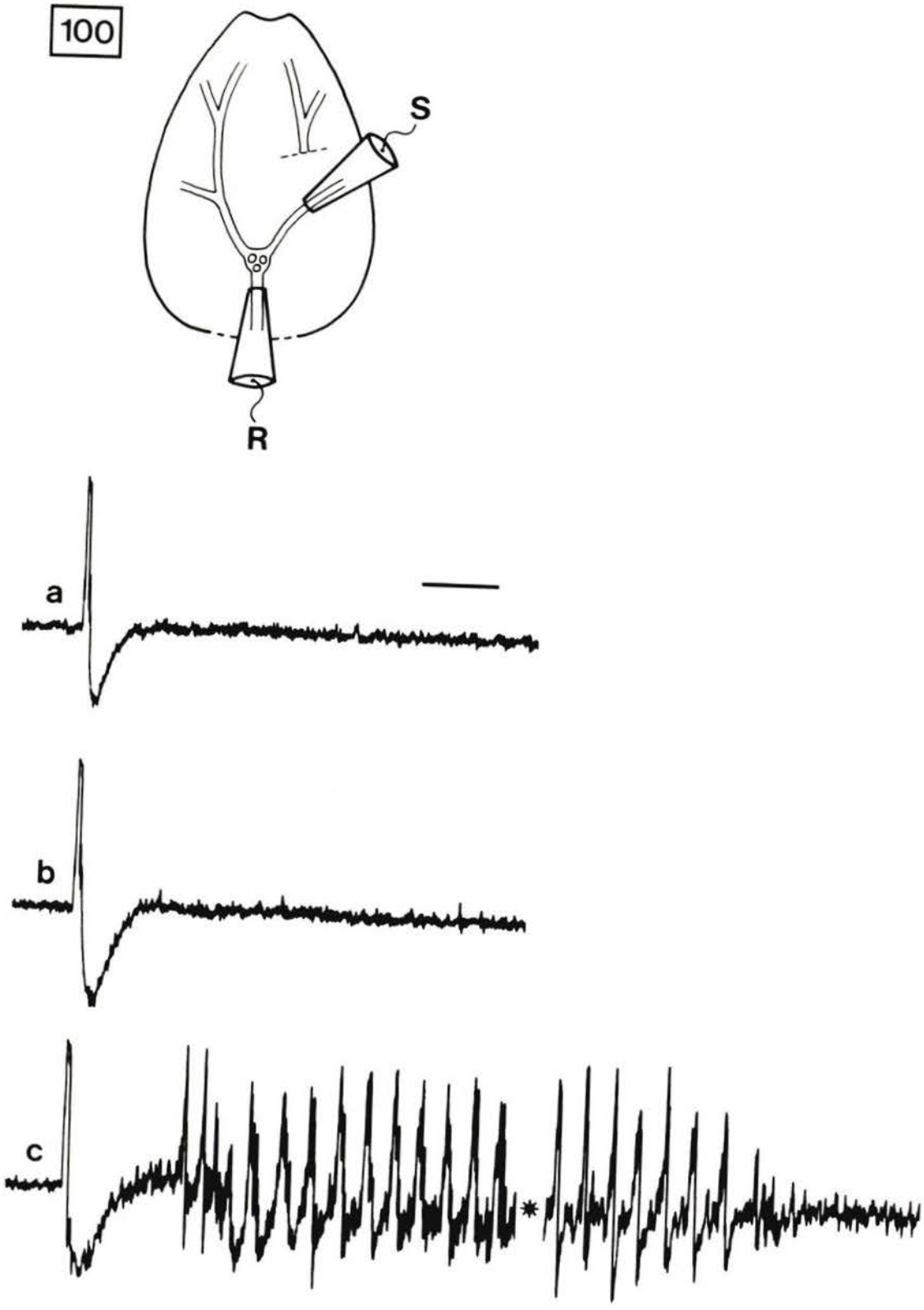
100
S
R
a
b
c

Figure 101: Synchrony of spike bursts during the patterned discharge recorded simultaneously from two nerves emerging from the basal ganglion. The diagram shows the position of two extracellular recording electrodes, R1 and R2, on a distal nerve and the ceratal nerve, respectively.

a. electrical stimulus of 8 V, 2 msec applied via S, as shown on the diagram, to proximal end of cut distal nerve; time scale = 500 msec

b. electrical stimulus of 10 V, 2 msec applied via S

c. application of a Pycnopodia tube foot to ceratal epidermis (recorded from different preparation than a and b)

101

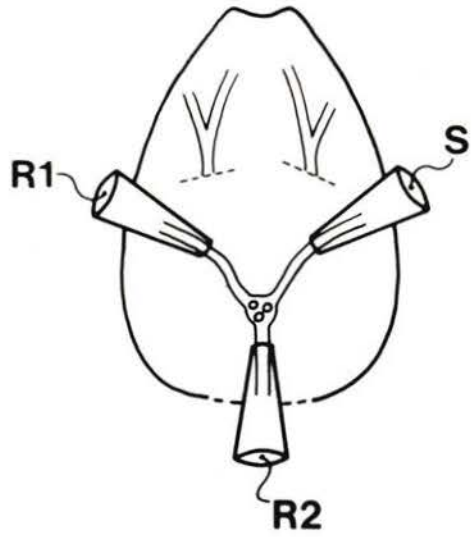

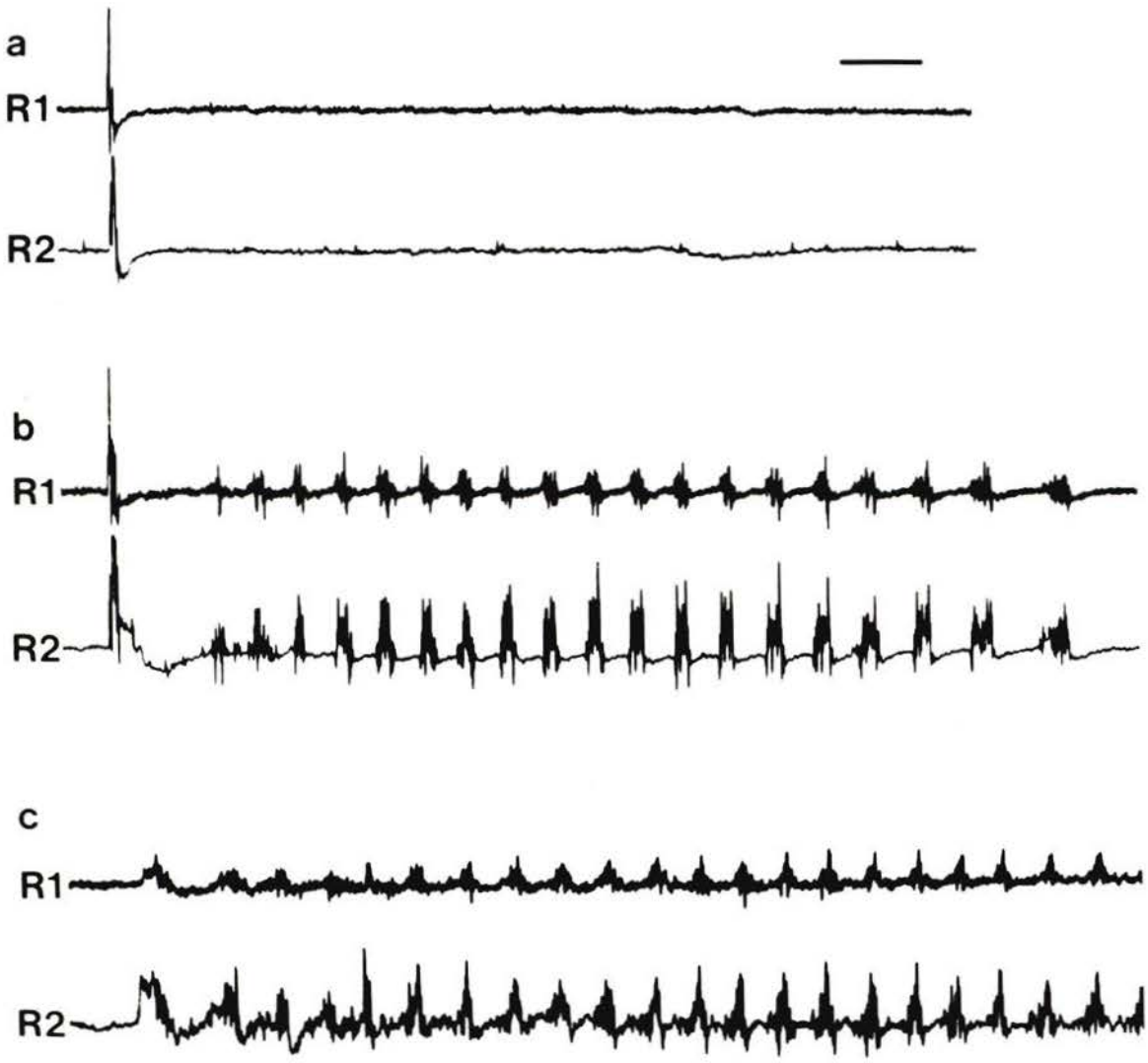

Figure 102: Demonstration of pattern generating ability by both the basal ganglion and a secondary ganglion. The diagram shows the layout of nerves and ganglia in this preparation. Anatomical abbreviations are: BG, basal ganglion; C, connective between basal and secondary ganglion; CN, ceratal nerve; DN, distal nerve; and SG, secondary ganglion. The chart records were obtained from the ceratal nerve (R1) and from a distal nerve arising from the secondary ganglion (R2) during the following manipulations:

a. 6.5 V, 2 msec stimulus applied via S1 as shown on diagram; connective intact; time scale = 500 msec

b. 6.5 V, 2 msec stimulus applied via S1; connective previously cut

c. 10 V, 2 msec stimulus applied via S2; connective previously cut

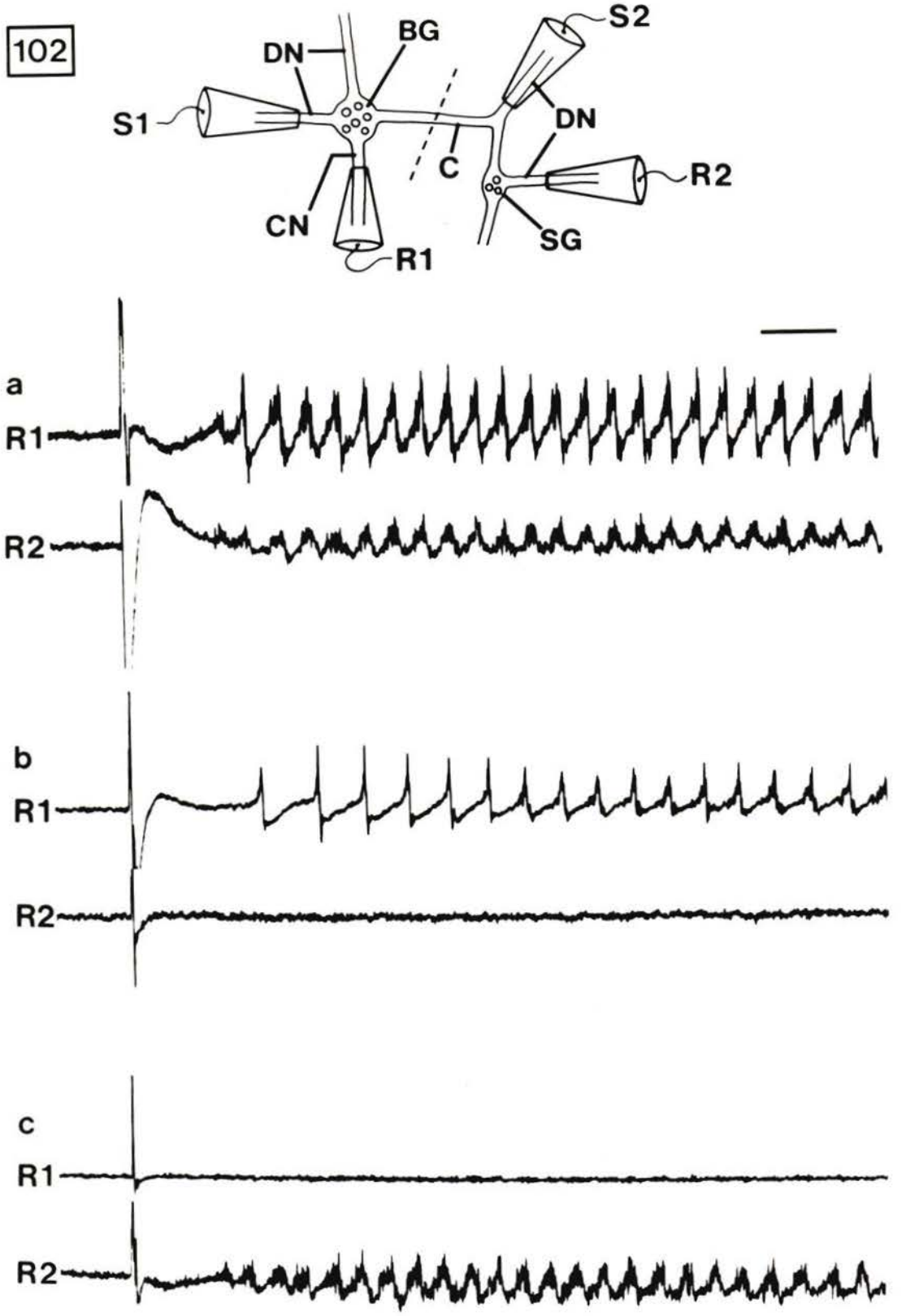
102
DN
BG
S2
S1
DN
C
R2
CN
SG
R1
a
R1
R2
b
R1
R2
c
R1
R2

Figure 103: Extracellular records (R1) from the ceratal nerve and simultaneous intracellular records (R2) from basal ganglion neurons. Electrical stimuli were applied to the proximal end of a distal nerve.

a. Category no. 2 neuron. Stimulus produced an antidromic spike (open asterisk) followed by a series of action potentials not coincident with the spike bursts recorded from the ceratal nerve. Each action potential is preceded by a slowly depolarizing prepotential. Time scale for R1 and R2 = 300msec; vertical scale for R2 = 20 mV.

b. Category no. 4 neuron. Stimulus produced an antidromic spike (open asterisk) followed by a series of action potentials that begins and ends in synchrony with the extracellular train of spike bursts. The closed asterisks mark gaps of 10 sec. Time scale for R1 and R2 = 100 msec; vertical scale for R2 = 20 mV.

c. Category no. 4 neuron. Oscilloscope sweep during the recording shown in Fig. 103b. Note the synchrony between each intracellular action potential and each spike burst recorded from the ceratal nerve. Also note epsps (arrows) between the action potentials. Time scale for R1 and R2 = 100 msec; vertical scale for R2 = 20 mV.

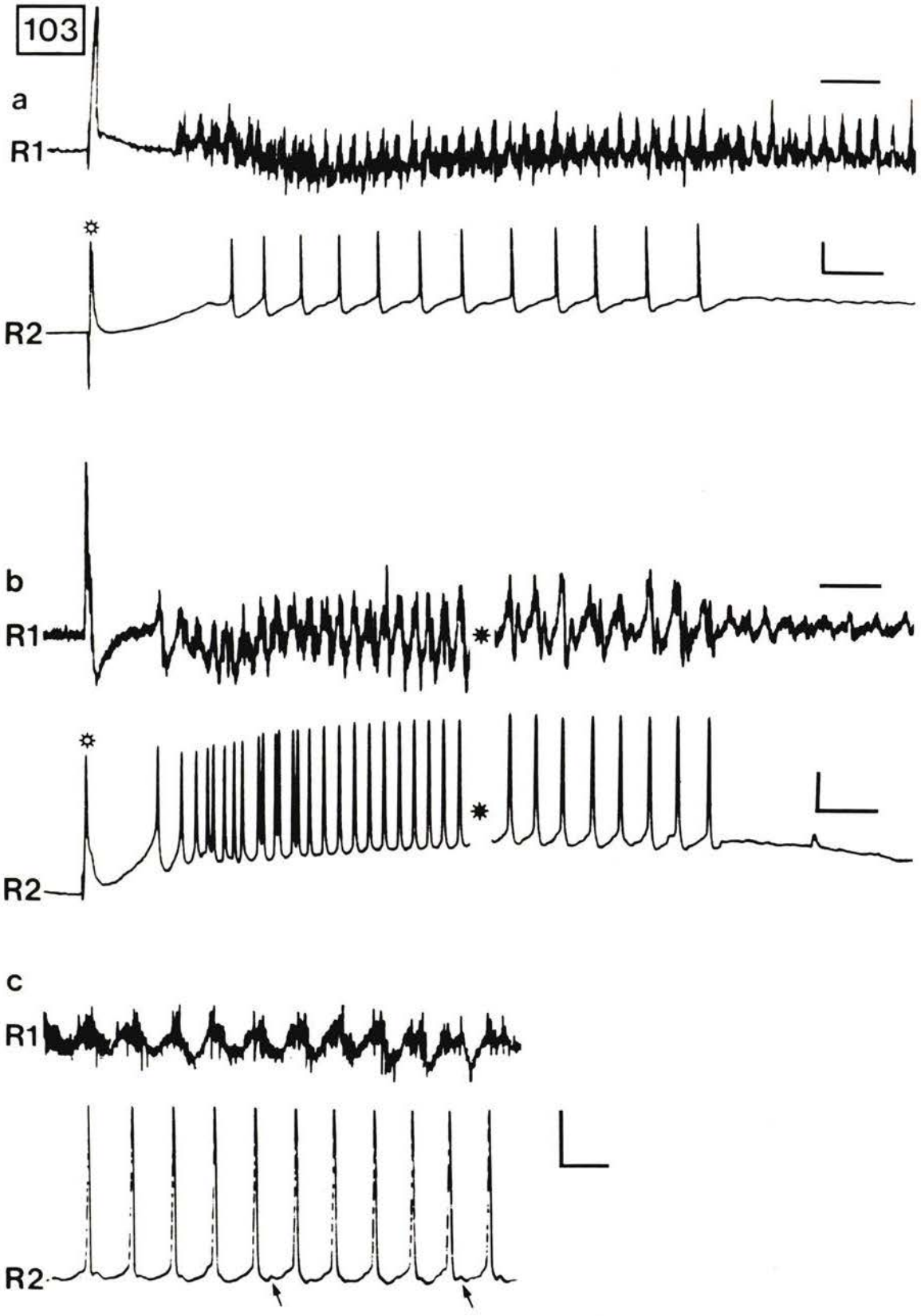
103
a
R1
R2
b
R1
R2
c
R1
R2

Figure 104: Extracellular recordings from a distal nerve (R on the accompanying diagram) during ceratal autotomy in two different preparations. The CNS was completely removed prior to each experiment.

a. Severing a distal nerve within the ceras induced a patterned discharge of spike bursts within the recorded distal nerve and autotomy of the ceras (arrow) as determined by visual inspection of the preparation. Time scale = 500 msec

b. Electrical stimulus applied to the proximal end of a distal nerve (S on the accompanying diagram) induced a train of spike bursts within the recorded distal nerve and ceratal autotomy (arrow). Note the 3 sec barrage of non-patterned, high frequency impulses that begins at the onset of autotomy (arrow).

104

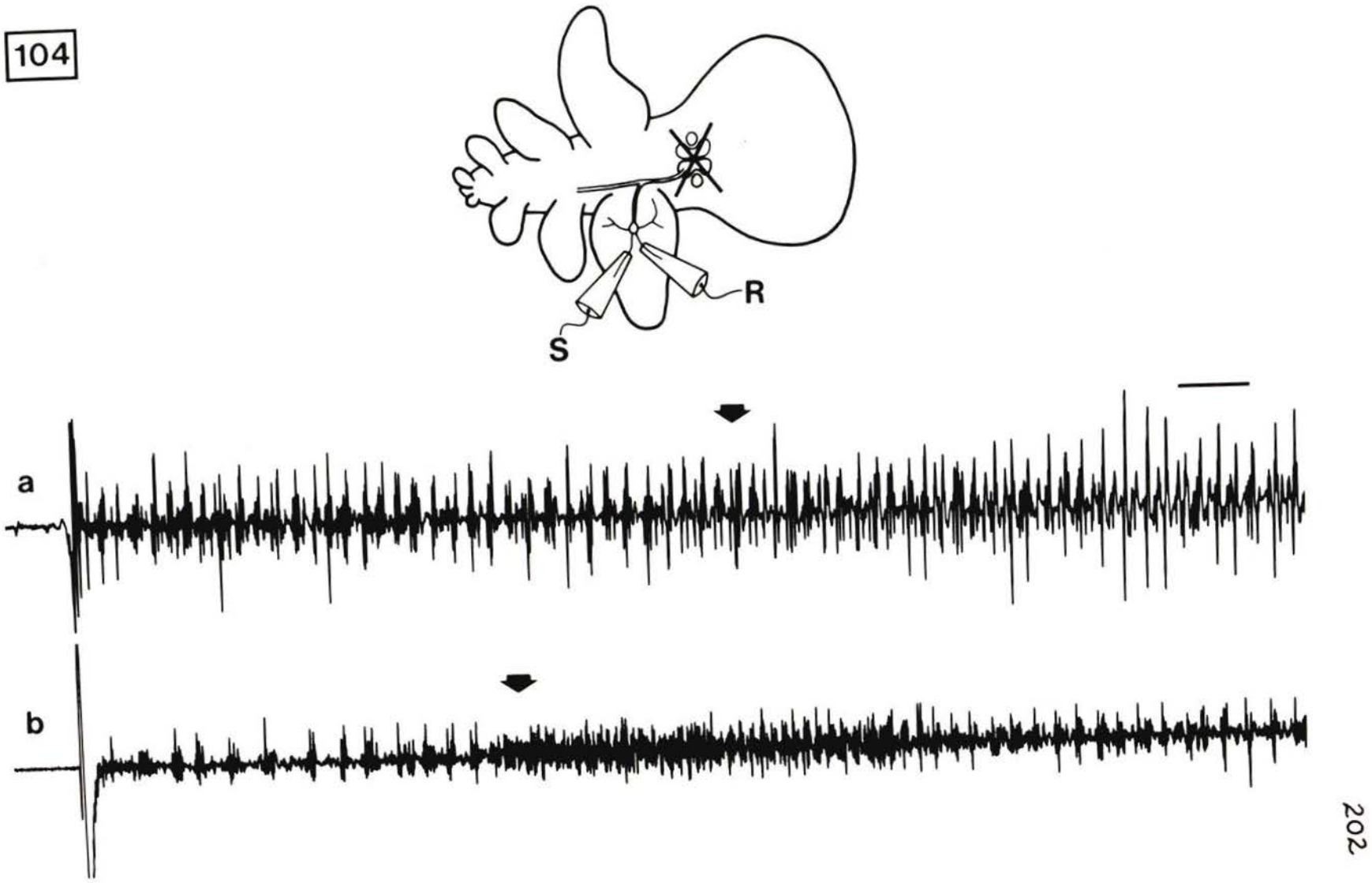

Figure 105: Continuous extracellular recording from a distal nerve following electrical stimulation to a second distal nerve (R and S, respectively in the diagram shown in Fig. 104). A train of large amplitude spike bursts followed the electrical stimulus but arrested 7 seconds prior to the onset of ceratal autotomy (arrow). Time scale = 500 msec.

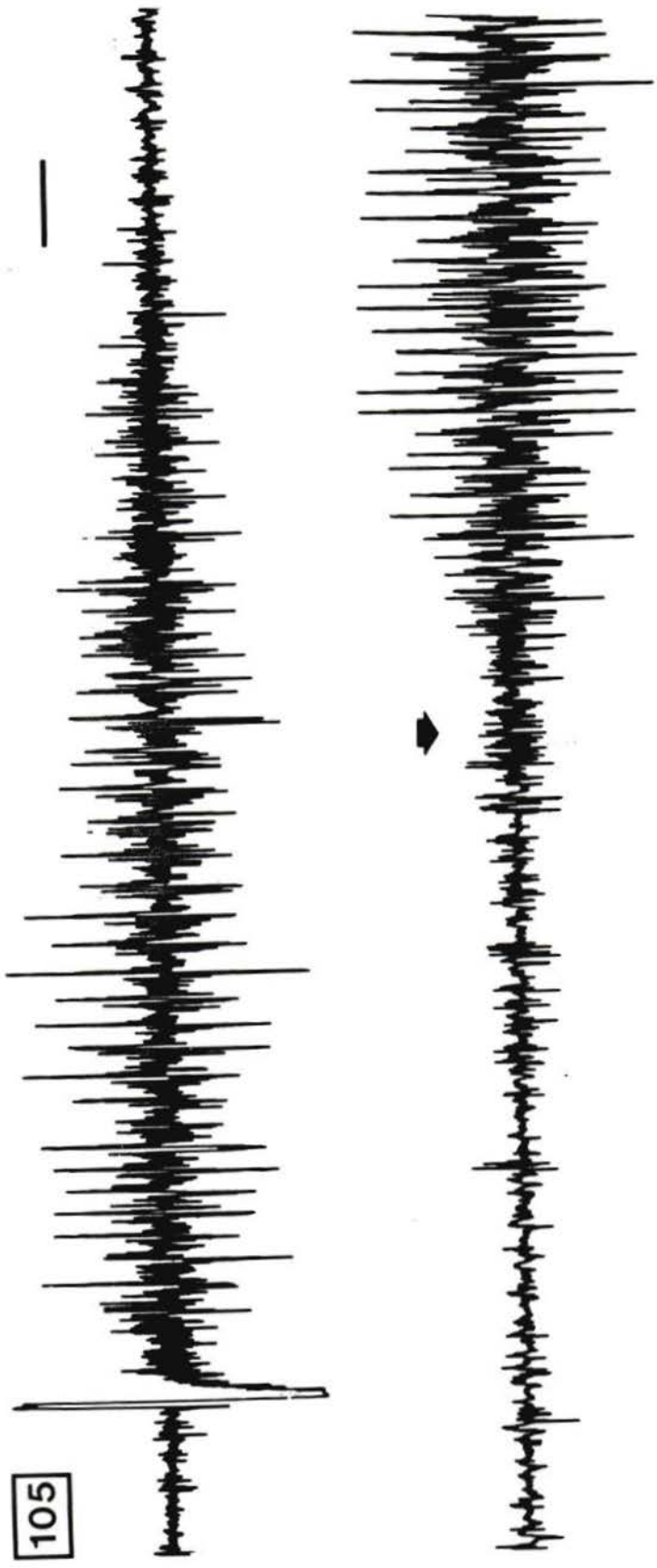
105

Chapter 4

STRUCTURE AND FUNCTION OF THE REPUGNATORIAL GLANDS AND THEIR ASSOCIATED SENSORY CELLS IN MELIBE LEONINA (GOULD, 1852)

INTRODUCTION

The reduction or loss of the protective shell in opisthobranch gastropods is correlated with the development of various alternative defense mechanisms against potential predators (Faulkner and Ghiselin, 1983). These defenses include cryptic colouration, spicules within the dorsal epidermis, nematocysts sequestered from cnidarian prey, escape behaviours, acid secretions, and other toxic or unpalatable chemical substances (see T. Thompson, 1960a; b; 1984; Edmunds, 1966; 1968; Farmer, 1970; Harris, 1971; Ros, 1976). The effectiveness of these methods is attested to by the fact that most opisthobranchs are rarely preyed upon under natural conditions and are rejected by fish in laboratory feeding experiments (Herdman, 1890; T. Thompson, 1960b; Russell, 1966).

Recent research by organic chemists has identified a large number of unusual secondary metabolites in nudibranchs. Some of these, particularly certain terpenoid compounds, are toxic or unpalatable to fish predators (Burreson et al., 1975; Schulte et al., 1980; Ayer and Andersen, 1982; Cimino et al., 1982; 1985; Hellou et al., 1982; J. Thompson et al., 1982; Okuda et al., 1983; Carté and Faulkner, 1986; Gunthorpe and Cameron, 1987). Unfortunately, other types of marine predators, notably crabs and seastars, have not been used in feeding bioassays of these chemicals. The unpalatable metabolites are frequently derived from the prey of nudibranchs, including sponges, bryozoans, and soft corals (Schulte and Scheuer, 1982; J. Thompson et al., 1982; Carté and Faulkner, 1983; Grode and Cardellina, 1984; Coll et al., 1985; Mebs, 1985), but some are the product of de novo synthesis (Cimino et al., 1983; 1985; Gustafson and Andersen, 1985). Interestingly, several of the defensive chemicals from nudibranchs are identical or related to antipredator substances found in insects (Ayer and Andersen, 1982; Cimino et al., 1985;) and terrestrial plants (Cimino et al., 1981; Schulte and Scheuer, 1982).

Studies by J. Thompson et al. (1982) on Cadlina luteomarginata and Cimino et al. (1983; 1985) on the dorid nudibranchs Dendrodoris limbata and D. grandiflora, indicate that the dorsum, exclusive of the hepatopancreas, contains the highest concentrations of terpenoids that are unpalatable to fish. Furthermore, toxic or unpalatable metabolites have been isolated directly from secretions of Phyllidia varicosa (Burreson et al., 1975) and Tambja abdere (Carté and Faulkner, 1986). These findings imply that the active substances are located within epidermal skin glands, yet little is known about the detailed structure or secretory mechanism of these glands. Drawings from histological work by T. Thompson (1960b) and Edmunds (1966) show distinctive epidermal glands in the dorsum of several dorid nudibranchs and the cerata of some eolid nudibranchs. As illustrated by these authors, the glands exhibit considerable interspecific differences in structure, but in each species they tend to be concentrated in areas of the body most vulnerable to predators. Furthermore, Thompson (1960b) observed that the slugs often react to disturbances by concealing areas lacking these distinctive glands (henceforth called repugnatorial glands) and exposing areas well-endowed with glands. Edmunds (1966) described ciliated sensory cells concentrated at the apices of the cerata in all but one of the eolids he examined. He speculated that vigorous prodding of the cerata induces secretion from the presumed repugnatorial glands by first stimulating the ciliated sensory cells.

The dendronotid nudibranch Melibe leonina, which can reach very high population densities within eel grass and kelp beds off the west coast of North America, has a distinctive odour when prodded or handled. Kjerschow-Agersborg (1921; 1923) suggested that the odour derives from the secretion of notable multicellular glands distributed liberally beneath the epidermis of this nudibranch. More recently, Ajeska and Nybakken (1976) found that the predatory sea star, Pycnopodia helianthoides, is repelled by direct physical contact with M. leonina and by contact with a glass rod previously wiped over the

surface of M. leonina. These authors suggested the aromatic substance was the responsible deterrent. Finally, Ayer and Andersen (1983) isolated two degraded monoterpenes from M. leonina; one had no antifeedant activity in a standard goldfish bioassay while the other, which embodied the characteristic odour of M. leonina, was said to be "too volatile for reliable testing".

I examined the repugnatorial glands and their associated sensory cells of M. leonina using light microscopy and scanning and transmission electron microscopy in order to further the structural observations made by Kjerschow-Agersborg (1923) and to determine the effective stimulus and mechanism for glandular discharge. In addition, I observed responses of seastars, fish, and crabs to M. leonina to confirm and extend Ajeska and Nybakken's (1976) claim that M. leonina is rejected by some, but not all, potential predators.

MATERIALS AND METHODS

A. Electron Microscopy

All ultrastructural observations were made on repugnatorial glands from the cerata of laboratory reared, young juveniles (4 to 6 weeks postmetamorphosis) of M. leonina. Observations made by Nomarski differential interference contrast microscopy (NDIC) suggest that the structure of the ceratal repugnatorial glands in young animals is identical to that of older individuals.

Prior to fixation, isolated cerata from small specimens of M. leonina were partially anaesthetized in artificial seawater containing increased concentration of magnesium ion and reduced concentration of calcium ion (high Mg^{2+}, low Ca^{2+} seawater; recipe given by Audesirk and Audesirk, 1980) for 2 hours. Initial fixation was in phosphate buffered (pH 7.6) 2.5% glutaraldehyde, made isosmotic to seawater with 0.34M NaCl (Cloney and Florey, 1968), for 12 hours at 4 degrees C. The tissue was subsequently fixed in phosphate buffered 2% osmium tetroxide for 1 hour at room temperature.

Tissue for scanning electron microscopy was dehydrated in a graded acetone series, critical point dried from liquid carbon dioxide (Bomar SPC critical point dryer; 1100 psi, 31 degrees C), mounted on stubs with double-sided sticky tape, and coated with gold-palladium (Technics hummer-sputter system). The prepared specimens were examined with a JEOL JSM-35 scanning electron microscope.

Tissue for transmission electronmicroscopy was dehydrated in a graded ethanol series, followed by propylene oxide, and embedded in Epon plastic. Silver-grey sections were cut with a Dupont diamond knife on a Riechert ultramicrotome and examined with a Philips EM300.

B. Predator Experiments

These experiments were done using adult M. leonina collected by SCUBA divers from Patricia Bay, Vancouver Island, Canada. The predator species were obtained from various sites around the southern end of Vancouver Island by SCUBA divers or by intertidal collection at low tide. Animals were held either in the recirculating natural seawater system at the University of Victoria or in the flow-through seawater system at Friday Harbor Laboratories, University of Washington, U.S.A.

Whole specimens of M. leonina were offered to seastars, fish, and crabs. I considered these to be the most likely categories of potential predators of M. leonina in its natural environment. The seastar species were: Pycnopodia helianthoides, Leptasterias hexactis, Dermasterias imbricata, Pisaster ochraceus, and Crossaster papposus. The fish were: Oligocottus maculosus and Gobiesox meandricus. The crabs were: Cancer productus, Pugettia producta, and Scyra acutifrons.

Tests with the seastars and crabs were conducted by pairing each predator with a specimen of M. leonina and placing the two in a large glass bowl. The size of each member of the pair was chosen so as to reasonably permit a predator - prey interaction and to facilitate observations within the experimental design. The response of the predator following physical contact with M. leonina was scored as avoidance, neutral, or attack.

In a second type of experiment, a small specimen of Pycnopodia helianthoides was placed in each of five bowls that also contained single specimens of M. leonina and the limpet Collisella digitalis. The bowls were observed following a 24 hour interval and instances of predation were recorded.

The two fish species that were tested for their acceptance of M. leonina as a possible food had been accustomed for several months previously to aquarium conditions and to being fed chunks of fresh limpet offered by forceps. At the time of testing, each fish was

offered chunks of both limpet and excised cerata of M. leonina and scored for acceptance or rejection of the offered item.

RESULTS

A. Distribution and Structure of Repugnatorial Glands and Sensory Cells

The repugnatorial glands of Melibe leonina appear to the unaided eye as tiny opaque 'spots' embedded within the otherwise transparent epidermis of this nudibranch. The glands are distributed over the entire dorsal and lateral surface of M. leonina but are most abundant on the cerata, particularly the distal portions, and on the dorsal surface of the large oral hood. They are absent from the ventral surface of the hood and from the sole of the foot.

Examination of the epidermis by light microscopy (NDIC) reveals that each of the repugnatorial glands, which range in diameter from 40 to 120 µm, is composed of 3 to 6 transparent spheres embedded within a surrounding sheath (Figs. 106 and 107). The glands are located at terminals of small nerve branches that ramify beneath the epidermis (Fig. 107). NDIC microscopy and scanning electron microscopy show that two or more bundles of short, stiff cilia arise from the epithelium overlying each gland (Figs. 108 and 109). These ciliary tufts are found nowhere else on the ceratal epidermis.

The detailed structure of the repugnatorial glands and the adjacent ciliated sensory cells, as determined by transmission electron microscopy, is sketched in Figure 110 and a low magnification transmission electron micrograph of a gland is shown in Fig. 111. Each of these multicellular glands consists of two types of large secretory cells located completely below the thickness of the epidermis. The apices of the secretory cells impinge upon the proximal end of a short secretory duct that is excavated within the overlying epidermis. The duct opens to the outside via a small pore. The sheath that envelops the secretory cells is composed of muscle cells.

Additional description of the various components of the repugnatorial glands of M. leonina and their associated sensory cells is given below.

1. Secretory Duct

The secretory duct is formed by epidermal cells that are invaginated within the epidermis (Figs. 112 and 113). The site of invagination remains open to form a secretory pore (Fig. 112). The secretory duct does not extend below the thickness of the general epidermis and the apices of the secretory cells line the floor of the duct. A felt-work of microfilaments lies immediately beneath the apical cell membrane of the duct cells (Fig. 114). This cytoskeleton may strengthen the apical cytoplasm of the duct cells so as to maintain the shape of the short lumen of the duct.

2. Secretory Cell Types

I have designated the two secretory cell types of the repugnatorial gland as types A and B. Both have a large central vacuole containing the product of synthesis, but the two cell types can be distinguished by cytoplasmic characteristics and by the ultrastructural appearance of their secretory product.

Type A: In thin sections, the material elaborated by the type A secretory cell appears as a diffuse meshwork of fine fibrils (Figs. 111, 112, 115, and 116). The large central vacuole containing this substance is very irregular in outline (Figs. 111 and 112), probably due to fusion of smaller cytoplasmic vacuoles with the large central vacuole at the time of fixation. At the apex of the type A secretory cell, the layer of cytoplasm lying between the limiting membrane of the central vacuole and the outer membrane of the secretory cell is very thin and devoid of organelles and inclusions (Figs. 112, 113, and 115). Thus, the secretory product is separated from the lumen of the secretory duct by little more than these two membranes. Along the lateral and basal portions of the type A secretory cells, the cell membrane is elaborated into many elongate, interdigitating processes (Fig. 116).

The large, ovoid nucleus of the type A secretory cell is located toward the base of the cell. A large nucleolus is present and the nuclear chromatin is uniformly dispersed with only occasional small clumps of heterochromatin (Fig. 111).

As shown in Fig. 116, many free ribosomes and polyribosomes are distributed throughout the cytoplasm of the type A cell and profiles of rough endoplasmic reticulum are present but not abundant. Each type A cell has many Golgi fields that give rise to primary vesicles containing a uniformly electron-dense substance. The primary vesicles appear to mature into secondary vesicles having a less electron-dense content, and these subsequently become the larger tertiary vesicles containing a flocculent material identical to that in the central lumen.

The most distinctive cytoplasmic features of the type A secretory cell are their high density of mitochondria and the presence of bundles of microtubules having various orientations (Fig. 116). The microtubule bundles are always situated close to the membrane of the central vacuole.

Finally, synaptic profiles containing a mixture of clear and slightly electron-opaque vesicles contact the type A secretory cells (Fig. 117).

Type B: The secretory product of the type B secretory cells appears as closely packed, electron-dense granules (Figs. 116, 118, and 119) contained within a central vacuole that is generally more regular in outline than that of the type A cell (Fig. 111). However, as in the type A cell, the distal portion of the type B cells narrows as it approaches the secretory duct and the secretory product within the central vacuole is separated from the lumen of this duct by only a thin layer of featureless cytoplasm and the apical membranes of the cell and central vacuole (Fig. 115).

The nuclear structure of the type B secretory cells is similar to that of the type A. The most distinctive feature of the cytoplasm in B cells is the abundance of rough endoplasmic

reticulum that is arranged in regular, parallel lamellae around the central vacuole (Fig. 118). The many, large Golgi profiles within these cells give rise to electron-dense vesicles that subsequently appear to fuse to form compound vesicles containing material similar to that in the central vacuole (Fig. 119). Type B cells contain fewer mitochondria than the type A cells and these are concentrated around the Golgi fields. Bundles of microtubules were not found within type B cells and the cell membrane is not elaborated into digitiform processes.

Like the type A secretory cells, the B cells are innervated and the synaptic terminals contain both clear and slightly opaque vesicles (Fig. 120).

3. Muscle:

Muscle tissue is a prominent component of each repugnatorial gland; it accounts for approximately 24% of the cross sectional area of each gland. This figure was obtained by first weighing cross-sectional profiles of five repugnatorial glands cut from photographic prints and then weighing the muscle portion alone. The muscle cells are organized into two layers: the inner layer invests each secretory cell and the outer layer encapsulates the entire gland (Fig. 111). The long axes of the muscle cells are oriented in various directions, so that sections through neighboring cells often show their respective myofilaments oriented in opposing directions (Fig. 121).

Unlike the longitudinal muscle bands of the ceras (see Ch. 2), the myofilaments of the repugnatorial gland muscle are sufficiently ordered to cause alignment of the dense bodies into distinct rows. Sobieszek (1973), among others, has shown that the dense bodies of molluscan muscle are sites of thin filament attachment. The muscle shows characteristic features of obliquely striated muscle (see Rosenbluth, 1972; Chantler, 1983). Single fibres cut in cross section show a non-homogeneous pattern of filament composition, in that areas consisting of both thick and thin filaments are intermingled with areas of thin filaments

only (Fig. 116). In longitudinal section, the rows of dense bodies are oriented at an oblique angle to the long axis (Fig. 121). However, this angle (the striation angle) is never less than 45 degrees from the long axis.

The thick filaments of this muscle are short. A mean sarcomere length of 1.3 µm (range 1.1 to 1.7 µm) was obtained from micrographs of 6 different muscles.

Dense bodies with attached arrays of thin filaments are also located along the sarcolemma (Fig. 116). These sites look like hemidesmosomes, but Nunzi and Franzini-Armstrong (1981) suggest the term hemifasciae adherentes to distinguish the fact that the associated intracellular filaments contain of actin and are not intermediate filaments. Membrane-associated dense bodies may be sites where thin filaments of the sarcoplasm are anchored to extracellular elements of the external lamina and surrounding connective tissue (Twarog et al., 1973; Nunzi and Franzini-Armstrong, 1981).

In general, tubules of the sarcoplasmic reticulum (SR) are confined to the peripheral, subsarcolemmal cytoplasm and do not extend along the lines of Z-bodies. Rare instances of SR located within myofilament bundles were confined to regions adjacent to the nucleus. Peripheral elements of the SR often form surface couplings (also called peripheral couplings or dyads) with the sarcolemma. In these regions, the opposing membranes of the sarcolemma and the SR are closely aligned and electron-dense material fills the intervening gap (Fig. 119).

The nuclei of the muscle cells, with associated Golgi, rough endoplasmic reticulum, and mitochondria are confined to the periphery of the gland (Fig. 111). Infrequent mitochondria and electron-dense granules that may be glycogen occur outside the myofilament bundles, beneath the sarcolemma.

I distinguished two general types of neuromuscular synapses based on the appearance of the synaptic vesicles. The first type, which is most abundant, contained many, small

vesicles with a clear or slightly electron-opaque content (Figs. 121 and 122). These are similar to the vesicles within the neuroglandular synaptic profiles. In the second, relatively rare type of neuromuscular synapse, the synaptic vesicles are similar in size to the former type but contain a very electron-dense material (Fig. 123).

4. Sensory Cells:

Each tuft of cilia that lies adjacent to the pore of a repugnatorial gland arises from a bundle of dendrites that extends through the thickness of the epidermis (Figs. 124, 125, and 126). The cell bodies of these primary sensory cells are located beneath the epidermal epithelium and the bundle of dendrites is flanked by several ciliated supporting cells with intraepithelial cell bodies (Fig. 124).

Each dendrite contributes 2 to 5 cilia to the ciliary tuft. The cilia are relatively short (less than 10 μm), have a 9 plus 2 axoneme, and are interspersed among microvilli. The ciliary axoneme arises from a basal plate that is elevated above the level of the apical membrane of the dendrite (type II transition zone as defined by Pitelka, 1974) and the basal bodies bear a basal foot and a striated rootlet (Fig. 127). Mitochondria are clustered immediately beneath the ciliary basal bodies (Fig. 126). Beginning in the region of mitochondria, the dendrites narrow and contain longitudinally arranged microtubules (Fig. 125).

The cytoplasm of the subepidermal, sensory cell bodies includes one or more Golgi bodies located distal to the nucleus, multivesicular bodies, and numerous small vesicles (Fig. 128). The cluster of sensory cell bodies is associated with a neuropil where synapses are frequently encountered (Fig. 124).

B. Stimulus and Mechanism for Glandular Secretion

The repugnatorial glands of an isolated ceras of Melibe leonina can be induced to secrete by touching a fine glass, wooden, or metal probe to the epidermis overlying each gland. Each repugnatorial gland behaves as an independent effector in that a probe elicits discharge from the gland touched, but not from neighboring glands, and glands can be induced to secrete even after the distal nerves of the ceras are cut. As viewed under a dissecting microscope, the capsule of the gland contracts abruptly as the secretory product is extruded from the central portion of the gland in the form of a coiled strand of mucous-like material. The secreted substance is sticky, in that it tends to adhere to the probe that evoked the discharge. After secretion, the cluster of refractile spheres that are characteristic of undischarged glands is absent (compare Figs. 129 and 130).

If secretion from several discharged glands is collected into a fine glass pipette and transferred to filter paper, the paper acquires the distinctive odour of a physically disturbed specimen of M. leonina. Kjerschow-Agersborg (1923) likened the odour to oil of bergamot, although a better description might be a combination of lime and melon.

Direct touch was the only stimulus I could identify that induced secretion from the repugnatorial glands. The intensity of these touch stimuli was not quantified, but very light touches rarely caused glandular discharge and some of the glands failed to discharge even following vigorous prods. Between these two extremes, individual glands varied with respect to their stimulus threshold for secretion.

Electrical stimuli applied via suction electrode to the distal stump of cut peripheral nerves (see Ch. 3 for method) failed to cause secretion from repugnatorial glands.

A filtered solution obtained by grinding tube feet from the sea star Pycnopodia helianthoides in a small amount of sea water did not elicit secretion from the repugnatorial glands when gently pipetted over the ceratal epidermis. Nevertheless, a cursory

experiment was performed to determine if unidentified tube foot chemicals might lower the threshold for touch-induced secretion from the repugnatorial glands. One primary ceras was removed from each of 12 adult M. leonina and these were secured by two pins to the bottom of separate Sylgard-lined petri dishes. The seawater within the dishes was held at 12 degrees C by partial immersion in a water bath. Ten glands on one side of the midline of each ceras were touched with a clean glass probe having a diameter similar to that of a seastar tube foot, and 10 glands on the opposite side of the midline were touched with a freshly excised tube foot from P. helianthoides. The results, as shown in Table I, indicate that touches with a P. helianthoides tube foot cause a significantly greater number of glands to secrete than touches with a glass probe.

Glandular secretion is inhibited by bathing cerata in high Mg^{2+}, low Ca^{2+} seawater for 12 hours and the inhibition is reversible. This dispels the notion that prodding the glands effects discharge by simply puncturing the distended secretory cells.

C. Predator Experiments

All seastar species, except Crossaster papposus, showed avoidance behaviour after their tube feet touched M. leonina. As previously described by Ajeska and Nybakken (1976), either the tip or the entire arm(s) that contacted the nudibranch flexed aborally and the seastar altered its direction of movement. When P. helianthoides was placed in bowls containing both M. leonina and the limpet Collisella digitalis, the limpet was ingested but the nudibranch was unmolested after a 24 hour interval.

Crossaster papposus also exhibited aboral flexion of the arm(s) that contacted M. leonina. However, instead of retreating from further contact, C. papposus crawled rapidly on top of M. leonina and everted its stomach. This 'pounce' behaviour is similar to that described by Mauzey et al. (1968) for attacks by the seastar Solaster dawsoni on its prey, Solaster stimpsoni.

Like most seastars, the two fish species consistently rejected cerata of M. leonina, but all 3 crab species attacked and, if capture was successful, ingested M. leonina.

DISCUSSION

In order for an unpalatable chemical secretion to be used economically but effectively against potential predators, it might be expected that the release of the substance should fulfill at least four criteria. The defensive chemical should be: 1) released only at the appropriate time (Faulkner and Ghiselin, 1983), 2) released from a site likely to be encountered first by an attacking predator (T. Thompson, 1960b; Edmunds, 1966; Faulkner and Ghiselin, 1983), 3) released in sufficient quantity to deter predators, and 4) released rapidly to prevent lethal damage before the distastefulness is detected by the predator. These criteria appear to be fulfilled in the present instance.

The widespread distribution of many small repugnatorial glands over the body of M. leonina ensures that all body surfaces exposed to predators are defended. With respect to the size and distribution of repugnatorial glands, it is interesting to compare M. leonina with the shell-less pulmonate Onchidella borealis that inhabits crevices and kelp holdfasts in the middle to high intertidal (Young et al., 1986). Unlike M. leonina, O. borealis is a small gastropod (usually less than one cm length) with a compact, limpet-like shape. The defensive chemical is concentrated in 20 or fewer large glands located around the margin of the dorsum and the secretion is elicited by and repels seastars (Young, et al., 1986). However, concentration of defensive chemical within a few large repugnatorial glands would seem particularly inappropriate for a large animal such as M. leonina with a large surface area due to many outstretched appendages (the cerata and oral hood). Furthermore, relative to O. borealis, the habit and habitat of M. leonina must impose much greater risk from fish predators that would attack sparsely protected appendages; even if the nudibranch were eventually rejected, damage to non-autotomizing structures such as the oral hood might be lethal.

Whatever the nature of the defensive chemical, it is sufficiently potent to repel seastars after contact-induced secretion from only a small percentage of the total number of glands. Therefore, distribution of potent defensive chemical among many small glands and the contact requirement for glandular secretion conserves defensive chemical and ensures that some, indeed most, of the nudibranchs's chemical defense system is left intact after a predator encounter.

Crossaster papposus was the only seastar out of five species tested that attacked and ingested M. leonina. This result supports field observations made by Mauzey et al. (1968). Crab predators are not repelled by the defensive chemical of M. leonina. I have argued in Ch. 3 that ceratal autotomy is M. leonina's defense against crab predators.

Examination of the repugnatorial glands of M. leonina by light and electron microscopy provides a morphological explanation for their behaviour as 'independent effectors'. Tufts of short, non-motile cilia, each arising from a bundle of sensory dendrites with subepidermal cell bodies, are located close to the secretory pore of each repugnatorial gland. This type of molluscan primary sensory cell has been recognized since the last century (see Crisp, 1971) and their ultrastructure has been described for a wide variety of molluscs (Crisp, 1971; Zylstra, 1972; Wright, 1974a, b; Kataoka, 1976; Emery and Audesirk, 1978; Phillips, 1979; Chia and Koss, 1982; Hodgson and Fielden, 1984). Among these, much variation exists regarding such things as number of cilia per cell, length of cilia, number and length of ciliary rootlets, and microtubule arrangement within the ciliary axoneme. Many authors have suggested that these structural differences reflect differences in the sensory modality that stimulates the receptors. However, in the absence of direct neurophysiological evidence, these are tentative speculations (see review by Croll, 1983).

The close spatial association between the ciliated sensory cells and repugnatorial glands, and the fact that glandular discharge can be elicited only by direct touch to the epidermis overlying each gland suggests that a touch stimulus activates a local circuit involving the ciliated sensory cells and efferents to the secretory cells and the investing musculature of the repugnatorial gland. This hypothesis was previously proposed by Edmunds (1966), whose histological work revealed both ciliated sensory cells and probable repugnatorial glands within the ceratal epidermis of several eolids.

While the possibility that some aspects of the discharge process, for instance the variable discharge threshold, are regulated by nerves coming from other parts of the animal, there is at present no evidence for such extrinsic control. Therefore, the glands may be provisionally regarded as independent effectors (Parker, 1919).

Additional evidence, albiet circumstantial, suggesting a mechanoreceptive role for the ciliated sensory cells associated with repugnatorial glands comes from neurophysiological recordings of impulse activity within distal nerves during touches to the ceratal epidermis (Ch. 3; Figs. 97, 98, and 99). These afferent responses likely originate from the ciliated receptors associated with the repugnatorial glands because: no other ceratal receptors were identified by scanning and electron microscopy, peripheral branches of distal nerves extend to each repugnatorial gland, and the distribution of the ciliated sensory cells and the combined receptive fields of distal nerves to touch stimuli both cover the entire ceratal epidermis.

Extracellular neurophysiological recordings from distal nerves of the ceras show greater neural activity during touch to the ceratal epidermis by Pycnopodia tube foot than that induced by a glass probe (Ch. 3; Figs. 97 and 99). Furthermore, touches by a Pycnopodia tube foot were a more effective stimulus for eliciting secretion from repugnatorial glands than were touches by a glass probe (Table I). The latter result was

also found for the repugnatorial glands of Onchidella borealis (Young et al., 1986). Pycnopodia releases dramatic escape responses from many marine invertebrates (see Mauzey et al., 1968), suggesting a high concentration of saponins within the tube feet of this seastar (see Mackie et al., 1970). Saponins are potent surfactants that lyse biological membranes by interacting with cell membrane cholesterol (Mackie et al., 1975). They are believed to provide a chemical defense for seastars (Mackie et al., 1977), although ironically, they also release avoidance and escape behaviours by their prey (Mackie et al., 1968; Mackie, 1970). Mackie (1970) suggested that saponins actually damage sensory cells of other invertebrates. Therefore, the potentiation effect of Pycnopodia tube feet on touch induced discharge of repugnatorial glands and on touch induced afferent responses from distal nerves of the ceras may result from injury discharges of the sensory cells associated with the repugnatorial glands.

During extracellular recordings from the pallial nerve of two limpet species (Acmaea limatula and Acmaea scutum), Phillips (1975b) found afferent response to a probe touched to the mantle margin and enhanced response to touch by tube feet of several predatory seastars. However, he also described a second category of afferent activity that responded to effluent from predatory seastars. This was consistent with experimental results showing distinct behavioural responses by the limpet depending on whether seastars were at a distance or had actually made contact (Phillips, 1975a; b). A subsequent ultrastructural study showed two types of ciliated receptor endings on the pallial tentacles (Phillips, 1977; 1979), one of which (the type II receptor), is similar to that of the ceratal sensory cells of M. leonina. Yoshii et al. (1978) also obtained evidence from extracellular electrophysiological recordings for distance chemoreception of predatory seastars in the clam, Spisula sachalinensis. Neither Acmaea nor Spisula is known to possess defensive chemicals, so avoidance behaviour initiated by distance chemoreception of approaching sea stars is appropriate.

Although receptors sensitive to dissolved chemicals from distant seastars may be present on the rhinophores or hood tentacles M. leonina, my unquantified observations did not suggest that M. leonina avoids approaching seastars. Avoidance behaviour may be unecessary due to the effectiveness of the defensive chemical released by contact stimulation of areas of epidermis provided with repugnatorial glands.

As described below, the structure of the repugnatorial glands exhibits several characteristics that ensure rapid release of the entire store of secretory product within each gland.

Storage of secretory product within a single large vacuole must facilitate rapid, all-or-none secretion upon appropriate stimulation of the synthesizing cell. A single fusion event between the membranes of the central vacuole and the limiting membrane of the glandular cell exposes the entire bulk of secretory product to the extracellular environment. The phenomenon is the same as occurs during the acrosome reaction of some types of sperm (see Colwin and Colwin, 1961; Summers et al., 1975). The acrosome reaction is also a secretion event that demands rapid and complete extrusion of an intracellularly-stored secretory product, the contents of the acrosomal vesicle.

Ultrastructural data show that each secretory cell within the repugnatorial gland complex receives synaptic input. The work of Kater and co-workers on molluscan salivary glands (Kater et al., 1978a, b; Goldring et al., 1983) showed that nervous excitation of glandular cells, either by direct synaptic contact or by electrotonic spread from innervated cells, opens voltage sensitive ion channels in the glandular cell membrane. The overshooting membrane depolarization is carried by calcium ions and results in release of the glandular product. A similar mechanism may open the central storage vacuoles of the repugnatorial gland cells in M. leonina, with the ciliated receptors acting as presynaptic cells.

Alternatively, the apical membrane of each secretory cell and its underlying storage vacuole may be mechanically ruptured by contraction of the investing muscle. However the central vacuole is opened, muscle contraction must expel the secretory product from each gland cell and subsequently from the secretory pore.

The structure of this muscle is interesting in several respects. Firstly, obliquely striated muscle is relatively uncommon in adult gastropods and tends to be restricted to components of the buccal mass (Matisson and Arvidsson, 1966; Nisbet and Plummer, 1968; Plesch, 1977). Secondly, the effective sarcomere length (1.3 µm), and therefore the thick filament length of the repugnatorial gland muscle is short compared to thick filament lengths of greater than 2 µm that are typical of most obliquely striated molluscan muscles (Hanson and Lowy, 1961; Schlote, 1963; Nisbet and Plummer, 1968; Plesch, 1977; Amsellem and Nicaise, 1980; Kier, 1985).

Obliquely striated molluscan muscles have contraction speeds that are less than cross striated fibres but considerably greater than molluscan non-striated (smooth) muscle (see Millman, 1967). The short sarcomere length of the repugnatorial gland muscle must contribute to a high shortening velocity. According to Josephson (1975) shortening velocity of striated muscle is directly proportional to muscle length and inversely proportional to sarcomere length (other factors being equal). The latter relationship is due to the fact that short sarcomeres result in a greater number of sarcomeres per unit length of muscle, and shortening velocities of elements connected in series are additive. The length of the muscle investing each repugnatorial gland is short; even the outer muscle layer must have a maximum length that is no greater than the circumference of the gland. Therefore, the unusually short sarcomere length may compensate for a short overall muscle length to allow a reasonably fast contraction velocity. In this respect, it is interesting that another short, obliquely striated molluscan muscle, the muscles that expand the chromatophores of

Loligo, have a length of only 30 µm and a sarcomere length of less than 1 µm (measurements taken from micrographs in Cloney and Florey [1968]).

Direct observations of living glands confirm the phasic contraction of the investing muscle, yet fast contraction must be coupled with the ability to generate large contractile force (tension) in order to abruptly expel the bulky, viscous secretory product through the narrow secretory pore. The required force may be a simple result of the pronounced thickness of the muscular investment of each secretory cell, because maximum tension produced by striated muscle is proportional to its cross sectional area (Josephson, 1975).

Finally, although mitochondria are common within the restricted perinuclear cytoplasm of the repugnatorial gland muscle, they are scarce alongside the myofilaments. In contrast, many mitochondria are found throughout the length of obliquely striated myofibres that operate the radula of gastropods (Matisson and Arvidsson, 1966; Nisbett and Plummer, 1968; Plesch, 1977). This difference can be explained by the fact that radular muscles must perform long-term repetitive contractions requiring a high and continuous supply of metabolic energy, whereas functional contractions of the repugnatorial gland muscle occur only at the time of glandular discharge.

The significance of two types of glandular cells with morphologically distinct secretory products is unknown. Previous investigators have noted that mucus is released concurrently with the defensive chemicals of certain other nudibranchs (Schulte and Scheuer, 1982; T. Thompson, 1960b; Edmunds 1966; Carté and Faulkner, 1986). T. Thompson (1960b) suggested that mucus may retard the diffusion of volatile defensive chemicals and thus prolong their protective function to the threatened nudibranch. One of the secretory cell types of the repugnatorial gland of M. leonina may be a mucocyte. The combination of mucocytes and glandular cells that release defensive chemical within a single, multicellular gland would ensure the mixing of these two materials within the secretory duct during glandular discharge.

LITERATURE CITED

Ajeska, R.A., and J. Nybakken. 1976. Contributions to the biology of Melibe leonina (Gould, 1852) (Mollusca: Opisthobranchia). Veliger 19: 19-26.

Amsellem, J., and G. Nicaise. 1980. Ultrastructural study of muscle cells and their connections in the digestive tract of Sepia officinalis. J. submicrosc. Cytol. 12: 219-231.

Audesirk, G., and T. Audesirk. 1980. Complex mechano- receptors in Tritonia diomedea 1. Responses to mechanical and chemical stimuli. J. comp. Physiol. 141: 101-109.

Ayer, S.W., and R.J. Andersen. 1982. Steroidal anti-feedants from the dorid nudibranch Aldisa sanguinea Cooperi. Tetrahedron Letters 23: 1039-1042.

Ayer, S.W., and R.J. Andersen. 1983. Degraded monoterpenes from the opisthobranch mollusc Melibe leonina. Experientia 39: 255-256.

Burreson, B.J., P.J. Scheuer, J. Finer, and J. Clardy. 1975. 9-Isocyanopupukeanane, a marine invertebrate allomone with a new sesquiterpene skeleton. J. Am. chem. Soc. 97: 4763-4764.

Carté, B., and D.J. Faulkner. 1983. Defensive metabolites from three nembrothid nudibranchs. J. org. Chem. 48: 2314-2318.

Carté, B., and D.J. Faulkner. 1986. Role of secondary metabolites in feeding associations between a predatory nudibranch, two grazing nudibranchs, and a bryozoan. J. chem. Ecol. 12: 795-804.

Chantler, P.D. 1983. Biochemical and structural aspects of molluscan muscle. Pp. 77-154 in The Mollusca, Vol. 4. Physiology, part 1, A.S.M. Saleuddin and K.M. Wilbur, eds. Academic Press, N.Y.

Chia, F.-S., and R. Koss. 1982. Fine structure of the larval rhinophores of the nudibranch, Rostanga pulchra, with emphasis on the sensory receptor cells. Cell Tiss. Res. 225: 235-248.

Cimino, G., S. De Rosa, S. De Stefano, and G. Sodano. 1981. Novel sesquiterpenoid esters from the nudibranch Dendrodoris limbata. Tetrahedron Lett. 22: 1271-1272.

Cimino, G., S. De Rosa, S. De Stefano, and G. Sodano. 1982. The chemical defense of four Mediterranean nudibranchs. Comp. Biochem. Physiol. 73B: 471-474.

Cimino, G., S. De Rosa, S. De Stefano, G. Sodano, and G. Villani. 1983. Dorid nudibranch elaborates its own chemical defense. Science 219: 1237-1238.

Cimino, G., S. De Rosa, S. De Stefano, R. Morrone, and G. Sodano. 1985. The chemical defense of nudibranch molluscs. Structure, biosynthetic origin and defensive properties of terpenoids from the dorid nudibranch Dendrodoris grandiflora. Tetrahedron 41: 1093-1100.

Cloney, R.A., and E. Florey. 1968. Ultrastructure of cephalopod chromatophore organs. Z. Zellforsch. mikrosk. Anat. 89: 73-79.

Coll, J.C., B.F. Bowden, D.M. Tapiolas, R.H. Willis, P. Djura, M. Streamer, and L. Trott. 1985. Studies of australian soft corals. XXXV. The terpenoid chemistry of soft corals and its implications. Tetrahedron 41: 1085-1092.

Colwin, L.H., and A.L. Colwin. 1961. Changes in the spermatozoan during fertilisation in Hydroides hexagonus (Annelida). I. Passage of the acrosomal region through the vitelline membrane. J. biophys. biochem. Cytol. 10: 231-254.

Crisp, M. 1971. Structure and abundance of receptors of the unspecialized external epithelium of Nassarius reticulatus (Gastropoda, Prosobranchia). J. mar. biol. Ass. U.K. 51: 865-890.

Croll, R.P. 1983. Gastropod chemoreception. Biol. Rev. 58: 293-319.

Edmunds, M. 1966. Protective mechanisms in the Eolidacea (Mollusca Nudibranchia). J. Linn. Soc. (Zool.) 46: 27- 71.

Edmunds, M. 1968. Acid secretion in some species of Doridacea (Mollusca: Nudibranchia). Proc. malacol. Soc. Lond. 38: 121-133.

Emery, D.G., and T.E. Audesirk. 1978. Sensory cells in Aplysia. J. Neurobiol. 9: 173-179.

Farmer, W.M. 1970. Swimming gastropods (Opisthobranchia and Prosobranchia). Veliger 13: 73-89.

Faulkner, D.J., and M.T. Ghiselin. 1983. Chemical defense and evolutionary ecology of dorid nudibranchs and some other opisthobranch gastropods. Mar. Ecol. Prog. Ser. 13: 295-301.

Goldring, J.M., J.W. Kater, and S.B. Kater. 1983. Electrophysiological and morphological identification of action potential generating secretory cell types isolated from the salivary gland of Ariolimax. J. exp. Biol. 102: 13-23.

Grode, S.H., and J.H. Cardellina II. 1984. Sesquiterpenes from the sponge Dysidea etheria and the nudibranch Hypseladoris zebra. J. nat. Prod. 47: 76-83.

Gunthorpe, L., and A.M. Cameron. 1987. Bioactive properties of extracts from Australian dorid nudibranchs. Mar. Biol. 94: 39-43.

Gustafson, K., and R.J. Andersen. 1985. Chemical studies of British Columbia nudibranchs. Tetrahedron 41: 1101-1108.

Hanson, J., and J. Lowy. 1961. The structure of the muscle fibres in the translucent part of the adductor of the oyster Crassostrea angulata. Proc. R. Soc. (Lond.) 154B: 173-196.

Harris, L.G. 1971. Nudibranch associations as symbioses. Pp. 77-90 in Aspects of the Biology of Symbioses, T.C. Cheng, ed. University Park Press, Baltimore.

Hellou, J., R.J. Andersen, and J.E. Thompson. 1982. Terpenoids from the dorid nudibranch Cadlina luteomarginata. Tetrahedron 38: 1875-1879.

Herdman, W.A. 1890. Some experiments on feeding fishes with nudibranchs. Nature 42: 201-203.

Hodgson, A.N., and L.J. Fielden. 1984. The structure and distribution of peripheral ciliated receptors in the bivalve molluscs Donax serra and D. sordidus. J. moll. Stud. 50: 104-112.

Josephson, R.K. 1975. Extensive and intensive factors determining the performance of striated muscle. J. exp. Zool. 194: 135-154.

Kataoka, S. 1976. Fine structure of the epidermis of the optic tentacle of a slug, Limax flavus L. Tiss. Cell 8: 47-60.

Kater, S.B., J.R. Rued, and A.D. Murphy. 1978a. Propagation of action potentials through electrontonic junctions in the salivary glands of the pulmonate mollusc, Helisoma trivolvis. J. exp. Biol. 72: 77-90.

Kater, S.B., A.D. Murphy, and J.R. Rued. 1978b. Control of the salivary glands of Helisoma by identified neurones. J. exp. Biol. 72: 91-106.

Kier, W.M. 1985. The musculature of squid arms and tentacles: ultrastructural evidence for functional differences. J. Morph. 185: 223-239.

Kjerschow-Agersborg, H.P. 1921. Contribution to the knowledge of the nudibranchiate mollusk, Melibe leonina (Gould). Amer. Nat. 55: 222-263.

Kjerschow-Agersborg, H.P. 1923. The morphology of the nudibranchiate mollusc Melibe (syn. Chioraera) leonina (Gould). Quart. J. microsc. Sci. 67: 507-592.

Mackie, A.M. 1970. Avoidance reactions of marine invertebrates to either steroid glycosides of starfish or synthetic surface-active agents. J. exp. mar. Biol. Ecol. 5: 63-69.

Mackie, A.M., R. Lasker, and P.T. Grant. 1968. Avoidance reactions of a mollusc Buccinum undatum to saponin-like surface-active substances in extracts of the starfish Asterias rubens and Marthasterias glacialis. Comp. Biochem. Physiol. 26: 415-428.

Mackie, A.M., H.T. Singh, and T.C. Fletcher. 1975. Studies on the cytoloytic effects of seastar (Marthasterias glacialis) saponins and synthetic surfactants in the plaice Pleuronectes platessa. Mar. Biol. 29: 307-314.

Mackie, A.M., H.T. Singh, and J.M. Owen. 1977. Studies on the distribution, biosynthesis and function of steroidal saponins in echinoderms. Comp. Biochem. Physiol. 56B: 9-14.

Matisson, A.G.M., and J.A. Arvidsson. 1966. Some effects of electrical stimulation and exogenous metabolites on the contractile activity and the ultrastructure of the radula muscle of Buccinum undatum. Z. Zellforsch. mikrosk. Anat. 73: 37-55.

Mauzey, K.P., C. Birkeland, and P.K. Dayton. 1968. Feeding behavior of asteroids and escape responses of their prey in the Puget Sound area. Ecology 49: 603-619.

Mebs, D. 1985. Chemical defense of a dorid nudibranch Glossodoris quadricolor, from the Red Sea. J. chem. Ecol. 11: 713-716.

Millman, B.M. 1967. Mechanism of contraction in molluscan muscle. Am. Zool. 7: 583-591.

Nisbet, R.H., and J.M. Plummer. 1968. The fine structure of cardiac and other molluscan muscle. Symp. zool. Soc. Lond. 22: 193-211.

Nunzi, M.G., and C. Franzini-Armstrong. 1981. The structure of smooth and striated portions of the adductor muscle of the valves in a scallop. J. ultrastruct. Res. 76: 134-148.

Okuda, R.K., P.J. Scheuer, J.E. Hochlowski, R.P. Walker, and D.J. Faulkner. 1983. Sesquiterpenoid constituents of eight porostome nudibranchs. J. org. Chem. 48: 1866-1869.

Parker, G.H. 1919. The Elementary Nervous System. Lippincott, Philadelphia, Pennsylvania.

Phillips, D.W. 1975a. Distance chemoreception-triggered avoidance behavior of the limpets Acmaea (Collisella) limatula and Acmaea (Notoacmea) scutum to the predatory starfish Pisaster ochraceus. J. exp. Zool. 191: 199-209.

Phillips, D.W. 1975b. Localization and electrical activity of the distance chemoreceptors that mediate predator avoiodance behaviour in Acmaea limatula and Acmaea scutum (Gastropoda, Prosobranchia). J. exp. Biol. 63: 403-412.

Phillips, D.W. 1977. A scanning electron microscope study of sensory tentacles on the mantle margin of the gastropod Acmaea (Notoacmea) scutum. The Veliger 19: 266-271.

Phillips, D.W. 1979. Ultrastructure of sensory cells on the mantle tentacles of the gastropod Notoacmea scutum. Tiss. Cell 11: 623-632.

Pitelka, D.R. 1974. Basal bodies and root structures. Pp. 437-469 in Cilia and Flagella, M.A. Sleigh, ed. Academic Press, London.

Plesch, B. 1977. An ultrastructural study of the musculature of the pond snail Lymnaea stagnalis (L.). Cell Tiss. Res. 180: 317-340.

Ros, J. 1976. Sistemas de defensa en los opisthobranquios. Oecologia Aquatica 2: 41-71.

Rosenbluth, J. 1972. Obliquely striated muscle. Pp. 389-420 in The Structure and Function of Muscle, Vol. I, 2nd ed. G.H. Bourne, ed. Academic Press, New York.

Russell, E. 1966. An investigation of the palatability of some marine invertebrates to four species of fish. Pac. Sci. 20: 452-460.

Schlote, F.-W. 1963. Neurosekretartige Grana in den peripheren Nerven und in den Nerv-Muskel-Verbindungen von Helix pomatia. Z. Zellforsch. mikrosk. Anat. 60: 325-347.

Schulte, G.R., and P.J. Scheuer. 1982. Defensive allomones of some marine molluscs. Tetrahedron 38: 1857-1863.

Schulte, G.R., P.J. Scheuer, and O.J. McConnell. 1980. Two furanosesquiterpene marine metabolites with antifeedant properties. Helv. chim. Acta 63: 2159-2167.

Sobieszek, A. 1973. The fine structure of the contractile apparatus of the anterior byssus retractor muscle of Mytilus edulis. J. ultrastruct. Res. 43: 313-343.

Summers, R.G., B.L. Hylander, L.H. Colwin, and A.L. Colwin. 1975. The functional anatomy of the echinoderm spermatozoon and its interaction with the egg at fertilization. Amer. Zool. 15: 523-551.

Thompson, J.E., R.P. Walker, S.J. Wratten, and D.J. Faulkner. 1982. A chemical defense mechanism for the nudibranch Cadlina luteomarginata. Tetrahedron 38: 1865-1873.

Thompson, T.E. 1960a. Defensive acid-secretion in marine gastropods. J. mar. biol. Ass. U.K. 39: 115-122.

Thompson, T.E. 1960b. Defensive adaptations in opisthobranchs. J. mar. biol. Ass. U.K. 39: 123-134.

Thompson, T. 1984. Histology of acid glands in Pleurobranchomorpha. J. moll. Stud. 50: 65-67.

Twarog, B.M., M.M. Dewey, and T. Hidaka. 1973. The structure of Mytilus smooth muscle and the electrical constants of the resting muscle. J. gen. Physiol. 61: 207-221.

Wright, B.R. 1974a. Sensory structure of the tentacles of the slug Arion ater (Pulmonata, Mollusca) 1. Ultrastructure of the distal epithelium, receptor cells and tentacular ganglion. Cell Tiss. Res. 151: 229-244.

Wright, B.R. 1974b. Sensory structure of the tentacles of the slug, Arion ater (Pulmonata, Mollusca) 2. Ultrastructure of the free nerve endings in the distal epithelium. Cell Tiss. Res. 151: 245-257.

Yoshii, K., N. Kamo, K. Kurihara, and Y. Kobatake. 1978. Electrophysiological studies on the responses of the surf clam, Spisula sachalinensis, to the starfish saponins. Comp. Biochem. Physiol. 61C: 301-307.

Young, C.M., P.G. Greenwood, and C. Powell. 1986. The ecological role of defensive secretions in the intertidal pulmonate Onchidella borealis. Biol. Bull. 171: 391-404.

Zylstra, U. 1972. Distribution and ultrastructure of epidermal sensory cells in the freshwater snails Lymnaea stagnalis and Biomphalaria pfeifferi. Netherlands J. Zool. 22: 283-298.

Table 1: Number of repugnatorial glands that secreted in response to touches with a glass probe, compared to number that secreted in response to touches with a freshly excised tube foot of the seastar Pycnopodia helianthoides. The results are highly significantly different ($p << .01$; Chi squared test for homogeneity with correction for continuity).

Test Ceras	Number of Glands Secreted (x/10)	
	Glass Probe	Tube foot
1	4	7
2	0	8
3	3	6
4	4	9
5	6	6
6	7	10
7	9	9
8	4	9
9	8	7
10	6	7
11	3	5
12	2	7
	---	---
Total:	56 (46.7%)	90 (73%)

Figure 106: Light micrograph (NDIC) of a portion of the ceratal epidermis of Melibe leonina showing three repugnatorial glands (arrowheads). Scale bar = 100 µm.

Figure 107: Light micrograph (NDIC) showing a ceratal repugnatorial gland located at the end of a small peripheral nerve (arrowheads). Scale bar = 25 µm.

Figure 108: Light micrograph (NDIC) of a repugnatorial gland in lateral view showing a tuft of short, stiff cilia (arrowhead) arising from the ceratal epidermis (E) overlying the gland. Scale bar = 25 µm.

Figure 109: Scanning electron micrograph of the ceratal epidermis showing the secretory pore (P) of a repugnatorial gland surrounded by tufts of sensory cilia (arrowheads). Scale bar = 5 µm.


106

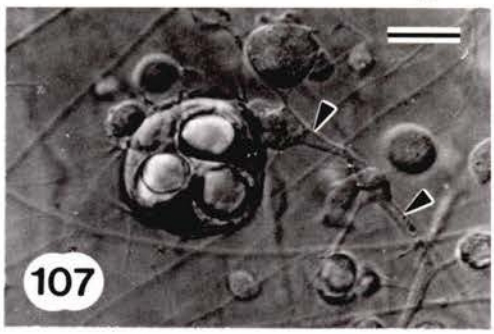
107

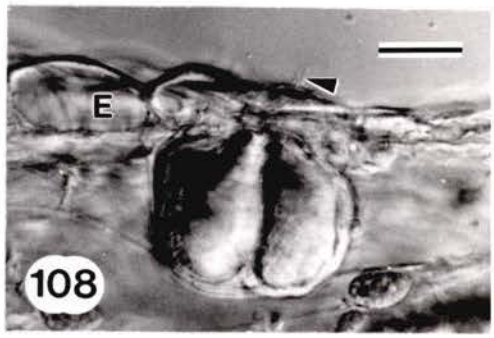
E
108


P
109

Figure 110: Sketch of a repugnatorial gland of Melibe leonina in longitudinal section showing the types A and B secretory cells, each with a large central vacuole (CV) containing the secretory product, and the muscle (MU) that encircles the gland and extends between the individual secretory cells. A bundle of ciliated sensory dendrites (CD) having subepidermal cell bodies (CB) lies adjacent to the secretory duct (D) and secretory pore (P) of the gland. Ciliated supporting cells (S) flank the bundle of dendrites as they traverse the epidermis (E). A nerve (N) extends to each repugnatorial gland. Drawing not to scale.

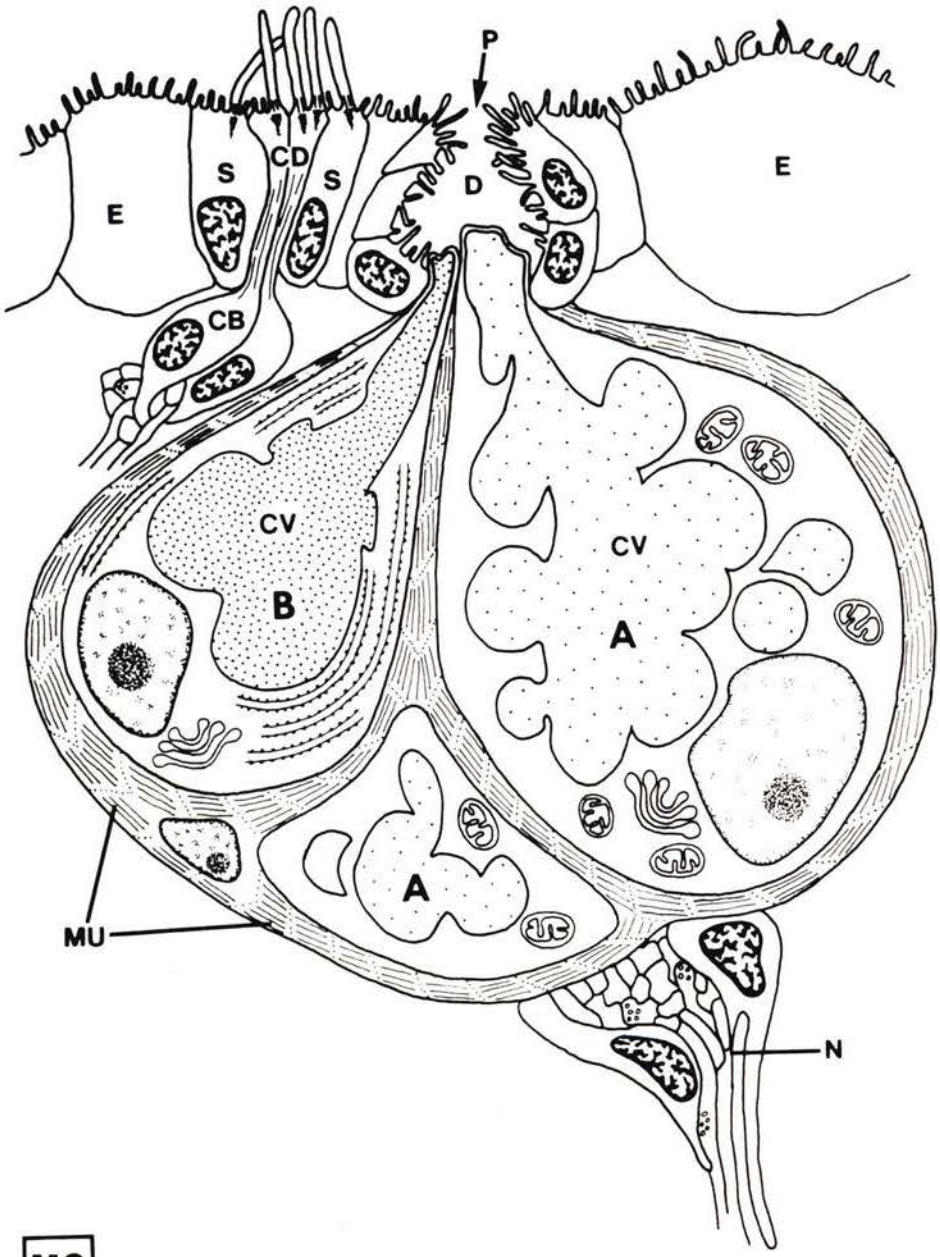

110

Figure 111: Transmission electronmicrograph (TEM) of a repugnatorial gland of Melibe leonina in oblique transverse section. The section passes through the central vacuole (CV) of two type A cells and one type B cell, and the nuclues (NU) of a type A cell and a muscle cell. Note the inner and outer muscle layers (IM and OM). Scale bar = 5 µm.

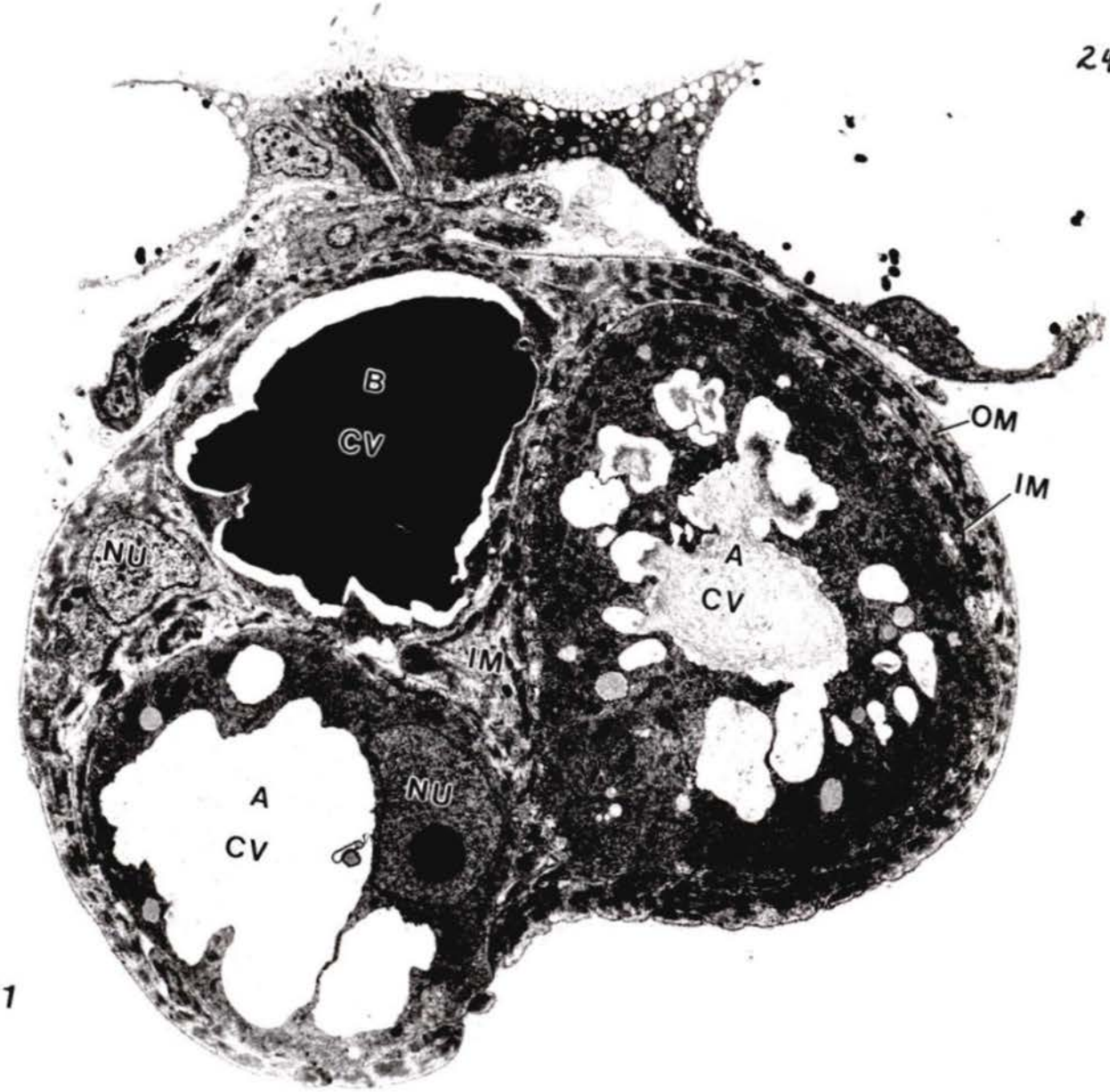

111

Figure 112: TEM of the secretory duct (D) and the distal portion of a type A and B secretory cell cut in longitudinal section. The extreme apical membrane of the secretory cells (arrowheads) forms part of the floor of the secretory duct, which in turn opens externally via the secretory pore (P). The section also passes through a tuft of sensory cilia (C) located close to the pore. Scale bar = 5 µm.

Figure 113: TEM of a cross section through a secretory duct (D) within the ceratal epidermis (E). The section passes through the apices of two type A secretory cells where they project into the lumen of the duct. Scale bar= 5 µm.

Figure 114: TEM of a duct cell showing the felt-work of microfilaments (arrowheads) immediately beneath the microvilli (MI) of the apical cell membrane. Scale bar = 1 µm.

Figure 115: Higher magnification of the apices of the type A and B secretory cells where they form the floor of the secretory duct (D) (enlarged from Fig. 112). In both cells, the apical membrane of the central vacuole (single arrows) is closely apposed to the apical membrane of the secretory cell (double arrows). Scale bar = 1 µm.

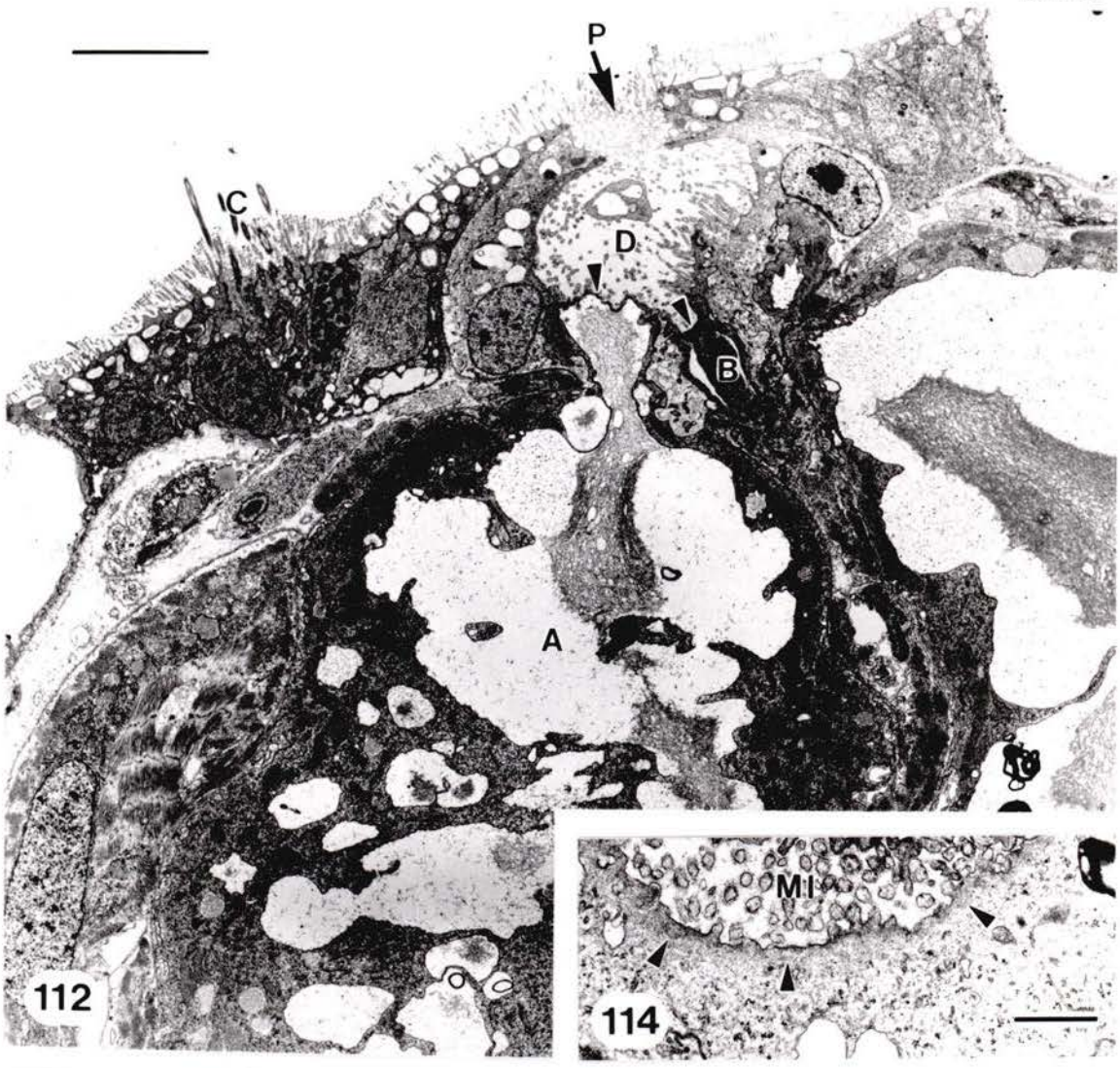
P
C
D
B
A
112

MI
114

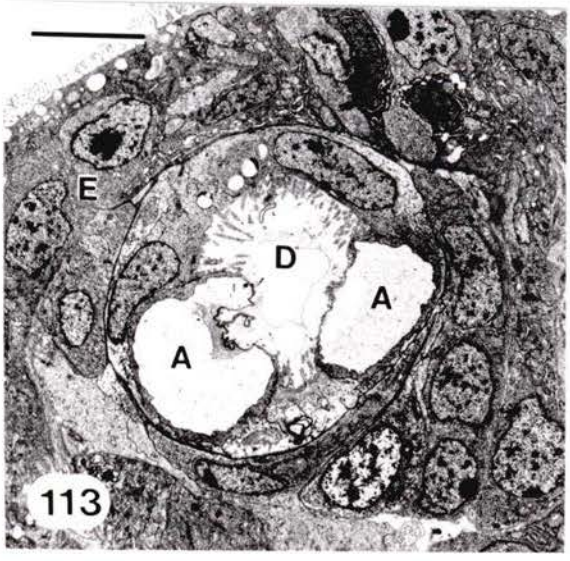
E
D
A
A
113

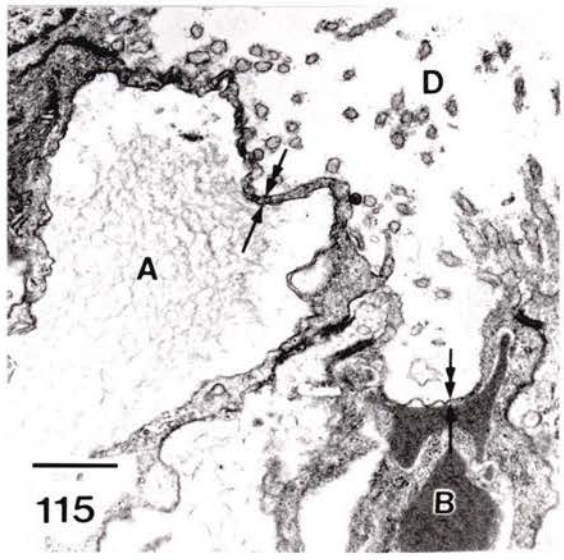
D
A
B
115

Figure 116: TEM through the cytoplasm of a type A secretory cell showing a Golgi profile (G) and primary (1V), secondary (2V), and tertiary (3V) cytoplasmic vesicles. The cytoplasm also includes bundles of microtubules (arrowheads) adjacent to the central vacuole (CV) and many mitochondria (M). The basal membrane is elaborated into interdigitating processes (P). The adjacent muscle fibres show several hemifasciae adherentes (arrows). Scale bar = 0.5 µm.

Figure 117: TEM of a neuroglandular synapse onto a type A secretory cell. Scale bar = 0.5 µm.

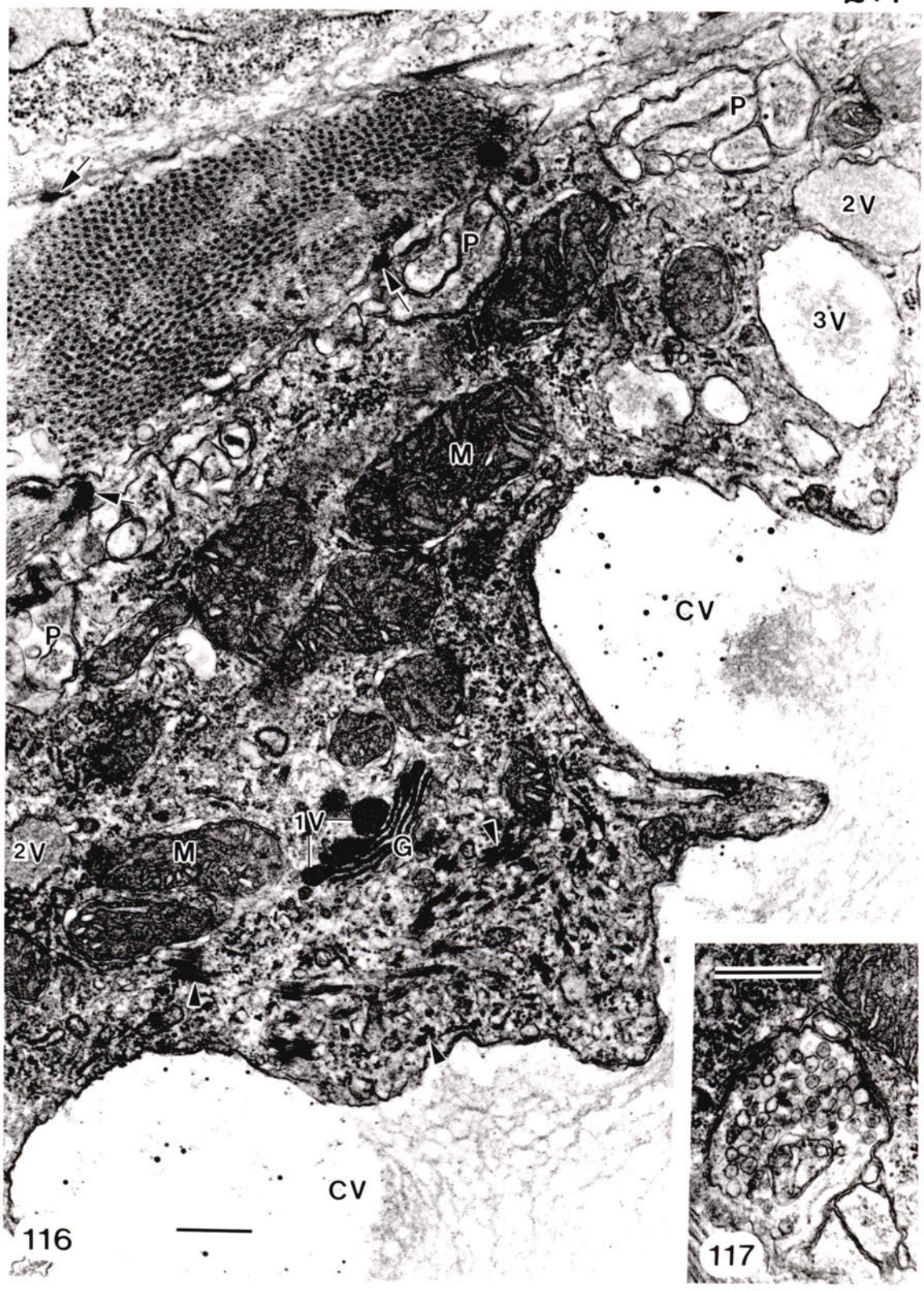
P
2V
P
3V
M
CV
P
1V
2V
M
G
CV
116
117

Figure 118: TEM of a portion of a type B secretory cell showing the parallel lamellae of rough endoplasmic reticulum (ER) arranged circumferentially around the central vacuole (CV). Scale bar = 1 µm.

Figure 119: TEM of the cytoplasm of a type B secretory cell showing mitochondria (M), rough endoplasmic reticulum (ER), and a Golgi body (G) with associated vesicles (V) having an electron-dense content. The largest of these vesicles appears to be merging (arrowheads) with the central vacuole (CV). Also note the surface coupling (circled) between the sarcolemma of an adjacent muscle cell (MU) and a tubule of sarcoplasmic reticulum. Scale bar = 0.5 µm.

Figure 120: TEM of a neuroglandular synapse onto a type B secretory cell. Scale bar = 0.5 µm.

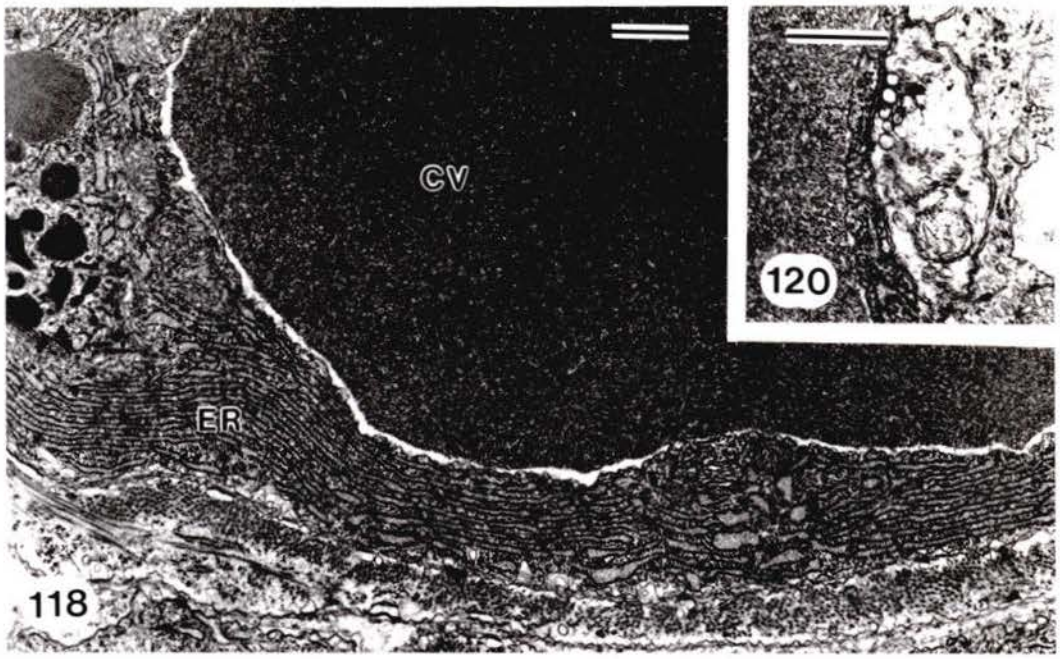
CV
ER
118
120

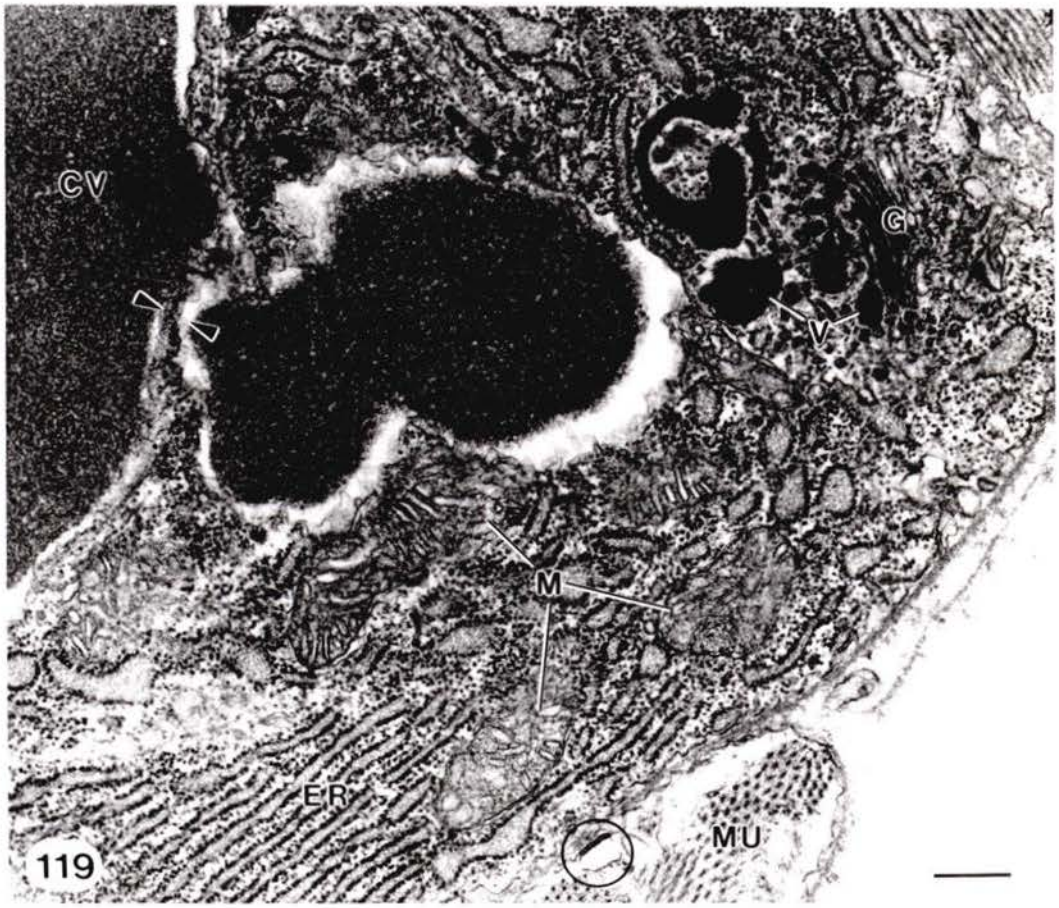
CV
G
V
M
ER
MU
119

Figure 121: TEM of two muscle cells labelled MU1 and MU2 adjacent to a type A secretory cell. Axonal varicosities (arrowheads) containing clear and slightly electron-opaque vesicles lie close to both muscle cells and the myofilaments of the two are oriented in opposing directions. The section through MU1 passes through its nucleus (NU) and also shows the oblique orientation of Z-bodies (arrowheads). Scale bar = 1 µm.

Figure 122: TEM of a neuromuscular synapse within a repugnatorial gland. Scale bar = 0.5 µm.

Figure 123: TEM of several axonal profiles (A) extending between muscle fibres (MU) within a repugnatorial gland. The arrowhead indicates a neuromuscular synapse in which the content of the synaptic vesicles is highly electron-dense. Scale bar = 1 µm.

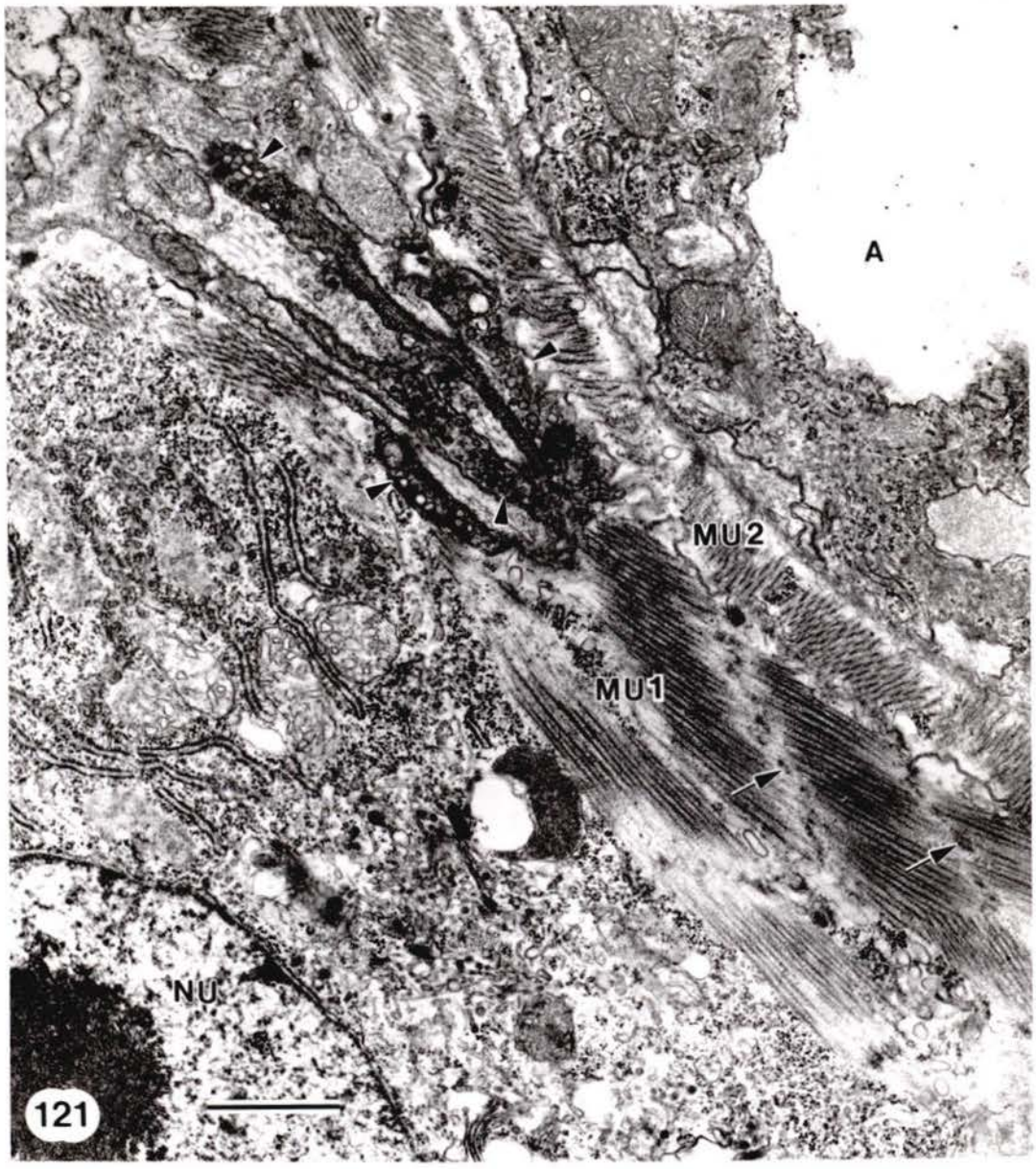
A
MU2
MU1
NU
121

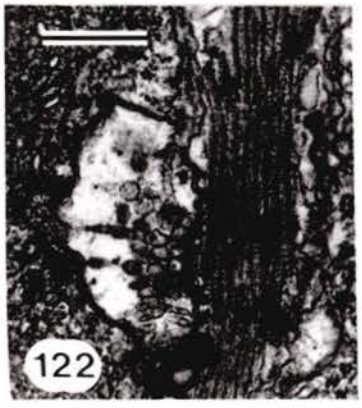
122

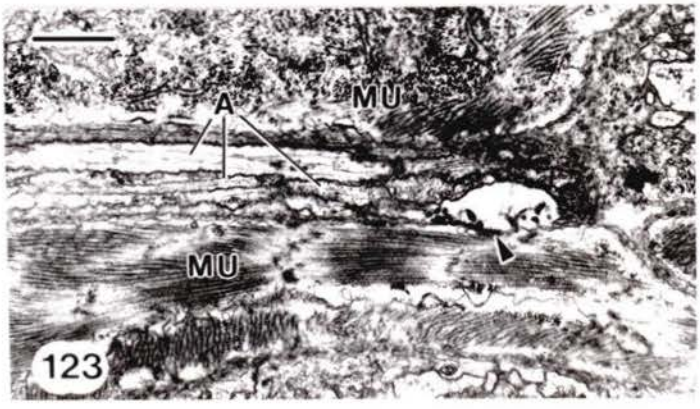
A
MU
MU
123

Figure 124: TEM showing a bundle of ciliated sensory dendrites (CD) flanked by 2 ciliated supporting cells (S). The arrowheads demarcate one side of a sensory dendrite as it penetrates the basal lamina of the epidermis and merges with its subepidermal cell body (CB). A neuropil (NP) showing a synapse (arrow) lies adjacent to the sensory cell body. Scale bar = 1 µm.

Figure 125: TEM of a portion of sensory dendrite cut in longitudinal section just distal to the basal lamina of the ceratal epidermis. Note the microtubules (arrowheads). Scale bar = 0.25 µm.

Figure 126: TEM of a transverse section through a bundle of sensory dendrites. The dendrites contain an aggregation of mitochondria (M) at this level of section (just proximal to the ciliary basal bodies). The many small circular profiles (arrowheads) are microtubules in cross section. Scale bar = 0.5 µm.

Figure 127: TEM of cilia at the distal end of a group of sensory dendrites (CD). Note the basal plate (BP), ciliary rootlet (R) and basal foot (F). Scale bar = 0.5 µm.

Figure 128: TEM showing a portion of the nucleus (NU) and perinuclear cytoplasm of a sensory cell. The cytoplsam contains a multivesicular body (MB) and a group of many small vesicles (arrowheads). Scale bar = 0.5 µm.

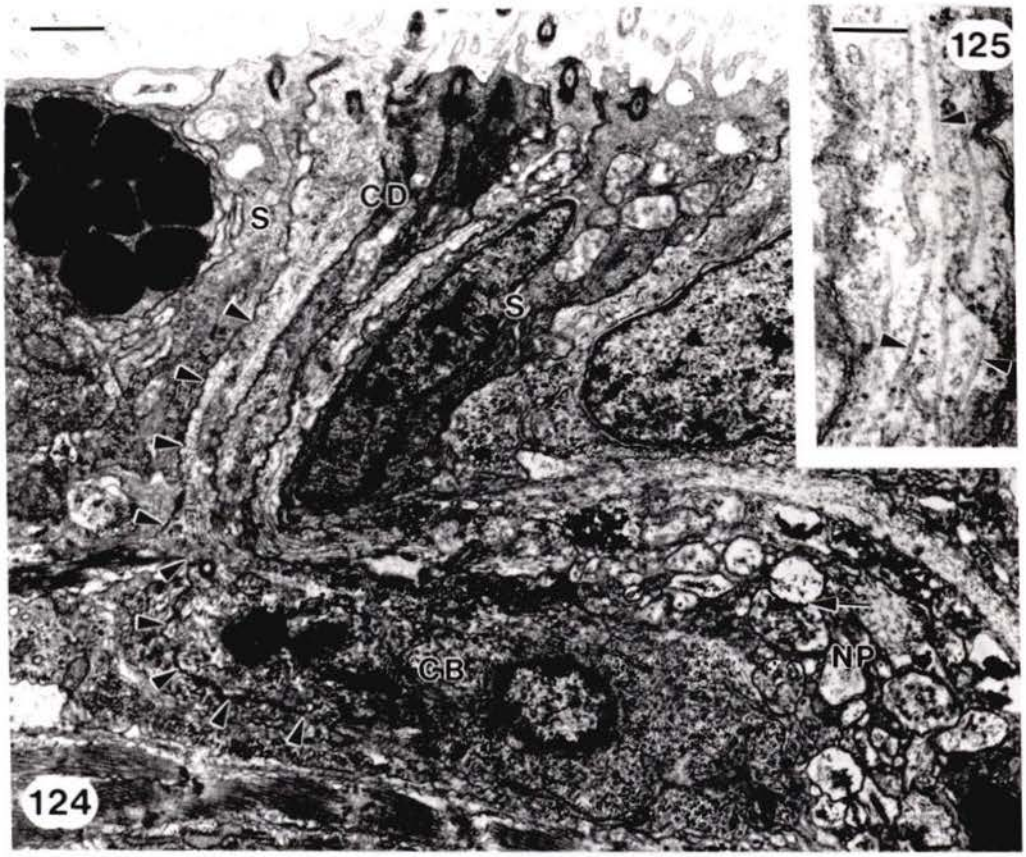
S
CD
S
CB
NP
124
125

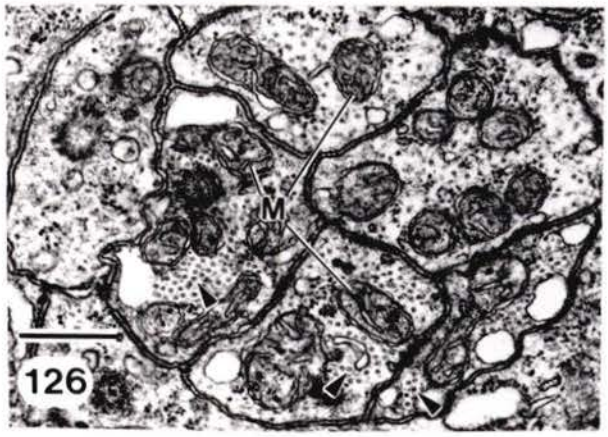
M
126

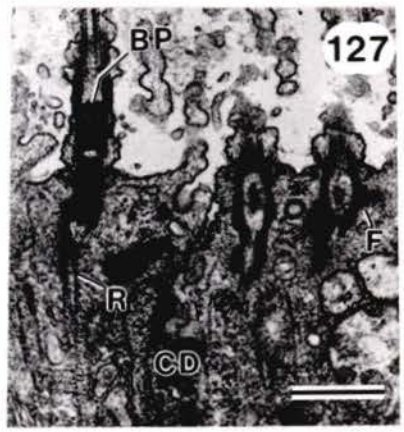
BP
127
F
R
CD

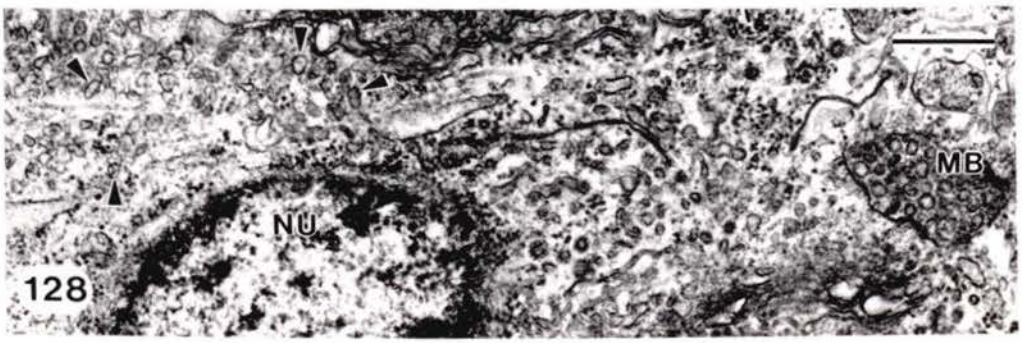
NU
MB
128

Figure 129: Light micrograph of an undischarged repugnatorial gland (RG) beneath the ceratal epidermis of Melibe leonina. The prominent spheres within the capsule of the gland are secretory cells filled with secretory product. Scale bar = 50 µm.

Figure 130: Light micrograph of the same gland (RG) as shown in Fig. 129 photographed after touch by a probe induced discharge of the secretory product. The capsule of the gland has contracted and the prominent spheres are absent. Scale bar = 50 µm.

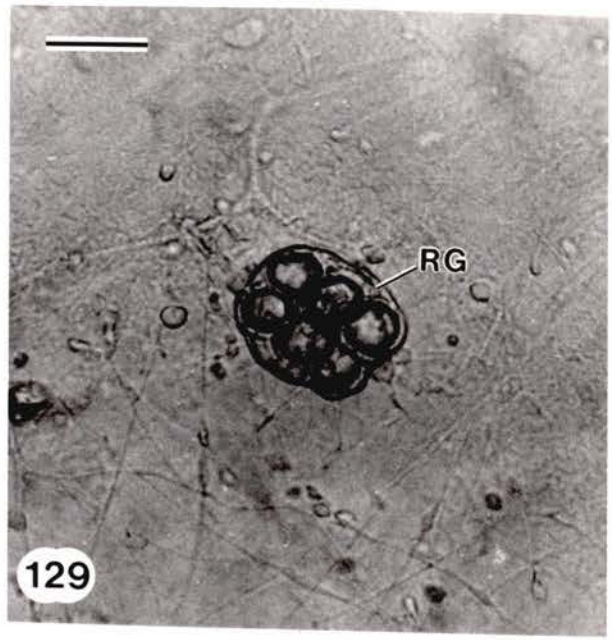
RG
129

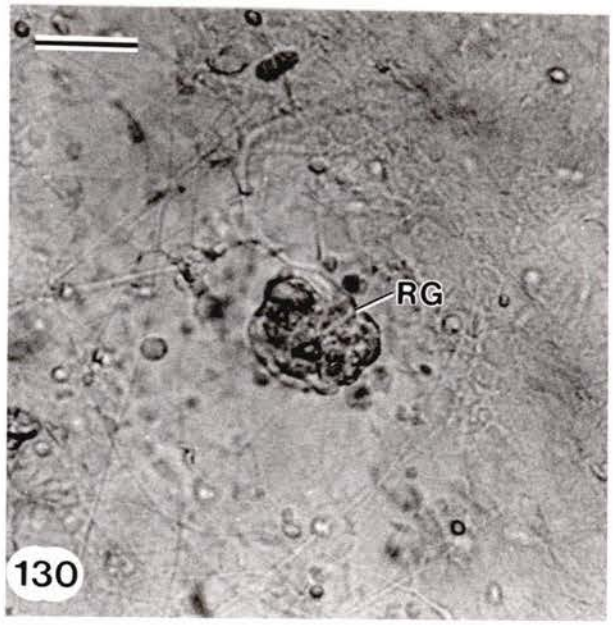
RG
130

VITA

Surname: PAGE (Bickell) Given Names: LOUISE ROBERTA

Birthplace: CALGARY, ALBERTA Birthdate: SEPT. 27, 1954

Educational Institutions Attended, With Dates of Entering and Leaving:

UNIVERSITY OF ALBERTA	1971 to 1975
UNIVERSITY OF ALBERTA	1975 to 1978
UNIVERSITY OF VICTORIA	1980 to 1988

DEGREES, DIPLOMAS, ETC. AWARDED, WITH DATES AND NAMES OF INSTITUTIONS:

B.Sc. (1st class honours)	1975	Univ. of Alberta
M.Sc.	1978	Univ. of Alberta

Honours and Awards:

N.R.C. Post-Graduate Scholarship, 1975/76 and 1976/77

University of Victoria Fellowship, 1980/81, 1981/82, 1982/83

Publications:

Chia, F.-S., and L.R. Bickell. 1978. Mechanism of larval attachment and the induction of settlement and metamorphosis in coelenterates: a review. Pp. 1-12 in Settlement and Metemorphosis of Marine Invertebrate Larvae, F.-S. Chia and M.E. Rice, eds. Elsevier/North-Holland, New York.

Bickell, L.R., and F.-S. Chia. 1979. Organogenesis and histogenesis in the planktotrophic veliger of Doridella steinbergae (Opisthobranchia: Nudibranchia). Mar. Biol. 52: 291-313.

Bickell, L.R., F.-S. Chia, and B.J. Crawford. 1980. A fine structural study of the testicular wall and spermatogenesis in the crinoid, Florometra serratissima (Echinodermata). J. Morph. 166: 109-126.

Bickell, L.R., F.-S. Chia, and B.J. Crawford. 1981. Morphogenesis of the digestive system during metamorphosis in the nudibranch Doridella steinbergae (Gastropoda): conversion from phytoplanktivore to carnivore. Mar. Biol. 62: 1-16.

Chia, F.-S., R. Koss, and L.R. Bickell. 1981. Fine structural study of the statocysts in the veliger larva of the nudibranch, Rostanga pulchra. Cell Tiss. Res. 214: 67-80.

Bickell, L.R., and S.C. Kempf. 1983. Larval and metamorhpic morphogenesis in the nudibranch Melibe leonina (Mollusca: Opisthobranchia). Biol. Bull. 165: 119-138.

Chia, F.-S., and L.R. Bickell. 1983. Echinodermata. Pp. 545-620 in Reproductive Biology of Invertebrates, Vol. II: Spermatogenesis and Sperm Function, K.G. and R.G. Adiyodi, eds. John Wiley and Sons, Chichester.

PARTIAL COPYRIGHT LICENSE

I hereby grant the right to lend my dissertation to users of the University of Victoria Library, and to make single copies only for such users or in response to a request from the library of another university, or similar institution, on its behalf or for one of its users. I further agree that permission for extensive copying of this dissertation for scholarly purposes may be granted by me or a member of the University designated by me. It is understood that copying or publication of this dissertation for financial gain shall not be allowed without my written permission.

Title of Dissertation

THE CERATA OF MELIBE LEONINA (GOULD, 1852) (MOLLUSCA; NUDIBRANCHIA): MORPHOGENESIS, NEUROGENESIS, AUTOTOMY, AND REPUGNATORIAL GLANDS

Author

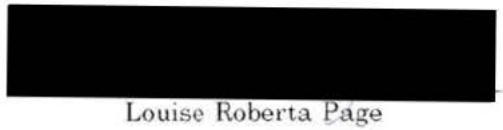

Louise Roberta Page

January 29, 1988